

THÈSE

Pour obtenir le grade de

DOCTEUR DE L'UNIVERSITÉ DE GRENOBLE

Spécialité : **Matériaux, Mécanique, Génie civil, Electrochimie**

Arrêté ministériel : 7 août 2006

Présentée par

Pierre LEITE

Thèse dirigée par **Yves BRECHET** et **Marc THOMAS**

préparée au sein du **Laboratoire DMSM/MAT ONERA**
dans l'**École Doctorale I-MEP2 – Ingénierie - Matériaux,**
Mécanique, Energétique, Procédés et Production

Optimal design of architected sandwich panels for multifunctional properties

Thèse soutenue publiquement le **16 Octobre 2013**,
devant le jury composé de :

Pr. Luc SALVO

Professeur, Institut National Polytechnique de Grenoble, Président.

Dr. Rodolphe LE RICHE

Chargé de recherche, Ecole des Mines de Saint-Etienne, Rapporteur.

Dr. Hervé WAGNIER

Maître de conférences, Université de Bordeaux, Rapporteur.

Pr. Paul WEAVER

Professeur, University of Bristol, Examineur.

M. Pierrick PECHAMBERT

PDG, Sainte-Marie Constructions Isothermes, Invité.

Pr. Yves BRECHET

Professeur, Institut National Polytechnique de Grenoble, Directeur de thèse.

Dr. Marc THOMAS

Ingénieur de recherche, DMSM, ONERA, Encadrant de thèse.



Remerciements

La réussite d'une thèse dépend de beaucoup de facteurs et surtout de beaucoup de personnes. Tous n'interviennent pas au même niveau ni au même moment mais font partie intégrante du processus.

Une thèse se termine généralement par une soutenance au cours de laquelle le travail du doctorant est jugé par des personnes de la communauté. Je tiens donc à remercier en premier lieu les membres de mon jury de thèse pour cet exercice critique. Je remercie Rodolphe Le Riche et Hervé Wagnier d'avoir rapporté ce manuscrit. Leurs remarques ont été très instructives. Je remercie également Luc Salvo qui a présidé ce jury et Paul Weaver qui a fait le déplacement depuis Bristol avec autant d'enthousiasme.

J'ai été très honoré d'avoir parmi les membres de mon jury Pierrick Péchambert de la société SMCI car il a apporté un point de vue critique essentiel à ce travail : le point de vue de l'industriel. Je le remercie pour sa présence et pour les échanges que nous entretenons.

Avant d'en arriver à la soutenance de thèse et au manuscrit, il faut fournir un travail construit et original. Je suis reconnaissant envers Yves Bréchet, mon directeur de thèse, qui a monté mon sujet de recherche. Ses conseils avisés et nos discussions du soir (ou du matin) m'ont été d'un grand réconfort au cours de ces trois ans. Il est plaisant de voir autant d'enthousiasme pour la science et plus particulièrement pour les matériaux architecturés.

Je dois aussi beaucoup à Marc Thomas, mon encadrant Onera au quotidien. Je le remercie pour son soutien et son implication dans une thématique de recherche nouvelle pour le département. Je pense qu'il faut avoir beaucoup de courage pour se lancer dans ce genre d'aventure.

Je remercie messieurs Shigehisa Naka, directeur du DMSM à mon arrivée, et Frank Gallerneau, directeur du DMSM à mon départ, de m'avoir accueilli au sein du département. Je remercie également Marie-Pierre Bacos, chef de l'unité Matériaux et ArchiTectures, pour son soutien et sa bienveillance. J'exprime également ma gratitude à Thierry Ochin, Sylvie Ruffault et plus particulièrement Sophie Garabédian qui ont la lourde tâche de nous simplifier la vie (ce qui représente un travail de titans), sans eux rien ne tournerait rond.

La communauté « matériaux architecturés » se développe en France depuis plusieurs années, et ce fut une chance pour moi de pouvoir côtoyer une partie de ses membres au sein du projet MANSART. Je salue tous les collaborateurs et les remercie pour les échanges que nous avons eus au cours de ces quelques années passées ensemble. Evoluer dans un groupe comme celui-ci est une incroyable source de richesse scientifique et personnelle. Je remercie plus particulièrement les doctorants Marion Amiot, Justin Dirrenberger, Loïc Courtois, Amélie Kolopp et Magali Dugué mais aussi Samuel Forest, Eric Maire, Rémy Dendievel, Marc Fivel, Anne Perwuelz, Marilyne Lewandowski, Dominique Poquillon, Christophe Bouvet, Sophie Gourdet, Valia Fascio et Dominique Bissières.

Je remercie également les collègues de l'Onera qui m'ont aidé et accompagné au cours de cette thèse en commençant par Frank Simon du DMAE pour son aide et pour avoir été mon professeur d'acoustique le temps d'une journée. En ce qui concerne l'optimisation, je dois

beaucoup à mon professeur Gonzalo Cabodevila mais aussi à Itham Salah-El-Din du DAAP qui m'a lancé de manière remarquable dans ce projet. Je remercie ce dernier pour le temps qu'il m'a accordé et pour son implication.

Cécile Davoine mérite une place particulière dans ces remerciements. Je lui dois mon arrivée à l'Onera mais aussi mon intérêt pour les matériaux architecturés. Merci pour les cours de cuisine (truffes, gaufres et sandwiches). Tout a commencé par un tube...

La réussite du travail dépend aussi de l'ambiance et donc des relations que l'on entretient avec ses collègues. Je salue tous les membres de l'équipe avec qui j'ai partagé les moments de pause : Cécile, Sébastien, Jean-François, Etienne, Pierre Josso, Marie-Pierre ; les doctorants : Antoine, Olivier, Anna ; les stagiaires et apprentis : Jonathan B, Jonathan C, Anaïs, Jérémy, David, Quentin, Alexandre Pelourdeau, Félix, Naïma, Aliénor, Pierre Defaye, Cédrik, Isabelle, Maxime, Mame, Antsa, Julie, Alexandre Tanguy, Pascal Bilhe, Manuel, Fabien et Benjamin.

Une pensée pour mon maître de la blague, Kevin, parti trop tôt (dans le sud). Je ne pensais pas un jour rencontrer quelqu'un avec un humour aussi particulier que le mien.

Même si je ne les nomme pas directement, je remercie tous les collègues avec qui j'ai passé du temps au sein du département.

Mes derniers remerciements seront pour ceux qui n'ont pas contribué à mon travail de thèse mais qui ont contribué à mon équilibre personnel. J'embrasse bien fort Elodie et Pitchou, le reste de la dream team. Nous sommes des fous mais nous y sommes arrivés. Je salue et remercie très chaleureusement Emeline, Mathieu, Delphine et Christophe pour leur amitié, leur patience et leur indulgence. Le hasard fait bien les choses parfois. Vive Berthelot ! Je remettrais la chaîne en partant...

J'embrasse toute ma famille, des côtés Leite et Busschaert. Merci pour votre soutien, c'est quelque chose de précieux.

Je remercie aussi mon chat pour les séances de ronron thérapie gratuite (ou pas) qui m'ont apporté beaucoup de réconfort à certains moments.

Je conclurai cette partie très personnelle en remerciant la femme de ma vie, Clotilde, qui m'a inconsciemment entraîné là-dedans. Je me nourris de tes forces et la balance commence à avoir mal. Il est impossible d'écrire ici ce que je ressens vraiment mais je ne suis rien sans toi, a minha mulher. Ça a été, on y est arrivé.

CONTENTS

<i>Résumé étendu – French summary</i>	9
1. Introduction	10
2. Méthode mise en place	11
3. Optimisation par voie “réelle” : conception de panneaux avec cœur en mousse	14
4. Optimisation par voie “virtuelle” : influence de l’architecture de cœur	22
5. Méthodes mixtes	26
6. Conclusion	30
 <i>Chapter 1: General introduction</i>	 35
1. Context	37
2. MANSART project (Architected Sandwich Materials)	40
3. Scope of the present study	41
 <i>Chapter 2: Literature review</i>	 45
1. Materials selection	47
1.1. Principles	47
1.2. Multi-criteria materials selection.....	48
1.3. Mixed mode index.....	50
1.4. Determination of performance index by coupling DOE and FEM.....	51
2. Introduction to architected materials	51
2.1. Definition and objectives of architected materials	52
2.2. Maxwell’s stability criterion	52
2.3. Overview of architected materials.....	53
3. Sandwich panels	59
3.1. Introduction	59
3.2. Mechanical properties	60
3.3. Thermal properties	63

Optimal design of architected sandwich panels for multifunctional properties

Pierre Leite

3.4. Acoustical properties	66
3.5. Blast mitigation properties.....	67
4. Presentation of multi-objective optimization methods.....	68
4.1. Generalities.....	68
4.2. Multi-objective optimization	70
4.3. Optimization algorithms	73
4.3.1. Deterministic algorithms	73
4.3.2. Stochastic algorithms	74
4.3.3. Comparison between the two types of algorithm.....	75
4.4. Genetic algorithm.....	76
 Chapter 3: Design process	 79
1. Principles	81
1.1. Process: individuals – evaluation – selection	81
1.2. Specificities of discrete/continuum problems	82
1.3. Path for material selection in the optimization process	85
1.3.1. Optimization based on a discrete database – “real path”	85
1.3.2. Optimization based on a semi-continuous database – “virtual path”	86
2. Analysis of properties	91
2.1. Mass	91
2.2. Flexural properties	91
2.3. Thermal properties	93
2.4. Acoustic damping.....	96
2.5. Blast mitigation	97
3. Performance space	101
3.1. Assessment of compatibility through Pareto front shape	102
3.2. Assessment of design variable influence.....	106
4. Genetic algorithm/implementation (DAKOTA)	108
4.1. Interfacing between analysis tools and optimization algorithm	108
4.2. Specificities of DAKOTA MOGA.....	109
 Chapter 4: Design of foam core sandwich panels: “optimization by real path”	 113
1. Introduction	115
2. Design at minimal weight for a single other objective	116

2.1. Flexural stiffness	117
2.2. Flexural strength.....	122
2.3. Acoustic damping.....	128
2.4. Thermal resistance	133
2.5. Thermal insulation	137
2.6. Blast mitigation	141
3. Design at minimal weight for multiple objectives	146
3.1. A case of beneficial competition between specifications: flexural stiffness and acoustic damping specifications.....	147
3.2. A case of non-beneficial competition between specifications: flexural strength and thermal resistance specifications.....	153
3.3. A case of compatibility between specifications: thermal insulation and blast mitigation specifications	158
3.4. A case of incompatibility between specifications: acoustic damping and blast mitigation specifications	162
4. Overview of the results of multi-objective design by “real path”	168
 <i>Chapter 5: Influence of core architecture: “optimization by virtual path”</i>	
	171
1. Introduction	173
2. Design at minimal weight for a single other objective	175
2.1. Flexural stiffness	175
2.2. Flexural strength.....	179
2.3. Acoustic damping.....	183
2.4. Thermal resistance	189
2.5. Thermal insulation	192
2.6. Blast mitigation	197
3. Design at minimal weight for multiple objectives	199
3.1. A case of beneficial competition between specifications: flexural stiffness and acoustic damping specifications.....	200
3.2. A case of non-beneficial competition between specifications: flexural strength and thermal resistance specifications.....	203
3.3. A case of compatibility between specifications: thermal insulation and blast mitigation specifications	206
3.4. A case of incompatibility between specifications: acoustic damping and blast mitigation specifications	211

4. Overview of the results of multi-objective design by “virtual path”	214
--	-----

Chapter 6: Improvement of the optimization process: mixed methods 219

1. Value of mixed methods.....	221
1.1. Link between optimization method, analysis and models complexity	221
1.2. Behaviour of the genetic algorithm – presentation of a reference case.....	223
2. Coupling genetic algorithm with a branch and average approach.....	226
2.1. Principles: branch-average-rank-select-delete.....	226
2.2. Mixed method applied on the reference case.....	228
2.3. Mixed method applied for the design of sandwich panels for stiffness and acoustic damping at minimal weight.....	232
2.4. Conclusion/Recommendations	235
3. Using design of experiments to create performance indices	236
3.1. Determination of the approximated performance index.....	236
3.2. Using approximated performance index for the design of sandwich panels for stiffness and acoustic damping at minimal weight.....	238
3.3. Conclusion/Recommendations	240
4. Conclusion on the value of mixed methods	240

Chapter 7: Conclusion 243

1. Summary	244
2. Further work.....	246

Glossary..... 249

Appendices 251

A. Additional case studies.....	252
B. Performance of the genetic algorithm	271
C. Design Of Experiments for acoustic damping	274

References..... 277

Résumé étendu

French summary

Ce résumé étendu présente en quelques pages les principaux résultats de cette thèse. Une brève introduction présente le contexte de l'étude. Une deuxième partie se concentre sur la méthode d'optimisation mise en place. Les parties 3 et 4 donnent un exemple d'étude de cas et établissent une synthèse de l'ensemble des résultats présentés dans le manuscrit. Une présentation des approches mixtes utilisées est fournie en partie 5. La partie 6 conclut cette étude.

1. Introduction

Dans la vie d'un produit, l'étape de conception est primordiale pour assurer à la fois ses qualités fonctionnelles mais aussi son usinabilité, sa durée de vie et son recyclage. De manière générale, la conception se base sur un cahier-des-charges, définissant la ou les fonctions du produit, et doit déterminer différents paramètres définissant de manière spécifique le produit :

- le ou les matériaux constitutifs.
- la forme du produit, aussi interne qu'externe.
- les procédés à employer afin de fabriquer le produit.

Ainsi la conception d'un produit peut se résumer à trois actions : sélection de matériaux, dimensionnement et définition du procédé d'élaboration. Ces trois actions sont liées par des interactions plus ou moins fines. L'étape d'élaboration n'a pas été abordée au cours de cette thèse. Le sujet central est la conception, i.e. la sélection de matériaux et le pré-dimensionnement, de structures sandwichs architecturés.

Les matériaux architecturés peuvent être définis comme la combinaison de plusieurs matériaux dans un certain arrangement spatial et qui aboutissent à des propriétés inhabituelles. Ici, matériau est à prendre au sens large. Ainsi, l'on considère un matériau cellulaire tel qu'une mousse, comme la combinaison d'un matériau de base et constitué de porosités. L'air compris dans les porosités est donc le deuxième matériau.

Ces matériaux aux propriétés particulières sont étudiés afin de répondre aux spécifications multicritères des cahiers-des-charges aéronautiques. En effet, ces dernières décennies ont vu s'établir une tendance pour laquelle les produits développés se doivent d'être de plus en plus multifonctionnels. De manière classique, la fonction d'un produit était souvent remplie par sa forme, le matériau étant choisi pour remplir certaines conditions considérées comme des contraintes. Définir une forme optimale pouvant remplir plusieurs fonctions s'avère délicat. Les concepteurs cherchent donc à transférer autant que possible des fonctionnalités dans le choix du matériau, plutôt que dans la définition de la forme. Les spécifications qui nous intéressent sont donc principalement multicritères et la méthode de conception développée pour cette thèse prend en compte ces aspects multi-objectifs.

Ceci soulève donc plusieurs questions. Les techniques classiques de sélection de matériaux, basées sur la notion d'indice de performance, ne sont applicables qu'à des cas de chargement simple et à des géométries simples. De plus, l'aspect multicritère des spécifications implique un mode de décision basé sur la notion de compromis. Un choix au cours du processus de conception pourra soit satisfaire à tous les critères, soit présenter un compromis entre les différents critères étudiés. L'approche adoptée se base sur une notion de compromis basée sur la dominance de Pareto, utilisée dans le cadre d'une optimisation par algorithme génétique.

Au cours de cette thèse nous nous sommes intéressés à l'optimisation multi-objectif de panneaux sandwichs architecturés pour plusieurs fonctions, représentatives des applications habituelles de ces panneaux :

- rigidité et résistance en flexion
- isolation phonique
- résistance et isolation thermique
- résistance aux chocs impulsifs

La première approche que l'on peut considérer est de partir d'une base de données fermée, ce qui est une approche classique de sélection de matériaux. On sélectionne dans une liste de possibilités le candidat idéal. Une évolution possible de cette méthode est d'ouvrir la base de données en incluant des variables géométriques continues dans la description des matériaux. Les matériaux ne sont plus seulement sélectionnés, mais ils sont créés à des fins bien précises. Toutefois, analyser les performances de ce genre de matériaux peut nécessiter des modèles complexes, coûteux en temps de calculs. Il est donc souhaitable de mettre en place des méthodes mixtes permettant de lever l'incompatibilité entre la complexité de l'optimisation et la complexité de l'analyse.

2. Méthode mise en place

La méthode de conception mise en place se sert du principe d'optimalité au sens de Pareto afin de gérer les compromis entre performances. Considérons un problème d'optimisation à n objectifs, évalués via les fonctions objectifs f_i . L'optimalité de Pareto définit la relation d'ordre suivante :

$$"b \text{ domine } a" \Leftrightarrow b < a \Leftrightarrow \begin{cases} \forall i \in \{1, 2, \dots, n\}, f_i(b) \leq f_i(a), \\ \exists j \in \{1, 2, \dots, n\}, f_j(b) < f_j(a), \end{cases} \quad (1)$$

Le cas le plus simple est celui pour lequel b est strictement meilleur que a , c'est-à-dire que pour tous les objectifs considérés, $f_i(a) < f_i(b)$. Cette notion d'optimalité est intéressante car elle admet un compromis entre objectifs à travers l'équivalence de Pareto. Considérons deux solutions pour lesquelles aucun dominant ne peut être identifié, alors ces solutions sont équivalentes au sens de Pareto. Ceci permet de définir deux groupes de solutions dans l'espace des performances¹. Comme le montre la Figure 1, un certain nombre de solutions, noté ici solutions de type A , sont des solutions dominées. En effet, on peut trouver parmi les autres candidats des individus possédant de meilleures performances. En revanche, il y a aussi un certain nombre de solutions pour lesquelles aucun dominant n'existe. Ces solutions, noté solutions de type B , sont des solutions non-dominées. Si l'on compare deux solutions non-dominées S_1 et S_2 dans un problème bi-objectifs P_1 et P_2 , S_1 sera meilleure que S_2 selon P_1 mais S_2 sera meilleure que S_1 selon P_2 . Il y a bien un compromis entre ces performances.

Grace à cette notion d'optimalité au sens de Pareto, l'optimum n'est pas un point mais une surface appelé Front de Pareto². La forme de ce front offre une indication sur la compatibilité entre les performances étudiées (voir Figure 2). On distingue trois cas de figure différents :

- Le front est concave. On parle alors de compétition désavantageuse entre performances. Si l'on considère deux solutions sur ce front, les solutions intermédiaires sont moins intéressantes que les solutions fictives obtenues en utilisant une loi des mélanges des solutions initiales.
- Le front est linéaire. Dans ce cas il y a proportionnalité entre les performances. Néanmoins, le fait d'augmenter l'une des performances aboutit à la réduction de l'autre.

¹ L'espace des performances trace les différentes solutions évaluées selon la valeur de leurs fonctions objectifs. Voir Figure 1.

² On l'appelle aussi surface de compromis ou groupe des solutions non-dominées.

Optimal design of architected sandwich panels for multifunctional properties

Pierre Leite

- Le front est convexe. On parle alors de compétition avantageuse. C'est en général le cas le plus favorable en optimisation multi-objectif. A l'inverse du front concave, si l'on considère deux solutions sur le front, les solutions intermédiaires auront de meilleures performances que des solutions fictives obtenues par la loi des mélanges des deux solutions initiales.

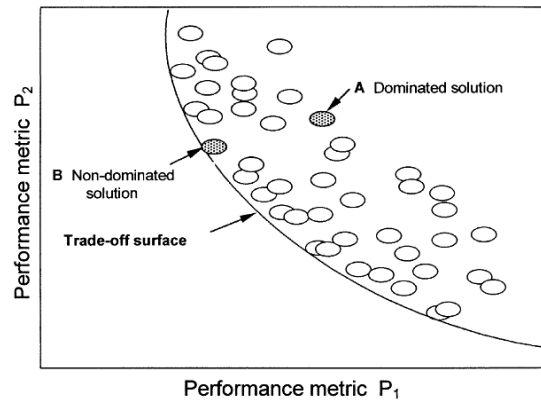


Figure 1 : Illustration schématique d'un espace de performance constitué de deux types de solutions : les solutions de type A sont des solutions dominées tandis que les solutions de type B, qui peuplent le front de Pareto, sont des solutions non-dominées (illustration issue de [ASH00a]).

L'algorithme d'optimisation utilisé est un algorithme génétique. Cet algorithme, imitant le principe de l'évolution selon Darwin, se sert d'une population d'individus dans l'espace de recherche pour évaluer quelles sont les zones intéressantes. Il crée ensuite de nouveaux individus et sélectionne les meilleurs qui resteront dans la population. Au bout d'un certain nombre de générations, l'algorithme aboutit à un ensemble de solutions optimales.

L'efficacité de ces algorithmes dépend en partie de la manière de coder les solutions. On distingue deux approches différentes :

- Une première approche que l'on qualifie d'optimisation par voie « réelle » considère le panneau sandwich symétrique comme l'ensemble de quatre paramètres : les matériaux de peaux et de cœur, les épaisseurs de peaux et de cœur. Les matériaux sont considérés comme existants et listés dans une base de données. Ce sont donc des matériaux réels.
- La seconde approche est qualifiée d'optimisation par voie « virtuelle ». On considère que le matériau architecturé employé en tant que cœur du sandwich peut aussi être décrit de manière semi-continue. Son matériau constitutif est décrit par une variable discrète faisant référence à une information dans une base de données, mais sa géométrie est maintenant définie par des variables géométriques qui ne sont plus figées. On passe donc de quatre variables de conception à cinq voire six selon le nombre de variables géométriques décrivant le cœur.

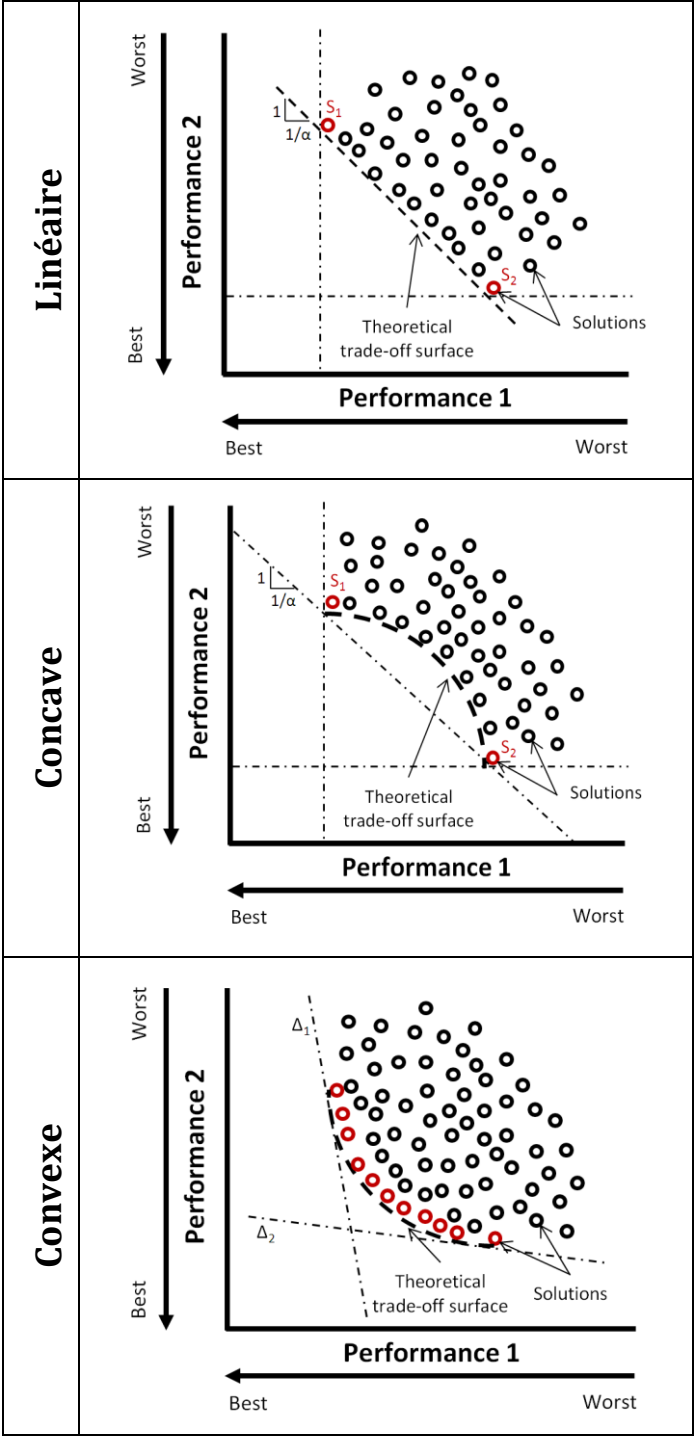


Figure 2 : Formes possibles du front de Pareto.

3. Optimisation par voie « réelle » : conception de panneaux avec cœur en mousse

3.1. Introduction

Ici on s'intéresse à la conception de panneaux sandwichs avec cœur en mousse en utilisant une optimisation par voie « réelle ». Les matériaux sont donc des variables discrètes listés dans une base de données matériaux. Les mousses ont alors l'avantage d'être bien connues et référencées dans de telles bases de données.

Plusieurs fonctions caractéristiques ont été étudiées. Elles sont listées dans le Tableau 1. Le point principal de cette thèse étant l'optimisation multi-objectifs des panneaux sandwichs, ces différentes fonctions ont dans un premier temps été optimisées à masse minimale, i.e. en considérant la réduction de la masse comme second objectif. Dans un deuxième temps, des optimisations tri-objectifs ont été menées afin d'observer l'interaction des performances entre elles. Différentes combinaisons de performances ont été testées, en incluant pour chaque la réduction de la masse comme objectif.

Pour chaque étude de cas, une approche préliminaire par indices de performances est utilisée afin de déterminer les matériaux idéaux. Le front de Pareto permet de déterminer la compatibilité entre performance tandis qu'une analyse de la variance des variables de design sur l'espace des performances permet de mieux comprendre la structure du front de Pareto et de déduire des guides de conception. Enfin, une comparaison entre les performances optimales des panneaux sandwichs et d'une plaque en acier permet de souligner l'intérêt de ce genre de structure par rapport à des structures monolithiques.

Tableau 1 : Combinaisons de performances testées. Les croix en gras représentent les cas qui ont été sélectionnés comme étude de cas pour le reste du manuscrit.

	<i>Rigidité en flexion</i>	<i>Résistance en flexion</i>	<i>Affaiblissement acoustique</i>	<i>Résistance thermique</i>	<i>Isolation thermique</i>	<i>Résistance aux chocs</i>
<i>Réduction de la masse</i>	X	X	X	X	X	X
<i>Rigidité en flexion</i>		X	X	X		X
<i>Résistance en flexion</i>			X	X		X
<i>Affaiblissement acoustique</i>						X
<i>Résistance thermique</i>						
<i>Isolation thermique</i>						X

3.2. Etude de cas : résistance en flexion à masse minimale

Espace de design :

- Matériaux peaux : Métaux, Polymères et composites.
- Epaisseurs des peaux : de 0,5 à 10 mm.
- Matériaux cœurs : Mousses métalliques, Mousses de céramique, Mousses de polymère.
- Epaisseur de cœur : de 10 à 500 mm.
- Type de panneaux sandwich : symétriques.

Objectifs :

- Résistance en flexion : maximiser l'effort critique correspondant à l'endommagement d'une poutre sandwich de 1 m soumise à un essai de flexion trois-points.
- Légèreté : minimiser la masse surfacique du panneau.

Contraintes :

- Effort critique > 2 kN.
- Masse surfacique < 50 kg/m².

Conception préliminaire : approche par Indice de Performance

L'indice de Performance correspondant à une plaque résistante à masse minimale est le suivant : $\sigma^{1/2}/\rho$, avec σ la limite élastique et ρ la masse volumique du matériau. Cet indice est tout à fait adapté pour la sélection du matériau peau. En revanche, le cœur s'endommagera soit par indentation soit par cisaillement. Dans tous les cas, l'indice de performance adéquat pour la sélection du matériau de cœur est : σ/ρ .

Ces indices de performance sont tracés graphiquement sur des cartes de performance³ comme le montre la Figure 3. La première ligne correspond au matériau cœur tandis que la seconde correspond au matériau peau.

Ces cartes permettent d'identifier la mousse de Polyméthacrylimide (PMACR) comme solution optimale en tant que constituant du cœur et le composite à matrice d'Aluminium renforcé de fibres de Carbone (Al-60%C) comme solution idéale pour constituer les peaux.

Conception avancée

Compatibilités

L'espace des performances généré par l'algorithme génétique est donné en Figure 4. On peut y observer un front de Pareto concave, avec un grand rayon de courbure. Il s'agit donc d'un cas de compétition désavantageuse.

Les solutions sont caractérisées par une résistance de 2 kN pour une masse surfacique de 7 kg/m² pour la solution la plus légère et une résistance de 28,5 kN et une masse surfacique de 44 kg/m² pour la solution la plus résistante.

³ Une carte de performance trace sur graphe des matériaux référencés dans une base de données selon deux propriétés matériaux. Ces cartes permettent d'effectuer une sélection de matériaux de manière graphique.

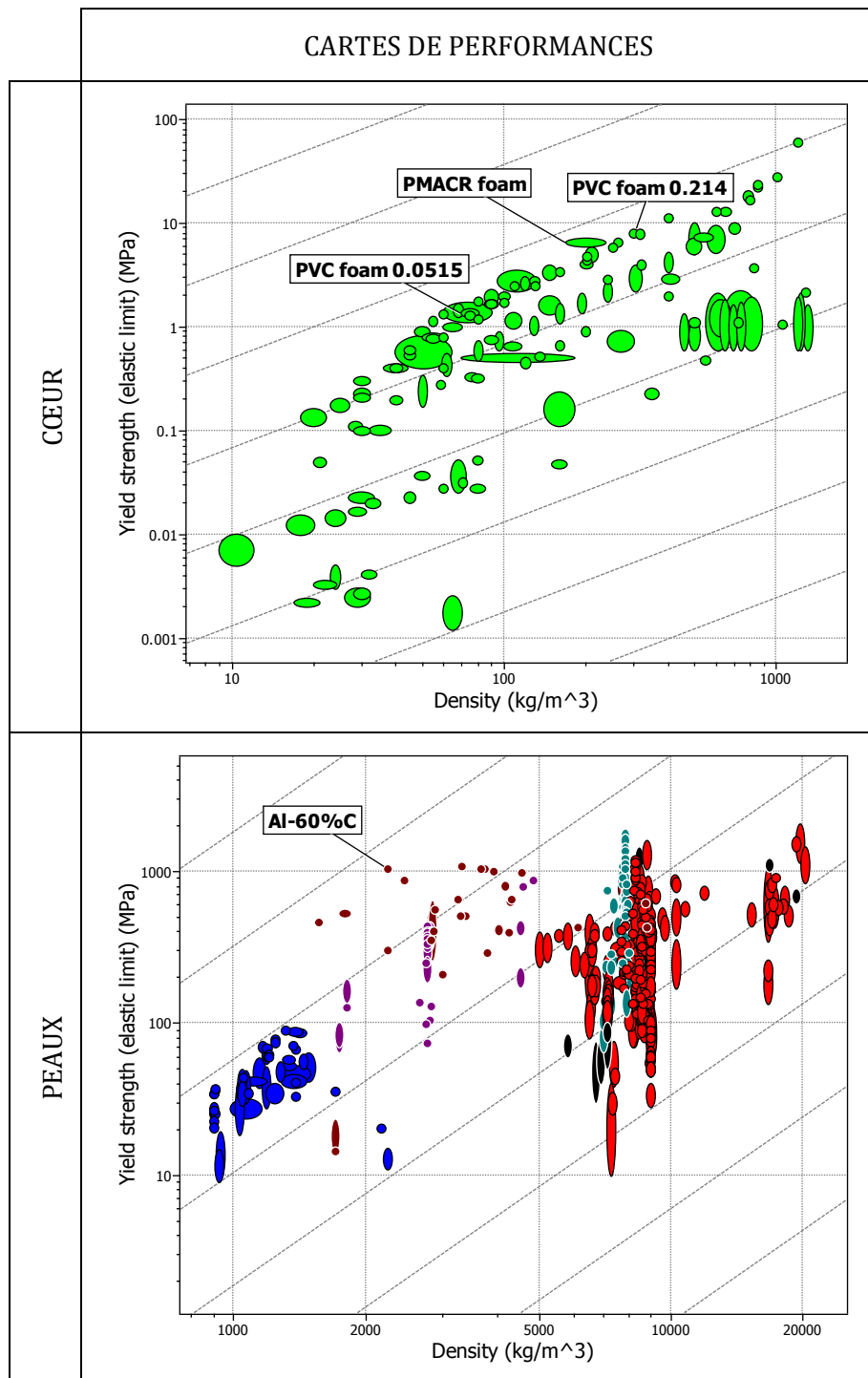


Figure 3 : Cartes de propriétés traçant la limite élastique (Yield Strength) en fonction de la masse volumique (Density) des matériaux. Les droites en pointillés représentent les iso-valeurs des indices de performance. Les solutions optimales se retrouvent en haut à gauche : mousse de PMACR pour le cœur et Al-60%C pour les peaux.

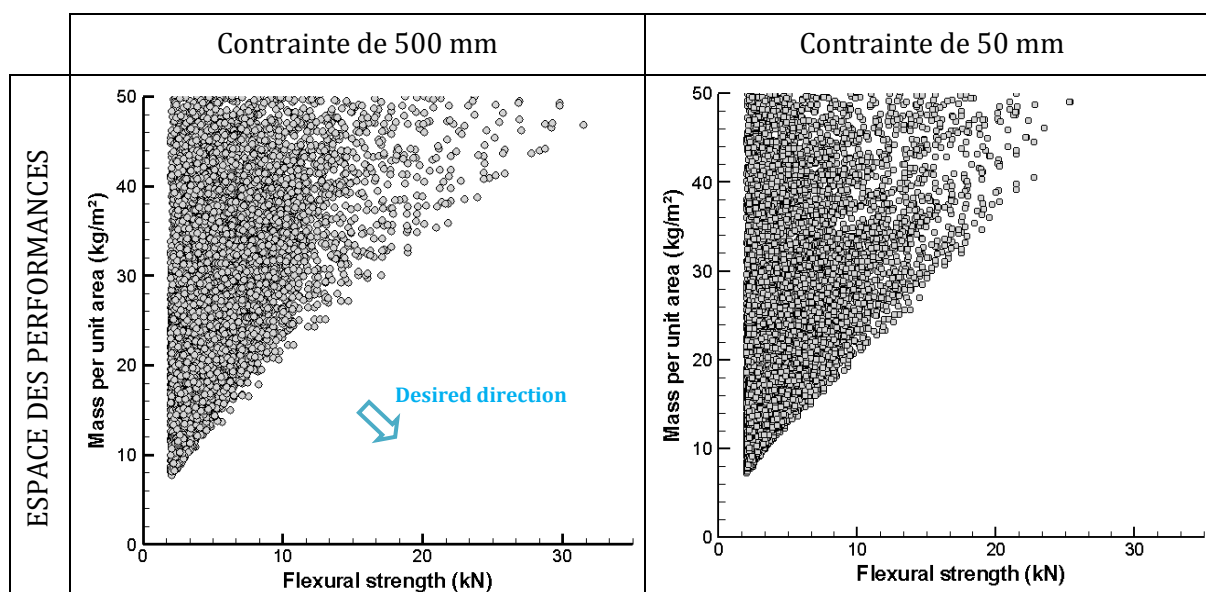


Figure 4 : Espace des performances pour la conception d'un panneau sandwich en résistance en flexion à masse minimale pour deux contraintes d'encombrement différentes.

Analyse de la variance

En Figure 5 sont représentés les effets des variables de conception sur l'espace des performances. La première ligne correspond aux peaux et la deuxième ligne au cœur. La première colonne représente le matériau constitutif et la deuxième colonne les épaisseurs.

On peut observer sur cette figure qu'un matériau ressort comme solution optimale : il s'agit d'un composite à matrice d'Aluminium renforcé en fibre de carbone (Al-60%C). La méthode par indice de performance a prédit de manière exacte la solution optimale en tant que matériau de peau. On retrouve aux basses résistances des alliages d'Aluminium comme autre solution compétitive en tant que peau.

En terme de matériau cœur, deux différentes solutions se détachent. La mousse de PMACR identifiée comme solution optimale par les indices de performances se retrouve effectivement sur le front de Pareto mais uniquement pour de faibles valeurs de résistance et de manière limitée. La majeure partie du front de Pareto est peuplée de solutions constituées de mousse de PVC de densité relative variable. On constate que plus la solution est résistante, plus la mousse de PVC possède une densité relative élevée.

En ce qui concerne les variables géométriques, i.e. les épaisseurs des couches, deux comportements peuvent être remarqués. L'épaisseur du cœur trouve une valeur optimale correspondant à 40 mm. En revanche, l'épaisseur des peaux n'a pas de valeur optimale sur tout le front mais évolue selon la résistance de la solution. Plus la solution sera résistante, plus les peaux seront épaisses.

Effet de la contrainte d'encombrement

Sur la Figure 4 sont représentés deux espaces des performances correspondant à deux contraintes d'encombrement différentes. En modifiant la contrainte de 500 à 50 mm d'épaisseur autorisée, l'effet reste négligeable. Cela s'explique facilement par le fait que les solutions optimales calculées avec une contrainte d'encombrement supérieure possèdent une épaisseur

Optimal design of architected sandwich panels for multifunctional properties

Pierre Leite

comprise environ entre 40 et 55 mm. On peut observer une différence pour les fortes valeurs de résistance mais dans l'ensemble le front reste très similaire.

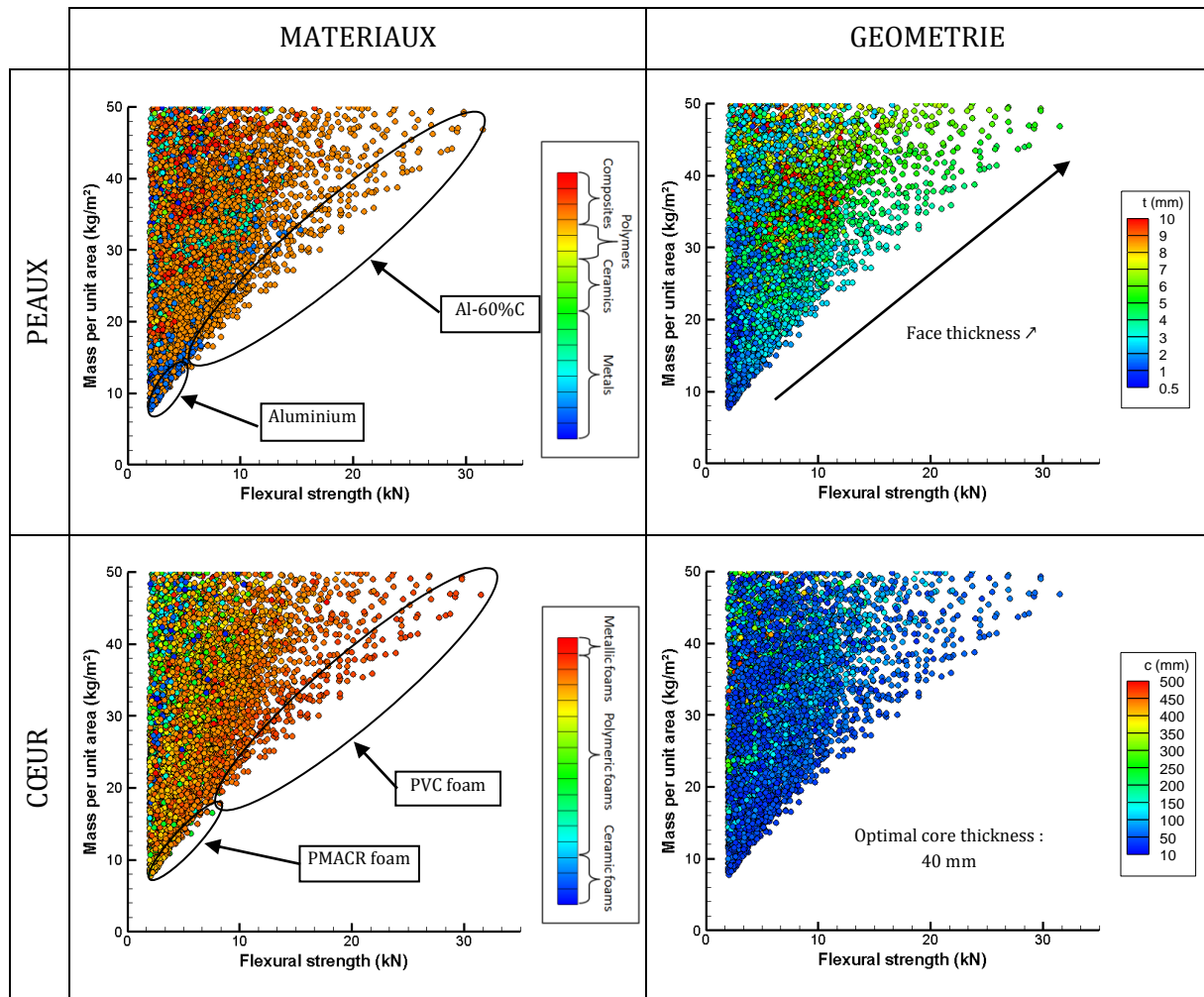


Figure 5 : Influence des variables de conception sur les performances des panneaux sandwichs optimisés en résistance en flexion à masse minimale.

Avantage des structures sandwichs comparées aux solutions monolithiques

Plusieurs études ont eu pour sujet d'étude l'optimisation de panneaux sandwichs en résistance à masse minimale. Celles-ci ont montré que l'on pouvait envisager plusieurs modes d'endommagement du panneau sandwich, conditionnant la sélection des matériaux et le dimensionnement. Une des conclusions de ces études est que le design⁴ optimal favorise une compétition entre plusieurs modes d'endommagement comme illustré en Figure 6 [DES01b]. Cela se traduit par un front de Pareto irrégulier si l'on considère un panneau constitué de matériaux figés, pour lesquels seules les épaisseurs sont des variables de conception (voir Figure 7) [CHE01].

Ce phénomène permet de mieux comprendre les raisons pour lesquelles la mousse de PVC apparaît comme solution optimale au détriment de la mousse de PMACR. Comme l'illustre la Figure 7, aux faibles valeurs de résistance, le mode prépondérant est la rupture des peaux. En

⁴ Ici design signifie définition en termes de conception. Dans le cas de panneaux sandwichs, le design est la donnée des matériaux constitutifs et des épaisseurs.

effet, afin d'obtenir une structure légère, des peaux fines sont préférables, ce qui entraîne par conséquent leur fragilité. Afin d'augmenter la résistance de la structure, il convient donc d'augmenter l'épaisseur des peaux. Cependant, il existe une valeur limite à partir de laquelle l'endommagement est transféré des peaux au cœur, modifiant la pente de la courbe entre résistance et masse. Pour augmenter la résistance de la structure, il convient à présent d'augmenter la résistance du cœur, ce qui peut être obtenu en augmentant sa densité relative. L'espace des performances est en réalité constitué de la superposition de courbes comme celles montrées en Figure 7, avec une densité relative de cœur qui varie, créant une continuité au niveau du front de Pareto.

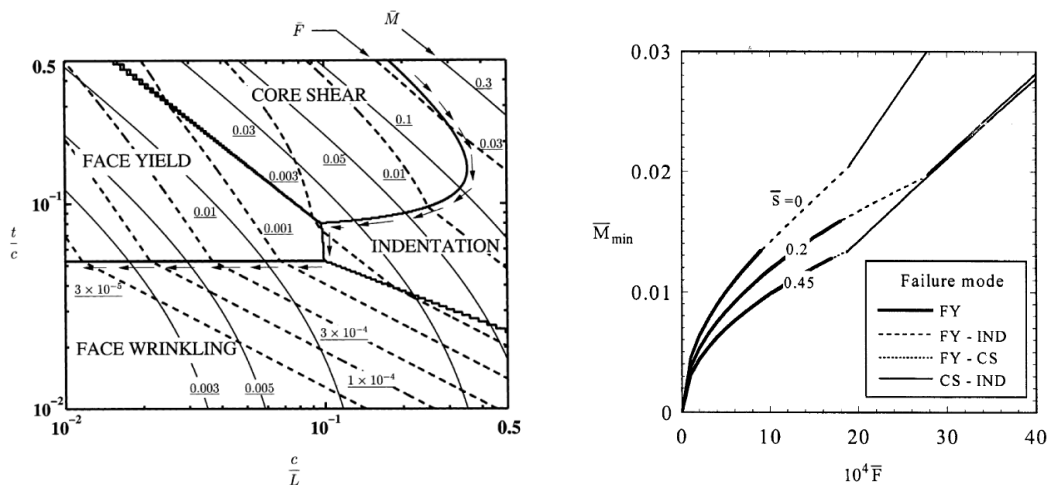


Figure 6 : Sur la gauche : carte d'endommagement de panneau sandwich. Les différentes régions correspondent à des modes d'endommagement différents. Le chemin optimal de résistance à masse minimale est représenté par des flèches et suit la frontière entre plusieurs modes. Illustration tirée de [DES01b]. Sur la droite : front de Pareto correspondant à un panneau sandwich pour une résistance en flexion à masse minimale. On y observe la transition entre modes dans les solutions optimales. Illustration tirée de [CHE01].

En ce qui concerne la mousse de PMACR identifiée comme optimale par l'indice de performance, il n'y a pas dans la base de données de mousse de PMACR plus résistante tandis qu'il existe un nombre non négligeable de mousses de PVC avec des densités relatives différentes, y compris des mousses plus rigides que la mousse de PMACR. C'est pourquoi la mousse de PVC est considérée comme plus optimale que la mousse de PMACR.

Une condition pour obtenir un design optimal est donc de favoriser la compétition entre différents modes d'endommagement. Or, pour une plaque monolithique il n'y a qu'un seul mode d'endommagement. La Figure 8 permet de comparer les performances des solutions optimales calculées précédemment aux performances d'une plaque en acier d'épaisseur t variable. Le panneau sandwich possède de bien meilleures performances pour ces spécifications.

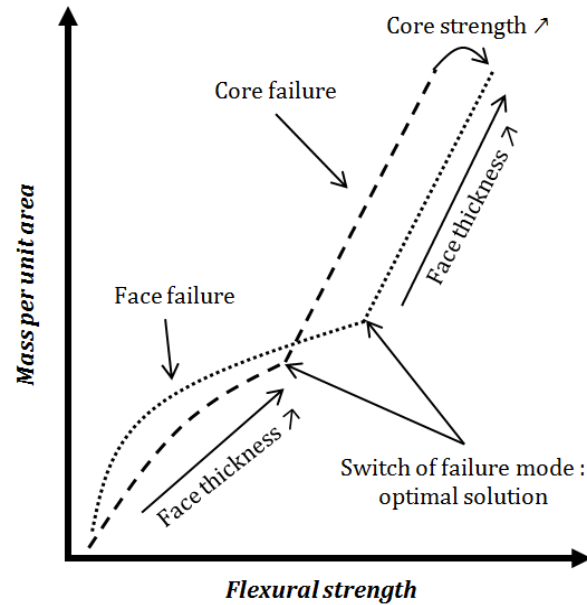


Figure 7 : Illustration de l'évolution des propriétés de résistance en flexion en fonction de la masse surfacique d'un panneau sandwich.

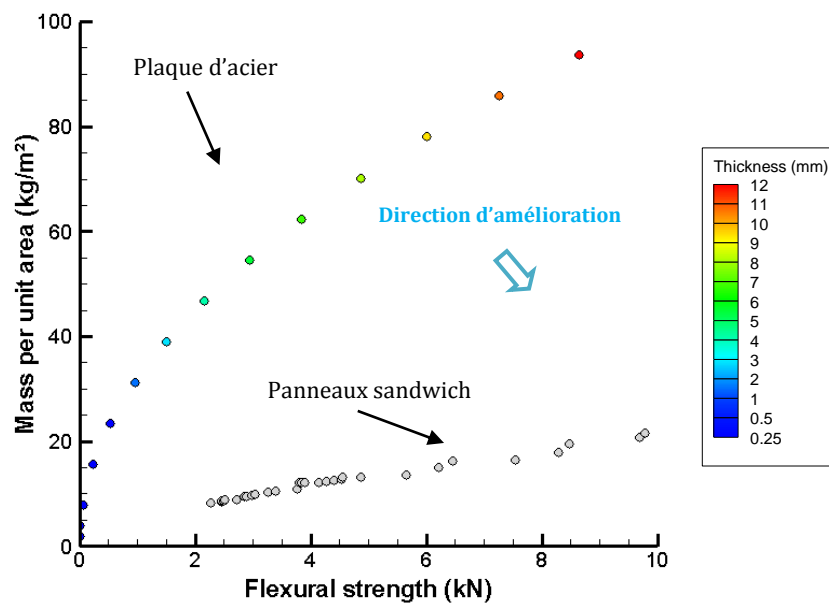


Figure 8 : Comparaison entre les performances optimales de panneaux sandwichs et les performances d'une plaque d'acier. La direction d'amélioration correspond à la direction dans laquelle les deux objectifs désirés, réduction de la masse et augmentation de la résistance, sont améliorés simultanément.

3.3. Synthèse des résultats et conclusions sur l'optimisation par voie « réelle »

Les principaux résultats obtenus en optimisation par voie « réelle » sont synthétisés dans les Tableaux 2 et 3. Dans un premier temps, pour chaque fonction considérée, une optimisation bi-objectif incluant la réduction de la masse a permis d'identifier les solutions optimales selon chaque fonction. En analysant la forme du front de Pareto, la compatibilité entre les performances a aussi pu être identifiée.

Une approche par indice de performance permet dans un certain nombre de cas de prédire correctement les matériaux optimaux. Cette approche est effective pour des spécifications simples et des géométries simples. Cependant, elle peut difficilement prendre en compte des interactions entre variables de conception ou prendre en compte des non-linéarités en terme de réponse de la structure.

De plus, une comparaison systématique entre les performances optimales calculées pour les panneaux sandwichs et les performances d'une plaque d'acier a montré le grand intérêt de ce genre de structures. Il faut toutefois rappeler que pour des raisons d'encombrement, des solutions monolithiques peuvent éventuellement être préférables à des solutions sandwichs. En effet, les sandwichs sont plus efficaces à masse équivalente, mais cela s'effectue au détriment du volume d'encombrement.

Tableau 2 : Synthèse des résultats obtenus en optimisation à masse minimale avec une fonction supplémentaire.

Objectifs	Forme du front de Pareto	Matériau peau optimal	Matériau cœur optimal	Variable la plus influente
<ul style="list-style-type: none"> Rigidité en flexion 	Convexe	Al-60%C	PVC, Glass	<ul style="list-style-type: none"> Matériau cœur Matériau peau
<ul style="list-style-type: none"> Résistance en flexion 	Concave	Al-60%C	PVC	<ul style="list-style-type: none"> Matériau cœur Matériau peau
<ul style="list-style-type: none"> Affaiblissement acoustique 	Convexe	Aucun	Polyuréthane	<ul style="list-style-type: none"> Matériau cœur Epaisseur du cœur
<ul style="list-style-type: none"> Résistance thermique 	Linéaire	Polypropylène	Mélamine, Polyuréthane, Phenolic	<ul style="list-style-type: none"> Matériau cœur
<ul style="list-style-type: none"> Isolation thermique 	Convexe	CMC (C/C)	Graphite	<ul style="list-style-type: none"> Matériau cœur Matériau peau
<ul style="list-style-type: none"> Résistance aux chocs 	Convexe	Al-60%C	Polystyrène, PVC, Polyéthylène	<ul style="list-style-type: none"> Epaisseur du cœur Matériau peau

Dans un deuxième temps, des optimisations tri-objectifs, incluant la réduction de la masse et deux autres fonctions comme objectifs ont permis d'explorer les capacités multifonctionnelles des panneaux sandwichs. Dans ces cas-là, on peut distinguer deux types d'interactions entre les fonctions considérées :

- Un premier type correspond à une compétition entre les performances, comme observé précédemment. Cette compétition peut être avantageuse ou désavantageuse.
- Le deuxième type est caractérisé par une absence de compétition ; dans ce cas il y a soit compatibilité, soit incompatibilité.

En tout, quatre cas de figures peuvent apparaître. Afin d'illustrer ces quatre cas de figures, quatre études de cas représentatives ont été présentées. Les principaux résultats qui en découlent sont synthétisés dans le Tableau 3.

Optimal design of architected sandwich panels for multifunctional properties

Pierre Leite

Tableau 3 : Synthèse des résultats obtenus en optimisation à masse minimale avec deux fonctions supplémentaires.

Objectifs	Compatibilité	Matériau cœur optimal	Variable influençant le compromis
<ul style="list-style-type: none">• Rigidité en flexion• Affaiblissement acoustique	Compétition avantageuse	<ul style="list-style-type: none">• Rigidité : glass• Affaiblissement : PS	<ul style="list-style-type: none">• Epaisseur du cœur• Densité relative du cœur
<ul style="list-style-type: none">• Résistance en flexion• Résistance thermique	Compétition désavantageuse	<ul style="list-style-type: none">• Résistance en flexion : PVC• Résistance thermique : Phenolic	<ul style="list-style-type: none">• Epaisseur du cœur• Densité relative du cœur
<ul style="list-style-type: none">• Résistance aux chocs• Isolation thermique	Compatibilité	<ul style="list-style-type: none">• PS	NA
<ul style="list-style-type: none">• Résistance aux chocs• Affaiblissement acoustique	Incompatibilité	<ul style="list-style-type: none">• Résistance : PS• Affaiblissement : Polyuréthane	<ul style="list-style-type: none">• Matériau cœur

En conclusion, la définition du cœur peut être considérée comme l'étape la plus importante. Le matériau cœur est le paramètre qui influe le plus sur les performances. De plus, pour des propriétés multifonctionnelles, c'est souvent le cœur qui est à l'origine de la compatibilité ou de l'incompatibilité entre les performances. C'est donc sur cette variable de conception qu'il faut accentuer les efforts.

4. Optimisation par voie « virtuelle » : influence de l'architecture du cœur

4.1. Introduction

Dans la partie précédente, on considère un matériau architecturé comme étant un matériau existant possédant ses propriétés effectives et pouvant être rangé dans une base de données. Ici on considère que le matériau architecturé n'est pas une variable discrète, mais une variable semi-continue. Son matériau constitutif est toujours représenté par une variable discrète, mais ses propriétés effectives seront calculées à partir de sa géométrie, définie par des variables continues. On obtient donc une variation continue des propriétés du matériau architecturé à matériau constitutif donné.

Cette approche devient alors tout à fait adaptée pour comparer différentes architectures de cœurs entre elles. Les trois architectures choisies sont les mousses, les nids-d'abeilles et les treillis de poutre tétraédrique. Ces architectures font partie des plus représentatives en tant que matériau d'âme pour un panneau sandwich. La Figure 9 donne un aperçu de ces matériaux.

La mousse est définie de manière géométrique par sa densité relative, qui est le ratio entre le volume de matière contenu dans une cellule unitaire représentative et le volume de cette cellule. Les mousses sont en général stochastiques, dans le sens où la répartition des pores est aléatoire. C'est une structure qualifiée de dominée par des modes de déformation en flexion. En effet, certains auteurs ont montré [DES01a] que les poutres constituant la mousse se déforme en flexion lorsqu'un chargement est appliqué au matériau.

Le nid-d'abeilles est une structure 2D extrudée. Dans le plan, elle est dominée par des modes de déformation en flexion. Cependant, hors-plan, on peut considérer que les parois se déforment en traction/compression. Cette architecture sera considérée comme dominée par des modes de traction. Cela peut se justifier par le fait que souvent lorsque le nid-d'abeilles est intégré dans un sandwich, la direction d'extrusion du nid-d'abeilles (la direction hors-plan) correspond à la direction dans l'épaisseur du sandwich. Cette architecture est décrite par le rapport entre épaisseur de parois et longueur de paroi.

La structure treillis est un matériau qui a fait l'objet de beaucoup d'études ces dernières années. Elle possède l'avantage d'être dominée par des modes de traction. Cette structure est décrite par deux variables géométriques, alors que les deux précédentes ne sont décrites que par une seule variable. Ces variables sont le facteur de forme des poutres (le rapport entre rayon et longueur) et l'angle entre les poutres et le plan horizontal comme le montre la Figure 9.

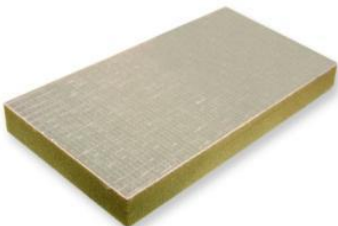

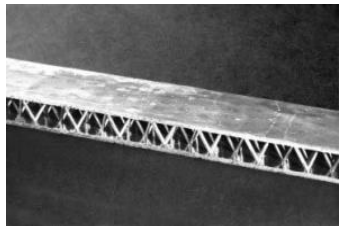
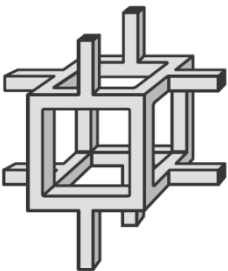
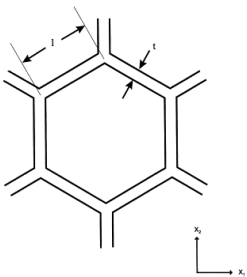
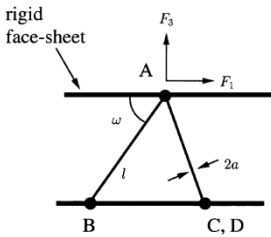
	MOUSSE	NIDS-D'ABEILLES	TREILLIS
ILLUSTRATION			
CELLULE UNITAIRE			
ESPACE DE DESIGN	$\rho^* \in [0,005; 0,4]$	$\frac{t}{l} \in [0,01; 0,2]$	$\omega \in [35^\circ; 75^\circ]$ $\frac{a}{l} \in [0,02; 0,05]$

Figure 9 : Présentation des trois architectures de cœur considérées.

Les études de cas réalisées par voie « réelle » sont ici traitées par voie « virtuelle » afin de comparer les architectures de cœur entre elles et de déterminer, pour chaque architecture quelles sont les designs optimaux. L'étude de cas présentée précédemment est brièvement reprise à titre d'exemple.

4.2. Etude de cas : résistance en flexion à masse minimale

Espace de design :

- Matériaux peaux : Métaux, Polymères et composites.
- Epaisseurs des peaux : de 0,5 à 5 mm.
- Matériaux cœurs : Métaux et Polymères.
- Epaisseur de cœur : de 10 à 200 mm.
- Type de panneaux sandwich : symétriques.

Objectifs :

- Résistance en flexion : maximiser l'effort critique correspondant à l'endommagement d'une poutre sandwich de 1 m soumise à un essai de flexion trois-points.
- Légèreté : minimiser la masse surfacique du panneau.

Contraintes :

- Effort critique > 2 kN.
- Masse surfacique < 50 kg/m².

Comparaison entre architectures

La Figure 10 nous montre les fronts de Pareto obtenus pour les trois architectures de cœur considérées. On constate que les mousses sont largement dominées par les structures dominées par des chargements locaux de type traction/compression.

Les nids-d'abeilles et les treillis ont des performances similaires bien que les premiers soient plus performants aux hautes valeurs de résistance.

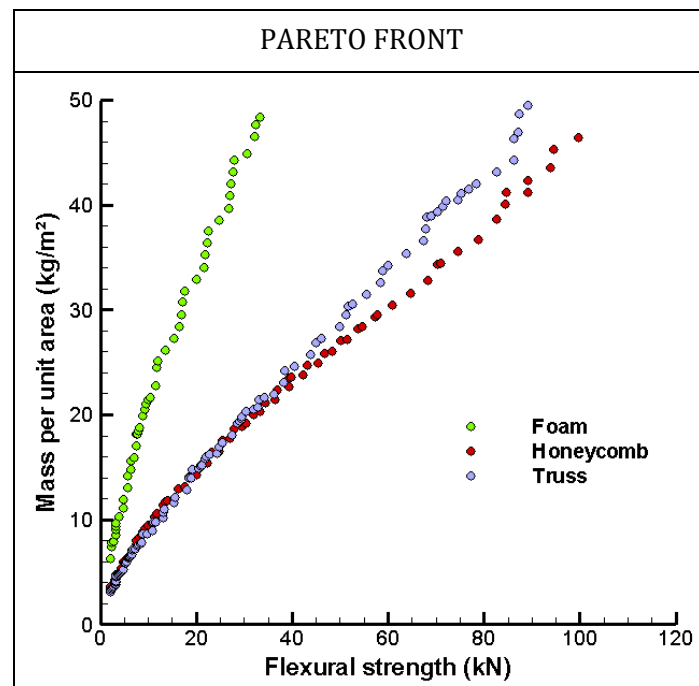


Figure 10 : Fronts de Pareto correspondant aux trois architectures étudiées pour une spécification de résistance à masse minimale.

4.3. Synthèse des résultats et conclusions sur l'optimisation par voie « virtuelle »

L'optimisation par voie « virtuelle » permet de comparer et de classer de manière objective les différentes architectures testées selon les propriétés étudiées. Le Tableau 4 dresse un récapitulatif des résultats obtenus. On peut y observer que selon les fonctions souhaitées, la topologie optimale de cœur varie. Pour l'acoustique par exemple, un cœur souple est préférable, et donc les mousses sont une solution plus adaptée que les autres. Pour des propriétés mécaniques en revanche, les nids-d'abeilles et les treillis sont plus efficaces.

Une approche par indice de performance est possible en utilisant des indices généralisés qui prennent en compte le chargement local dans l'architecture. Les mêmes remarques que dans la partie précédente peuvent être faites.

Tableau 4 : Synthèse des résultats d'optimisation multi-objectifs en considérant une fonction en supplément de la réduction de la masse. Un classement entre architectures est établi pour chaque cas ainsi que le matériau constitutif optimal correspondant. Le type de sollicitations local optimal est aussi indiqué afin de généraliser le résultat. La dernière colonne propose un indice de performance généralisé pour chaque architecture selon la fonction étudiée.

Fonction	Classement	Matériau cœur optimal	Mode de chargement local optimal	IP correspondant
Rigidité	1) Nids-d'abeilles 2) Treillis 3) Mousse	- Cr/Al/Mg - Cr/Al/Mg - Mg	Traction	- E/ρ - E/ρ - $E^{1/2}/\rho$
Résistance en flexion	1) Nids-d'abeilles 2) Treillis 3) Mousse	- Al - Steel/Ti/Al - Al	Traction	- σ/ρ - σ/ρ - $\sigma^{2/3}/\rho$
Affaiblissement acoustique	1) Mousse 2) Treillis 3) Nids-d'abeilles	- MDPE - MDPE - MDPE	Flexion	$1/E$
Résistance thermique	NA	PP/PS	NA	$1/k\rho$
Isolation thermique	1) Treillis 2) Mousse 3) Nids-d'abeilles	- UMC0-50 - UMC0-50 - IN-100 - UMC0-50	Traction	$1/a\rho$
Résistance aux chocs	1) Treillis 2) Nids-d'abeilles 3) Mousse	- Mg - Mg - Al	Traction	-

Tous les cas traités en optimisation par voie « réelle » l'ont aussi été par voie « virtuelle ». De manière générale, la forme du front de Pareto ne dépend pas de l'architecture de cœur.

En ce qui concerne les propriétés multifonctionnelles, une synthèse des résultats est donnée dans le Tableau 5. On constate que les treillis peuvent presque être considérés comme la meilleure architecture. Ceci est en partie dû à la description adoptée. En effet, deux variables géométriques permettent de décrire le treillis, en l'occurrence le facteur de forme des poutres et l'angle entre les poutres et les peaux. Cet angle permet de passer de manière continue d'une

Optimal design of architected sandwich panels for multifunctional properties

Pierre Leite

structure très rigide, lorsque les poutres sont orientées dans l'épaisseur, à une structure très souple, lorsque les poutres sont quasiment dans le plan du sandwich. Cette souplesse dans la conception permet d'obtenir des propriétés multifonctionnelles exceptionnelles.

Tableau 5 : Synthèse des résultats d'optimisation multi-objectifs en considérant deux fonctions en supplément de la réduction de la masse. Un classement entre architectures est établi pour chaque cas. Et le matériau constitutif optimal correspondant est donné dans la dernière colonne.

Fonctions	Classement	Matériau cœur optimal
<i>Rigidité et affaiblissement acoustique</i>	1) Treillis Rigidité → Nids-d'abeilles Acoustique → Mousse	- Ni/Cu/PS - Mo/PC/PBT - Mg
<i>Résistance en flexion et résistance thermique</i>	1) Nids-d'abeilles 2) Treillis 3) Mousse	- PMMA/PS - Ti/PMMA/PS - PMMA
<i>Isolation thermique et résistance aux chocs</i>	1) Treillis Isolation thermique → Mousse Chocs → Nids-d'abeilles	- UMC0-50/IN-100 - IN-100/Inco713/MAR-M200 - UMC0-50/IN-100
<i>Affaiblissement acoustique et résistance aux chocs</i>	1) Treillis Acoustique → Mousse Chocs → Nids-d'abeilles	- MDPE/PS/Mg - MDPE/Al - Mg/Al

Il est possible de comparer les résultats obtenus par voie « réelle » et « virtuelle » pour les sandwichs avec un cœur en mousse. On constate alors que l'on ne retrouve pas les mêmes résultats. Il y a deux raisons à cela :

- La base de données utilisée pour l'optimisation par voie « réelle » ne contient que des mousses existantes et dont les propriétés ont été mesurées. Il est donc tout-à-fait possible de créer des mousses par voie « virtuelle » avec des matériaux qui ne possèdent aucun équivalent dans la base de données réelle.
- La base de données utilisée pour créer virtuellement les mousses ne contient pas tous les matériaux imaginables. Notamment, des matériaux comme la mélamine ou le phénol (base de la mousse phénolique), ne sont pas toujours considérés comme des matériaux au sens structural du terme. Il est donc possible de trouver des mousses « réelles » possédant des propriétés exceptionnelles que l'on ne pourra pas créer de manière virtuelle.

Cependant, les matériaux qui n'ont pas été considérés pour l'optimisation par voie « virtuelle » correspondent à des matériaux qui sont difficilement usinables sous forme de poutre ou de nids-d'abeilles. Afin de permettre une comparaison objective entre les architectures, ces matériaux ont donc été écartés de la base de données.

5. Méthodes mixtes

La méthode de conception utilisée jusqu'à présent permet une optimisation globale en prenant en compte plusieurs objectifs et contraintes. De plus, les variables de conception sont constituées de variables discrètes (les matériaux) et de variables continues (géométrie). Il s'agit

du cas le plus complexe en optimisation. La résolution de ce type de problème nécessite un grand nombre d'évaluation, i.e. un grand nombre de calculs des performances. Or, pour des problématiques industrielles, il est souhaitable d'utiliser des modèles d'analyse qui soient précis et prédictifs. Il en découle une éventuelle incompatibilité entre la complexité de l'analyse et la complexité de l'optimisation pour des raisons de temps de calculs (voir Figure 11).

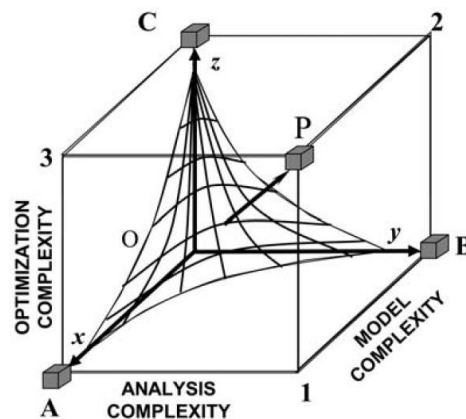


Figure 11 : Venkataraman et Haftka représente les interactions entre complexité d'optimisation, d'analyse et de modèle. Pour des raisons de limites de puissance de calcul, il est impossible de résoudre un problème possédant une complexité maximale selon les trois axes. Afin d'augmenter la complexité de l'une de ces parties, il convient de réduire la complexité des deux autres. Illustration tirée de [VEN04].

Afin de réduire le nombre d'évaluations, plusieurs pistes peuvent être explorées. Ici nous proposons d'explorer deux pistes inspirées des principes classique de sélection de matériaux.

La première approche consiste à tirer profit de la structure de l'espace de design en termes de matériaux. En effet, les bases de données sont souvent conçues sous forme d'arborescence. Les matériaux sont rangés par famille, classe et sous-classe. De manière classique en conception, la sélection de matériaux s'effectue de manière incrémentale. Dans un premier temps, on sélectionne la famille, puis la classe, la sous-classe et finalement le matériau adéquat. Cet état d'esprit est reproduit ici en couplant une démarche dite de « séparation & moyennage » avec l'algorithme génétique.

La nouvelle démarche se décompose comme suit et est illustré en Figure 12 :

- Dans un premier temps, un représentant de chaque famille de matériaux est créé en lui attribuant la moyenne des propriétés de tous les matériaux compris dans cette famille. Une nouvelle base de données est donc créée.
- Dans une deuxième étape, on effectue une optimisation classique en se servant de la nouvelle base de données.
- On détermine sur le front de Pareto les familles qui ne sont pas prometteuses, i.e. les familles qui ne sont pas sur le front de Pareto.
- Finalement on élimine de l'espace de recherche tous les matériaux appartenant aux familles jugées non prometteuses. On reprend ces étapes pour les classes et sous-classes jusqu'à une base de données réduite contenant de véritables matériaux.

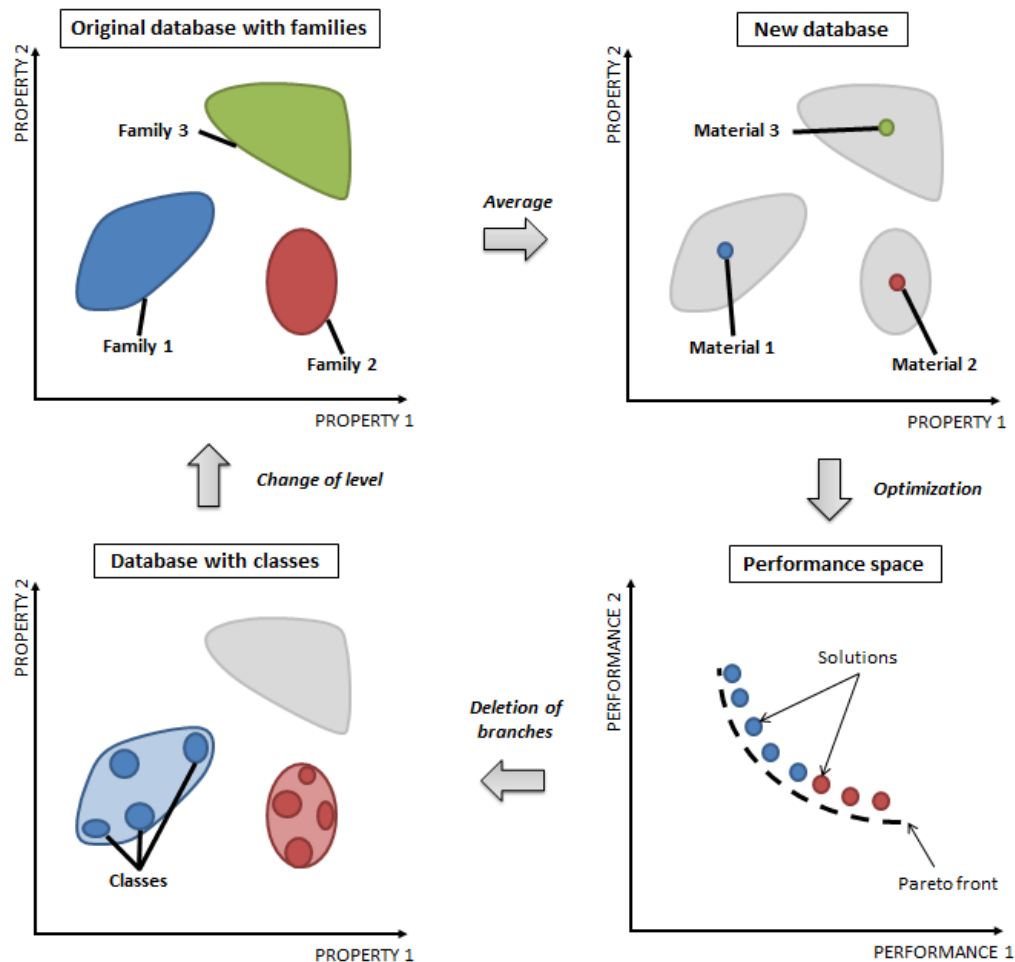


Figure 12 : Fonctionnement de la méthode mixte. Première étape : moyennage des familles de matériaux afin de les représenter par un seul candidat. Deuxième étape : optimisation en se servant d'une base de données alimentée par les candidats générés dans l'étape précédente. Troisième étape : détermination des familles à supprimer de l'espace de recherche. Quatrième étape : suppression des familles non-prometteuses et passage au niveau inférieur (classes, sous-classes puis membres).

Cette approche a été testée sur deux cas d'optimisation multi-objectif. Le premier est principalement limité par la sélection de matériaux cœur dans le sens où l'espace des solutions faisables est très restreint. L'algorithme génétique classique doit donc déployer un certain effort pour la localiser. En utilisant la nouvelle méthode mixte, la localisation de la zone correspondant aux solutions réalisables est beaucoup plus rapide. Ainsi, une réduction de 80% du nombre de calculs a été enregistrée pour ce cas avec une restitution du front de Pareto qui est excellente comme le montre la Figure 13.

Le deuxième cas est beaucoup plus complexe car il est multimodal. En effet, selon les matériaux sélectionnés, les interactions entre les performances sont différentes. Lors des différentes étapes de séparation et d'élimination, une partie entière de l'espace des performances a été perdue comme le montre la Figure 14. En revanche, le reste de l'espace des performances, qui en constitue la majeure partie, est parfaitement restituée et avec une réduction du nombre de calculs de 66%. On peut donc en déduire que l'algorithme est tombé dans un optimum local.

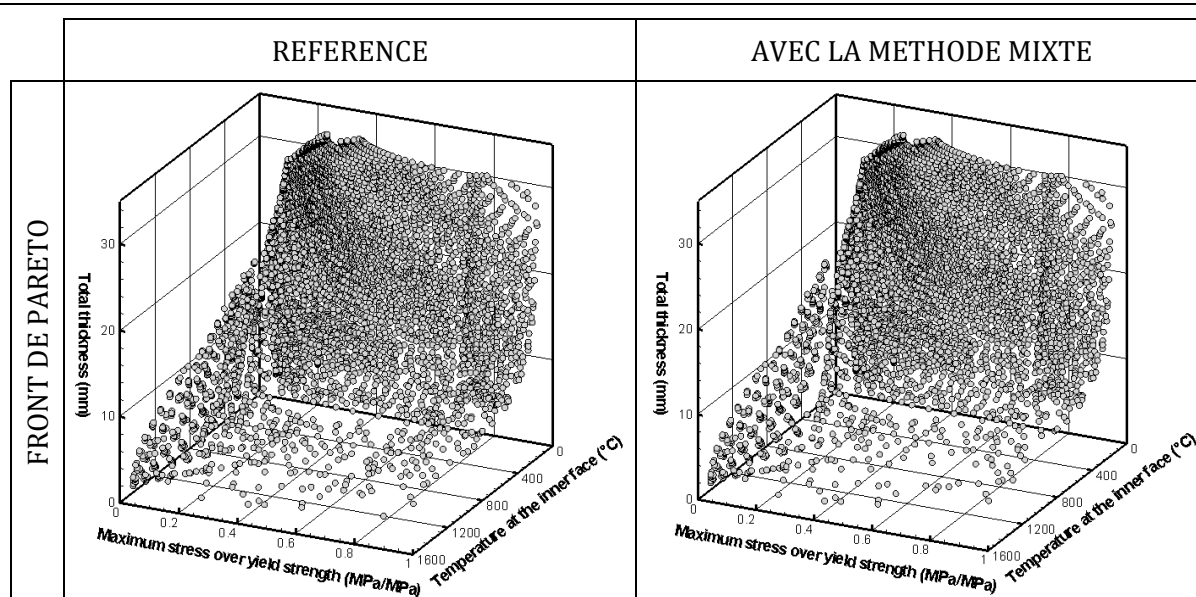


Figure 13 : Comparaison entre le front de Pareto de référence et celui obtenu en utilisant une approche couplant algorithme génétique et « séparation & moyennage ». Les deux fronts sont semblables.

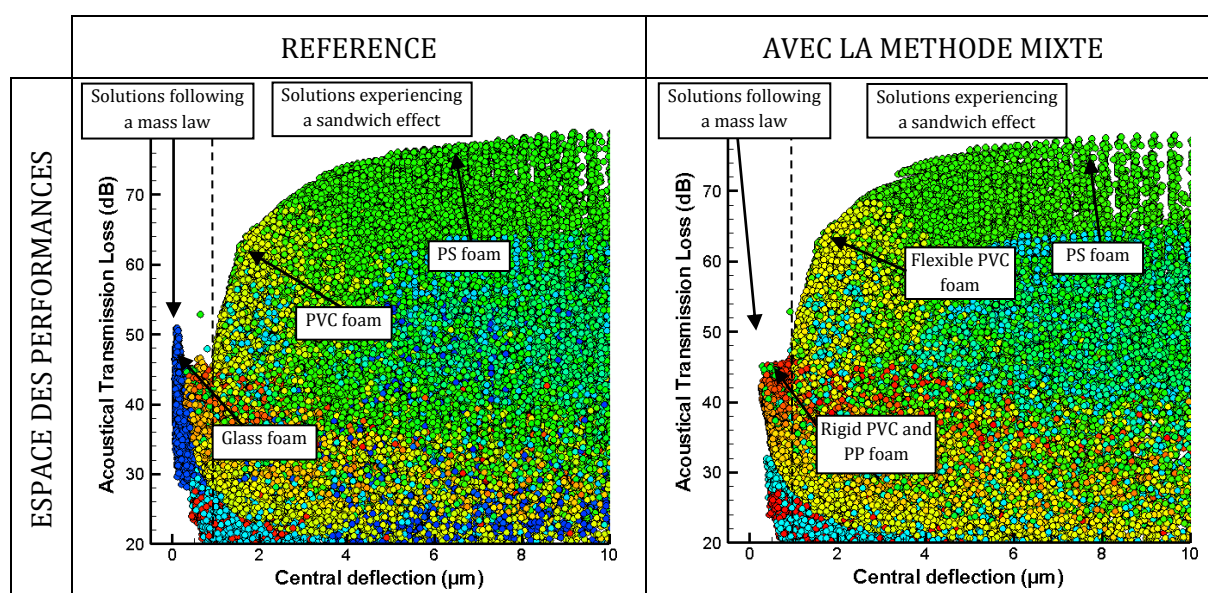


Figure 14 : Comparaison entre l'espace des performances du cas de référence et celui obtenu avec la méthode mixte. L'espace peut être divisé en deux parties, correspondant à deux comportements acoustiques différents. La démarche de « séparation & moyennage » aboutit à la suppression d'une partie de l'espace de recherche qui est pourtant optimal dans une petite gamme de performance. Sur le reste de l'espace, la méthode fonctionne correctement.

La deuxième méthode s'inspire des travaux de Castillo et al. et utilise une approche de type plans d'expériences pour créer un indice de performance approché qui vient se substituer à un calcul numérique plus complexe [CAS09]. L'idée est de transférer les efforts de calculs dans l'établissement d'un modèle analytique simple ne faisant intervenir que des propriétés matériaux et des variables géométriques, ceci afin d'effectuer la sélection de matériaux directement sur la base de données.

Cette démarche a été testée sur le cas multimodal présenté ci-dessus. Dans ce cas, deux modèles approchés ont été utilisés afin de restituer avec un maximum de fidélité l'aspect de

Optimal design of architected sandwich panels for multifunctional properties

Pierre Leite

l'espace des performances. Le plan d'expériences a permis de créer un modèle approché de prédiction du taux d'affaiblissement acoustique, qui est l'une des performances recherchées, en effectuant uniquement 90 calculs. Un deuxième modèle se base sur une loi tirée de la littérature, appelée la loi de masse.

On constate sur la Figure 15 que la zone correspondant au modèle généré par le plan d'expérience est relativement fidèle au cas de référence. La loi utilisée pour restituer le reste de l'espace des performances aboutit à des résultats erronés et doit donc être revue. Compte tenu de l'effort de calcul déployé, le résultat est très satisfaisant pour le modèle généré par le plan d'expérience.

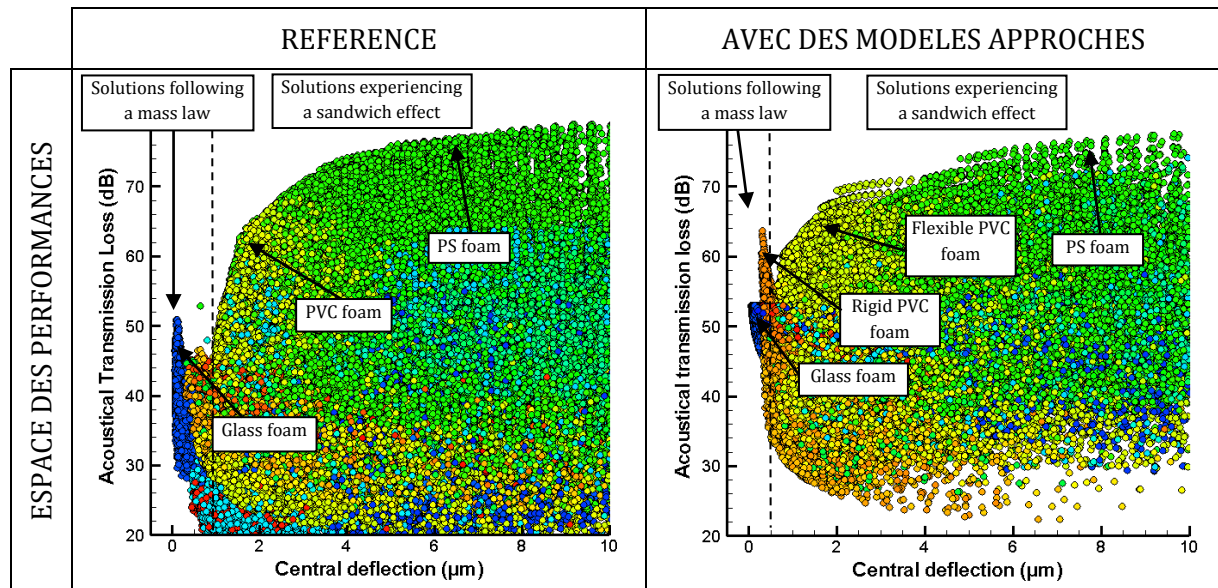


Figure 15 : Comparaison entre les espaces des performances obtenus avec les modèles d'analyse exacts et avec les modèles approchés. L'espace peut être divisé en deux parties, correspondant à deux comportements acoustiques différents. Le plan d'expérience a permis de créer le modèle approché sensé rendre compte des performances observées dans la partie droite de l'espace des performances. Dans cette partie, la restitution de l'information est très satisfaisante. Dans l'autre partie, les solutions optimales sont erronées. La loi utilisée pour évaluer ces solutions doit être révisée.

6. Conclusion

Cette thèse a eu pour objectif d'étudier l'optimisation de panneaux sandwichs architecturés pour des propriétés multifonctionnelles.

Une première approche, qualifiée d'optimisation par voie « réelle » est basée sur une description des matériaux par une variable discrète faisant référence à un matériau « existant » dans une base de données. Des modèles simples ont permis d'évaluer les propriétés de panneaux sandwich avec un cœur en mousse. Un algorithme génétique est utilisé afin de déterminer les solutions optimales.

A partir de la forme des fronts de Pareto, plusieurs situations typiques ont été mises en évidence dans la conception de panneaux sandwichs à masse minimale en considérant une fonction supplémentaire :

- Un front concave correspond à une compétition désavantageuse entre performances.
- Un front linéaire correspond à une proportionnalité.
- Un front convexe, le plus recherché, correspond à une compétition avantageuse.

A travers une approche d'optimisation multi-objectifs, nous avons aussi étudié des cas pour lesquels on considère la réduction de la masse et deux autres fonctions comme objectifs. Dans ces cas, les interactions entre les deux fonctions peuvent être rangées en deux catégories :

- Il existe une compétition entre les performances, dans ce cas on retombe sur les situations décrites précédemment.
- Il n'y a pas de compétition, et alors les performances sont soit compatibles, soit incompatibles.

On a pu constater à travers les différentes études de cas que le matériau cœur est le paramètre le plus influent. La capacité d'un panneau sandwich à développer des propriétés multifonctionnelles vient la plupart du temps des propriétés du matériau cœur. Pour cette raison, la méthode d'optimisation a évolué afin d'adopter une description semi-continue du cœur permettant plus de souplesse de conception et une comparaison directe entre différentes architectures. Cette approche est appelée optimisation par voie « virtuelle ».

Un changement d'architecture de cœur ne modifie pas les interactions entre performances mais a un impact conséquent sur les performances. A travers les trois architectures étudiées, que sont la mousse, le nid-d'abeilles et la structure treillis, on a pu comparer les performances selon les modes de chargements locaux. En effet, la mousse est une architecture dominée par des modes de déformation en flexion tandis que les deux autres peuvent être apparentées à des architectures dominées par des modes de déformation en traction. Ces dernières possèdent des propriétés mécaniques supérieures à celle des mousses à matériau et masse donnés.

Toutefois, dans le cas de spécifications multifonctionnelles, il est possible de trouver un front de Pareto global peuplé à la fois des deux types d'architectures. Ce sera notamment le cas lorsque l'une des spécifications requiert un cœur souple tandis que l'autre requiert un cœur rigide.

Dans ce genre de situations, la structure treillis offre un avantage considérable. En effet, elle possède une souplesse de conception qui permet de passer de manière continue d'une structure souple à une structure rigide. La rigidité optimale peut donc être adaptée aux spécifications recherchées via l'angle entre les poutres et le plan du panneau.

Concernant la précision de la méthode, il est évident qu'elle dépend de la capacité de l'algorithme d'optimisation à trouver l'optimum global mais aussi de la précision des outils d'analyse utilisés pour évaluer les solutions. Au cours de cette thèse, des modèles simples et pratiques ont été utilisés. Ce sont des modèles dédiés aux panneaux sandwichs qui permettent un pré-dimensionnement et un classement entre solutions. Toutefois, dans un problème industriel, il est souhaitable que les modèles employés soient prédictifs. Les modèles prédictifs sont généralement coûteux en temps de calculs. Il y a donc une incompatibilité entre la volonté d'effectuer une optimisation complexe (car globale, multi-objectifs et sur des variables mixtes) et celle d'utiliser des modèles complexes.

Dans l'optique de lever cette incompatibilité, deux approches ont été présentées :

- Une méthode de type « séparation & moyennage » couplée à l'algorithme génétique permet de supprimer une plus ou moins grande partie de l'espace recherche tout en restant multi-objectifs. Cependant, il y a un risque de se retrouver dans un optimum local comme cela a été montré précédemment.

- Une deuxième méthode s'appuie sur le principe des indices de performances. En utilisant un modèle approché, on peut relier les propriétés matériaux et géométriques à la performance recherchée. Pour cela, les plans d'expériences offrent un outil intéressant car ils permettent de déterminer les effets et interactions entre paramètres (ou facteurs) et permettent également de créer un modèle polynômial approché [CAS09]. Un exemple traité dans cette thèse montre l'intérêt mais aussi les inconvénients d'une telle méthode. En effet, le modèle approché doit être suffisamment élaboré pour restituer correctement le comportement d'un panneau sandwich sur tout l'espace de recherche.

En conclusion, l'optimisation par voie « réelle » est une approche pratique pour des problématiques industrielles, aboutissant à une solution constituée de matériaux existants. Cette approche permet à la fois une sélection de matériaux et un pré-dimensionnement.

L'optimisation par voie « virtuelle » permet quant à elle d'explorer de nouvelles voies de conception du point de vue du chercheur en mettant en évidence les interactions entre géométrie et matériau constitutif. Cette démarche permet une comparaison objective entre architecture et d'une manière générale, elle donne la possibilité d'étudier les différentes situations multifonctionnelles des matériaux architecturés.

Chapter 1

General introduction

This introduction aims at presenting the context of this study and the addressed problematic. It also gives a brief introduction of the MANSART project which includes the present work. Finally, the outline of the present thesis is developed.

Optimal design of architected sandwich panels for multifunctional properties

Pierre Leite

Chapter content

1. Context.....	37
2. MANSART project (architected sandwich materials).....	40
3. Scope of the present study	41

1. Context

In a product life time, the design step is crucial. It comes right after the specification step, in which the functions of the product are specified. It is through the design that the product can complete its function and it is through the design that one can guess a product function. Practically, the design step consists of translating the functions/specifications into a detailed description of the product. It should answer the questions: What does it made of? What are the dimensions? How do I manufacture it? And so on. This can be illustrated by interactions between the function of the product and the three main parts of the design as shown in Figure 1.1: material, shape and process.

Consistent efforts have been made by engineers to rationalize the design process. Different techniques have been developed to answer the questions raised during the design step according to the specifications. One of the main issues that have been addressed these past decades is how to choose the right material which has led to the creation of a specific field: material selection.

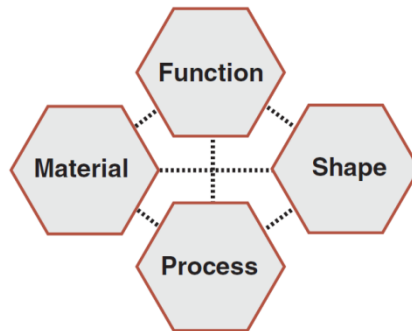


Figure 1.1: Interaction between function, material, shape and process. Function is the main identity of a product. Material and shape should be determined in order to help the product completing its function. Process should be compatible with material and shape and can have a significant role in product functionality.

Material selection techniques have been extensively studied, developed and exposed by Pr. Ashby in a series of books and papers [ASH89, ASH99, ASH00a, SIR04, SIR06, ASH07]. The main idea is to use performance indices in order to evaluate and rank the materials from the most promising to the less promising. A performance index is an analytical expression involving materials properties that can measure the performance of a material for a given objective, prescribed constraints and preselected loading mode and geometry. This method, when combined with a material database, is really efficient in guiding the choice of the decision-maker. However, deriving analytical expressions which involve materials properties can only be achieved for simple geometries and simple loadings.

These methods can be displayed graphically using property charts as the one presented in Figure 1.2 [ASH11]. In this chart, materials are plotted as a function of their Young's modulus and density. The performance indices are transformed into guidelines used to determine the optimal material for minimum mass design.

While design techniques have been improved, materials science has been pushed forward to provide more and more efficient materials. This trend is motivated by the desire to integrate consistently more functions at the material scale rather than integrate all of them at the shape

Optimal design of architected sandwich panels for multifunctional properties

Pierre Leite

scale. This would avoid complex geometries which are difficult and expensive to manufacture. This desire is translated into materials requirements that are pushed towards more multifunctionalities. But, there are “holes” in some regions of the materials properties space. These “holes” usually represent regions in which having a solution would be an improvement of multifunctional properties. Then, it becomes interesting to try filling the “holes” of the material space as shown in Figure 1.2.

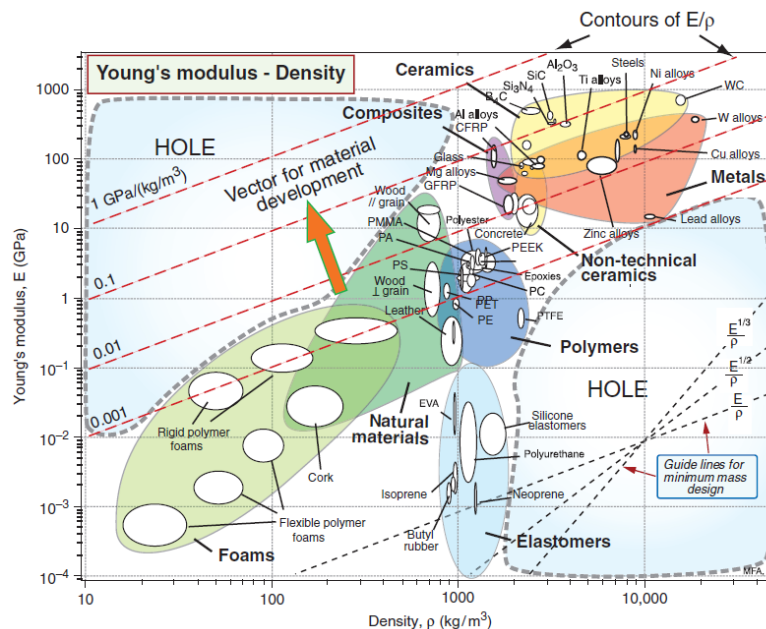


Figure 1.2: Property chart plotting materials as a function of their Young's modulus and density. Guide lines corresponding to performance indices are drawn in order to identify the optimal material regarding stiffness specifications at minimal weight. “Holes” are observed in some regions of the property chart. It is desirable to fill these “holes” in order to obtain better performances. Figure taken from [ASH11].

It seems obvious that classical materials science, such as by new alloy development or novel processing routes, will be able to fill some of the holes, but only in a very limited manner. Metallurgical optimization is not sufficient to get out of monolithic materials boundaries. In the past decades, extensive efforts have been made to integrate an intermediate design scale between the microstructure scale which is the research field of metallurgists and the macroscopic scale which is the research field of mechanics and structure engineers. This length scale is the one of architected materials as defined by Bréchet and Embury and illustrated in Figure 1.3 [BRE13, BOU08]. Using this new design scale, a great range of opportunities has been opened in terms of performances by designing new kinds of materials.

Since the sixties, sandwich structures have been studied, manufactured and used as structural parts. In this context, a sandwich structure is usually composed of two thin and stiff face sheets and a thick low-density core as shown in Figure 1.4. This structure has become the common lightweight panel solution. One of the first striking designs was a balsa wood core with plywood faces. This structure was used for the “de Havilland Mosquito”, an aircraft that flew during World War II [DAV01]. Since then, sandwich constructions have been optimized and were part of the success of the Apollo campaign to land a spaceship on the moon. Metal face sheets with a honeycomb core was used to provide lightweight panels with sufficient strength to

tolerate the applied stresses due to acceleration and landing [DAV01]. Most of sandwich constructions are made of architected cores, such as honeycombs and foams. These structures are found in a wide range of applications [BAN08]. They can be used in very demanding applications such as aerospace and naval constructions for which high performances are sought [DAN09]. They can be observed in building trade for their multifunctional possibilities and their relatively low cost.

This evolution on sandwich constructions has been made possible by the evolution of the constitutive materials. The great number of possible combinations of materials and geometries in the design of a sandwich structure can give access to a new range of multifunctional properties.

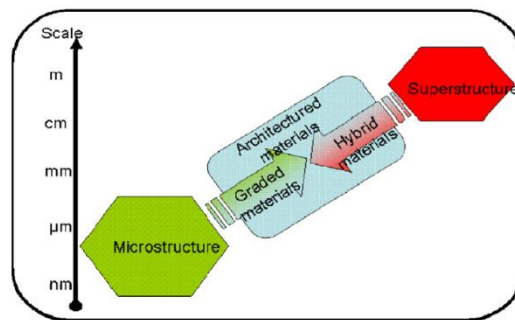


Figure 1.3: The design length scale of an architected material is between the scale of microstructure and the one of superstructure. Architected materials are materials, possibly multi-materials arranged in a particular shape and with a design length scale close to the one of the component being designed. Designing them requires then design methods from both micro and macro scales. Figure taken from [BRE13].

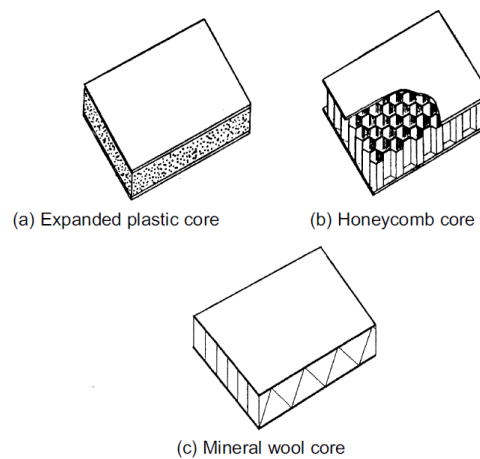


Figure 1.4: Examples of structural sandwich panels made of different core materials.

Sandwich panels are commonly used for their strong flexural properties, for instance stiffness and strength, at minimal weight. But they can also be advantageously used for functional applications. One of the main functional applications of concern is thermal insulation. By integrating porous core material, a sandwich panel possesses a low thermal conductivity, which is desirable in some applications (building trades, refrigerated trunks). Furthermore, several work showed that their acoustic damping properties can be very interesting for some applications [DYM74, SIM95, WAN09]. In building trades, Phenolic foam can be used as core material for both thermal insulation and acoustic damping. Another promising application that has seen sandwich panels as emerging solution is impact mitigation. The usual high resistant

Optimal design of architected sandwich panels for multifunctional properties

Pierre Leite

monolithic solutions can be replaced by lighter sandwich solutions which deform by core crushing to dissipate the incoming energy.

The breakthrough of architected materials and sandwich structures raised a major question about dedicated design methods. Indeed, the classical design method based on material selection techniques and on geometrical optimization is mainly dedicated to the design of monolithic solutions for which simple loadings are considered.

Every design method is based on an optimization principle. Material selection techniques using performance indices to rank the possible solutions are based on the enumeration principle. Every possibility is considered, evaluated and ranked. Enumeration is in general a very expensive method in terms of computational cost. For instance, considering sandwich structures defined by the combination of two materials, face and core, the number of possibilities rapidly reaches several billions, which might be not compatible with computing time. Moreover, if the analysis tool used to evaluate the solutions is not based on analytical expressions but on numerical simulations, the calculation time should further increase, thus leading to a prohibitive computational cost.

An optimization method was used for the design of laminate materials based on evolutionary algorithms [LeR95]. This is a particular case where the material is considered as defined by the ply orientation and the material properties of the fibres. In the present work, we have adapted this approach to sandwich structures.

However, including material selection in the optimization process remains sparse in the literature, at least in the way intended by material selection techniques. In order to keep all possibilities open, we have to implement an efficient optimization algorithm.

Therefore, a new design process for architected sandwich panels which considers both material selection and geometrical design is needed. This design process should be able to deal with multiple criteria, as the main advantage of a sandwich panel is its multifunctional properties. The present work, which was part of the MANSART project, aims at providing a design process adapted to the case of architected sandwich panels. This design process is used to explore the functional possibilities of sandwich panels regarding common specifications: flexural stiffness and strength, Acoustical Transmission Loss, thermal resistance and insulation and finally blast resistance.

The first approach that can be considered is to optimise the solutions in regard to a closed database which is the classical method. The idea is to select among the existing material the best one. A natural evolution of the method would be to open the database and to pass from a discrete set of materials to a semi-continuous one. In this case, the material is no more selected, it is created on purpose. Evaluating such solutions requires accurate models that can be expensive in terms of computing time. This cost can be prohibitive if coupled with a complex optimization process. In order to eliminate the incompatibility between analysis and optimization complexity, mixed methods could then be required.

2. MANSART project (architected sandwich materials)

The MANSART project is dedicated to the study of architected sandwich materials for a wide range of aeronautical and terrestrial applications. This project was funded by the French National Research Agency ANR (Agence Nationale de la Recherche) and ran for 4 years from

January 2009 to January 2013. This project gathered 4 industrial partners: Airbus, EADS-IW, Ateca and SMCI; and 7 academic partners: SIMaP/Grenoble-INP, CdM/Mines-ParisTech, MATEIS/INSA-Lyon, GEMTEX/ENSAIT, ICA/ISAE, CIRIMAT/ENSIACET together with ONERA as the coordinator.

The considered work has been divided into 5 work packages: specification, elaboration, characterization, modelling and optimization. The present work is encompassed in the last work package dealing with optimization. Based on specifications given by the industrial partners, a “materials-by-design” approach has been set in order to develop new design techniques and to propose innovative architected solutions. The applications were mainly focused on crashworthiness and mechanical properties of layered structures. In addition, thermal and acoustic requirements were occasionally issued.

The project included Ph.D. work on several topics:

- Para-aramid non-woven and porous composite structures for acoustic absorption and impact (Ph.D. work of Marion Amiot at GEMTEX) [AMI12].
- Fibrous reticulated networks for sandwich panels (Ph.D. work of Laurent Mezeix at CIRIMAT) [MEZ10].
- Sandwich structures for impact loadings (Ph.D. work of Amélie Kolopp at ICA) [KOL12].
- Homogenization methods for predicting the effective properties of architected materials, including negative Poisson’s ratio structures (Ph.D. work of Justin Dirrenberger at CdM) [DIR12b].
- Monofilament entangled materials (Ph.D. work of Loïc Courtois at MATEIS) [COU12].
- Fragmented interlocking materials for damage tolerance (Ph.D. work of Magali Dugué at SIMaP) [DUG13].
- Optimal design of sandwich structures for multifunctional applications (the present work).

3. Scope of the present study

The aim of this study is to develop and explore the possibilities of a design process dedicated to architected sandwich panels for multifunctional properties.

First, following the introduction in Chapter 1, a literature review is provided in **Chapter 2**. Materials selection techniques based on the performance index principle and its evolutions over the last decades are presented. If this method is perfectly suited for classical situations, it is not so well adapted to the design of multi-materials and of architected materials.

As we are looking for multifunctional properties, architected materials as core members in sandwich panels constitute the basis of this work. A brief overview of actual architected materials is then given as example. Only three representative architectures will be considered for the case studies. The specific properties that can be expected for sandwich panels made of architected cores are also described.

Finally, different optimization methods are introduced. First, common mono-objective optimization is presented. Then, multi-objective optimization is explained leading to the Pareto set approach. The most common optimization algorithms are indicated, and their advantages/drawbacks are discussed. A comparison between these algorithms helped emphasize that the best choice for the design process is a genetic algorithm. The specificities of this algorithm are documented at the end of Chapter 2.

The established design process is presented in **Chapter 3**. A genetic algorithm is used, coupled with a material database to determine the optimal solutions. An analysis step is comprised in the process in order to compute the performances of the solutions from the definition of material and geometrical variables. An architected material can be described in different manners. From a macroscopic point of view, it can be considered as a material with its effective properties similar to other materials. From a point of view related to its architecture, it can be considered as a particular architecture made of a particular material. Then the effective properties of the architected material are evaluated from both the geometry and the material.

Using this design process, sandwich panels can be optimized following two different paths which will be explored in Chapters 4 and 5. Considering the sandwich panel as a superposition of three materials referenced in the database, the design at the level of the sandwich structure is explored. In **Chapter 4**, the optimal design of foam core sandwich panels is studied considering the foam materials in the database.

The main challenge is to figure out if, by designing a sandwich panel, it is possible to develop multifunctional properties and what is the nature of the interactions between properties. Different scenarios are considered here. Properties can be compatible in the sense that the design guides to improve the properties is common to the two considered specifications. On the other hand, contradictory guide lines between the properties lead to an incompatibility in the sense that the solutions will be split into two groups. One group will gather solutions that have good properties regarding the first objective but poor ones regarding the second objective. The second group will gather solutions with good performances regarding the second objective but being inefficient for the first objective. The intermediate case, which is one of the most common, is when a competition occurs between the different design requirements. In this case, improving one property leads to a reduction of the other one. In some instances, this competition can be interesting depending on the relative loss performance compared to the gain on the other one.

In addition to the nature of the interactions between the specifications, the optimal design in terms of material and geometry is provided for each case study. A comparison between the performances of sandwich solutions and the ones of monolithic plates is given in order to emphasize the possible advantage of sandwich panels.

In **Chapter 5**, the influence of the nature of core architecture is assessed. A design process similar to the one of Chapter 4 is used. The main change lies in the core material description. This part of the panel is no longer considered as a classic material but as a structure. Then, its effective properties are calculated using scaling laws. These laws are analytical expressions that give the effective properties of the architected materials from its constitutive material together with its geometry. Using this approach, a comparison between different types of architectures is possible. Each case study treated in Chapter 4, is once again treated in Chapter 5 in order to compare and rank the core architectures regarding their fitness for the specifications.

The purpose of **Chapter 6** is to provide a brief sight of the possible ways to improve the design process. A general introduction on the value of mixed method emphasizes the needs of advanced methods by enlightening the drawbacks of the genetic algorithm used for the optimization process. Two different mixed methods are presented and tested.

The last Chapter, **Chapter 7**, gives an overview of the principal results presented in this work and, hopefully, this can be a springboard to future work on the topic of designing architected sandwich panels.

Chapter 2

Literature review

This literature review starts by presenting the principles of material selection techniques based on performance indices and its evolutions. The class of architected materials is introduced as well as the most common architected materials. A specific attention is brought to sandwich panels which are the object of this work. The last section is dedicated to optimization methods, presenting the specificities of multi-objective optimization and a set of familiar algorithms, with in particular genetic algorithms.

Chapter contents

1. Materials selection.....	47
1.1. Principles	47
1.2. Multi-criteria material selection.....	48
1.3. Mixed mode index.....	50
1.4. Determination of performance index by coupling DOE and FEM.....	51
2. Introduction to architected materials.....	51
2.1. Definition and objectives of architected materials	52
2.2. Maxwell's stability criterion	52
2.3. Overview of architected materials.....	53
3. Sandwich panels.....	59
3.1. Introduction	59
3.2. Mechanical properties	60
3.3. Thermal properties	63
3.4. Acoustical properties	66
3.5. Blast mitigation properties.....	67
4. Presentation of multi-objective optimization methods.....	68
4.1. Generalities.....	68
4.2. Multi-objective optimization	70
4.3. Optimization algorithms	73
4.3.1. Deterministic algorithms	73
4.3.2. Stochastic algorithms	74
4.3.3. Comparison between the two types of algorithm.....	75
4.4. Genetic algorithm.....	76

1. Materials selection

In this first part several investigations on materials selection techniques are presented. A short presentation of the performance index method and of its evolution is given, and its range of applicability and limits are discussed.

1.1. Principles

A component in an industrial device is defined by its function which imposes its shape and constitutive material. Material and process selection is a crucial step of the part conception. This selection is not easy as the number of materials available to the engineer lies between 40 000 and 80 000 [ASH99]. A systematic materials selection method was developed in the 1990's by M.F. Ashby based on the principle of the performance indices [ASH89, ASH99]⁵. This method mainly addresses structural parts conception for which the required specifications are mechanical properties at minimal weight, minimal cost, minimal volume and so on.

The principle of a performance index is to find out an analytical expression allowing the evaluation of the materials performance in order to compare them for a given set of constraints/objectives. This expression is obtained by derivation of the equations describing the performances of the component for a given problem, which involves several intrinsic properties of the materials. For that purpose, external loads are considered as known data whereas geometrical parameters are either fixed or free variable. Let us illustrate this by a simple and classical example, i.e. a beam in bending. The problem is to find the material that will have the lowest mass for a given flexural stiffness. The length of the beam is noted l , the beam has a square section of dimension a and the applied load in a three-point bending test is F . E is Young's modulus, ρ is the density and M the total mass of the beam. The equations of mechanics give the elastic deflection δ due to bending load and the total mass is easily written:

$$\delta = \frac{Fl^3}{4Ea^4} \quad (2.1)$$

$$M = \rho la^2 \quad (2.2)$$

Eliminating the free variable a between equation (2.1) and equation (2.2) gives:

$$a^2 = \sqrt{\frac{Fl^3}{4\delta E}} \quad (2.3)$$

$$M = \sqrt{\frac{Fl^3}{4\delta E}} l \rho \rightarrow M = Cte \frac{\rho}{\sqrt{E}} \quad (2.4)$$

The ratio \sqrt{E}/ρ depends exclusively on materials properties and dictates the performance of the beam. The higher the ratio, the lower the mass. This ratio is the performance index of material for a beam subjected to a three-point bending load and corresponds to the minimal weight design at a given stiffness. For more details on the use and derivation of performance indices, one can refer to the following literature [ASH89, ASH99].

⁵ It has been implemented in commercial software (CES) which encompasses large materials and process databases.

This method is even more efficient by using a materials database graphically [ASH99, CES]. Indeed, the set of known materials can be represented in a materials space of dimension n regarding materials properties (n being the number of properties). Then, property charts can be extracted from this materials space by choosing two different properties. An example is given in Figure 2.1, with a property chart plotting density against Young's modulus in a log-log scale. The equi-performance contour index \sqrt{E}/ρ can be drawn (guidelines of slope equal to 2) allowing the selection of materials. On the same guideline, materials possess the same value of performance index while those above this line have a higher performance. This method helps compare materials, proposes a substitutive material having the same performance index or allows the determination of the best material.

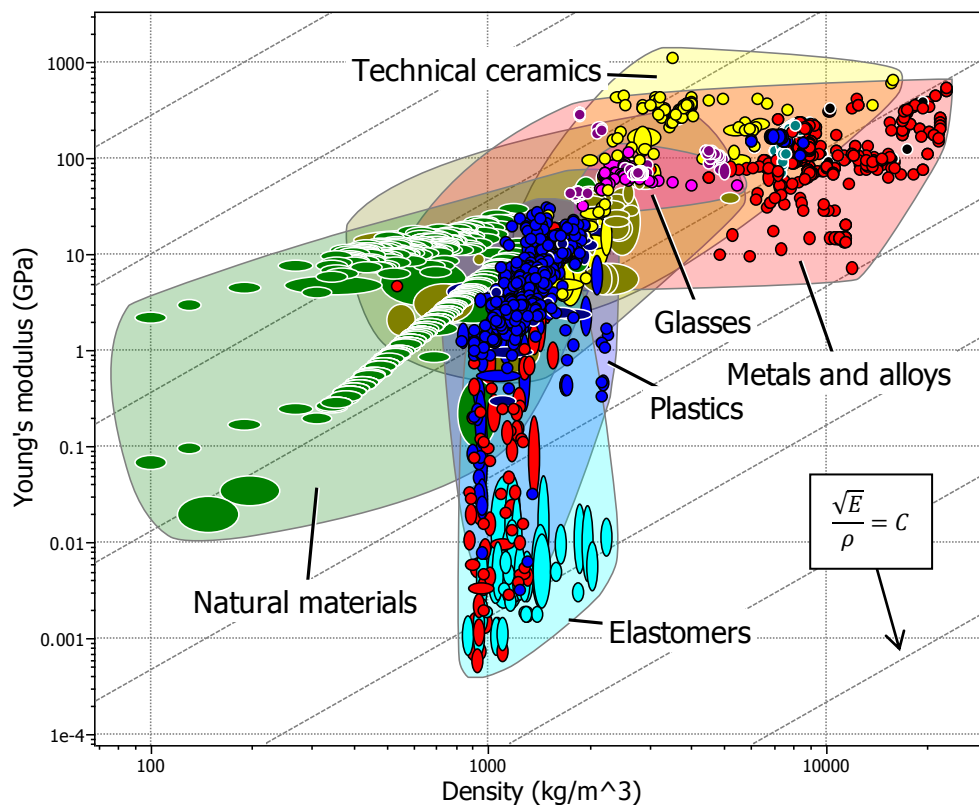


Figure 2.1: Property chart Young's modulus vs. Density. The dotted guidelines correspond to the performance index of a beam for a minimal weight design at a given flexural stiffness. Graph taken from CES software [CES].

Analytical expressions involving material properties can be derived only for simple geometrical shapes and classical loadings. Moreover, a graphical method can only handle two different performance indices. Figure 2.2 gives an overview of the mostly used performance indices, and more details can be found in [ASH99].

1.2. Multi-criteria materials selection

However, materials selection aided computer tools allowed to manage quite many objectives by working directly on the database [BAS98, LAN00]. A weighting method of objectives is

coupled to fuzzy logic in order to rank materials from the most suitable one to the less adapted one given a specific set of requirements [FUZ].

Function, objective, and constraints	Index
Tie, minimum weight, stiffness prescribed	$\frac{E}{\rho}$
Beam, minimum weight, stiffness prescribed	$\frac{E^{1/2}}{\rho}$
Beam, minimum weight, strength prescribed	$\frac{\sigma_y^{2/3}}{\rho}$
Beam, minimum cost, stiffness prescribed	$\frac{E^{1/2}}{C_m \rho}$
Beam, minimum cost, strength prescribed	$\frac{\sigma_y^{2/3}}{C_m \rho}$
Column, minimum cost, buckling load prescribed	$\frac{E^{1/2}}{C_m \rho}$
Spring, minimum weight for given energy storage	$\frac{\sigma_y^2}{E \rho}$
Thermal Insulation, minimum cost, heat flux prescribed	$\frac{1}{\lambda C_p \rho}$
Electromagnet, maximum field, temperature rise prescribed	$\frac{C_p \rho}{\rho_e}$

ρ = density; E = Young's modulus; σ_y = elastic limit; C_m = cost/kg λ = thermal conductivity; ρ_e = electrical resistivity; C_p = specific heat

Figure 2.2: Example of material indices, taken from [ASH99].

The use of a weighted sum of objectives was also described by M.F. Ashby adapting the graphical materials selection method for a bi-objective problem [ASH00a]. Indeed, performance indices can be plotted by pairs along the axes of a graph. It is then possible to determine a decision vector regarding the weighting of objectives, and so the optimal material can be identified. Using a Pareto dominance notion, as described in Section 4, it is possible to determine a trade-off surface which is the group of non-dominated solutions as shown in Figure 2.3.

Considering a set of performances noted P_i , the decision vector is written using exchange constants α_i , as follows:

$$V = \alpha_1 P_1 + \alpha_2 P_2 + \dots + \alpha_i P_i \quad (2.5)$$

Then a new metric based on this weighted sum can be drawn to identify the optimal solution for the decision vector V .

A few years later, Sirisalee et al. used these principles to draw decision charts as a function of the value of the exchange coefficients⁶. In a first paper [SIR04], these authors proposed a method to process the multi-objective material selection for a bi-objective problem as shown in Figure 2.4. In the presented case, exchange constants convert the units of performance into the unit of currency. This way, the choice of α reflects the price per unit raise of performance that the decision-maker considers as worthwhile.

This method can also be adapted for a problem with three or four objectives. The authors treated the case of a disk brake calliper for which mass and cost were to be minimized while the

⁶ Exchange constants can be obtained for instance via a value analysis between mass and cost.

Optimal design of architected sandwich panels for multifunctional properties

Pierre Leite

heat transfer was to be maximized. A decision chart as the one in Figure 2.4 has been drawn, plotting the different optimal solution as a function of the exchange constants value. These authors also treated the optimization of a casing for a mini-disk player with four objectives, concluding that with more than four objectives this method becomes cumbersome. The considered objectives were the minimization of the thickness, the mass, the cost and the environmental impact of the material. To visualize the results, particular values of the exchange constant between cost and environmental impact were chosen to draw decision charts as for a three-objective optimization problem.

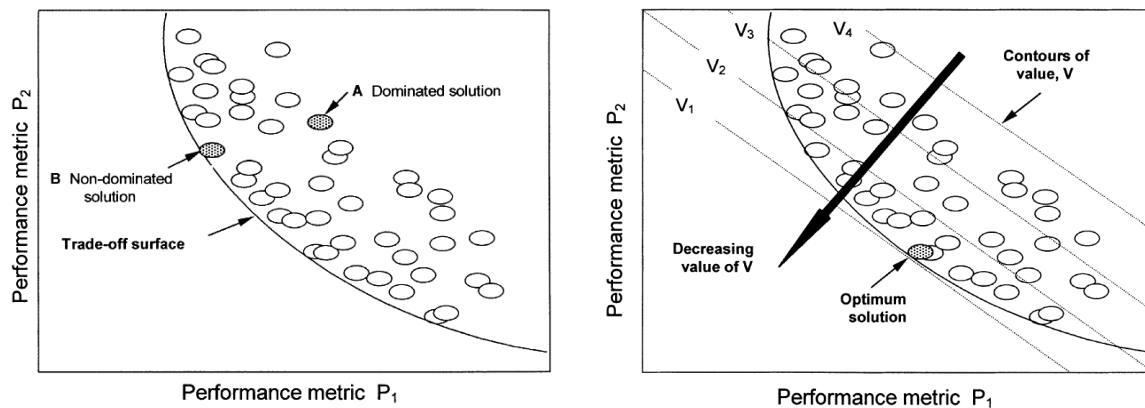


Figure 2.3: On the left hand side: the trade-off surface between two performance metrics with solutions of A-type being dominated solutions and solutions of B-type being non-dominated ones. On the right hand side: graphical method to identify the optimal solution for a given decision vector V (taken from [ASH00a]).

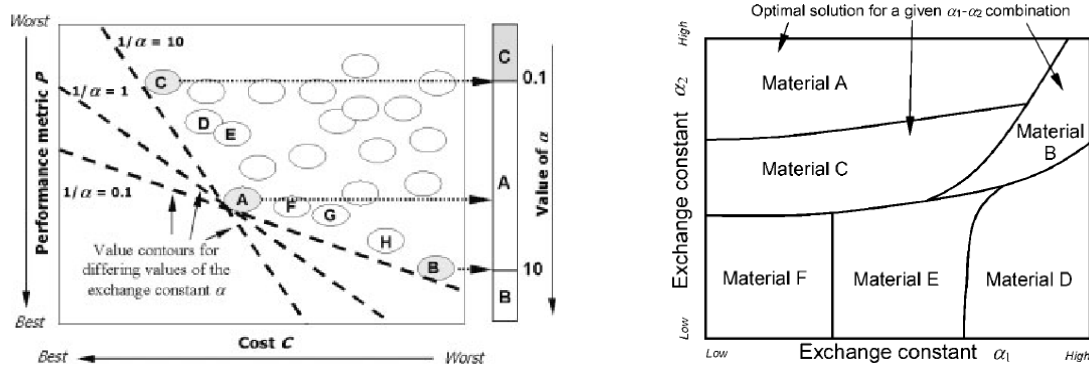


Figure 2.4: On the left hand side: identification of the optimal solution as a function of an exchange constant for a bi-objective optimization. On the right hand side: decision chart giving the optimal material as a function of exchange constants for a three-objective optimization (taken from [SIR04]).

1.3. Mixed mode index

Bouaziz and Masse extended the idea of performance index to the case of a plate subjected to a mixed load of tension and bending [BOU12]. This extended mixed mode index can be used to identify the appropriate material depending on the relative weight of the tension mode compared to the bending mode. This relative weight is taken into account by a parameter proportional to the ratio between tension and bending. This method is similar to the one

developed by Ashby in [ASH00a] by introducing the weighting into the expression of the performance index.

Thanks to the last evolutions, the performance index method is able to deal with materials selection problems involving simple shape (rods, beams, plates) and solicitations (tension, bending torsion) with simple analytical expressions. This method is still adapted to problems with a limited number of objectives and can only be applied to select mono-materials in the set of known materials.

1.4. Determination of a performance index by coupling Design Of Experiments and Finite Element Modelling

As already mentioned, a performance index is an analytical expression giving the fitness of a material/solution to a given situation. In line with this principle, Castillo et al. proposed an interesting way to obtain an approximated material performance index for a complex situation [CAS09]. When the situation is complex, for instance when the geometry is not simple enough to obtain analytical expressions of the performances of the solution, classical performance indices fail to evaluate the fitness of a material. However, evaluating the fitness can be achieved by numerical simulations. The problem is related to the fact that there is no link between the evaluated performance and the material properties. Moreover, performing material selection using numerical simulations instead of analytical expressions would imply prohibitive computational costs.

The approach proposed by Castillo et al. consists in using a Design Of Experiments (DOE) in order to link the material properties with the evaluated performance by an approximated analytical expression. The authors focused on the design of a machine tool frame. Their objective was to maximize its thermal stability, for instance minimizing the relative displacement between the part and the tool during temperature variations.

This relative displacement depends on the geometry of the machine tool frame and the material properties, these parameters will be called factors for the DOE. The geometry can be described by a free variable e , the other parameters being fixed. The material properties influencing the displacement induced by temperature variations are the density ρ , the Young's modulus E , the thermal conductivity λ , the thermal expansion coefficient α and the specific heat capacity c . Using filtration methods, the authors narrowed the variability range of each factor. Then a full factorial design has been used to evaluate the influence coefficients of each factor, as well as for interactions between factors. This expression has been used as a performance index to select the optimal materials for the machine tool frame, which are ceramics such as marbles, cements and concretes according to the authors.

2. Introduction to architected materials

The method described above allows the analysis of multifunctional specifications, but solutions that can be obtained are selected from a list of known materials. In this next part, a new class of materials is presented, i.e. architected materials.

After defining what an architected material is, a specific criterion, used to class the architected materials, is presented. Finally, examples of the most common architected materials are given in order to foresee the great potential of this kind of materials for the present study.

2.1. Definition and objectives of architected materials

Architected materials are defined as a combination of materials with a particular spatial arrangement that exhibit unusual combination of properties [BRE13]. This definition encompasses bi-materials but also porous/cellular materials (air being the second “material”) and other man-made materials. Designing architected materials fills the need to design a material for a specific purpose with enhanced properties.

Initially, a definition for architected materials was given by Kromm et al.: “an architected material is the combination of two or more materials in a predetermined geometry and scale, optimally serving a specific engineering purpose” [KRO02]. It was reformulated by Ashby and Bréchet in “architected = A + B + geometry + shape” with A or B being possibly a gas [ASH03]. Using this working definition, a classification of architected materials can be proposed in Table 2.1.

Thus, those materials lie between the classical dense material and the structure, creating new design variables allowing the exploration of performance space and pushing back the limits of known materials [ASH03, BRE13, ASH13].

2.2. Maxwell’s stability criterion

Usually the deformation of a truss network is bending-dominated just as in foams, while for certain conditions in connectivity they are stretching-dominated. These conditions are summarized by Maxwell’s stability criterion [MAX64].

This criterion predicts the stability of a pin-jointed frame made up of b trusses and j frictionless joints. In this case, stability means that the frame is rigid and can support a load without tumbling. The criterion is:

$$M = b - 2j + 3 = 0 \text{ in 2D} \quad (2.6)$$

$$M = b - 3j + 6 = 0 \text{ in 3D} \quad (2.7)$$

Considering a framework with locked joints representing the topology of an architected material, two cases emerge:

- If $M < 0$, the frame is not able to carry load. As the joints are locked, it does not tumble but the trusses will bend if the frame is loaded.
- If $M > 0$, the frame is load bearing. Even if the joints were not locked, the framework would be able to support load and trusses would be loaded in tension/compression.

The main information given by this criterion that is relevant for architected materials is the nature of the deformation of the trusses of the architecture. There is a direct link between the local deformation mode and the effective stiffness of the architected material [ASH03].

For bending-dominated patterns, just as foams, the effective elastic modulus will have a quadratic dependence of relative density:

$$E^* = C \left(\frac{\rho^*}{\rho_s} \right)^2 E_s \quad (2.8)$$

For stretching-dominated patterns, the effective elastic modulus will depend linearly of relative density:

$$E^* = C \left(\frac{\rho}{\rho_s} \right) E_s \quad (2.9)$$

A similar development can be done for the strength of the architected material as a function of the local deformation mode. Ashby illustrates the difference in the achievable performances in a property chart computing the effective properties of foams and truss lattice structures made of the same constitutive material as shown in Figure 2.5 [ASH11]. At a given density, truss structures are stiffer than foams.

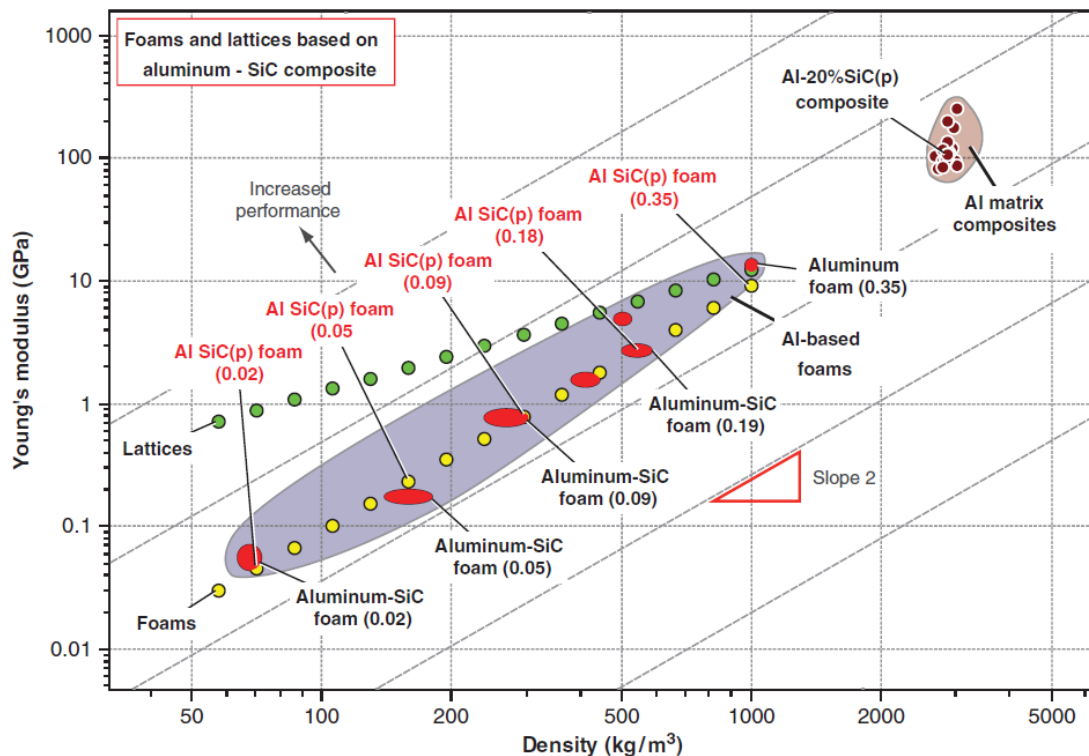


Figure 2.5: Property chart plotting Young's modulus as a function of density. Effective properties of foams (in red) and truss lattice structures (in green) made of the same constitutive material are plotted. For a given density, stretching-dominated structures are stiffer than bending-dominated ones.

2.3. Overview of existing architected materials

Composites

Composite materials commonly refer to a bi-material, $A + B$ with both A and B being solid materials. Being a filled polymer, an unidirectional composite or a laminate, the main idea is to have a relatively soft and light matrix reinforced by a stiffer (or/and stronger) compound. The effective properties of composites often follow a rule of mixtures, or the inverse rule of mixtures. Composites are weight saving materials. Such materials are largely used for their high-standard specific mechanical properties in the transport industry (aerospace industry, automotive and train building) but also in sport industry and for military applications. A huge literature concerns composites but this will not be introduced or discussed here. The interested reader can

Optimal design of architected sandwich panels for multifunctional properties

Pierre Leite

refer to the book from Berthelot on generalities dealing with mechanical behaviour of composites [BER96] or to this review on optimization of this kind of materials [VEN99].

Table 2.1: Classification of architected materials.

Class	Materials		Shape			Geometry		Specific Functions
	Mono-material	Multi-material	1D	2D	3D	Organized	Random	
Composite particulate		X			X		X	<ul style="list-style-type: none"> • Axial and flexural stiffness and strength / wt • Thermal insulation
Composite fibrous		X		X		X		<ul style="list-style-type: none"> • Axial and flexural stiffness and strength / wt • Thermal insulation • Toughness • Energy absorption
Cellular (foams, hollow sphere stacking)	X				X		X	<ul style="list-style-type: none"> • Axial and flexural compliance • Energy absorption • Thermal insulation
Architected (Honeycombs, truss structures, egg-box)	X				X	X		<ul style="list-style-type: none"> • Axial and flexural stiffness and strength / wt
Sandwich panel		X		X		X		<ul style="list-style-type: none"> • Flexural stiffness and strength / wt • Thermal insulation
Cable	X	X	X			X		<ul style="list-style-type: none"> • Flexural compliance • Tensile strength • Damage tolerance • Thermal conductivity • Electrical conductivity
Interlocked segmented material	X	X			X	X		<ul style="list-style-type: none"> • Damage tolerance

Foams

Foams are cellular solids made of a constitutive material and gas, usually air (see Figure 2.6). They are represented as a stochastic material with a mean cell size determining the macroscopic behaviour of the foam. They are made by expanding the material which can be a polymer, a metal or a ceramic with a foaming agent. It is a bending-dominated structure. Cell walls or edges locally bend when the material is mechanically loaded. The presence of gas in the porosities, either opened or closed, is important even though its mechanical properties are negligible. But in low density foam, air is the main contributor for thermal or electrical properties.

This structure allows lighter materials to be obtained while having good functional properties. It is an attractive thermal insulation solution and has a high densification strain, making foams ideal for packaging and shock absorbers. It is worthwhile noting that foams can often be considered as isotropic materials. More information is provided in specific references [GIB97, ASH00b, BAN08].



Figure 2.6: Example of Aluminium foam (ERG Duocel®).

Honeycombs

Another cellular solid which is widely used is the honeycomb structure (see example in Figure 2.7). This material, whose architecture is inspired by nature, owns interesting orthotropic mechanical behaviour. Indeed, honeycomb patterns are obtained by extrusion of a unit cell which has been reproduced periodically in the plane. The most famous honeycomb is the hexagonal one, but other shapes can be used to build a honeycomb such as triangles, squares or a re-entrant pattern. Honeycombs can be manufactured by extrusion processes or sheet folding and bonding depending on the nature of the constitutive material.

In compression, honeycombs exhibit a stiffer behaviour in the out-of-plane direction than in the in-plane one. But this anisotropy is clearly advantageous compared to foams since the out-of-plane shear modulus of honeycombs is higher for a given out-of-plane compressive modulus.

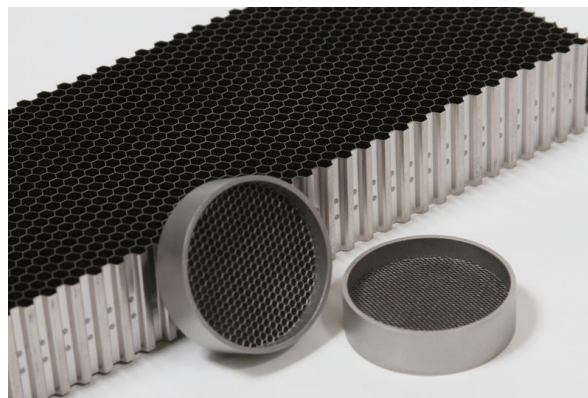


Figure 2.7: Illustration of a regular hexagonal honeycomb.

Truss structure

As stated above, architected materials can be either bending or stretching dominated. Among the stretching-dominated patterns, the lattice truss structure has become popular in

Optimal design of architected sandwich panels for multifunctional properties

Pierre Leite

recent years. A particular structure has been extensively investigated, i.e. the octet truss lattice (illustrated in Figure 2.8) that was proposed by the architect R.B. Fuller in 1954 for building trade industry.

This architected material possesses very high specific mechanical stiffness and strength. They are perfectly suited for load bearing and impact mitigation applications [WIC01, FLE01, DES01b].

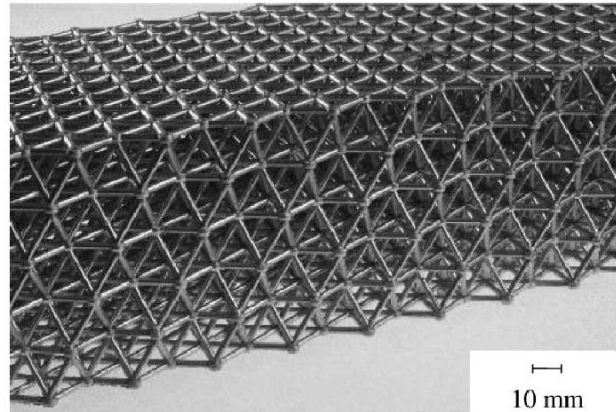


Figure 2.8: Picture of an octet truss lattice structure. Taken from [DES01b].

Interlocked segmented materials

Interlocked materials are a really special example of architected materials as they take advantage of a segmentation of the material in order to increase the macroscopic tolerance to crack propagation for brittle structures [DYS03a, DYS03b, AUT07]. Interlocked topologies can be achieved through simple geometries such as cubes (see Figure 2.9), or through complex shapes such as osteomorphic structures.



Figure 2.9: Interlocked segmented material made of topologically interlocked cubes. Taken from [DUG13].

Hollow spheres stacking

Hollow spheres clearly demonstrate how the understanding of mechanisms involved in architected materials behaviour is important and contributes to the improvement of materials. By combining open and closed porosities in the same material (see Figure 2.10), hollow spheres stackings display good mechanical properties (closed porosities) and good

acoustical absorption (open porosities). Compared to metal foams, hollow spheres stacking has a better acoustical behaviour for a given stiffness or strength [GAS04, GAS05, DAV09].

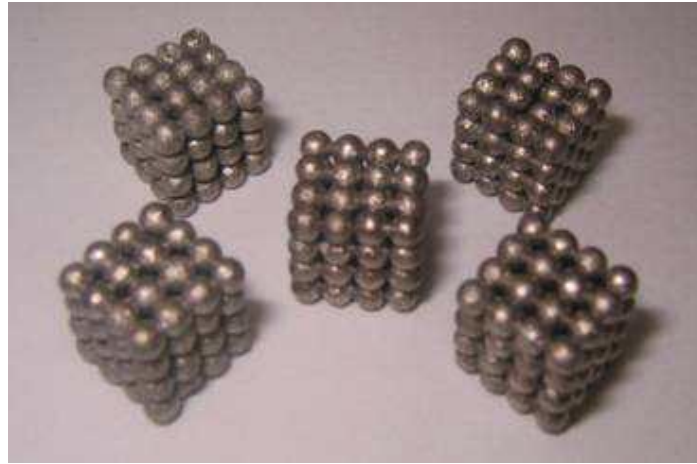


Figure 2.10: Pictures of regular hollow spheres stacking. Taken from [DAV09].

Egg-box

Another structure which could compete with truss structures and honeycombs for mechanical applications corresponds to the egg-box structure illustrated in Figure 2.11. This one corresponds to an embossed geometry. Such structures can be made from embossed metal sheets [ZUP03] or composites [CHU07].

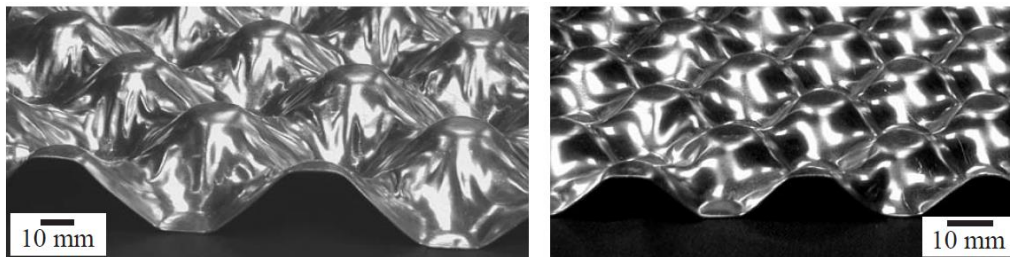


Figure 2.11: Pictures of metallic egg-box. Taken from [ZUP03].

Auxetic materials

Architected materials can also repel the limits of materials science. Auxetic materials (see Figure 2.12) are an example of that. By being able to exhibit a negative Poisson's ratio, such materials can display a strong increase of shear modulus. They can also be used to build synclastic panels. For more details, one can refer to the following papers [EVA91, ALD10, DIR12a, DIR12b].

Entangled materials

Entangled materials are very light and relatively compliant materials. Such cellular structures can stand as a common solution in building trades for multifunctional applications involving thermal and sound insulation. The manufacturing process has been optimized through many decades, making this structure easy to manufacture with a very low cost [AMI12].

Optimal design of architected sandwich panels for multifunctional properties

Pierre Leite

However, their mechanical stiffness is poor even though the involved mechanism promotes them as good solutions for energy dissipation. Efforts are being made in order to increase their mechanical properties, including studies on reticulated entangled materials as shown in Figure 2.13 [MEZ10].

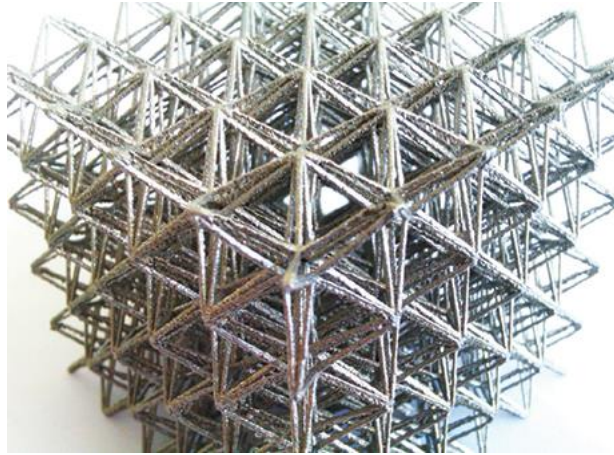


Figure 2.12: The hexatruss lattice, a 3D auxetic material. Taken from [DIR12b].

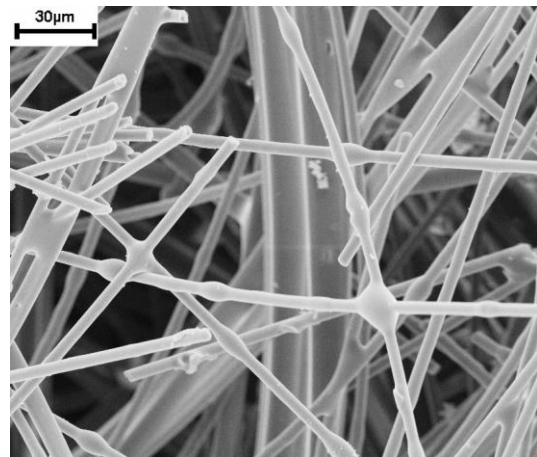


Figure 2.13: On the left hand side: picture of entangled para-aramid fibres, taken from [AMI12]. On the right hand side: micrograph of reticulated entangled materials, taken from [MEZ10].

Cables

One of the most familiar architected material is the cable. It can be considered as a segmented material composed of strands as illustrated in Figure 2.14. Compared to a monolithic rod of equal mass, the cable has a far better flexural compliance, which is a required specification in many applications, and a very good tensile strength.

In addition, by manufacturing multi-material cables, one can tailor the functional properties of the cable. For instance, using steel and copper, the cable can be stronger than a cable only made of copper and have better electrical conductivity than a cable only made of steel [ASH03].



Figure 2.14: Picture of a stranded cable made of steel.

3. Sandwich panels

3.1. Introduction

This finally brings us to the most familiar hybrid material together with the cable: the sandwich panel. A classical sandwich panel is composed of 3 layers as illustrated in Figure 2.15. The outer layers are called faces while the inner layer is called core. The main interest of these structures is to efficiently distribute the material in space regarding the external load in bending. Panel structures being usually submitted to flexural solicitations, sandwich panels are consistently made of stiff and strong faces and of a lightweight core in order to move away the material from the neutral axis and to preserve a constant distance between faces. This increases the moment of inertia with a reduced increase of mass resulting from a light core.

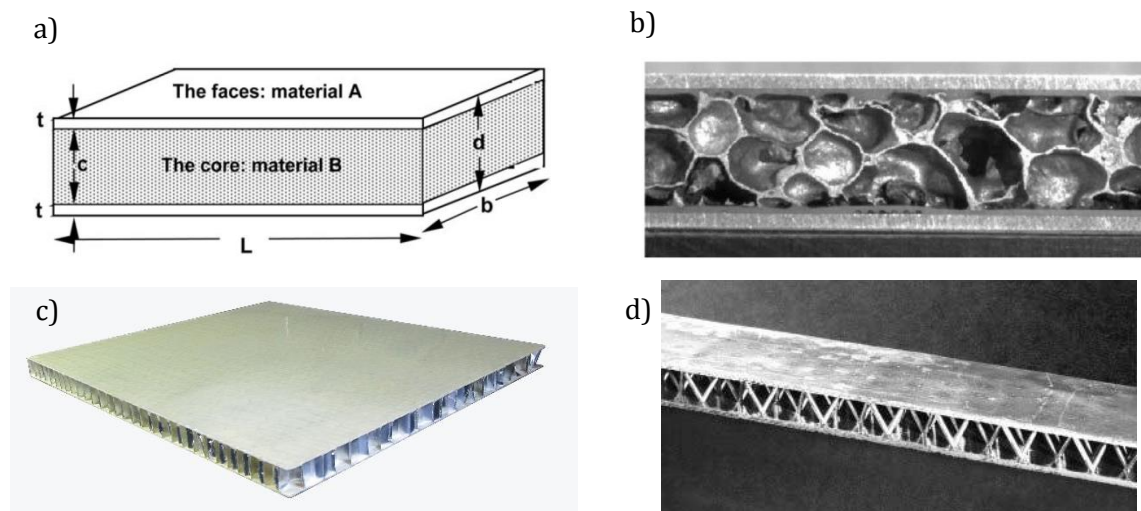


Figure 2.15: Schematic description of a sandwich panel (a) and pictures of sandwich panels with different cores: foam (b), honeycomb (c) and truss structure (d).

The design possibilities for sandwich panels are quite huge. The first sandwich panels were made of metallic faces and of a balsa wood core. With the appearance of composites and foams, sandwich panels became architected at different scales, from the panel itself to the constitutive core. The architected materials presented above are usually used as constitutive materials in sandwich panels design.

Optimal design of architected sandwich panels for multifunctional properties

Pierre Leite

Sirisalee et al. have demonstrated that sandwich panels are competitive for multifunctional applications using decision charts as shown in Figure 2.16 [SIR06]. The authors studied the case of floor panels, drawing a decision map with sandwich panels.

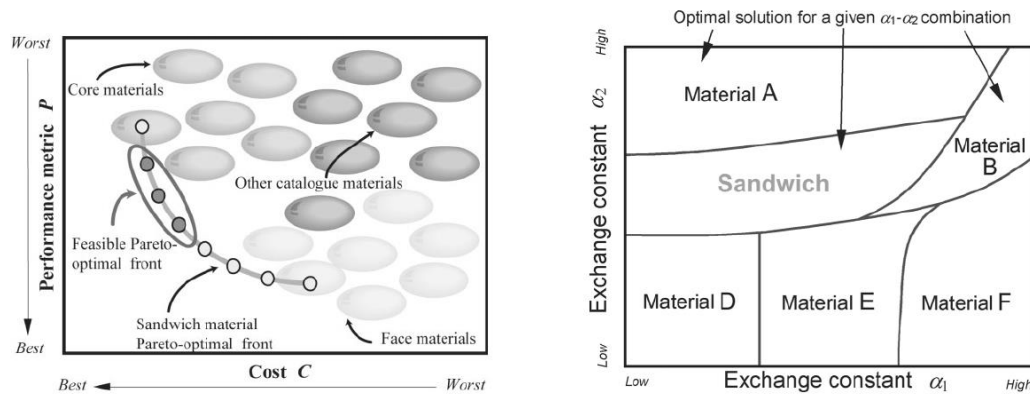


Figure 2.16: On the left hand side: sandwich panels can overcome dense materials for multifunctional applications. On the right hand side: a decision chart where sandwich panels can compete with dense materials for some exchange constants.

A brief review of the most common applications of sandwich panels is introduced in the next sections. For each tackled property, a summary of the main results from the literature is addressed.

3.2. Mechanical properties

The main property that promotes sandwich panels as competitive solutions is their high flexural stiffness at minimal weight. Usually panels are optimised either for stiffness or for strength with minimization of the mass as objective. As the main solicitation for a panel is bending, the different studies on the mechanical behaviour of sandwich panels addresses its behaviour under a bending test (three or four points).

The stiffness of sandwich panels has been subjected to extensive work since the sixties. Exact and approximated analytical expressions have been derived to evaluate the flexural stiffness of sandwich panels. These expressions take into account the shear deformation of the core in addition to the bending deformation of the panel. The behaviour of such panels regarding classical loading cases have been investigated by Allen and Zenkert, including the deflection of a panel submitted to a three-point bending test [ALL69, ZEN97].

Since then, the stiffness of sandwich panels made of all sorts of face and core material has been experimentally investigated. There is usually good agreement between these experimental results and the approximated expressions given by Allen.

The strength of the panel can also be assessed using an upper bound approach. The different possible failure modes of this panel under a three-point bending test have been identified into four instances. The first one is core indentation for which the core material collapses and the indenter pulls in the panel. The second one is face yielding. The wrinkling of the face loaded by the indenter represents the third instance. Finally, the last mode is core yielding by shear. A critical load corresponding to the onset of plastic deformation can be calculated for each mode. Then, the strength can be estimated by taking the lowest value of critical load, identifying the dominant failure mode. The possible failure modes are schematically represented in Figure 2.17.

A brief description of the different modes is presented in next chapter; for more details please refer to [ALL69, ZEN97, ASH00b, GIB97].

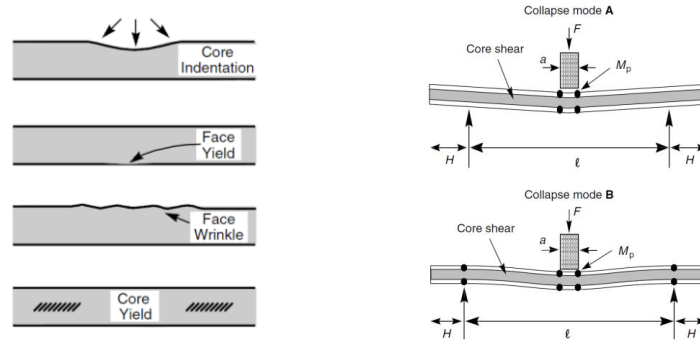


Figure 2.17: Illustrations of the different failure modes considered for a sandwich panel by bending.

Based on the previous models and on the different architected materials models, it is possible to trace failure mode maps giving the dominant mode as a function of the geometrical parameters. One of the first studies which used this approach is the one from Triantafillou and Gibson on sandwich beams subjected to three-point bending tests with Aluminium faces and a Polyurethane foam core [TRI87]. The authors used the Allen's model to determine the dominant failure mode and the critical load value. Experimental tests were performed and a good agreement was found between analytical predictions and experimental results.

Thereafter, Petras and Sutcliffe focused on sandwich panels composed of Glass Fibre Reinforced Polymer (GFRP) composite faces and of a Nomex honeycomb core subjected to bending [PET99]. By using the developed models, in particular by Allen and Zhang, failure mode maps were traced as a function of the ratio between the face thickness and total length of the beam and of the core relative density. Experimental results confirmed the obtained results.

2001 has been a prolific year concerning this issue with in particular the collaborative work of three different teams. The first study is about sandwich panels composed of Aluminium faces with Aluminium foam core in bending solicitations [McC01]. Stiffness and strength were evaluated using the models presented previously which allowed the authors to draw failure mode maps as a function of face thickness and of core thickness both normalized by the distance between supports. They used experimental tests to validate the analytical prediction and found good agreement with the experimental results.

Chen et al. produced a similar work but including numerical analysis by Finite Element Modelling (FEM) [CHE01]. Numerical, analytical and experimental results satisfactorily concord. Failure mode maps were traced as well as mass and load indices noted \bar{M} and \bar{F} (see Figure 2.18). These indices give estimation on the performances of the panel design regarding the mass and strength respectively. They are defined by dimensionless expressions:

$$\bar{M} = \frac{M}{\rho_f b l^2} \quad (2.10)$$

$$\bar{F} = \frac{F}{b l \sigma_{yf}} \quad (2.11)$$

with M the total mass of the panel, ρ_f the density of the face material, F the value of the critical load and σ_{yf} the yield strength of the face material. Depending on the desired strength, the design

Optimal design of architected sandwich panels for multifunctional properties

Pierre Leite

variables t and c minimizing the mass index can be identified from this map. Arrows show the optimal path of minimal weight, that is the design variables which offer the minimal weight for a given load index. In a general manner, this optimal path follows the frontier between different failure modes domains.

For their part, Bart-Smith et al. traced failure mode maps based on numerical simulations obtained by FEM and validated them by experimental results [BAR01]. The studied sandwich panels were made of Aluminium foam core while two different Aluminium alloys were used as faces. The constitutive material influence on the failure mode map is shown in Figure 2.19.

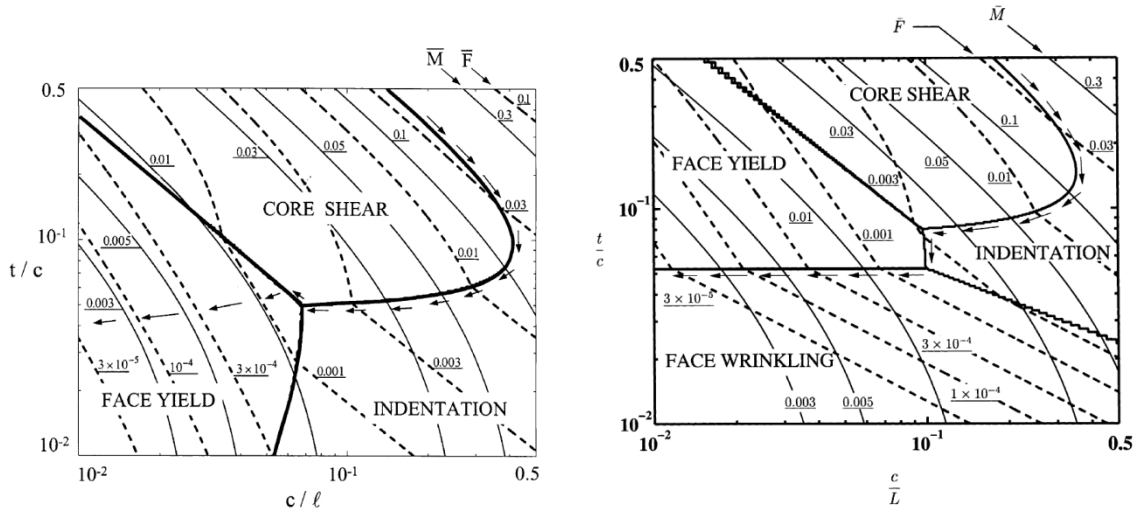


Figure 2.18: Failure mode maps plotting against geometrical parameters of the sandwich panel. These maps allow an optimization of the structure thanks to performance indices \bar{M} and \bar{F} (taken from [CHE01] and [DES01b]).

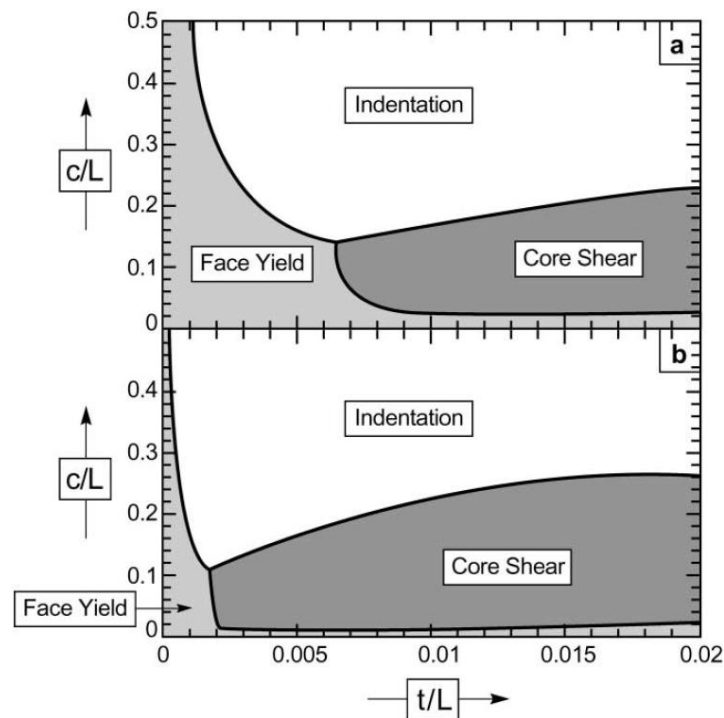


Figure 2.19: Influence of constitutive material on failure mode maps (taken from [BAR01]).

During the same year, two other papers were published about the mechanical behaviour of sandwich panels made of truss core. Wicks and Hutchinson established analytical models to predict the stiffness and strength of a truss network following the octet truss lattice pattern. They could then deduce the minimal weight design for a given strength without plotting failure mode maps [WIC01]. The tested panels could be made of solid faces or of planar trusses. An analytical comparison with optimized honeycomb sandwich panels enlightened the competitiveness of truss structures as core material. Actually, if honeycombs give lighter panels for a given strength, they must be thick. In order to have thinner panels, thus considering a size constraint, truss cores can compete with honeycombs for mechanical properties. These authors also led a similar study on the compression behaviour of this kind of panels, showing that their performances were comparable to that of hat-stiffened panels.

Deshpande and Fleck followed a different path to evaluate the strength of the truss structure [DES01b]. Still, they used their analytical model to plot failure mode maps and traced the minimal weight design path (see the arrows in Figure 2.18). Stiffness and strength were estimated and compared to experimental results with a satisfactory correlation for both of them.

Thereafter, Steeves and Fleck took over the study of Polymer foam core sandwich panels with composite faces plotting failure mode maps using the upper bound approach described previously [STE04a]. The path of minimal weight design was determined too. However, they readjusted the analytical model corresponding to the indentation mode by considering an elastic, perfectly plastic behaviour of the foam core and only elastic deformation for the composite faces. Their new model was validated using numerical and experimental results [STE04b].

The latest paper from Steeves and Fleck intended to summarize the method of plotting failure mode maps and the results obtained in a materials selection point of view [STE04c]. As shown in Figure 2.20, the optimal weight design for a given strength in terms of materials will depend on the desired strength. For a low load index, PVC foam cores are really competitive while honeycomb cores are ahead for high load index. Then, a full optimization should take into account materials selection and geometrical optimization. It is also observed that depending on the desired strength, the failure mode corresponding to the optimal design can change.

What is to be kept in mind from the presented method is that a primary design of the panel can be estimated using simple analytical expressions. Depending on stiffness and strength requirements, the minimum weight design can be found. In some cases, choosing the failure mode can be of interest, such as for shock absorbing applications where indentation minimizes the deflection of the panel. However, most of the studies mainly focus on geometrical optimization. Materials selection is performed by comparison of the optimized panels of each core architecture.

3.3. Thermal properties

Besides a good flexural stiffness, sandwich structures have many other qualities. Considering thermal properties, the presence of air in the core material implies a greater thermal resistance than the solid materials with a low density as shown in Figure 2.21 for foams and honeycombs.

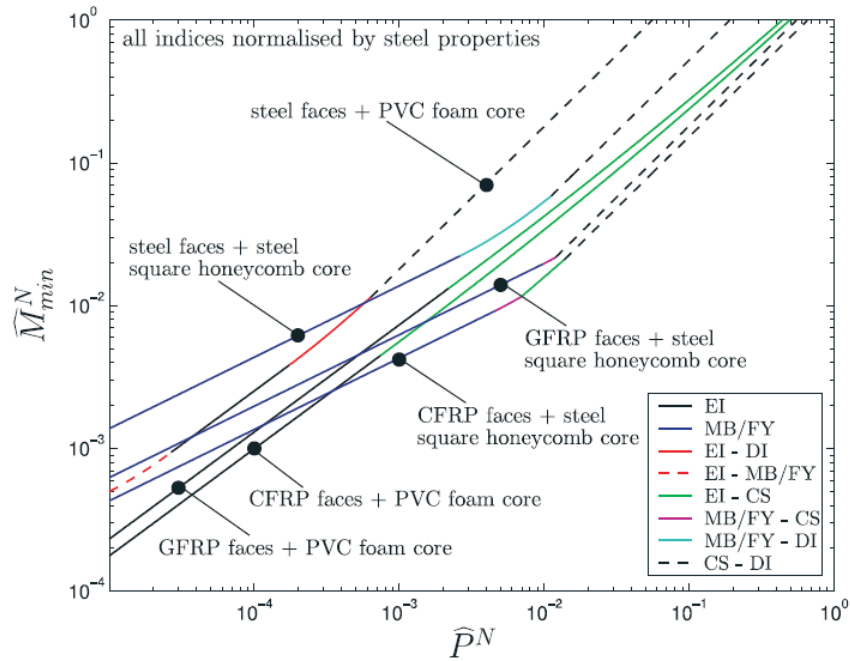


Figure 2.20: Influence of constitutive materials of the sandwich panel on the optimal design for bending performances (taken from [STE01c]).

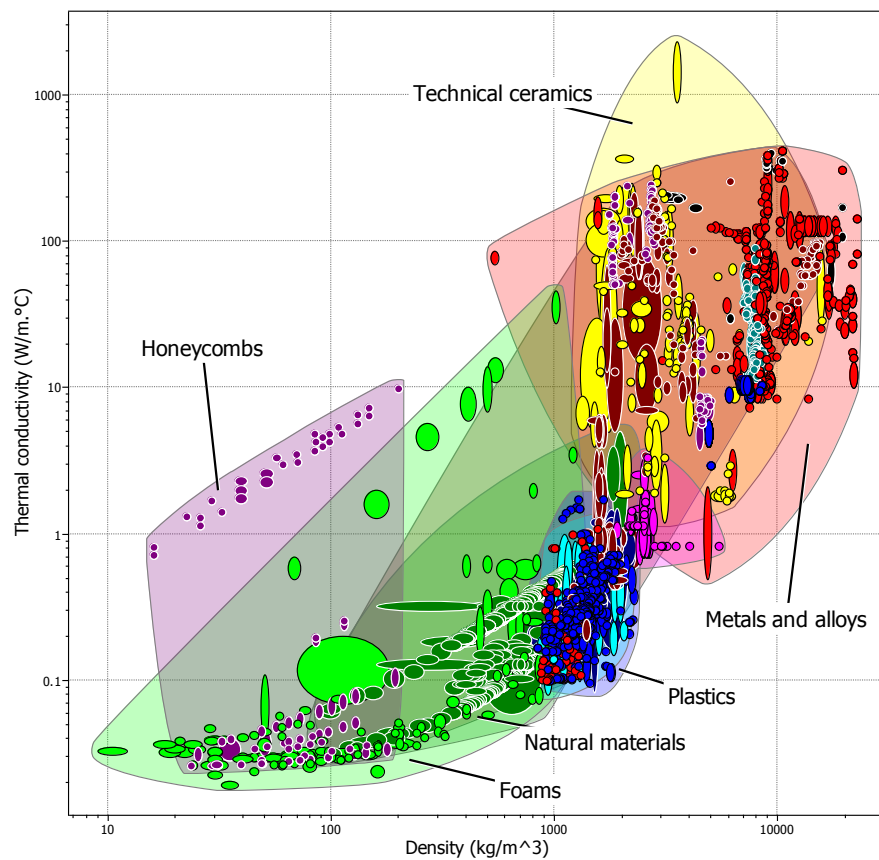


Figure 2.21: Property chart thermal conductivity vs. density.

The presence of open porosities in the core of the panels also offers attractive performances for heat exchange applications. Let us consider a panel heated at one face, then heat flow can be

dissipated by conduction from the hot face into the web structure while a coolant flows through the core. Heat transfer between solid and fluid reduces the temperature of the web structure and helps dissipate heat. The first studies run by Lu et al. led to the development of simple analytical models dedicated to metal foams [LU98] and honeycombs [LU99] allowing a topological optimization of the architectures for heat exchange applications. A simple analysis of an idealized topology helped the authors to evaluate the global heat transfer coefficient as well as the pressure drop needed for the coolant to flow. In particular, this work ended to the development of a performance index dedicated to the two architectures previously mentioned.

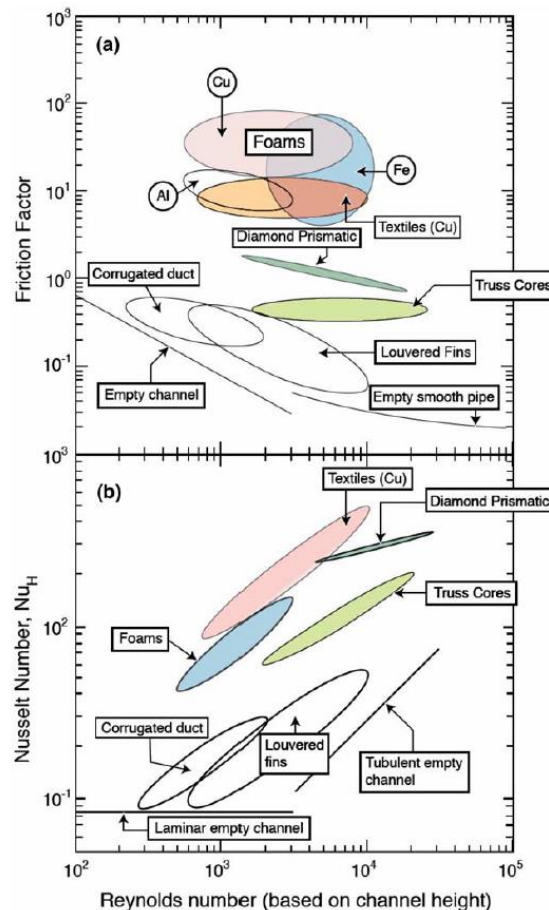


Figure 2.22: Comparison between several core architectures regarding some influent parameters involved in heat exchangers applications (taken from [LU05]).

Thereafter, several studies focused on a more accurate evaluation of thermal properties of metal foams, particularly of thermal conductivity [BHA01, B0001] as well as permeability and inertial coefficient involved in the behaviour of a fluid flowing into the foam [BHA01]. The authors developed several predictive models based on geometrical considerations. Experimental results, in particular for Aluminium and RVC foams served to validate their models [BHA01].

Concurrently with these studies on effective properties of foams, Gu et al. investigated the multifunctional design of sandwich panels with cellular cores for heat exchangers applications involving load bearing specifications [GU01]. The assessed architectures are honeycombs with a hexagonal pattern, two different types of square patterns and two different triangle patterns. The models which were used are based on previous work on mechanical behaviour of cellular materials [GIB97] and on Lu et al. work [LU99]. A topological optimization was performed to

determine the best core architecture. In a first stage, only mass and thermal properties were optimized, showing that hexagonal honeycombs were the most promising core for this kind of specifications. Next, a constraint on flexural stiffness of the panel was set and ended to slightly different optimal solutions. While the hexagonal pattern remains the most promising for high heat flux specifications, the triangle outperformed the other candidates for thinner structures.

Comparisons between experimental and numerical results (particularly FEM simulation) were used to validate the models and confirmed the good performances of architected sandwich panels for thermal applications such as heat exchangers. Other 2D structures [WEN06] but also truss cores [TIA04, LU06] and textile cores [TIA07] were analysed in order to trace property charts, thus allowing a graphical comparison between the different known structures as shown in Figure 2.22.

3.4. Acoustical properties

Acoustic damping is of major interest in some applications such as building trades. The main property characterizing a panel for acoustic damping is the Acoustical Transmission Loss, which is linked to the ratio between the incident acoustical energy and the transmitted one. The higher the Acoustical Transmission Loss is, the lower the transmitted energy is. The first analytical law predicting the Acoustical Transmission Loss R of a panel is dedicated to dense panel submitted to normal incident acoustic waves. This is called the “mass law” from its dependence on the mass per unit area M of the panel and on the frequency f of the acoustic wave, as given in equation 2.12. The acoustic behaviour of a panel according to this law is independent of the stiffness of the panel. The predictions made through this law are satisfactory for dense homogenous and monolithic walls. It predicts a decrease of R by frequency of 6 dB per octave.

$$R = 20 \log(Mf) - 47 \text{ dB} \quad (2.12)$$

Sandwich panels enabled to increase the possibilities in terms of acoustical insulation. Indeed, a first study from Dym and Lang showed that the presence of a flexible core inside the panel favours in some circumstances the occurrence of symmetric vibration modes which increase the Acoustical Transmission Loss [DYM74]. Dedicated models were developed to predict the panel acoustical behaviour and were used to demonstrate that sandwich panels were the best solution for this kind of applications. For more details on that field, please refer to [MUR98].

Studies on the acoustic behaviour from Simon et al. and Wang et al. showed that sandwich panels with a sufficiently soft core experience a “sandwich effect” consisting first on a decrease of the Acoustical Transmission Loss at a frequency called the symmetric coincidence frequency, and then on an increase of the Acoustical Transmission Loss of 20 dB per octave [WAN09, SIM95]. Then, as shown in Figure 2.23, a sandwich panel has better Acoustical Transmission Loss in some frequency ranges than a monolithic panel of equivalent mass for which only the “mass law” is applied.

Wang et al. used a genetic algorithm to perform a material selection on a short list of possible materials in order to optimize the Acoustical Transmission Loss of a sandwich panel. The authors considered constraints on flexural stiffness and mass. They proposed a 72 mm honeycomb core sandwich panel made of 1.3 mm Titanium face sheets exhibiting a 45.05 dBA Acoustical Transmission Loss in the frequency range [1 000; 4 000] Hz, a mass per unit area of

13.58 kg/m² and a deflection of 0.007 mm under a central load of 1 N in a three-point bending test with a span of 1 m.

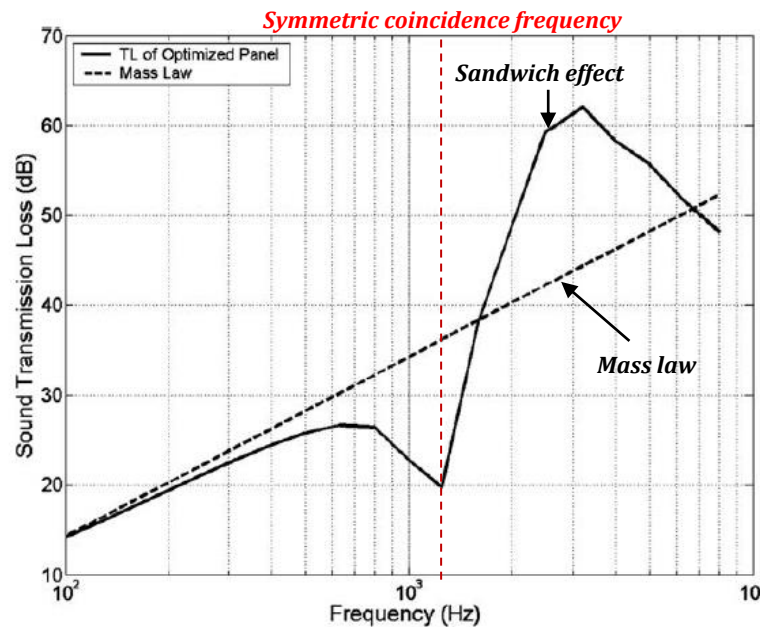


Figure 2.23: Evolution of the Acoustical Transmission Loss as a function of the frequency. Comparison between the performances of an optimized sandwich panel experiencing a “sandwich effect” and the performances of a panel of equivalent mass experiencing a “mass law”. Figure taken from [WAN09].

3.5. Blast mitigation properties

The ability of sandwich panels to absorb shocks has been investigated in many studies according to different core architectures. A first comparative study, held in 2003, focused on truss core panels and demonstrated the competitiveness of sandwich panels against solid plates of equivalent mass [XUE03]. Based on FEM simulations, the authors showed that sandwich panels, under some circumstances, are able to better absorb shocks compared to plates in the sense that the central deflection of the inner face is lower. The applied load is considered as representative of a blast load. The authors pointed out the necessity of optimizing the sandwich panel structure. Actually, the panel can behave worse than a plate of equivalent mass if not correctly designed; in other words, the deflection can be higher for the sandwich panel. Moreover, the mechanical constitutive laws used for the study neglected the strain rate dependence, and so the truss core was modelled using a homogeneous equivalent solid with a constitutive law adapted from foams. So the representativeness of these constitutive laws is to be considered with particular care. Then, the authors focused on three specific geometries to obtain more accurate results [XUE04]. The considered geometries are a pyramidal truss core, a square honeycomb and a folded plate. A 3D modelling of a unit cell of the architecture was used to evaluate the performance of such structures in order to rank them and compare them to solid plates. Based on an optimization stage, they showed that for these structures the deflection was lower than for a solid plate, which allows to conclude on the competitiveness of sandwich panels for blast mitigation. Actually, square honeycombs were the most effective architecture. Moreover, considerations on fluid-structure interactions showed that this advantage was intensified when considering an underwater blast.

On their own, Deshpande and Fleck focused on developing an analytical model to assess and optimize the behaviour of architected sandwich panels under blast loading [FLE04]. The model is based on three stages. The first one corresponds to the fluid-structure interaction, giving the velocity of the outer face after blast. During the second stage, crushing of the core occurs while in the last stage, all the structure deforms, thus leading to dissipate the remaining energy. In this last stage, deformation is by plastic bending and stretching of the structure. This model was then used to plot performance charts as a function of several geometrical parameters. The considered core architectures were metal foams, pyramidal truss, hexagonal and square honeycombs and the diamond celled folded plate. These charts allowed optimal design to be identified for each structure regarding weight for a given deflection. Comparison between numerical results obtained in [XUE04] and analytical results showed the limitations of the presented model. However, the correlation is good enough to consider this model as a tool for preliminary design.

Thereafter, several studies were dedicated to the improvement of the established models [HUT05, DES05] while others explored the field of blast mitigation by experimental tests giving a fruitful validation for the previous work [RAT06, RAD06, McS06, TAG10].

4. Presentation of multi-objective optimization methods

This new class of materials offers tremendous possibilities in terms of design with wide prospect of multifunctional applications. In industry, design often means multi-objective optimization under multiple constraints. In the case of architected materials, the semi-continuous nature of the design space (discrete for materials and continuous for dimensions) could make the optimization very complex. Thus, this section focuses on optimization methods. After introducing some generalities about optimization, a closer look will be given to multi-objective methods and to the different algorithms dedicated to solving this kind of problems.

4.1. Generalities

Optimization is a field of mathematics often involved in decision guidance [EHR05, COL02]. In this field, one wishes to minimize or maximize a function in order to guide the decision-maker to the best choice. In more specific terms, the design variables that will minimize (or maximize) the objective function have to be found while respecting the constraints set to the problem. In the following, a minimization problem is considered, reminding that maximization can easily be translated into minimization just by taking the inverse of the objective function.

Optimization problems can be found in our daily life. Sometimes, they are not expressed in mathematical terms. For example, let us consider a common person willing to buy a car. Here the design variable is the car. Assuming that the constraints imposed by this person are the maximal price, transmission type, motorization type and volume of trunk as well as number of passengers, then the objective function is to be defined. The most obvious one is price. Now, the problem is to find out the least expensive car having a manual transmission, a diesel engine, five passengers seats, and a 300 litre trunk while having a price lower than 20 k€. From a mathematical point of view, d is the variable (the car), f is the objective function ($f(d)$ is the car price), and g_i are the constraints with i from 1 to 5.

The problem is then reformulated as:

$$\underset{d \in D}{\text{minimize}} f(d), \quad (2.13)$$

$$\text{under constraints} \begin{cases} g_1(d) \leq 20\,000, \\ g_2(d) = \text{manual}, \\ g_3(d) = \text{diesel}, \\ g_4(d) = 5, \\ g_5(d) \geq 300, \end{cases} \quad (2.14)$$

With:

$$\begin{cases} D = \{\text{Ford}, \text{Citroën}, \text{Toyota}, \text{Mercedes}, \text{Ferrari}\}, \\ g_2(d) \in \{\text{manual}, \text{automatic}\}, \\ g_3(d) \in \{\text{essence}, \text{diesel}\}, \end{cases}$$

Assuming that the Mercedes is equipped with an automatic transmission and that its price is higher than 20 k€, constraints 1 and 2 are then violated. Ferrari car is a 2 passengers car and the trunk volume is lower than 300 litres while the price is far too high regarding constraint 1. The only feasible solutions, those that respect all the constraints, are Ford, Toyota and Citroën. Now, if we consider for simplicity that Citroën has the lowest price among all the feasible solutions, then this optimization problem is solved and the solution is straightforward.

Now, a more classical example is taken, which is the minimization of a continuous mathematical function. The problem is formulated as:

$$\underset{d \in D}{\text{minimize}} f(y_1), \quad (2.15)$$

$$\text{under constraint } \{g: y_1 \geq 1, \quad (2.16)$$

With $f(y_1) = y_2 = (y_1)^4 - 6 \cdot (y_1)^2 + 10$

This problem is easily solved using a variable substitution and a classical minima search by derivation of the equation. The solution is $\sqrt{3}$ as shown in Figure 2.24.

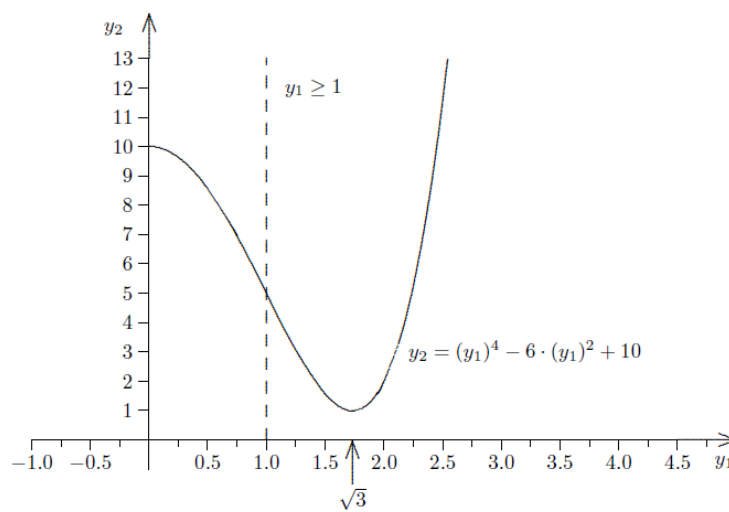


Figure 2.24: Example of a mathematical function minimization under constraint, taken from [EHR05].

Optimal design of architected sandwich panels for multifunctional properties

Pierre Leite

The general form taken by an optimization problem is [EHR05]:

$$\begin{aligned} & \underset{d \in D}{\text{minimize}} \ f(d), \\ & \text{under constraints} \ \begin{cases} g(d) \leq 0, \\ h(d) = 0, \end{cases} \end{aligned} \quad (2.17)$$

with g and h in system (2.17) an array of n inequality constraints and an array of m equality constraints respectively, $g(d) = (g_1(d), g_2(d), \dots, g_n(d))$ and $h(d) = (h_1(d), h_2(d), \dots, h_m(d))$.

Industrial optimization problems are often complex, particularly in the definition of the objective function. Being able to correctly define the constraints and the objective function can be tricky. Let us consider a structural part for which the designer wishes to add some extra-performances such as vibration absorption at minimal weight. The main purpose of the part is bearing loads, and it is expected to be designed in stiffness. The designer will then focus on its stiffness, mass and vibration properties (which will be expressed as a cut-off frequency). Several scenarios can be imagined for the formulation of the optimization problem.

The first step is to set apart constraints from objectives. As the main purpose of this part is to bear load, its stiffness must not be lower than a critical value; then there is a constraint on the stiffness even though mechanical performance is its main objective. Considering mass and vibration properties as performances, two constraints and two objectives can be defined in relation to those performances. Then three cases can be considered:

Minimize mass u.c. $\begin{cases} \text{stiffness} \geq r_{lim} \\ \text{frequency} \geq f_{lim} \end{cases}$	Maximize cut-off frequency u.c. $\begin{cases} \text{stiffness} \geq r_{lim} \\ \text{mass} \leq m_{lim} \end{cases}$	Minimize mass and maximize cut-off frequency u.c. $\text{stiffness} \geq r_{lim}$
--	--	--

The third case is a multi-objective problem for which usual methods are not adapted.

4.2. Multi-objective optimization

In the case of a multi-objective optimization, the mathematical formulation of the problem is the same than in (2.17) but with f being an array of objective functions. It has to be noted that the meaning of minimization and maximization in multi-objective optimization needs to be redefined. Indeed, objective functions can be contradictorily in the sense that improving one could lead to deteriorate the others. Here, appears the notion of trade-off between objectives. Then, two kinds of methods can be found. The first one consists of defining a type of trade-off before performing any calculation in order to find a unique solution. This is the “a priori” approach. The second kind is based on a dominance notion in order to find out a set of solutions forming a trade-off surface. This is the “a posteriori” approach. More detailed information can be found on these methods in [EHR05] and [COL02].

A priori methods

This method consists of getting back to a mono-objective problem as in (2.17) to find out a unique optimal solution. It is also known as an aggregative method as it aggregates in some manner the different objectives. The easiest way to do so is to use a weighted sum of objectives and to consider this sum as the objective function to minimize. This implies that weights can be

determined and that all objectives are comparable between each other. Accordingly, it can be of interest to normalize the objective functions and to use dimensionless expressions. The main difficulty is still the determination of weights which is a subjective choice from the decision-maker. Moreover, if the problem involves quantitative and qualitative objectives, expressing the sum can be a sensitive issue.

Another type of aggregative techniques is based on the idea of an ideal point. The multi-objective problem is translated into the minimization of the distance between the optimal solution and the ideal point, which is often utopian. Once again this implies being able to define correctly and wisely the ideal point. Among the techniques based on this idea, the MinMax and Target Vector Optimization techniques are the most famous ones.

Another way to go from multiple criteria to single criterion is to transform objectives into constraints. The ϵ -constraints technique proposes to optimize the most important objective, according to the decision maker choice, while setting constraints on the other objectives. The critical values used for the constraints have to be determined first.

However, another technique, the lexicographic optimization, is able to go over this determination by ranking objectives in a hierarchical manner. The most important one will be treated without constraints leading to the optimal value for this objective. The second objective is then optimized with a constraint on the first objective, setting up its value equal to the optimal solution found in the early stage. That way, all objectives are treated by transforming the objectives already optimized into constraints related to the optimal values that have been found.

A posteriori methods

Unlike aggregative methods, the use of a trade-off notion leads to a group of solutions with different trade-offs according to the considered trade-off notion. As an example, let us consider again the example given before of a common person willing to buy a car. To the minimization of the car price, the minimization of fuel consumption is added as second objective. The only cars respecting the constraints were Ford, Toyota and Citroën. Price and fuel consumption are represented schematically in Figure 2.25:

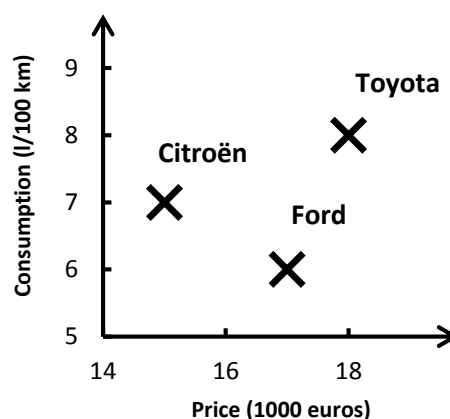


Figure 2.25: Multi-objective optimization example with a trade-off notion.

It has been noticed that Citroën minimizes price, but by looking at the fuel consumption, Ford is a better solution. In every case, Toyota is not an optimal choice as it is dominated by Ford and Citroën. The two latter exhibit a different trade-off between price and consumption. Then they

Optimal design of architected sandwich panels for multifunctional properties

Pierre Leite

are both optimal and the final choice has to be taken by the decision-maker according to the interest between price and consumption.

This approach based on a trade-off notion can be generalized to multi-objective problems by using the Pareto dominance [PAR96]. The trade-off surface composed by all the optimal solutions is called Pareto front. This front can sometimes be considered as a part of the frontier of the solutions plotted in the performance space (space obtained by plotting the objective function value on the axis of a graph). To define this front, a dominance notion is to be defined in order to compare two solutions between each other. Then, a solution a is dominated by b if for every objective, the value of the objective function applied to a is higher or equal to the value of the objective function applied to b and that at least one objective can be found for which b is strictly better than a :

$$"b \text{ dominates } a" \Leftrightarrow b < a \Leftrightarrow \begin{cases} \forall i \in \{1, 2, \dots, n\}, f_i(b) \leq f_i(a), \\ \exists j \in \{1, 2, \dots, n\}, f_j(b) < f_j(a), \end{cases} \quad (2.18)$$

The most striking example is the one for which b is strictly above a for every objective, because it clearly appears that b dominates a in that condition. When there is no dominance between two different solutions, they are considered as equivalent in a Pareto sense. This was the case for Ford and Citroën in the example given before. Then the Pareto front is the group of non-dominated solutions. For every solution A , a cone of dominance can be defined as the area where, if any solution is found, this solution will dominate A . Graphically, considering a bi-objective problem, the Pareto front is defined as the group of solutions for which there is no solution in the cone of dominance (see Figure 2.26).

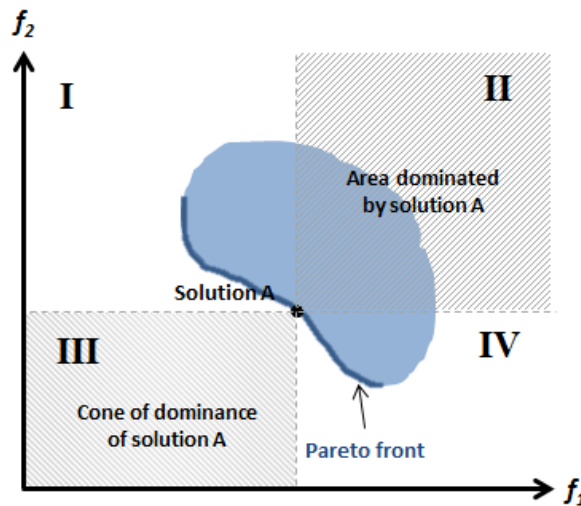


Figure 2.26: Illustration of a performance space. The plotted domain represents achievable solutions as a function of their fitness value f_1 and f_2 . A part of the frontier which gathers the non-dominated solutions is also called the Pareto front or trade-off surface. Non-dominated solutions are the ones for which no achievable solutions are present in their cone of dominance.

In Figure 2.26, the blue area represents the set of feasible solutions, the dark blue line being the Pareto front. The area II is the area dominated by A while area III is the cone of dominance. Areas I and IV are the area of Pareto equivalence.

The main interest of Pareto set optimization is to simply manage multiple criteria by using a ranking relation. However, two properties of the method can be considered as drawbacks. First,

all objectives have the same importance during the optimization process. Then, no objective is considered minor given that invested resources to solve it are the same as for the major ones. The user can then be tempted by the fact of setting some objectives as constraints at the risk of losing some information. Secondly, the set of optimal solutions can have a very large size and theoretically be infinite. Indeed, for geometrical design variables defined as a continuous variable, the Pareto front can be constituted by solutions with a continuous evolution of the design variable. The size of the Pareto front can become hardly manageable in terms of computing resources. It can also be a drawback for the decision-maker who will have to choose between numerous possibilities.

Alternatives to the Pareto dominance exist for multi-objective optimization problems. Among them, game theory such as Nash's equilibrium is able to handle multiple criteria. The main drawback is related to the fact that those methods are often developed to lead to a unique solution.

To conclude, aggregative methods allow the simplification of the problem by transforming multiple criteria into a single one. However, this is possible only by taking a priori decisions which are not always easy to take and certainly not objective unless further information is provided. "A posteriori" methods are more complex and more time-consuming as they need to explore the design space regarding several directions. However, the quantity of information obtained is much larger. From an industrial point of view, the possibility to make optimal choices a posteriori allows a strategic readjustment of objective weights which is appreciable for decision-makers and is certainly in line with material selection methods [LAN00]. This is why this study will mainly use Pareto set optimization.

4.3. Optimization algorithms

The Pareto dominance notion helps to understand what minimization means in a case of multiple criteria, yet it has to be coupled with optimization algorithm in order to explore the design space and to trace the solutions in the performance space. These algorithms explore the design space and use the Pareto dominance to converge to the Pareto front. There are many possible algorithms for that purpose. Two main types of algorithms can be identified, the deterministic ones and the stochastic ones. In this part, the most known algorithms will be shortly introduced. More detailed information will be given concerning genetic algorithms which are the better choice for the present application.

4.3.1. Deterministic algorithms

Deterministic algorithms, also known as exact methods, have the property of leading to an invariant solution when starting from the same input. The algorithm will pass through the same calculation steps to converge to a unique solution for a given problem. Usually, these algorithms use a starting point and assess the best direction in a neighbourhood of the current point to move and converge to the closest optimal solution. The best direction is the one that allows the highest minimization of the objective function.

Gradient based algorithms

The gradient based algorithms are surely the most frequently used optimization algorithms. They are based on the hypothesis that the derivative of the objective function is known and continuous all over the design space [MIN83]. Then, at each step the algorithm estimates the direction with the lowest value of objective function derivative, the one with the lowest slope.

Optimal design of architected sandwich panels for multifunctional properties

Pierre Leite

The main drawback of this kind of methods is its limited range as only the closest local optimum can be found. The system may get “stuck” in a local optimum. Then, the starting point choice is crucial to find the global optimum. However, this difficulty can eventually be overcome by the use of a “multi-start” approach. This evolution consists of running simultaneously several searches using several starting points scattered in the design space, thus increasing the chances to find out the global optimum. Still, the hypothesis on the regularity of the objective function is very strong and can be very sensitive.

Nelder-Mead's simplex

Gradient based algorithms are very efficient when applicable, however the objective function must be derivable. In the 1960's, Nelder and Mead developed an algorithm which is similar in its essence but which settled the problem of function derivation [NEL65]. The simplex method, also known as Nelder-Mead's algorithm, is based on a construction of a set of points, called simplex, which are used to assess the best direction search. This direction is evaluated by comparing the objective function value of each point forming the simplex. This algorithm is still a local optimization algorithm as the solution will depend on the starting simplex.

Branch and bound algorithm

The last deterministic algorithm presented here is the branch and bound algorithm [LAN60]. The main idea is to branch the design space and to bound the value of the objective function in each parts. Then, some parts can be set apart from the search process and the remaining search space is once again branched. Iterations should lead to the optimal solution. This method can be efficient if the bounds can easily be found and if the design space is wisely branched.

4.3.2. Stochastic algorithms

Stochastic algorithms are approximate methods as they are based on random process, particularly on creating and choosing the search points. Heuristics are used to explore the design space and to converge to the optimal solution. This way, the optimum obtained with a stochastic algorithm can differ for a given problem depending on the random exploration process.

Monte-Carlo

The most familiar stochastic algorithm is the Monte-Carlo algorithm [FIS97]. This technique starts from an initial solution and generates random search point using a probabilistic law (a Gaussian law for example). If the objective function value of the search point is better than the one of the current point, then the search point becomes the current point and a new search point is generated from it. Otherwise a new search point is generated from the last current point. Search continues while an ending condition is met. Several ending conditions can be found. Usually, this allows the calculation time to be bounded. A simple, yet useful, ending condition is to define a maximum number of iterations, after which optimization stops and the best solution that has been found is set as the optimal solution. Another ending condition which is more meaningful is to define a number of iterations and a progression ratio. If after this defined number of iterations, the best solution has not been improved by more than the progression ratio, then the solution is considered as stable and the optimization stops. If those parameters are wisely chosen, the obtained solution should be close enough to the global optimum to be acceptable within a relatively short calculation time.

Simulated annealing

The simulated annealing algorithm is inspired by the metallurgical process of annealing [KIR83]. As for a Monte-Carlo process, the algorithm starts with an initial point and generates randomly new solutions. If this search point is better than the current point then there is replacement. Otherwise, a random process following a probabilistic law related to a characteristic temperature is used to decide whether the search point is chosen or not. Then, even though the search point is not better, it can be chosen which allows a better exploration, and thus preventing the algorithm from getting “stuck” in a local optimum.

The probabilistic law is built so that at the beginning of the exploration process, the probability to accept a bad search point is high, then the exploration ability of the algorithm is improved. This exploration ability will decrease with time and then at the end of the process, the algorithm will converge following a process similar to Monte-Carlo’s one. This sequence mimics the physical processes during the cooling down of a metal. This is translated into the probabilistic law by a characteristic temperature that will be high at the beginning of the process and that will decrease with time. A multi-start approach can be used to accelerate the optimization process.

Tabu search

The Tabu search process is a local optimization process [GL097]. Starting from an initial point, the neighbourhood is analysed and chose the best neighbour which becomes the current point. It is to be noticed that this new point can be worse than the previous one. In order to avoid returning back to the last point, a list of unauthorized displacement is created and actualized during the process. This list is called the Tabu list. It has a predefined size. Then the exploration ability of the algorithm is related to the size of the list. The unauthorized displacements go out of the list after a certain time. The algorithm stops after a given number of iterations and the optimal solution will be the best solution found during all the process. This method is suited for global optimization as it can get out from a local optimum which is in the Tabu list.

Genetic algorithm

Genetic algorithms are the most famous ones among the evolutionary algorithms [HOL75, GOL89]. Its process is inspired by Darwin’s theory of evolution. By analogy, a solution will be called an individual and a set of solutions will be called population. Individuals are coded such as a genotype. This genotype gathers the design variables values. Contrary to most of the optimization algorithms, it does not start from a unique initial point but from an initial population. Moreover, it is based on a fitness notion of individuals which allows a comparison between them. It can easily be adapted to multiple criteria by selecting a ranking relation as fitness type and then it can easily be coupled with the Pareto dominance notion.

4.3.3. Comparison between algorithms

The advantages/drawbacks of deterministic and stochastic algorithms are summarized in Table 2.2. Given the specificities of our optimization problem (continuous and discrete variables, search of multi-objective optimum) stochastic algorithms should be the most adapted class of algorithms. Indeed, multiple criteria are more easily taken into account when the search is driven by a notion of fitness instead of a notion of direction. Among the stochastic algorithms,

Optimal design of architected sandwich panels for multifunctional properties

Pierre Leite

genetic algorithm has been chosen for the present study as it is a familiar approach in designing layered materials.

Table 2.2: Advantages/drawbacks of the two main classes of algorithms.

Class of algorithm	Advantages	Drawbacks
Deterministic	<ul style="list-style-type: none">• Accurate• Quick convergence/low number of evaluations	<ul style="list-style-type: none">• Local optimization• For continuum variables• Based on a direction notion
Stochastic	<ul style="list-style-type: none">• Global optimization• For every type of variables• Based on a notion of fitness	<ul style="list-style-type: none">• Requires high memory capacity• Requires high number of evaluations• Based on probabilistic phenomena

4.4. Genetic algorithm

The genetic algorithm used for this work is taken from the Dakota software [DAK] and a more detailed presentation of this algorithm can be found in [EDD01]. Advanced details are provided in Chapter 3, Section 4.

Algorithm architecture

Input variables:

- Population size: N_p
- Cross-over rate: T_c
- Mutation rate: T_m
- Maximum number of iterations: N_g
- Improvement rate: T_a
- Critical number of generation: N_l

Steps:

1. **Initialisation:** generation of a population of size N_p , this population being noted P_0 .
2. **Evaluation:** evaluation of the objective functions value for each individual of the population.
3. **Cross-over:** creation of new individuals by cross-over and their injection in the current population. The number of cross-over performed is equal to $T_c \times N_p$.
4. **Mutation:** creation of new individuals by mutation and their injection in the current population. The number of mutation performed is equal to $T_m \times N_p$.
5. **Evaluation of the new individuals:** evaluation of the objective functions value for each new individual.
6. **Fitness assessment:** evaluation of the fitness of individuals.
7. **Selection:** selection of the individuals following a probabilistic law depending on the fitness of individuals and creation of a new population P_{t+1} constituted by the selected individuals. The more the individual fits, the best chance it has to be selected.
8. **End condition:** if the end condition is met, the algorithm stops; otherwise it goes back to step 2 and $t \rightarrow t+1$.

An iteration corresponds to a step going from t to $t+1$. The obtained population after cross-over and mutation is called generation (this is on such a population that selection will be operated).

Genetic operators

Cross-over and mutation are called genetic operators. Cross-over is the one allowing convergence of the algorithm. What is expected is that by crossing the genes between two good solutions, an even better one is created. Several types of cross-over can be used. The one chosen for this work is the shuffle random consisting of randomly choosing one of the parents as the donor for each gene. This process is illustrated in Figure 2.27.

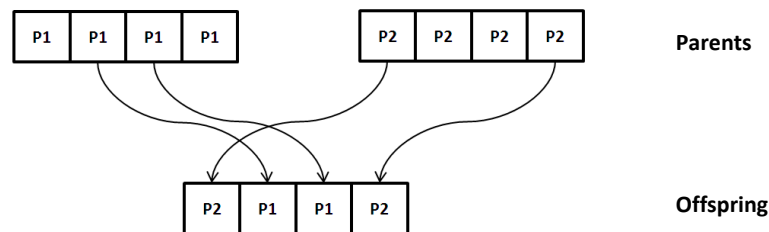


Figure 2.27: Illustration of the cross-over behaviour.

Mutation on its own is the operator ensuring good exploration ability. By randomly creating a new individual, it is expected that all the design space will be explored. This will prevent from being trapped into a local optimum. Once again several mutation types exist. Among them, the chosen one is the “replace uniform” which consists of randomly choosing one gene and assigning a random value taken from the possible values. This point is illustrated in Figure 2.28.

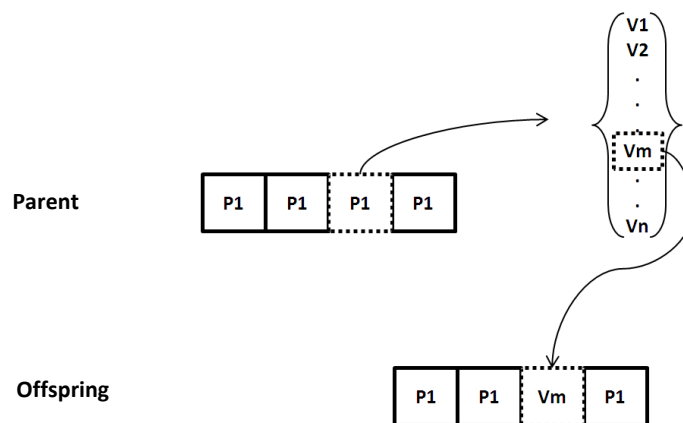


Figure 2.28: Illustration of the mutation behaviour.

The strength of genetic algorithms is to be able to explore a local area while still exploring the design space simultaneously by means of the two genetic operators.

Fitness assessment and selection

Fitness assessment is used to select the most promising individuals for future reproduction. It is this part of the algorithm that made it called an evolutionary algorithm. The selection method

Optimal design of architected sandwich panels for multifunctional properties

Pierre Leite

will mainly depend on the fitness assessor choice. One option is to use a domination count. For each individual, the number of dominating individuals can then be counted and is taken as the fitness value. Then, a non-dominated solution has a fitness of 0 as no dominant can be found. The associated selection method is the below limit method which consists of selecting only the individuals that have a fitness lower than a given value n , i.e. the individuals that have no more than n dominants. This parameter n is to be defined knowing that, the algorithm will be elitist if it is too small and the algorithm will not be selective enough to be efficient if it is too high.

Other selection approaches are based on the notion of rank. Non-dominated solutions are assigned the rank 0. The solutions of rank 1 are determined by identifying the non-dominated solutions when all solutions of rank 0 are deleted from the performance space. The solutions of higher order will be identified using the same scheme. This notion is illustrated in Figure 2.29.

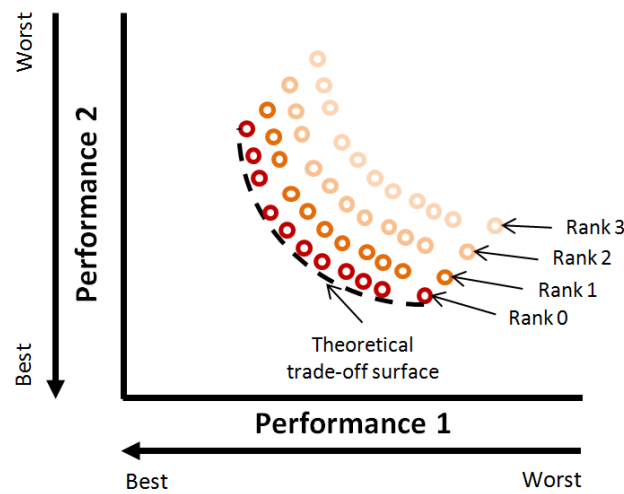


Figure 2.29: The rank of a solution depends on its distance to the trade-off surface. Non-dominated solutions are assigned the rank 0. The ranks of higher order are determined as described in the text.

End condition

The ending condition can be a condition on the number of calculation or a stability condition. Both conditions can be considered simultaneously to prevent from having a calculation time too long and to end up the algorithm by rapid convergence towards a stable solution. The stability condition consists of verifying if the population has improved of more than T_a after N_i generations. If so, the algorithm continues, if not the algorithm stops. Usually the optimal solution is identified after the end of the algorithm by analysing all the obtained solutions in order to correct the bias induced by the use of a stochastic process.

Chapter 3

Design process

The design of architected sandwich panels requires a dedicated design process. Starting with the principles of the proposed design process, which is based on the use of a genetic algorithm and of a materials database, two different paths are defined. The first path is based on a material selection performed on a list of existing materials. This is the “real path” approach. The second path is based on a semi-continuous description of the core material. This is the “virtual path” approach. The differences and specificities of each path are presented and discussed.

Optimization process exploits several models in order to evaluate the fitness of the generated solutions. These models are presented in Section 2, according to the properties they are assumed to evaluate.

Section 3 aims at familiarizing the reader with several notions regarding the performance space and the trade-off surface. The trade-off surface is the group of optimal solutions. According to its shape, one can assess the compatibility between the optimized functions. A discussion on the meaning of these shapes will help understand the results displayed in Chapters 4 and 5.

More details on the optimization algorithm used in the present work, DAKOTA MOGA, are provided in the last section.

Chapter contents

1. Principles	81
1.1. Process: individuals – evaluation – selection	81
1.2. Specificities of discrete/continuum problems	82
1.3. Path for material selection in the optimization process	85
1.3.1. Optimization based on a discrete database – “real path”	85
1.3.2. Optimization based on a semi-continuous database – “virtual path”	86
2. Analysis of properties	91
2.1. Mass	91
2.2. Flexural properties	91
2.3. Thermal properties	93
2.4. Acoustic damping.....	96
2.5. Blast mitigation	97
3. Performance space	101
3.1. Assessment of compatibility through Pareto front shape	102
3.2. Assessment of design variable influence.....	106
4. Genetic algorithm/implementation (DAKOTA)	108
4.1. Interfacing between analysis tools and optimization algorithm	108
4.2. Specificities of DAKOTA MOGA.....	109

1. Principles

In order to investigate the interactions between performances and the influence of design parameters, trade-off surfaces will be drawn. These surfaces are extracted from the performance space which is filled during the optimization process. This chapter will focus on the methodology used to determine the trade-off surfaces. The first section will briefly introduce the optimization process. Then, specificities of discrete and continuous design space in optimization problems will be discussed while the last section will focus on the two possible paths for selecting materials that have been used for the present study.

1.1. Process: individuals – evaluation – selection

The obtention of trade-off surfaces is based on an optimization loop involving an algorithm of optimization, the design space, the analysers and the performance space. As shown in Figure 3.1, the genetic algorithm starts by generating an initial population of individuals in the design space. The latter can be either continuous such as the geometrical variables, discrete such as a list of materials or both such as a list of composites or foams with a continuous variation of reinforcement volume fraction or porosity. The specificities of continuous and discrete design space will be introduced in the next paragraph. The number of individuals in the initial population is important as the population has to be representative of the whole design space. If the population is too small, a large number of generations could be required in order to converge, with a risk of remaining “stuck” into a local optimum. On the other hand, if it is too large, the number of evaluations per generation will increase the computing time. Let us consider an optimization problem with several design parameters which can take a pre-defined number of values in their range. As an empirical rule, a limit number of individuals in the initial population should be at least of the same order of magnitude than the highest number of possible values for the design parameters. Depending on the computational cost of the analysis tools, the initial population size will be taken as five to ten times this limit number. For example, if the design variables can have a hundred different values, the initial population size will lie between 500 and 1 000.

Once the initial population identified, the individuals are evaluated using the “analysis tools” presented in Section 2 of this chapter. In this stage, the array corresponding to the design parameters is transformed into an array corresponding to the values of objective functions defining the “performance space”. According to these values, the performance space is filled by the evaluated solutions. In order to perform the evaluation, the array of design parameters has to be transformed into a suitable form to be interpreted by the analysis tools. An interface is used to transform the files given by the genetic algorithm into inputs to the models used.

Once evaluated, solutions are ranked according to their “fitness value”. This ranking can be interpreted as the distance between the solution location in the performance space and the partial Pareto front. This fitness value is used to determine the probability a solution will have to be selected for the reproduction process, and this by using genetic operators described in Chapter 2 Section 4.4. These operators will create a new population that will be evaluated afterwards. To promote evolution, the next population will be constituted of the best solutions taken from the combination of the initial pool and of the new ones evolved by reproduction, as illustrated in Figure 3.2. This new population becomes the actual pool on which reproduction,

evaluation and selection will be performed. Thanks to genetic operators, the design space will be explored and the population will converge to the group of non-dominated individuals allowing the identification of the optimal solutions.

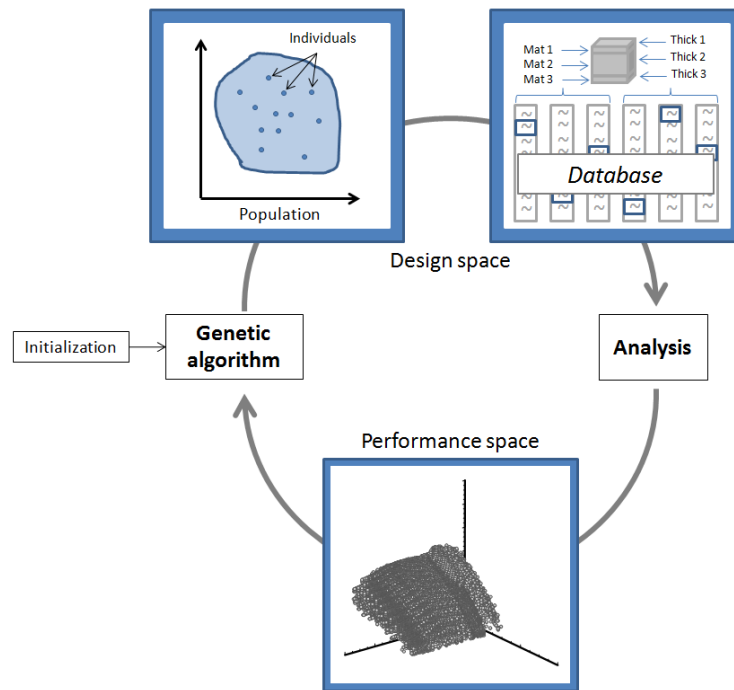


Figure 3.1: Optimization loop.

1.2. Specificities of discrete/continuum problems

The design space can be either continuous or discrete depending on the nature of design parameters.

When these variables are real numbers, there are two main options to define them:

- The first definition consists of determining a set of real numbers which often corresponds to a proper discretization of the range of possible values. The number of possible values can be tailored in order to monitor the computing time of the optimization process. The discretization can be homogeneous, meaning that a step size can be chosen, thus leading to a given number of possibilities. It can also be heterogeneous, especially if the design parameter is anticipated as having a specific behaviour in a limited range. In this case, the range of possible values is defined by its cardinal and the values within it.
- Design variables can also be defined by their entire range with two limit values. In this case, the algorithm can select any real value within this range. A minimal step size can be defined in order to avoid the algorithm to fall under a certain decimal place. Continuous design variables generally refer to physical parameters such as geometrical parameters or intrinsic properties. As a consequence, objective functions are often differentiable in relation to these parameters. In this case, deterministic optimization algorithm can be more efficient than stochastic ones and are more suitable to deal with a continuum design space.

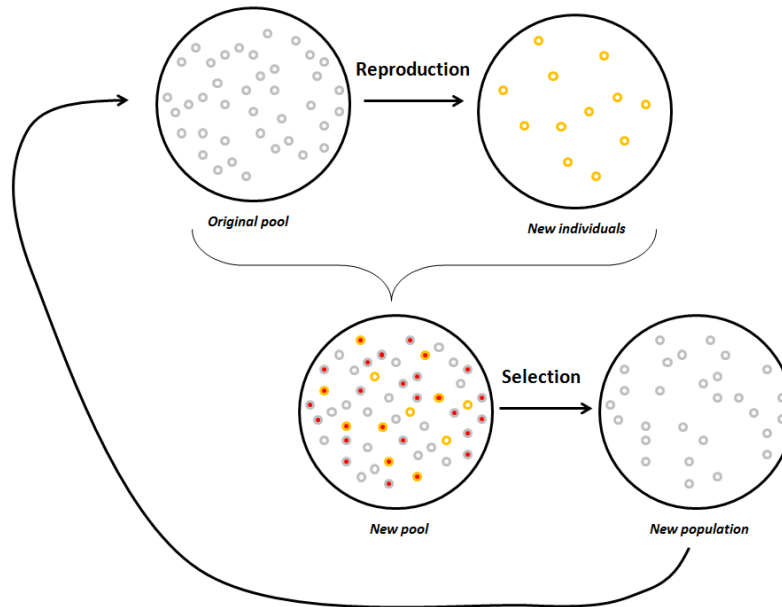


Figure 3.2: Creation of a new population based on an original pool and using reproduction and selection tools.

Some design parameters can be defined by discrete values, as a unit of the corresponding quantity cannot be divided into pieces. For instance, one can refer to a situation which is not a numerical quantity such as a given chemical composition or a particular process. In this case, the design parameter can take a value corresponding to the situation ranked in the list of possible situations.

For material selection problems, two main possibilities can be considered:

- Usually in computational mechanics, material is considered as a continuum defined by its materials properties that are properly bounded. The considered bounds should take into account materials possibilities and existence. Thus, the optimization problem is transformed into an inverse problem where the optimal material properties are known by calculation and where the corresponding material is to be identified. Ensuring the existence of this material can be difficult. Usually, the distance between the closest solution and the optimal virtual material is to be minimized. This approach has been used for example in the optimization of composite structures [IRI11a].
- However, in engineering design, material selection is more often performed on a materials database. Then, material is considered as a discrete value corresponding to an entry in this database. This entry is associated with relevant properties. This approach is in line with material selection techniques such as performance indices.

In the particular case of architected sandwich panels, two possibilities can be taken into account, as illustrated in Figure 3.3:

- The sandwich panel can be considered as a homogenous medium. Each possible sandwich panel would be represented by its calculated apparent properties. Sandwich panel selection could then be performed on a discrete database composed of a list of sandwich panels or on a continuous design space. If the last option is taken, the inverse problem would be summarized as determining the combination of

Optimal design of architected sandwich panels for multifunctional properties

Pierre Leite

materials and thicknesses that exhibit effective properties as close as possible to the optimal calculated solution.

- A more intuitive option is to consider the sandwich panel as the combination of three layers, every one described by its own properties. Once again, for each layer, material can be selected on a list of materials or described by its material properties with the freedom to vary in bounded ranges. The inverse problem is slightly less complicated as the problem is transformed from finding a sandwich panel with equivalent properties to finding materials with required material properties. However, the identification of the optimal core material given a certain mechanical behaviour is still sensitive. The number of design parameters will be increased as the media is divided into three subsets.

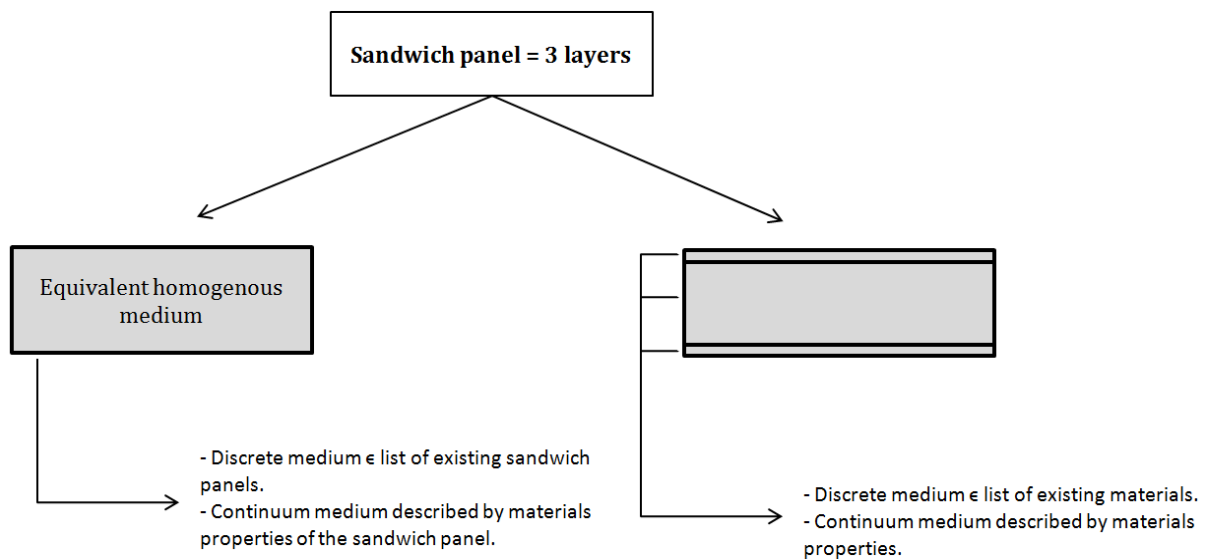


Figure 3.3: The two different ways of selecting sandwich panels. One approach is to describe the sandwich panel as a homogenous equivalent medium that can be selected either on a discrete or a continuous database. The second approach is to describe it as the combination of three layers, each layer being selected on a discrete or continuous database.

The last possibility is to consider an intermediate path, by considering a discrete/continuous description. The thickness of the layers will be considered as continuous variables while the material will be referenced in a materials database. This implies four to six design parameters considering the sandwich as symmetrical or unsymmetrical respectively. It is possible to go deeper in the description of the architected core material given that the medium can be described by continuous parameters corresponding to the geometrical pattern and by a discrete parameter corresponding to the constitutive material. One of the advantages of this description concerns the fact that it is based on the same kind of database used for material selection in engineering design. Moreover, decoupling thickness and material of each layer will help determine the relative importance of each type of design variables.

For the present study, a discrete/continuous description of the sandwich panel is used by considering thicknesses as continuous parameters and material selection as based on a materials database. Then the design space is partly discrete, partly continuous. Specifications on the path for material selection are given in the next section.

1.3. Path for material selection in the optimization process

In order to perform the analysis presented in the next section, several material properties are required for each layer constituting the sandwich panel. The face sheets are considered as dense materials and their properties can be extracted from a materials database. Core materials can be considered in two different ways. In a first approach, core material selection can be performed on a database, in which actual materials are referenced with their effective properties. This approach is called optimization by “real path” and is based on a discrete core design space. In the opposite approach, materials such as architected materials (foams, honeycombs, trusses) can be described by their geometrical pattern and the constitutive material. Scaling laws are then used to evaluate the effective materials properties as a function of geometrical parameters and of constitutive materials properties. It is clear that the range of achievable materials using this approach is wide and exceeds the range of real materials. This approach is called optimization by “virtual path” and is based on a semi-continuous core design space.

1.3.1. Optimization based on a discrete database – “real path”

In an optimization by “real path”, materials are all referenced in a materials database in which general properties are specified. In this kind of database, dense materials such as Steel or Aluminium are indicated, but also hybrid materials (composites or foams and honeycombs). Materials are then defined in the database by several entries, for example the chemical composition for alloys or a constitutive material and an effective density for foams. Data can be extracted for each material, for instance Young’s modulus, yield strength, thermal conductivity, density and so on. An example of materials property chart is given in Table 3.1 for Aluminium alloy.

Table 3.1: Example of an entry of the material database.

Property (symbol)	Value	Unit
Name	Aluminium alloy 7075	-
Density (ρ)	2820	kg/m ³
Price (P)	1.08	€/kg
Compressive strength (σ_c)	505	MPa
Elastic limit (σ_y)	505	MPa
Loss coefficient (η)	0.00105	-
Poisson’s ratio (ν)	0.33	-
Shear modulus (G)	26.4	GPa
Tensile strength (σ_{str})	570	MPa
Young’s modulus (E)	72	GPa
Max temp in service (T_{max})	140	°C
Specific heat capacity (c_p)	862	J/kg.°C
Thermal conductivity (k)	134	W/m.°C
Thermal expansion (α)	23.5	μstrain/°C

The considered face materials are made of metals, plastics and composites. The database that has been used gathers 85 metals and alloys, 30 ceramics, 17 polymers and 26 composite materials. Regarding the core material, only foams have been taken into account in the optimization by “real path”, but with a large number, i.e. 107 different foams, representing all

Optimal design of architected sandwich panels for multifunctional properties

Pierre Leite

types of foams (metallic, polymeric and ceramic). The property chart giving Young's modulus as a function of density for the materials listed in the database is plotted in Figure 3.4.

This is a reduced database compared to the whole set of available materials, but including representative materials. It is a starting point to develop and test the actual design process.

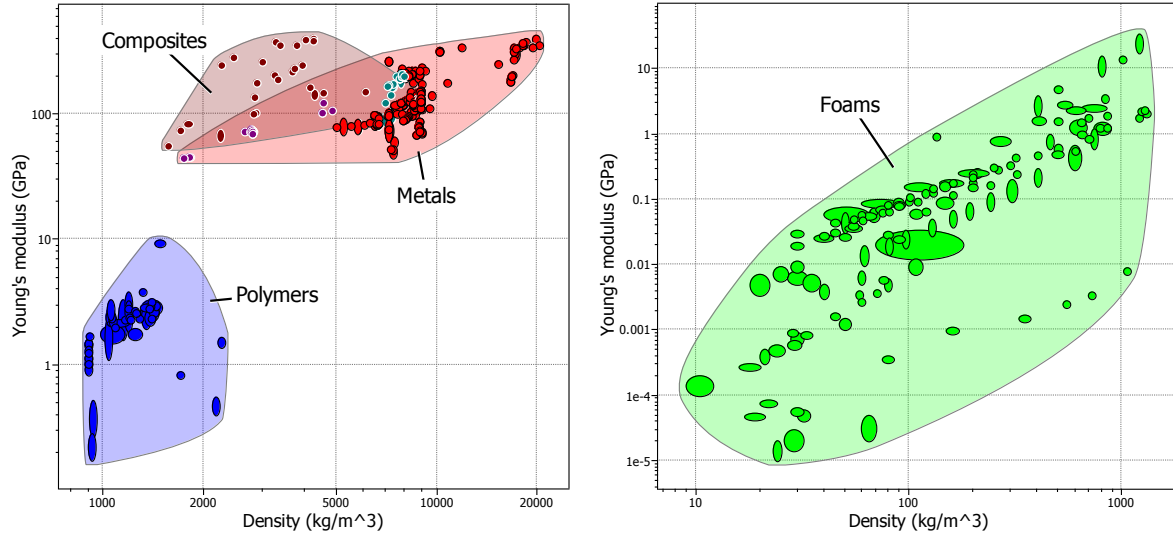


Figure 3.4: Property charts illustrating the materials listed in the database: Young's modulus as a function of density. On the left hand side: face materials. On the right hand side: core materials. Taken from the CES software.

During the optimization process, the algorithm of optimization will “build” sandwich panels to determine a population. Actually, the algorithm will define a sandwich panel by choosing three materials in the database and three thicknesses in the range of possible thicknesses, one for each layer of the panel. The simpler case is the one of a symmetrical sandwich panel for which only two materials (core and face) and two thicknesses (core and face thicknesses) are to be defined.

The design space is then of dimension 4 or 6 for symmetrical or asymmetrical sandwich panels respectively. As mentioned previously, in the algorithm, a panel is represented by an array. Let us consider an asymmetrical sandwich panel, then the algorithm will define a set of arrays of length 6 with 2 numbers corresponding to the entry in the database of face materials, 1 number corresponding to the entry of a core material and 3 thicknesses.

Since materials are referenced in the database, one main advantage of this method is that they are usually available from some suppliers. Moreover, their properties are already known and can be used to run calculation in order to evaluate the performances of the sandwich panel. This approach will help highlight the benefits of using sandwich structures over monolithic solutions. The relative importance of core design over face design will be discussed using this approach.

1.3.2. Optimization based on a semi-continuous database – “virtual path”

In an optimization by “virtual path”, architected materials are not directly referenced in a database but are defined by a constitutive material (referenced in the database) and geometrical parameters leading to a partly continuous design space. The length of the arrays defining the panels is greater than 6 (for unsymmetrical panels) and depends on the architecture of the core

material. Three core materials are investigated in this study. Foam is the architecture of reference to be compared to the “real path” approach. Two additional architectures are considered. Both are stretching-dominated architectures in order to compare the properties of bending-dominated over stretching-dominated ones. A regular hexagonal honeycomb is chosen as one of the most current core material used in industry. The last architecture is a tetrahedral truss structure made of cylindrical trusses. This structure has been chosen as a promising architecture from the recent literature. Moreover, it offers an additional degree of freedom compared to honeycombs owing to its mechanical behaviour which is defined by three geometrical parameters (truss aspect ratio, angle and core thickness) while honeycomb behaviour is defined by only two parameters (ratio between wall thickness and length and core thickness).

The constitutive materials are still referenced in the database, but the properties of the architected material are no longer referenced. Using this method implies the introduction of an intermediate step in the calculation process which consists of calculating the architected materials properties according to the constitutive parameters. Equations given below can be used for that purpose, by providing density and effective properties of the architected materials as a function of the constitutive material and of the geometrical parameters.

Foams

Foam properties can be extracted from scaling laws which involve constitutive material properties and relative density ρ^*/ρ_s . These laws are based on the representative unit cell shown in Figure 3.5 and are sum up here:

$$\frac{E^*}{E_s} = C_E \left(\frac{\rho^*}{\rho_s} \right)^2 \quad (3.1)$$

$$\frac{G^*}{E_s} = \frac{3}{8} E^* \quad (3.2)$$

$$\frac{\sigma^*}{\sigma_s} = C_\sigma \left(\frac{\rho^*}{\rho_s} \right)^{\frac{3}{2}} \quad (3.3)$$

$$\alpha^* = \alpha_s \quad (3.4)$$

$$k^* = \frac{2}{3} \frac{\rho^*}{\rho_s} k_s + \left(1 - \frac{\rho^*}{\rho_s} \right) k_g \quad (3.5)$$

with * referring to the effective properties of the foam, the subscript s referring to the properties of the constitutive material and C_E and C_σ being two constants. E , ρ and σ are the Young's modulus, the density and the yield strength respectively. α is the coefficient of thermal expansion, k is the thermal conductivity with k_g the one of the gas filling the void space in the architected material. It is assumed that the only significant thermal mechanisms are conduction through solid and conduction through gas. No convection is taken into account and the considered gas is air. Those equations are taken from [GIB97, ASH00b].

An efficiency factor 2/3 is applied on the contribution of solid conduction in equation (3.5) which corresponds to the effective thermal conductivity of the foam. This efficiency factor takes into account the tortuous shape of the cell walls [GIB97].

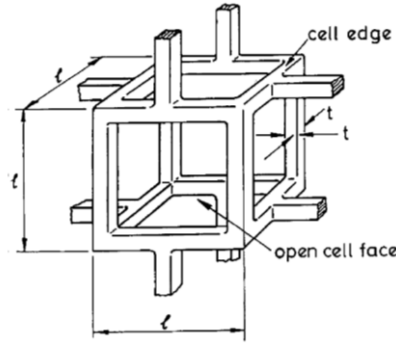


Figure 3.5: Representative unit cell of foams (taken from [GIB97]).

Honeycombs

As for foams, scaling laws have been proposed to determine the macroscopic behaviour of honeycombs. These laws are a function of constitutive material properties and of geometrical parameters. In general, hexagonal honeycombs are defined by the wall-thickness t , cell lengths l and h , finally a particular angle θ as shown in Figure 3.6. In the case of a regular and single walled honeycomb, $\theta = 30^\circ$ and $h = l$ and the only geometrical parameter that remains in scaling laws is the ratio t/l . The corresponding laws are given here:

$$\frac{\rho^*}{\rho_s} = \frac{2}{\sqrt{3}} \frac{t}{l} \quad (3.6)$$

$$\frac{E_{33}^*}{E_s} = \frac{\rho^*}{\rho_s} \quad (3.7)$$

$$\frac{G_{13}^*}{G_s} = \frac{\sqrt{3}}{3} \frac{t}{l} \quad (3.8)$$

$$\frac{G_{23}^*}{G_s} = \frac{\sqrt{3}}{3} \frac{t}{l} \quad (3.9)$$

$$\frac{(\sigma_{plast}^*)_{33}}{\sigma_s} = \frac{\rho^*}{\rho_s} \quad (3.10)$$

$$(\sigma_{el-buck}^*)_{33} = 5.2 E_s \left(\frac{t}{l} \right)^3 \quad (3.11)$$

$$\frac{(\sigma_{pl-buck}^*)_{33}}{\sigma_s} = 5.6 \left(\frac{t}{l} \right)^{5/3} \quad (3.12)$$

$$\tau_{13}^{plast} = \frac{2}{3} \sigma_s \frac{t}{l} \quad (3.13)$$

$$\tau_{23}^{plast} = \frac{2\sqrt{3}}{3} \sigma_s \frac{t}{l} \quad (3.14)$$

$$\tau_{13}^{buck} = \frac{2}{3} \frac{C E_s}{1 - \nu_s^2} \left(\frac{t}{l} \right)^3 \quad (3.15)$$

$$\tau_{23}^{buck} = \frac{2\sqrt{3}}{3} \frac{CE_s}{1-\nu_s^2} \left(\frac{t}{l}\right)^3 \quad (3.16)$$

$$\alpha^* = \alpha_s \quad (3.17)$$

$$k^* = \frac{\rho^*}{\rho_s} k_s + \left(1 - \frac{\rho^*}{\rho_s}\right) k_g \quad (3.18)$$

with t the wall thickness, l its length, E_{33}^* the compressive modulus in axis 3, G_{i3}^* the apparent shear modulus between axes i and 3, $(\sigma_{plast}^*)_{33}$ the compressive yield strength considering yielding of cells, $(\sigma_{el-buck}^*)_{33}$ the compressive yield strength considering elastic buckling of cells, $(\sigma_{pl-buck}^*)_{33}$ the compressive yield strength considering plastic buckling of cells, τ_{i3}^{plast} the shear strength between axes i and 3 considering yielding of cells and τ_{i3}^{buck} the shear strength between axes i and 3 considering buckling of cells. Those equations are taken from [GIB97, ZHA92].

The effective thermal conductivity is considered in the out-of-plane direction as thermal gradient will be in the out-of-plane direction. Unlike for foams, the efficiency factor applied on the solid conduction contribution of the effective thermal conductivity in equation (3.18) is taken as 1. This is a plausible assumption as the cell walls are perfectly plane and in the out-of-plane direction.

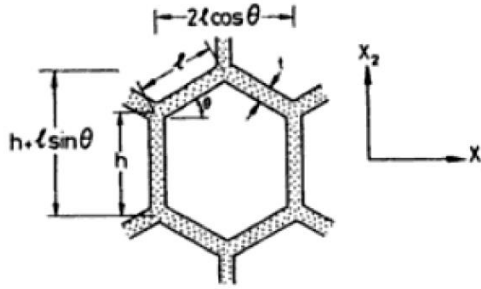


Figure 3.6: Hexagonal honeycomb structure.

Truss structures

The tetrahedral truss structure is defined by truss length l , radius a and the angle ω between the truss and the horizontal axis as shown in Figure 3.7. The mechanical behaviour of this structure as an architected material has led to the development of the following scaling laws [WIC01, FLE01, DES01b]:

$$\frac{\rho^*}{\rho_s} = \frac{2\pi}{\sqrt{3}} \frac{1}{\cos^2 \omega \sin \omega} \left(\frac{a}{l}\right)^2 \quad (3.19)$$

$$\frac{E_{33}^*}{E_s} = \frac{\rho^*}{\rho_s} \sin^4 \omega \quad (3.20)$$

$$\frac{G_{13}^*}{E_s} = \frac{1}{8} \frac{\rho^*}{\rho_s} \sin^2 2\omega \quad (3.21)$$

$$\frac{\sigma_{33}^*}{\sigma_s} = \frac{\rho^*}{\rho_s} \sin^2 \omega \quad (3.22)$$

$$\frac{\sigma_{buck}^*}{\sigma_s} = E \frac{\pi^2}{4} \left(\frac{a}{l}\right)^2 \frac{\rho^*}{\rho_s} \sin^2 \omega \quad (3.23)$$

$$\tau_{13}^{buck} = \frac{\pi^3}{4\sqrt{3}} \frac{E_s}{\cos \omega} \left(\frac{a}{l}\right)^4 \quad (3.24)$$

$$\tau_{13}^{plast} = \frac{1}{4} \frac{\rho^*}{\rho_s} \sin 2\omega \sigma_s \quad (3.25)$$

$$\alpha^* = \alpha_s \quad (3.26)$$

$$k^* = \frac{2}{3} \frac{\rho^*}{\rho_s} k_s + \left(1 - \frac{\rho^*}{\rho_s}\right) k_g \quad (3.27)$$

with a the radius of the struts, l their length and ω the angle between the horizontal axis and the axis directing the struts. These equations as well as the diagrams presented in Figure 3.7 were taken from [DES01b].

The efficiency factor in the effective thermal conductivity is taken as 2/3 like the one for foams. No more information has been found in the literature on the plausible evolution of this factor with the angle of inclination of the trusses.

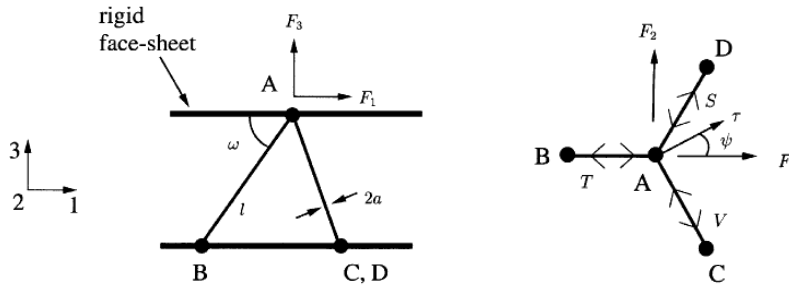


Figure 3.7: Tetrahedral truss structure.

Architected materials and especially foams, are characterized in terms of mechanical properties by their plateau stress and the densification strain. Core failure can occur by different mechanisms, for instance buckling and yielding. Scaling laws are used to evaluate the plateau stress corresponding to each considered mode. For the computation of the effective properties of the material, all the modes are taken into account. Using a lower bound approach, the minimum value of plateau stress is determined and the corresponding mechanism is considered as the limiting one.

The densification strain is given by the following equation [GIB97]:

$$\varepsilon_D = 1 - 1.4 \left(\frac{\rho^*}{\rho_s}\right) \quad (3.28)$$

The main advantage of this method is that an additional design scale is created, which is the one of the architected material. Setting geometry and material as parameters will help to assess the influence of each one as much as their respective weight. However, two main drawbacks can be mentioned. First, this method implies an increase of the dimension of the design space that can impact the optimization speed. Then, the optimization process can define

solutions which are not easy to manufacture. This is a quite sensitive situation since by following a restrictive approach, innovative solutions will not be allowed, whereas by following a not so restrictive approach, no realistic solutions could come out at the end of the optimization process. This issue can be overcome by choosing constitutive materials that can be processed into the considered architected materials and by choosing geometrical values that can be achievable with a classical manufacturing process.

2. Analysis of properties

The analysis step consists in computing the properties of a sandwich from its characteristics in terms of materials and geometry. The emphasis is laid upon simple analytical models.

The performance space plots the evaluated solutions as a function of their performances. In this study, several specifications are considered:

- Mass
- Flexural properties: stiffness and strength
- Acoustic damping
- Thermal properties: thermal resistance and thermal insulation
- Blast mitigation

Some of these performances can be easily evaluated, whereas some others involve much more complicated calculations. Each performance will be briefly commented.

2.1. Mass

The ability of sandwich panels to provide weight saving will be evaluated by the mass per unit area of the panels. Knowing the density ρ of each material and the thickness t of each layer, mass M is then expressed by:

$$M = \rho_u t_u + \rho_c t_c + \rho_l t_l \quad (3.29)$$

In the case of an optimization by “virtual path”, the density of the core material ρ_c is to be calculated using equations given above. Based on usual applications, a mass constraint will be considered in all optimization problems, even when mass is not considered as objective. This constraint is set at 50 kg/m² except for some cases involving blast mitigation for which it is raised to 300 kg/m².

2.2. Flexural properties

Stiffness

Performances of sandwich panels are assessed by considering a three-point bending test. Let us consider a sandwich beam of length L between the supports and of width b which is submitted to a three-point bending test of load F as shown in Figure 3.8. Based on the work of Allen [ALL69], the flexural stiffness of the panel, noted D , can be estimated analytically.

$$D = \frac{E_u b t_u^3}{12} + \frac{E_b b t_b^3}{12} + \frac{E_c b t_c^3}{12} + E_u b t_u (d - e)^2 + E_b b t_b e^2 + E_c b t_c \left(\frac{t_c + t_b}{2} - e \right)^2 \quad (3.30)$$

with E and t the Young's modulus and thickness with subscripts u , b and c referring to the upper face, lower face and core respectively. The variable d is the distance between centroid of the faces, and e is the distance between the mid-thickness of the lower face and the neutral axis.

Optimal design of architected sandwich panels for multifunctional properties

Pierre Leite

Considering a classical sandwich panel made of stiff faces and of a compliant light core, then faces are assumed to deform by bending while the core mainly deforms by shear. The central deflection of the panel is then the combination of a bending term, noted δ_b , and of a term corresponding to pure shear of the core, noted δ_s :

$$\delta_b = \frac{Fl^3}{48D}, \delta_s = \frac{Fl}{4S} \text{ with } S = \frac{Gbd^2}{t_c} \text{ where } G \text{ is the shear modulus of the core.}$$

For a symmetrical sandwich panel, an approximated estimation of the central deflection δ submitted to a load F is given by:

$$\delta = \frac{Fl^3}{24Ebt_d^2} + \frac{Flt_c}{4Gbd^2} \quad (3.31)$$

In this study, a sandwich beam of 1 m length between the supports and 50 mm width is considered. Flexural stiffness is estimated by calculating the central deflection of the beam subjected to a central load of 1 N using above equations and is constrained to be less than 10 μm .

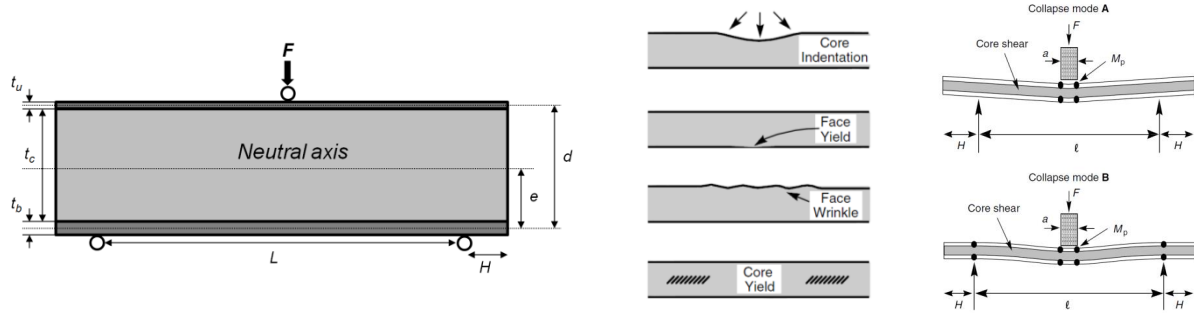


Figure 3.8: Sandwich panel submitted to a three-point bending test and corresponding failure modes.

Strength

The strength is estimated by calculating the critical load F corresponding to the onset of yielding. Four failure modes have been considered (see below). For each mode, a critical load is calculated. The strength is then estimated by a lower bound approach. The failure mode with the lowest value of critical load is considered as the limiting one as it will occur first. The strength is set to this critical load. The formulas corresponding to the different failure modes are given below. The strength will be constrained to be higher than 2 kN with an overhang $H = 0.1 \times L$.

(i) The first mode is indentation of the core. Presented in [ASH00b] for a squared indenter of size a , the occurrence of plastic hinges in the faces and of a plastic collapse of the core are considered and gives a critical load F_i . This mode is dominant when faces are thin and core is thick compared to the length of the panel.

$$F_i = 2bt_u\sqrt{\sigma_{yc}\sigma_{yu}} + ab\sigma_{yc} \quad (3.32)$$

(ii) The second mode is face yielding. This usually occurs for thick faces with a thin core. The critical load F_{fy} corresponds to the plastic yielding of the lower face due to tension:

$$F_{fy} = \frac{4bt_b d}{l} \sigma_{yb} \quad (3.33)$$

(iii) While face yielding mainly applies to the lower face, face wrinkling of the upper face appears when the faces are really thin compared to the core. This situation corresponds to an elastic instability between the face and the core. The critical load F_{fw} can be expressed as:

$$F_{fw} = 2.28 \sqrt[3]{E_u E_c^2} \frac{b t_u t_c}{l} \quad (3.34)$$

(iv) The last failure mode, which is shear yielding of the core, is slightly more complicated as it depends on the length of overhang, H , beyond the outer supports. If this length is small, the entire core will experience some shear stress. For higher values of overhang, only the part between the supports will experience shear stress. The first case is noted mode A while the second one is noted mode B as shown in Figure 3.8. Each mode comes with plastic hinges in the faces. The critical load of mode A, F_{sa} , linearly depends on H and is expressed by:

$$F_{sa} = \frac{b t_u^2}{l} (\sigma_{yb} + \sigma_{yu}) + 2 b t_c \tau_{yc} \left(1 + \frac{2H}{l} \right) \quad (3.35)$$

In mode B, the critical load F_{sb} is completely independent on the overhang and can be expressed by:

$$F_{sb} = \frac{2 b t_u^2}{l} (\sigma_{yb} + \sigma_{yu}) + 2 b t_c \tau_{yc} \quad (3.36)$$

The transition from mode A to mode B occurs at an overhang value, noted H_t , which can be calculated by equalizing F_{sa} and F_{sb} . The obtained expression is then:

$$H_t = \frac{1}{2} \frac{t^2 \sigma_y^f}{t_c \tau_y^c} \quad (3.37)$$

This model is only valid for sandwich panels made of stiff and thin faces and of a soft and thick core with a length between supports which is large compared to the total thickness of the panel.

2.3. Thermal properties

Two thermal properties are investigated corresponding to requirements involving a steady-state or a transient behaviour.

Steady-state regime – thermal resistance

In a steady-state regime, the main thermal property which was assessed corresponds to the thermal resistance through the sandwich panel.

For some applications, high thermal resistance r is required. This property is calculated for a cross section of unit area and is related to thickness t and thermal conductivity k of each layer by:

$$r = \frac{t_u}{k_u} + \frac{t_c}{k_c} + \frac{t_l}{k_l} \quad (3.38)$$

Optimal design of architected sandwich panels for multifunctional properties

Pierre Leite

The thermal resistance will be constrained to be higher than $1 \text{ m}^2\text{K/W}$. It is assumed that the thermal resistance of air contained in the core material is taken into account in core thermal conductivity and that bonding of layers does not significantly affect thermal properties. Indeed, considering an interface of thickness ε between layers, the thermal resistance of this interface becomes negligible as soon as $\varepsilon \ll t$.

Transient regime – thermal insulation

Considering a transient regime, both thermal insulation and thermal shock resistance are required. In this kind of specifications, the sandwich panel is supposed to protect what is at the back of the panel from an abrupt raise of temperature at the front for a given time. A limit value of temperature is defined regarding the specificities of the application. Then, the panel experiences high gradient of temperature from the heated side to the protected side, thus leading to internal thermo-mechanical stresses which should not reach the yield strength of the constitutive material.

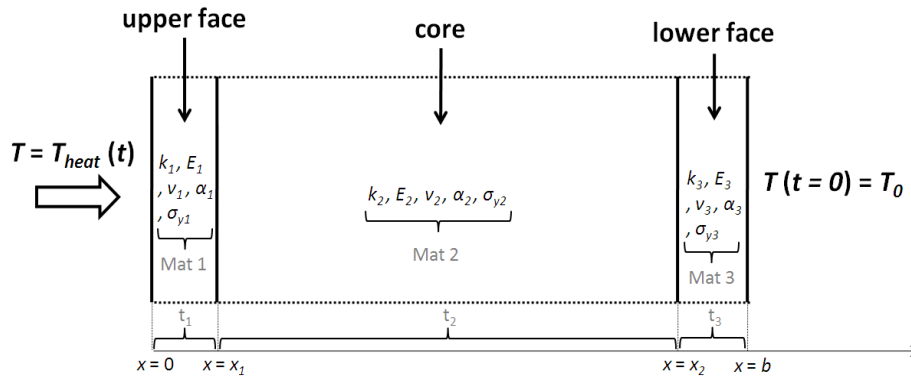


Figure 3.9: Schematic representation of a sandwich panel subjected to thermal load at one side.

Let us consider a sandwich panel submitted to a thermal load T_{heat} as shown in Figure 3.9. This thermal load is assumed to be composed of a first stage corresponding to the raise of temperature and of a second stage corresponding to an upholding of the maximum temperature value during a certain time. At the other side ($x = b$), the temperature is set to T_0 at $t = 0$ and released free for the rest of the calculation. The temperature field throughout the panel is obtained by solving the one-dimensional Fourier differential equation of transient heat equation:

$$\frac{\partial T(x, t)}{\partial t} = \frac{\partial}{\partial x} \left(a(x) \frac{\partial T(x, t)}{\partial x} \right) \quad (3.39)$$

with continuity conditions of temperature and heat flux at the interfaces between the different layers. The variable a is the thermal diffusivity and is different for each layer:

$$a = \frac{k}{\rho c_p} \quad (3.40)$$

with k the thermal conductivity (in $\text{W/m}^\circ\text{C}$), ρ the mass density (in kg/m^3) and c_p the specific heat capacity (in $\text{J/kg}^\circ\text{C}$). The one-dimensional heat equation is solved using a backward time, centred space scheme in a difference finite modelling.

The temperature field is discretized in time and space following the equation:

$$\frac{T_i^m - T_i^{m-1}}{\Delta t} = a(x) \frac{T_{i-1}^m - 2T_i^m + T_{i+1}^m}{\Delta x^2} + O(\Delta t) + O(\Delta x^2) \quad (3.41)$$

T_i^m is the temperature of grid point x_i and at the time t_m . This equation can be rewritten in matrix form:

$$\mathbf{A}\mathbf{T}^m = d\mathbf{T}^{m-1} \quad (3.42)$$

where \mathbf{T} is a column matrix containing the value of the temperature at each grid point at the time t_i , \mathbf{A} is a square matrix of size corresponding to the number of grid points and d is a scalar. \mathbf{A} is tridiagonal and can then be inversed using a LU decomposition. Solving this linear matrix system gives access to the temperature field at each grid point for each time step. At this point, it is possible to verify that the temperature at the back of the panel did not exceed the limit temperature and that the temperature at each point of the panel remained below the maximum service temperature of the constitutive material. This maximum service temperature is a property provided by the materials database that ensures for a material used under this temperature, that mechanical properties are not strongly affected. For example, an Aluminium alloy with a melting point of about 550 °C has a maximum service temperature of 140 °C.

To evaluate the stress field, a plane strain approximation is assumed (in the plane x, y), considering a geometry of the panel such that $L \gg l \gg b$. In order to simplify the calculations, edge boundaries are considered as free. The compatibility equations give:

$$2\varepsilon_{xy,xy} = \varepsilon_{xx,yy} + \varepsilon_{yy,xx} \quad (3.43)$$

As no mechanical loads are applied on the boundaries, σ_{xx} is expected to disappear. Moreover, strains are independent of the y -coordinates. Then, equation (3.43) becomes:

$$0 = 0 + \varepsilon_{yy,xx} \quad (3.44)$$

Considering linear thermo-elastic behaviour of the materials:

$$\varepsilon_{yy} = \frac{1 - \nu(x)^2}{E(x)} \left(\sigma_{yy} - \frac{\nu(x)}{1 - \nu(x)} \sigma_{xx} \right) + (1 + \nu(x))\alpha(x)(T(x) - T_0) \quad (3.45)$$

with $E(x)$, $\nu(x)$ and $\alpha(x)$ the Young's modulus, the Poisson's ratio and the thermal expansion coefficient, respectively. These parameters are dependent on the layer (and then depend on the x -coordinate). Replacing equation (3.45) in equation (3.44) and integrating twice, the thermal stress σ_{yy} is obtained throughout the thickness, with two integration constants.

$$\sigma_{yy} = \frac{\alpha(x)E(x)}{1 - \nu(x)} (T(x) - T_0) + \frac{E(x)}{1 - \nu(x)^2} (K_1x + K_2) \quad (3.46)$$

These constants are determined by solving the equilibrium conditions. As no external loads are applied, the resulting force and moment in the structure are to be equal to zero:

$$\int_0^b \sigma_{yy} dx = 0, \int_0^b \sigma_{yy} x dx = 0 \quad (3.47)$$

Solving equations (3.47) and (3.46) at each time steps gives access to the thermal stress at each grid point.

The ratio between the thermal stress and the yield strength of the material is a measurement of the thermal shock resistance, often noted TSR, and can be evaluated at each grid point at each time step. In order to ensure a satisfactory component lifespan, the thermal stress should never reach the yield strength. Then, the maximum value of this ratio along the duration of the simulation is constrained to be less than 1:

$$\max_{\forall x, \forall t} \left(\frac{\sigma_{yy}(x, t)}{\bar{\sigma}_y(x)} \right) < 1 \quad (3.48)$$

with $\sigma_{yy}(x, t)$ the thermal stress at a grid-point x and at a time t and $\bar{\sigma}_y(x)$ the yield strength of the material at a grid-point x .

Knowing the stress field at each grid point and at each time step allows to check if that stress has not reached the yield strength of the material. It is also assumed that the layers are perfectly bonded and that bonding has no significant effect on mechanical properties. Even though this assumption does not reflect a real case, taking different bonding forces into account through different manufacturing processes is complex and will not be investigated during this work.

For the present work, thermal load will consist on a front-side temperature of 700 °C with an initial temperature of 20 °C. The back-side temperature should not reach 140 °C after one hour.

2.4. Acoustic damping

The vibro-acoustical model used to evaluate the sound transmission loss has been developed at ONERA in the DMAE department [SIM95, SIM04] and is implemented in the PIAMCO® software. This model concerns dissymmetric structures with a thick orthotropic core and orthotropic multi-layered laminates. The formulation of displacement field with membrane, bending and shear terms allows a continuity of shear stress between each layer, which is a required condition because of orthotropic properties. Moreover, this takes into account a possible transverse expansion of a "soft core", whereas the laminates are treated as thin panels with the same transverse displacement through the thickness. Taking into account the possible transverse deformation of the core allows symmetric vibration modes to be developed in addition to antisymmetric ones as shown in Figure 3.10. The consequence of the superposition of these modes is to exhibit better acoustical insulation behaviour in a certain frequency range than panels without core transverse deformation.

The acoustical insulation power of a panel can be measured by its Transmission Loss, which is defined by:

$$TL(\theta, \varphi) = 10 \log \left(\frac{1}{\tau(\theta, \varphi)} \right) \text{ in dB} \quad (3.49)$$

with τ the acoustic coefficient transmission, θ and φ angles defining the direction of incident waves as shown in Figure 3.11.

In our case, we are interested in a diffuse field excitation. So, the transmission coefficient must be averaged over the incidence orientation to obtain the diffuse field Transmission Loss, as follows:

$$TL_d = -10 \log \left(\frac{\int_0^{2\pi} \int_0^{\theta_{lim}} \tau(\theta, \varphi) \sin(\theta) \cos(\theta) d\theta d\varphi}{\int_0^{2\pi} \int_0^{\theta_{lim}} \sin(\theta) \cos(\theta) d\theta d\varphi} \right) \quad (3.50)$$

with generally $\theta_{lim} = 78^\circ$. Theoretically, the limit value should be taken as 90° . In practice, the acoustic field is never totally diffuse and then the large angles are statistically disadvantaged.

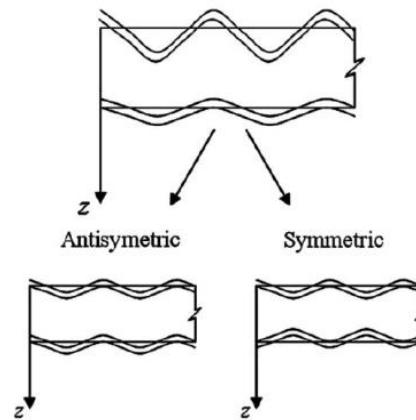


Figure 3.10: Illustration of the two types of vibration modes considered in the acoustic model.

The value used to assess the acoustic damping of a sandwich panel, noted R , is the mean value of TL_d in the frequency range 1 000 to 4 000 Hz which corresponds to the most relevant frequency range for the specific application of cabin noise reduction on a commercial aircraft. A minimum constraint of 20 dB is used for the optimization process.

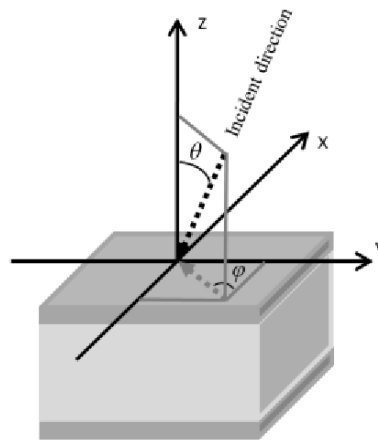


Figure 3.11: Definition of the incident direction of the acoustic wave on the sandwich panel.

2.5. Blast mitigation

The model used in the assessment of the blast resistance of sandwich panels is adapted from the model proposed by Deshpande and Fleck in [FLE04] for the assessment of the resistance of clamped sandwich beams to shock loading. In this model, the behaviour of a sandwich panel subjected to a blast impulse is divided into three stages. Let us consider a clamped sandwich beam of length $2L$ as shown in Figure 3.12. The modifications brought to the model concern asymmetrical sandwich beams with different face materials and different thicknesses, while the original model was dedicated to symmetrical solutions.

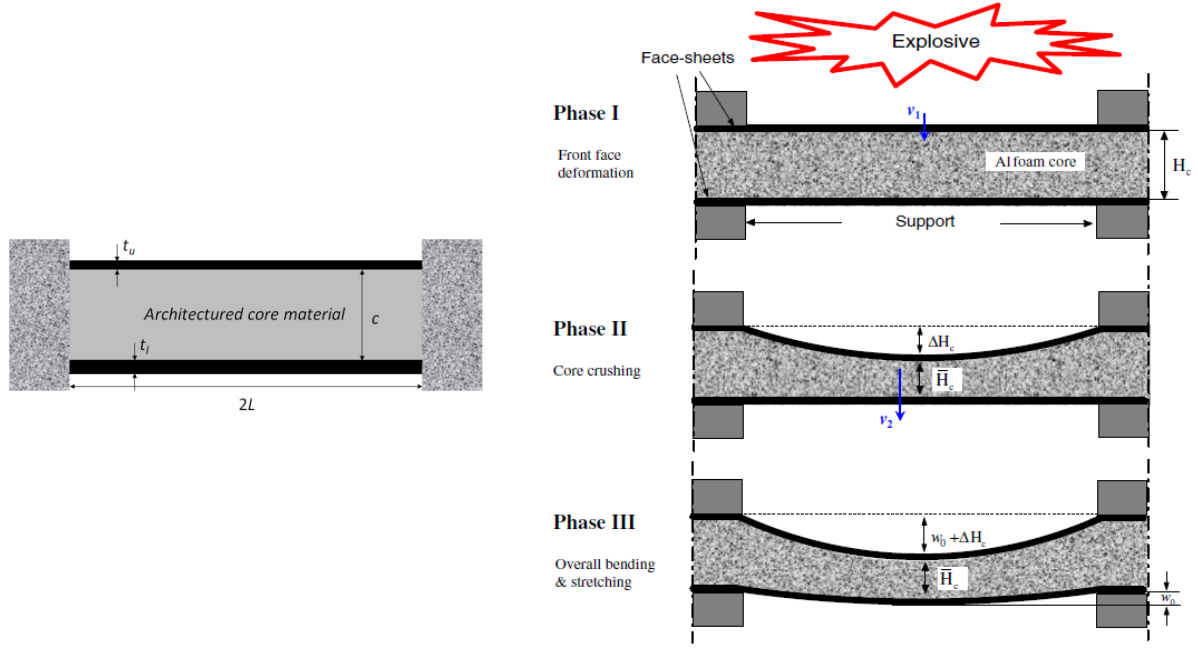


Figure 3.12: Geometry of the clamped sandwich beam and illustration of the three stages considered [ZHU09]. The first stage corresponds to the front face deformation and acceleration. The second stage corresponds to core crushing while the last stage corresponds to bending deformation of the sandwich and in-plane stretching of the faces and core.

Stage I: motion of the front face

In a first stage, stage I, the one-dimensional fluid-structure interaction problem is solved, leading to a uniform velocity of the upper face, which is the one impacted by the blast. Considering a blast of peak pressure p_0 and duration θ , then the maximum achievable impulse I is given by:

$$I = \int_0^\infty 2p_0 e^{-t/\theta} dt = 2p_0\theta \quad (3.51)$$

and the ratio between the maximum achievable impulse I and the impulse conveyed to the face I_{trans} is:

$$\frac{I_{trans}}{I} = \psi^{-\psi/\psi-1} \quad (3.52)$$

with $\psi = \rho_w c_w \theta / m_u$ a nondimensional measurement depending on the duration of the blast θ , the mass per unit area of the upper face m_u , the density of fluid ρ_w and the velocity of the wave in the fluid c_w . For example, for an air blast the following values are taken: $\rho_w = 51.24 \text{ kg/m}^3$, $c_w = 330 \text{ m/s}$ and $\theta = 0.1 \text{ ms}$.

It is then assumed that in this first stage the upper face undergoes acceleration to a velocity v_0 due to the transmitted blast impulse while the core and the lower face remain stationary. This initial velocity is given by:

$$v_0 = \frac{I_{trans}}{m_u} \quad (3.53)$$

Stage II: core crushing

During stage II, crushing of the core is considered. The upper face moving forward into the core is decelerating from v_0 to v_f , thus causing crushing of the core until a compressive strain ε_c . Then, the core and the lower face accelerate to the same velocity v_f as the upper face. The core is considered as a rigid, ideally plastic crushable material with crush strength σ_y and densification strain ε_d . The quantities needed to proceed with the next stage are the final velocity of the whole sandwich beam v_f and the compressive strain of the core ε_c .

A direct relationship exists between v_0 and v_f by the momentum conservation during crushing as stated hereafter:

$$(m_u + m_c + m_l)v_f = m_u v_0 \quad (3.54)$$

with m_u , m_c and m_l being the mass per unit area of the upper face, core and lower face respectively. The mass per unit area of the core can be expressed as $m_c = \rho_c c$ with ρ_c the core density and c the thickness of the core.

The energy U_{lost} dissipated during this stage can be expressed as a function of the initial kinetic energy of the upper face and the final kinetic energy of the whole sandwich beam:

$$\frac{m_u v_0^2}{2} = U_{lost} + \frac{m_u v_f^2}{2} + \frac{m_c v_f^2}{2} + \frac{m_l v_f^2}{2} \quad (3.55)$$

and combining equation (3.55) and (3.54):

$$\frac{U_{lost}}{m_u v_0^2 / 2} = \frac{m_c + m_l}{m_u + m_c + m_l} \quad (3.56)$$

It is assumed that the loss of energy occurs by plastic dissipation during compression of the core and then:

$$U_{lost} = \sigma_y \varepsilon_c c \quad (3.57)$$

By combining equations (3.56) and (3.57), an explicit expression of the core compressive strain ε_c is obtained:

$$\varepsilon_c = \frac{\varepsilon_D}{2} \frac{m_c + m_l}{m_u + m_c + m_l} \hat{I}^2 \quad (3.58)$$

with $\hat{I} = I_{trans} / \sqrt{m_u c \sigma_y \varepsilon_D}$.

Eventually, for high values of U_{lost} , ε_c can be higher than the densification strain ε_D . In this case, ε_c should be set to the value of ε_D . In the present analysis no additional dissipation mechanisms are considered even though additional dissipation is expected for the latter case in order to satisfy energy conservation. More details about the validity of this model can be found in [QIU03].

Stage III: dissipation of the remaining energy by bending and stretching

At the end of stage II, the sandwich beam has a uniform velocity v_f . Stage III corresponds to the dissipation of the remaining kinetic energy by bending and stretching of the beam. The displacements are assumed to be in the transverse direction with moderate deflection. The displacement w at the mid-span is then considered small compared to the length of the beam, and the longitudinal force N is assumed to be constant along the beam.

Optimal design of architected sandwich panels for multifunctional properties

Pierre Leite

The proposed analysis divides the phenomenon into two phases. During the first one, a central portion of the beam translates at a velocity v_f while a segment of length ξ rotates symmetrically at the supports. Thus the bending moment M varies from $-M_0$ at the support to M_0 at the end of the rotating segment. It is constant in the central portion. A schematic representation of the velocity and displacement profiles is shown in Figure 3.13.

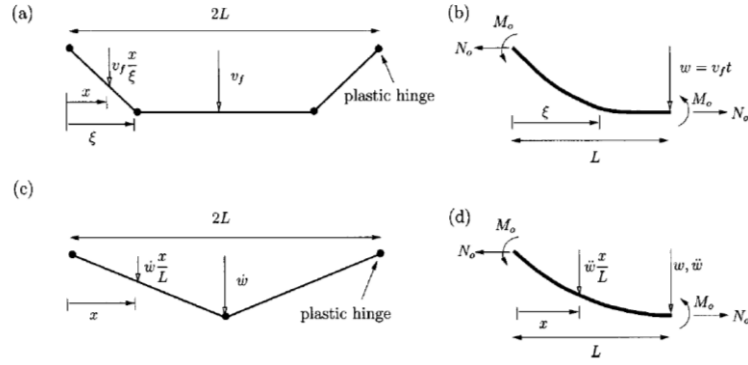


Figure 3.13: Schematic representation of velocity profile in phases 1 (a) and 2 (c) and of free-body diagram with the approximated shape of the half-beam in phases 1 (b) and 2 (d).

This phase ends when $\xi = L$ at a time T_1 with a central deflection w_1 . By equating the conservation of momentum about a fixed end, it is possible to evaluate the expression of ξ as a function of time and thus to obtain an expression of T_1 and w_1 :

$$T_1 = \frac{M_0}{N_0 v_f} \left[\sqrt{4 + \frac{mL^2 v_f^2 N_0}{3M_0^2}} - 2 \right] \quad (3.59)$$

$$w_1 = v_f T_1 = \frac{M_0}{N_0} \left[\sqrt{4 + \frac{mL^2 v_f^2 N_0}{3M_0^2}} - 2 \right] \quad (3.60)$$

with m the total mass per unit length of the sandwich beam and L the mid-length of the beam.

During the second phase, plastic hinges occur at the supports and at the mid-span, and the velocity profile is assumed to be triangular. Following the diagram of Figure 3.13 (d), the equation of motion is:

$$2M_0 + N_0 w = -\frac{\ddot{w}}{L} \int_0^L m x^2 dx = -\frac{mL^2}{3} \ddot{w} \quad (3.61)$$

which can be solved using initial conditions $w(T_1) = w_1$ and $\dot{w}(T_1) = v_f$.

Then the central deflection of the sandwich beam w is given by:

$$w = \sqrt{\frac{v_f^2}{\omega^2} + \left(\frac{2M_0}{N_0} + w_1 \right)^2} - \frac{2M_0}{N_0} \quad (3.62)$$

with $\omega = \sqrt{3N_0/m}/L$ a constant expressed in s^{-1} .

The longitudinal force and the bending moment are expressed as:

$$N_0 = \sigma_{yu}t_u + \sigma_{yl}t_l + \sigma_{lc}c \quad (3.63)$$

$$M_0 = \sigma_{yu}t_u(e_u) + \sigma_{yl}t_l(e_l) + \sigma_{lc}\left(\frac{c_u^2}{2} + \frac{c_l^2}{2}\right) \quad (3.64)$$

with e_u the distance between the centroid of the upper face and the neutral axis, e_l the distance between the centroid of the lower face and the neutral axis. Moreover, c_u and c_l are defined as $e_u = c_u + t_u/2$ and $e_l = c_l + t_l/2$. The variables σ_y refers to the yield strength of the face materials while the variable σ_{lc} is the in-plane strength of the core material. In some cases, such as for pyramidal truss cores and hexagonal honeycombs, this strength can be neglected and considered to be equal to zero.

When calculating M_0 , the compression of the core is to be taken into account and thus the thickness c is replaced by $(1 - \varepsilon_c)c$. For the longitudinal force N_0 , it is assumed that the effect of core compression can be neglected, thus the equation (3.63) can be used without modification.

All variables in equation (3.62) have been explicitly expressed and then the central deflection w of the sandwich beam can be evaluated such as the maximum deflection of the upper face w_u which is $w_u = w + \varepsilon_c c$.

A simple failure criterion corresponding to stretching of the faces can be expressed. While it can be expected that failure occurs at the supports in some cases, this criterion gives a first approximated tool for sandwich selection. As the tensile strain ε_m in the faces can be approximated by:

$$\varepsilon_m = \frac{1}{2} \left(\frac{w}{L} \right)^2 \quad (3.65)$$

it is possible to compare this value with the tensile ductility of the face materials ε_f . If $\varepsilon_m \geq \varepsilon_f$, then failure occurs. The same analysis can be performed with the upper face by replacing w by w_u .

This model helps to predict the deflection of a sandwich panel subjected to a blast load knowing few parameters. Moreover, a simple criterion takes into account failure of the faces at the mid-span. For a complete description of the initial model, refer to [FLE04]. Let us note that the failure criterion used is very simplistic and that optimized solutions may be discarded if a more refined model is used. In particular, the sandwich panel is considered as clamped and failure can occur by face sheet shear-off at the supports.

Different improvements have been brought to this model recently. However, these improvements have not been taken into account, the presented approach being considered sufficient for the purpose of our work.

For the present study, air blast is considered with $\rho_w = 51.24 \text{ kg/m}^3$, $c_w = 330 \text{ m/s}$, $\theta = 0.1 \text{ ms}$ and $p_0 = 50 \text{ MPa}$. The half-length of the sandwich panel is taken as 2 m. If faces are perforated, the solution is discarded. The inner central deflection will be constrained to be less than 0.4 m which represents a ratio between the deflection and the half-length of the beam of 0.2.

3. Performance space

Once the performance space has been filled via generation of new sandwiches and selection via the genetic algorithm, it is possible to extract the trade-off surface which is the group of non-

dominated solutions. This enables afterwards to assess the compatibility between the several specifications by looking at the form of the trade-off surface, as presented in the first part of this section. By plotting the contour values of the design variables in the performance space, it is also possible to obtain information on whether these variables have an influence on optimization, on the performances or no influence at all. This matter will be discussed in Section 3.2.

3.1. Assessment of compatibility through Pareto front shape

In the case of optimization problems with two criteria, the trade-off surface can exhibit three different types of shapes: linear, concave and convex. For each type of shapes, the possible interactions between performances are discussed. In Figure 3.14 are represented the different possible shapes of Pareto front qualified as linear, concave or convex.

Let us remind that a decision vector V can be expressed in that case as:

$$V = P_1 + \alpha P_2 \quad (3.66)$$

with α the exchange constant between the performances P_1 and P_2 .

Linear shapes

In terms of trade-off, the linear Pareto front can be expressed by a linear relation between the two performances:

$$P_2 = kP_1 \quad (3.67)$$

with k the slope of the Pareto front. Considering a decision vector corresponding to an exchange coefficient α , three cases emerge:

- If $\alpha = k$, all the solutions along the trade-off surface are optimal ones.
- If $\alpha > k$, the optimal solution is the best one in regard to P_1 .
- If $\alpha < k$, the optimal solution is the best one in regard to P_2 .

A linear shape of the trade-off surface means that along the Pareto front, the saving on one performance is proportional to the loss on the other performance.

Concave shapes

A case of concave shape trade-off surface is shown in Figure 3.15. For this kind of Pareto fronts, a critical value of exchange constant α_c can be defined as the one for which two optimal solutions are obtained. It is represented by a corresponding performance metric that passes through the two solutions at the corner of the concave shape. These particular solutions are plotted in red in Figure 3.15 and are noted S_1 and S_2 , being the best solutions regarding P_1 and P_2 respectively.

Then, in terms of trade-off, three situations occur:

- If $\alpha > \alpha_c$, the optimal solution is S_1 .
- If $\alpha = \alpha_c$, both S_1 and S_2 are optimal solutions.
- If $\alpha < \alpha_c$, the optimal solution is S_2 .

Only the two extreme solutions present a real interest in terms of trade-off. This situation is called non-beneficial competition as an intermediate solution has less interesting performances than a virtual solution that would correspond to a rule of mixture between solutions S_1 and S_2 .

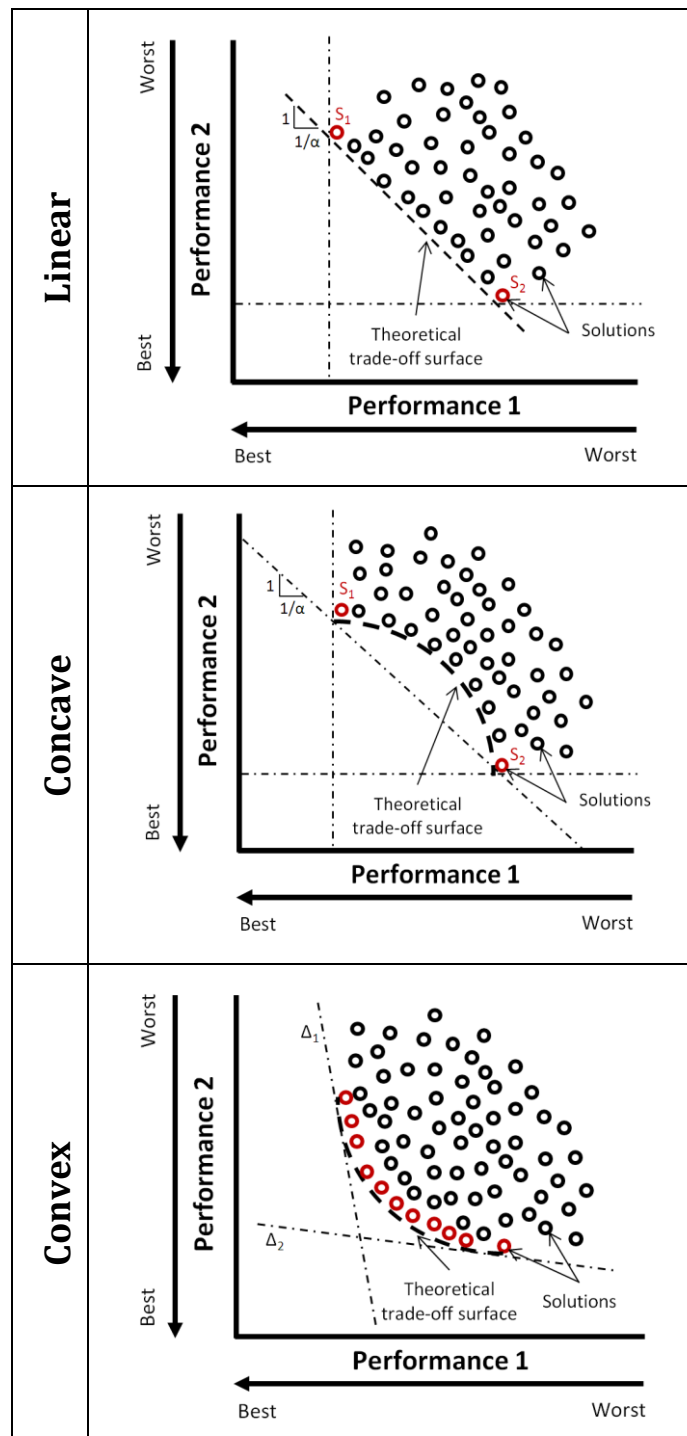


Figure 3.14: Possible shapes of trade-off surface.

A simple way to characterize the concavity of a trade-off surface is illustrated in Figure 3.16. It consists in measuring the ratio between δ_{max} and D with δ_{max} the distance between the Pareto front and the straight line joining the two extreme solutions and D the distance between the two extreme solutions S_1 and S_2 in the Pareto front. A high value of δ_{max} compared to D would mean that the two observed performances are not compatible in the design of a sandwich panel. Indeed, the two optimal solutions obtained in this case would represent solutions that exhibit an increase of one of the performances to the expense of the other one.

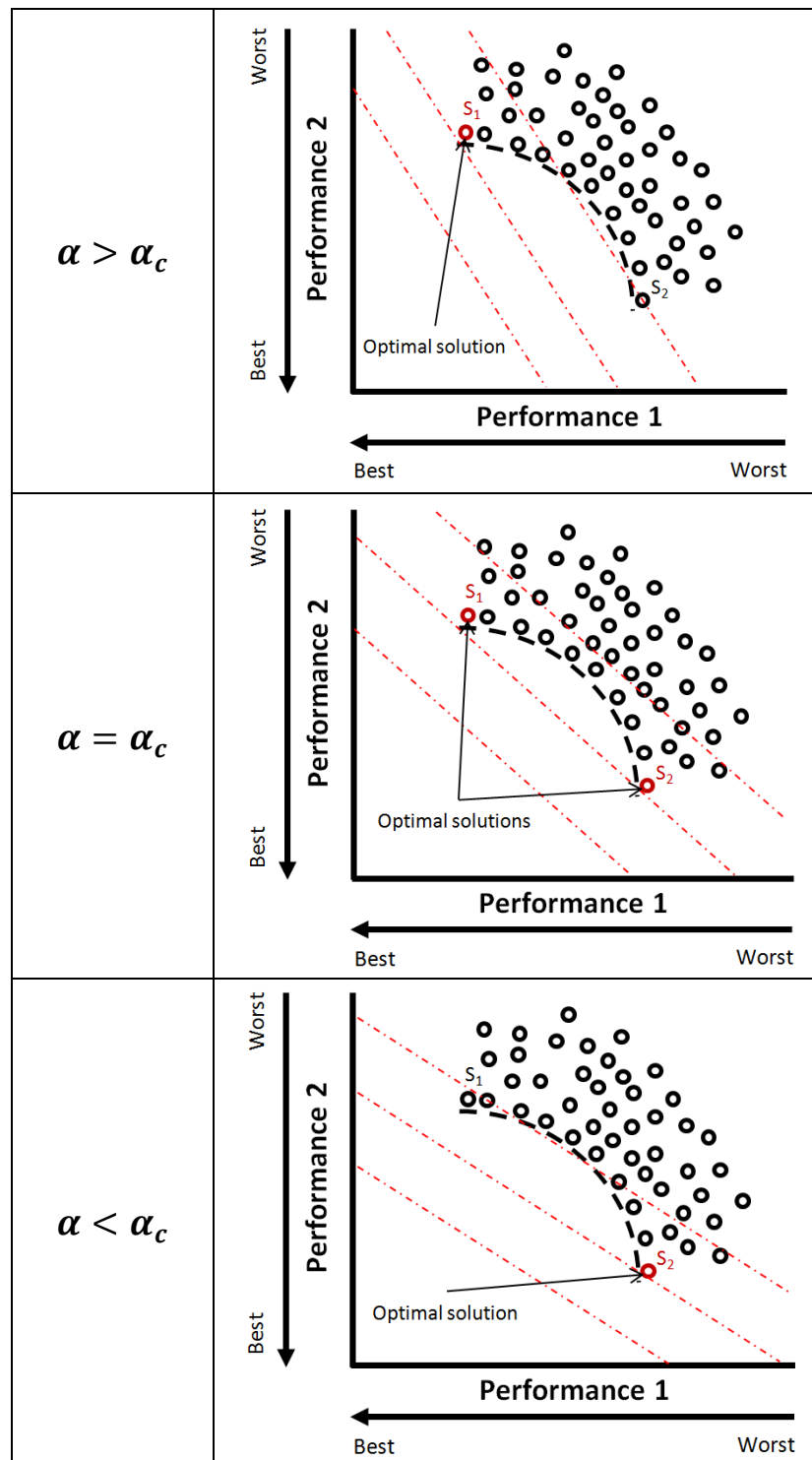


Figure 3.15: Illustration of the three possible cases when a decision vector is used to select the optimal solution in a concave trade-off surface. If the exchange constant equals the critical value α_c , two optimal solutions are identified, which are at the limits of the trade-off surface. Then, according to whether the constant value is higher or lower than this critical value, the optimal solution will correspond to one of the two limit solutions.

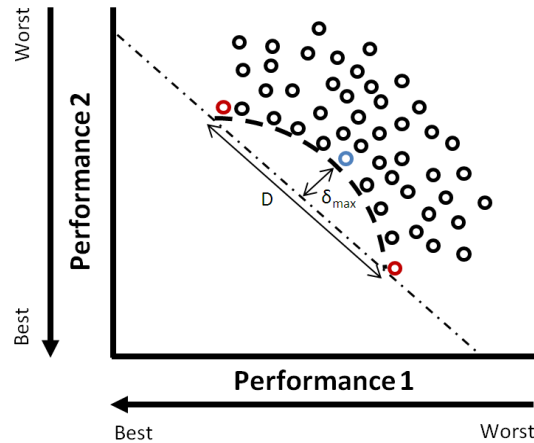


Figure 3.16: Definition of a metric δ_{max} for a concave shape trade-off surface.

Convex shapes

The case of a convex shape Pareto front is the most interesting one in terms of trade-off. An example of such Pareto front is plotted in Figure 3.17. In this particular situation, the optimal solution regarding an exchange constant α changes when this constant is modified as illustrated in Figure 3.17. For three different exchange constants, three different optimal solutions are determined.

This situation corresponds to a beneficial competition given that intermediate solutions have better performances than a virtual solution that would correspond to a rule of mixture.

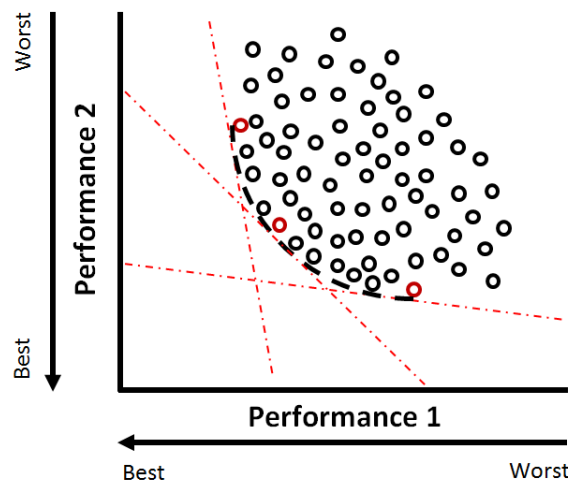


Figure 3.17: Illustration of a convex trade-off surface. In this case, changing the exchange constant can lead to a change of optimal solution in continuous manner. This is illustrated with three different decision vectors identifying three different optimal solutions.

As for the concave shape trade-off surface, a simple way to characterize the convex shape Pareto front is to calculate the ratio between the distance δ_{max} and D as shown in Figure 3.18. The sign of this ratio then gives direct information on the convexity of the trade-off surface. It would be assumed that a positive ratio is representative of a convex shape while a negative value represents a concave trade-off surface.

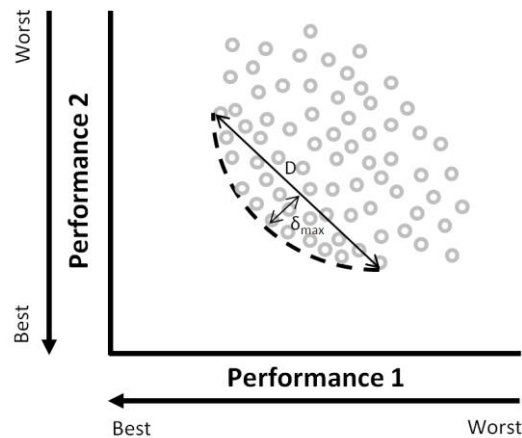


Figure 3.18: Definition of a metric δ_{max} for a convex shape trade-off surface.

A high value of δ_{max} over D could be synonymous with compatibility between the two performances that are being optimized. The best case is a right angled Pareto front leading to a unique optimal solution that maximizes both performances without loss. For usual convex trade-off surface, the higher δ_{max} over D is, the more beneficial it is to seek an intermediate solution presenting a real trade-off between performances.

3.2. Assessment of design variable influence

There are two different types of design variables in the optimization by “real path” of sandwich panels. The first one corresponds to material selection through the constitutive material of each layer. The second one corresponds to geometrical design through the thickness of each layer. These design variables may have or not an influence on the performances of the sandwich panel. Three main possibilities will be considered:

- The first one is that the design variable can modify the rank of a solution.
- The second one is that the variable mainly influences one of the performances but only slightly the other one.
- The last one occurs as the design variable has no influence on the rank nor on the performances.

Rank influential variables

The first mentioned case concerns variables that can affect the rank of the solutions. As developed in Part 2, the rank of a solution is linked to the number of dominating individuals. If a solution is not dominated, then its rank is equal to zero as shown in Figure 3.19. If these solutions were deleted from the performance space, the non-dominated solutions among the remaining ones would have a rank equal to one and so on. A design variable Var will be characterized as rank influential if, by plotting its contour values, there is a link between the value of this variable and the rank of the solutions as shown in Figure 3.19.

In this case, the design variable has a major influence on the rank of the solution and should be considered as a priority variable.

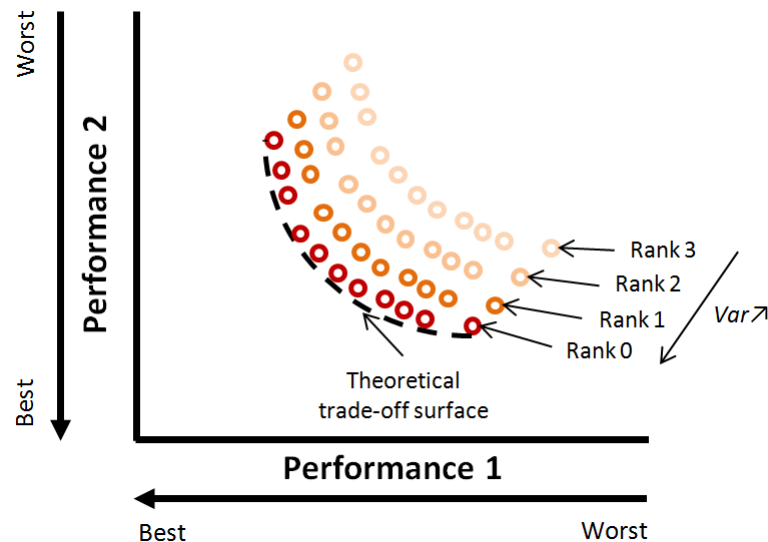


Figure 3.19: Illustration of the effect of rank influential variables on the performance space. The colours correspond to contour values of the design variables and to the rank of the solutions. There is a direct link between the design variable and the optimality of the solutions.

Performance influential variables

The second possibility addresses the case of a design variable Var influencing the performances but not the rank of the solutions. A schematic example is given in Figure 3.20 with a convex trade-off surface. In this case, the design variable mainly affects Performance 1 but not Performance 2. This is graphically translated by a banded pattern of the performance space.

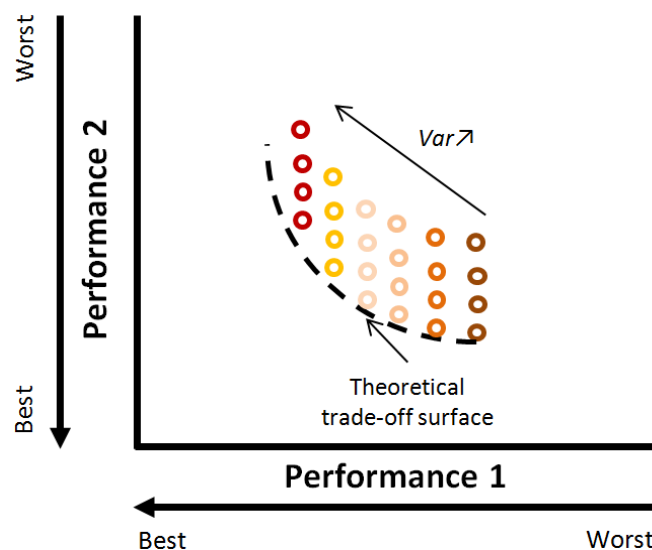


Figure 3.20: Illustration of the effect of performance influential variables on the performance space. The colours correspond to contour values of the design variables. There is a direct link between the design variable and Performance 1 while Performance 2 is independent of the design variable.

Non-influential variables

The last possibility is the one in which the design variable has no effect on the performances nor on the rank of the solutions. This leads to a performance space for which no clear pattern can be identified.

4. Genetic algorithm/implementation (DAKOTA)

The DAKOTA software (Design Analysis Kit for Optimization and Terascale Applications) is a GNU Lesser Public License tool for optimization and uncertainty analysis developed by the Sandia National Laboratories. It presents a flexible interface between simulation codes and iterative analysis methods that can be used for optimization problems, uncertainty quantification, parameter estimation and sensitivity/variance analysis. It is extensively used in academic research for all sorts of applications, including at the DAAP department at ONERA for aerodynamics applications. The first part of this section will briefly introduce how the interface works. The software also proposes a large number of algorithms for optimization, either gradient or non-gradient based methods. Within it, different evolutionary algorithms are proposed. The one used for the present study is the MOGA developed by Eddy and Lewis [EDD01]. Some specificities of the algorithm are given in Section 4.2.

4.1. Interfacing between analysis tools and optimization algorithm

In order to solve an optimization problem, DAKOTA uses a method which deals with variables and communicates with the analysis drivers through an interface in order to get a response. These four pieces (method, variables, interface and response) are specified in a users input file. In a few words, the method specifies how the optimization is performed, the variables specify on what it is performed, the interface specifies the external tools used (the analysis drivers for instances) and the response specifies what type of result is required. Each piece is described in the following paragraphs.

The method part gathers specifications on the algorithm used and the strategy employed. The maximum number of iterations and evaluations are defined here. They are taken as 200 and 1.10^7 respectively. This maximum number of evaluations seems to be extremely high but it is dictated by the size of the design space. Indeed, considering about 100 possible materials for each layers and a discretization of the thickness with 10 values, then the design space for an unsymmetrical sandwich panel would be composed of 1.10^{12} possible solutions. In order to have a representative population of the design space, it is required that the initial population in the genetic algorithm is about 1 000 individuals. As a consequence, a large number of evaluations can be performed during the optimization process.

The second set of parameters directly concerns the chosen algorithm. The main input parameters required for MOGA are the population size, the cross over and mutation rates, and the number of generations and percent change characterizing the convergence metric tracker. As explained above, the population size is taken as 1 000. The design space being large, an exploration step is then required. The mutation rate is set to 0.7 while the cross over rate is set to 0.4 which are default values from the software. For the convergence metric tracker, the number of generations is taken as 10 with a percent change of 0.05, which are default values.

The variables part defines the design space. The different design variables are defined by their name, their nature (real or integer) and their range. In the case of thickness parameters, a set of real numbers is given while for material parameters a list of integers is used. These integers correspond to the materials referenced in the database.

As shown in Figure 3.21, in order to move on the optimization process, DAKOTA generates a parameters file containing the genotype of the individuals to be evaluated. The analysis drivers should perform the evaluation and generate in their turn a result file containing the value of the objective functions. These values are read by DAKOTA and stored. The path of the analysis drivers are specified in the interface part. For the sake of flexibility, parameters and results file names can be specified according to what the analysis drivers need.

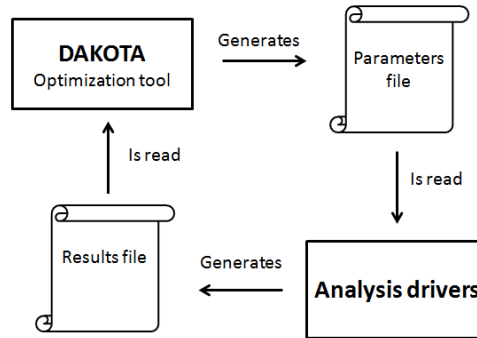


Figure 3.21: Dialogue between DAKOTA and the analysis drivers.

The last given specifications concern the response required by DAKOTA. The number of objective functions is specified according to the number of values that the analysis drivers write in the results file. In such a manner, the optimization algorithm knows how many values are expected and how to evaluate the rank of the solutions to drive the optimization.

During the optimization process, a file containing information on the population is generated at each generation. It contains the genotype of the individuals and the value of the corresponding objective functions. At the end of the process, the optimal solutions forming the trade-off surface are gathered in a different file and the whole performance space is stored in a distinct file.

4.2. Specificities of DAKOTA MOGA

DAKOTA MOGA is a Multi-Objective Genetic Algorithm. In order to determine the optimal solution of a given problem, this software creates new solutions via genetic operators, then selects some of them to generate new populations and eventually stops when convergence criteria are met. In this section, detailed information is given on the creation of the individuals, on their selection and on the convergence criteria.

To create new individuals from the initial population, genetic operators are used ; namely cross-over and mutation. Cross-over is the first operator used to create new individuals. At each generation, the number of individuals created by cross-over is equal to the number of individuals in the population multiplied by the cross-over rate.

The selection of the individuals used to perform the cross-over is based on the fitness of the individuals. Let us consider a mating pool. Every solution is represented once in this pool. Then, in order to promote the most promising solutions, the individuals are replicated in the pool proportionally to their fitness. The best individual will be the one that is the most replicated. Finally, two individuals are randomly selected as parents for cross-over.

Optimal design of architected sandwich panels for multifunctional properties

Pierre Leite

The individuals created by mutation follow the same scheme with a number of mutated solutions obtained by multiplying the initial population size by the mutation rate. Cross-over is performed by “*shuffle random*” and mutation by “*replace uniform*” as explained in Chapter 2 Section 4.4.

The selection rule to create the new population is based on the rank of the individuals in the population. The population containing the individuals of the initial population and the ones created by reproduction are ranked by the number of dominants. Every solution having more than 6 dominants is discarded while the others enter the new population.

To stop the optimization process, MOGA uses a convergence metric tracker based on 3 different metrics as illustrated in Figure 3.22:

- The first one monitors the expansion of the non-dominated group of solutions by measuring for each objective the distance between the maximum and minimum values of the objective function.
- The second metric monitors the density of the Pareto front by calculating the ratio between the number of solutions within it and the corresponding hypervolume.
- The last metric monitors the mean fitness of the partial Pareto front by determining the number of solutions of the previous population that are non-dominated by the solutions present in the current population. The metric is equal to this number divided by the size of the previous population.

These three metrics are percentages of improvement between two populations. The termination criterion used for the present work is the following: if after 10 generations, the improvement falls behind 0.05 for every metric then convergence is reached.

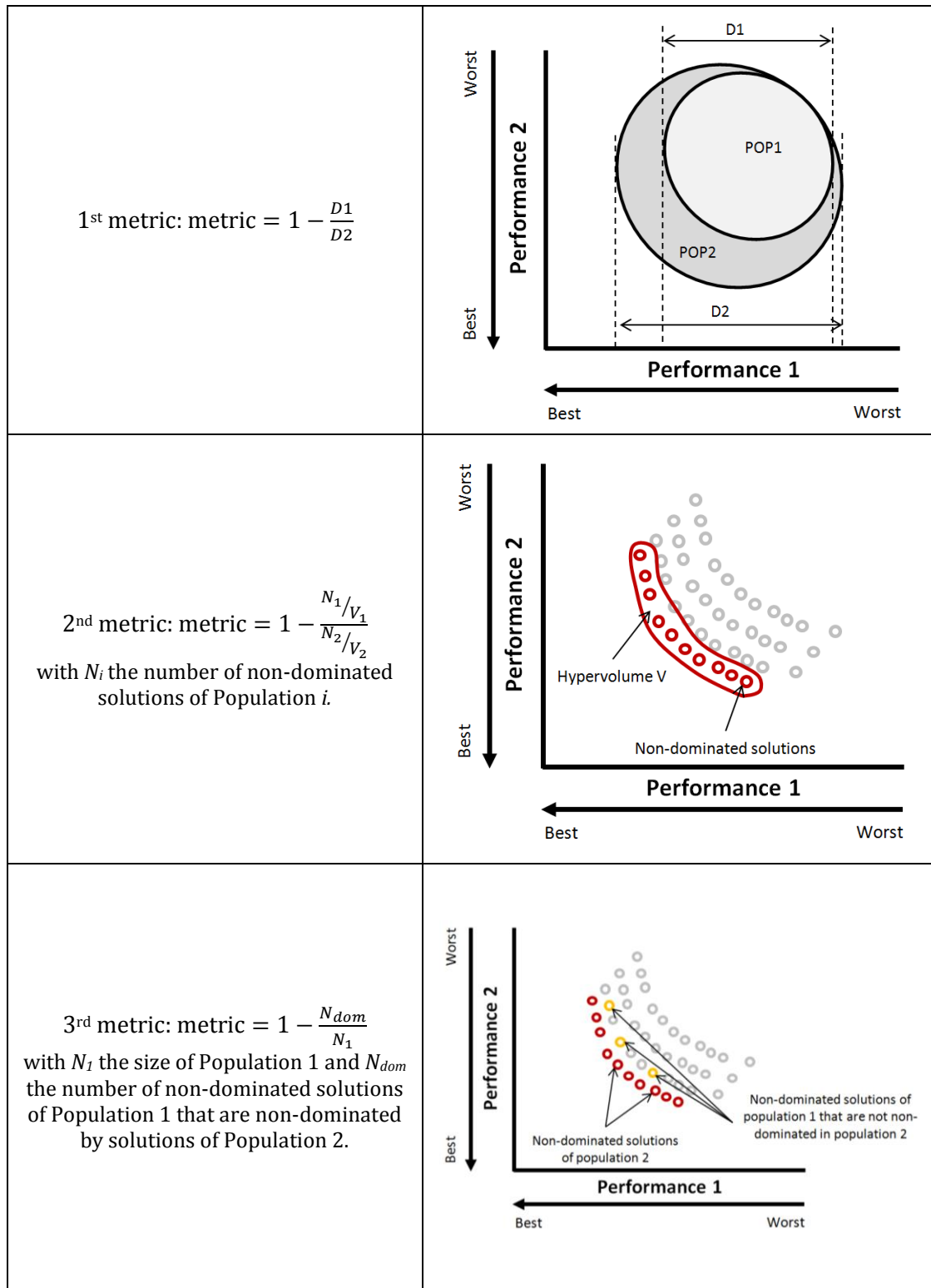


Figure 3.22: Illustration of the metrics used to monitor the convergence of the algorithm.

Chapter 4

Design of foam core sandwich panels: “optimization by real path”

The proposed design process, presented in the previous chapter, is used to investigate the multifunctional properties of architected sandwich panels. In the present chapter, several functions, classically allocated to sandwich panels, are optimized in a minimal weight design using a “real path” approach. The set of materials considered in this chapter includes different face materials but only foams as core material.

Firstly, in Section 2, the minimum weight design with a single other objective of foam core sandwich panel is treated. Thus, the optimal design in terms of material and dimensions is identified and the compatibility between mass and the objectives is discussed.

Secondly, in Section 3, the different possible situations that can occur in a multifunctional design are presented through four representative case studies. Tri-objective optimization problems are considered, in which mass reduction is one of the objective. The two other objectives are taken from the functions investigated in Section 2. For each case, a classical application is provided and a variability analysis is performed in order to identify the optimal designs.

Finally, the obtained results are summarized in the last section.

Chapter contents

1. Introduction	115
2. Design at minimal weight for a single other objective	116
2.1. Flexural stiffness	117
2.2. Flexural strength.....	122
2.3. Acoustic damping.....	128
2.4. Thermal resistance	133
2.5. Thermal insulation	137
2.6. Blast mitigation	141
3. Design at minimal weight for multiple objectives	146
3.1. A case of beneficial competition between specifications: flexural stiffness and acoustic damping specifications.....	147
3.2. A case of non-beneficial competition between specifications: flexural strength and thermal resistance specifications.....	153
3.3. A case of compatibility between specifications: thermal insulation and blast mitigation specifications	158
3.4. A case of incompatibility between specifications: acoustic damping and blast mitigation specifications	162
4. Overview of the results of multi-objective design by “real path”	168

1. Introduction

In this part, an optimization method called by “real path” is used to investigate the multifunctional design possibilities of sandwich panels.

A first section will focus on the optimal design at minimal weight for a single function, based on the models presented in the previous chapter. For each function, the performance space is filled by the solutions generated by the optimization algorithm in order to obtain the shape of the trade-off surface. The possible advantage of using sandwich panels instead of monolithic solutions is highlighted. Finally, a variability analysis is performed which helps identify design guides corresponding to each function. As two different size constraints have been used, its influence on the achievable performances is also discussed.

The second section addresses optimization problems with multiple functions. Four different cases have been selected which illustrate the different kinds of trade-offs that can be met with sandwich panels. For each case, the typical range of applications concerned by the considered specifications is presented. As for optimal design at minimal weight for a single function, the Pareto front is presented, the possible advantage of sandwich panels is discussed and a variability analysis is performed. In addition, the effects of several constraints on the optimal design are assessed by performing a multi-objective optimization. The addressed constraints are mass, size and the different functions that are at stake.

The last section will present an overview of the results in the form of a table gathering the main characteristics of the problems that have been studied.

Let us now identify the parameters used for the optimization process presented in this chapter.

The optimization problems consider classical three layers sandwich panels among which is a foam core. Foam has been chosen for two reasons. Firstly, it is a commonly used architected material in industry, moreover as a core material for sandwich structures. Secondly it is a well referenced material for which data is easily available. The material database used for the present work is partly composed of different kinds of foams. Material selection is then carried out on a discrete database. The panel will be taken as symmetric except when thermal insulation or blast resistance are considered as objective. Then, there are 4 design variables for symmetric sandwich panels and 6 for asymmetric ones. In this part, the considered performances are:

- Lightness
- Flexural stiffness
- Flexural strength
- Acoustic damping
- Thermal resistance
- Temperature insulation
- Blast resistance.

Different combinations of performances can be tested. Mass has been combined with all the other performances as weight saving is of major interest for sandwich panels and architecture materials in transportation industry in general. Some other combinations have been examined which are listed in Table 4.1. All these combinations have been tested in a three-objective optimization including mass reduction as the third objective. The cases which are not presented in this chapter are reported in Appendix A.

Optimal design of architected sandwich panels for multifunctional properties

Pierre Leite

Table 4.1: Tested combinations. The marks in bold identify the cases chosen as case studies for the optimal design with multiple functions.

	<i>Flexural stiffness</i>	<i>Flexural strength</i>	<i>Acoustic damping</i>	<i>Thermal resistance</i>	<i>Thermal insulation</i>	<i>Blast mitigation</i>
<i>Mass reduction</i>	X	X	X	X	X	X
<i>Flexural stiffness</i>		X	X	X		X
<i>Flexural strength</i>			X	X		X
<i>Acoustic damping</i>						X
<i>Thermal resistance</i>						
<i>Thermal insulation</i>						X

In addition, a size constraint is set on the total thickness of the sandwich panel. Two possible values have been chosen:

- The first one is a 50 mm thick constraint which is quite restrictive but representative of transport standards.
- The second one is a 500 mm thick constraint which is large enough to explore the effects of the variation of the total thickness on the trade-off surface.

In the performance spaces presented in this part, results for both size constraints will be represented. Though all observations are made on the 500 mm constrained problems, the effect of size constraint will be discussed separately.

For every optimization problem that does not involve mass as an objective, a weight constraint has been set. The sandwich panel weight is to be below 50 kg/m².

For the optimizations with a 50 mm thickness constraint, the face thickness can vary from 0.5 to 5 mm while the core thickness varies from 5 to 50 mm. In the case of a 500 mm thickness constraint, the face thickness ranges between 0.5 and 10 mm and the core thickness between 10 and 500 mm. Even though these variables are continuous ones, they are described by a set of real values. The variability range is divided into 20 possible face thicknesses and 50 possible core thicknesses.

2. Design at minimal weight for a single other objective

This section is dedicated to the optimal design of sandwich panels at minimal weight for a single function. Reducing the weight of structures is one of the driving force for designing sandwich panels and architected materials in transportation applications.

For each performance under consideration, a bi-objective optimization is performed. A boxed text summarizes what are the design space, objectives and constraints retained for each case study. A preliminary design based on a performance index approach gives a first result in terms of material selection.

Then our design process is used so as to produce an advanced design of the optimal sandwich panel. The performance space is filled by possible solutions in order to obtain the trade-off

surface. Each point in the performance space corresponds to a different sandwich panel generated by the genetic algorithm during the optimization process.

This performance space will help assess the compatibility between performances but also the influence of the design variables. In each performance space, an arrow points at the desired region.

A quick comparison between the results obtained by a performance index approach and the one presented in this work provides an overview of the benefits of the present approach.

2.1. Flexural stiffness

Design space:

- Face materials: Metals, Polymers, and Composites.
- Face thickness: from 0.5 to 10 mm.
- Core materials: Metal foams, Ceramic foams, Polymer foams.
- Core thickness: from 10 to 500 mm.
- Type of sandwich panel: symmetrical.

Objectives:

- Flexural stiffness: minimize the central deflection of a 1 m span sandwich beam submitted to a 1 N in a three-point bending test.
- Lightness: minimize the mass per unit area.

Constraints:

- Central deflection $< 10 \mu\text{m}$.
- Mass per unit area $< 50 \text{ kg/m}^2$.

Preliminary design: Performance index approach

The performance index corresponding to a stiff panel at minimal weight is $E^{1/3}/\rho$. The corresponding guide lines are drawn in the property charts given in Figure 4.1 for core and face material selection.

According to the performance index approach, the optimal core material should be PVC foam and the optimal face material should be a Metal Matrix Composite (Al-60%C).

Advanced design

Compatibilities

The performance space plotting central deflection and mass per unit area of the solutions generated by the genetic algorithm is given in Figure 4.2. The Pareto front is the combination of two different convex surfaces corresponding to two different sub-domains according to core nature. The transition is smooth but can be more easily observed in Figure 4.3.

The sandwich mass per unit area ranges from 3.9 to 50 kg/m² while the central deflection ranges from 0.07 to 10 μm .

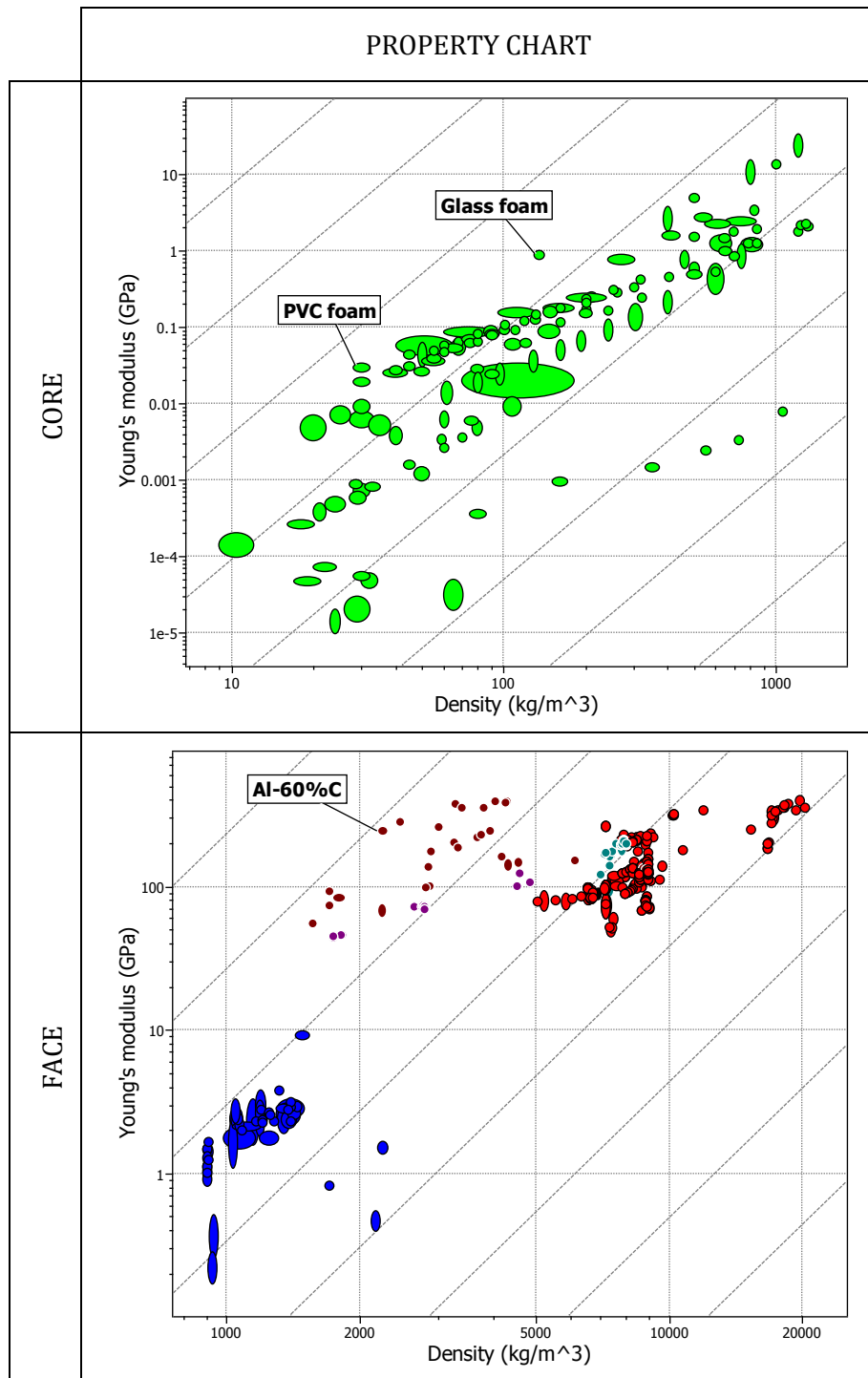


Figure 4.1: Property charts and guide lines corresponding to optimal material for flexural stiffness at minimal weight. Optimal core material is PVC foam while optimal face material is Al-60%C.

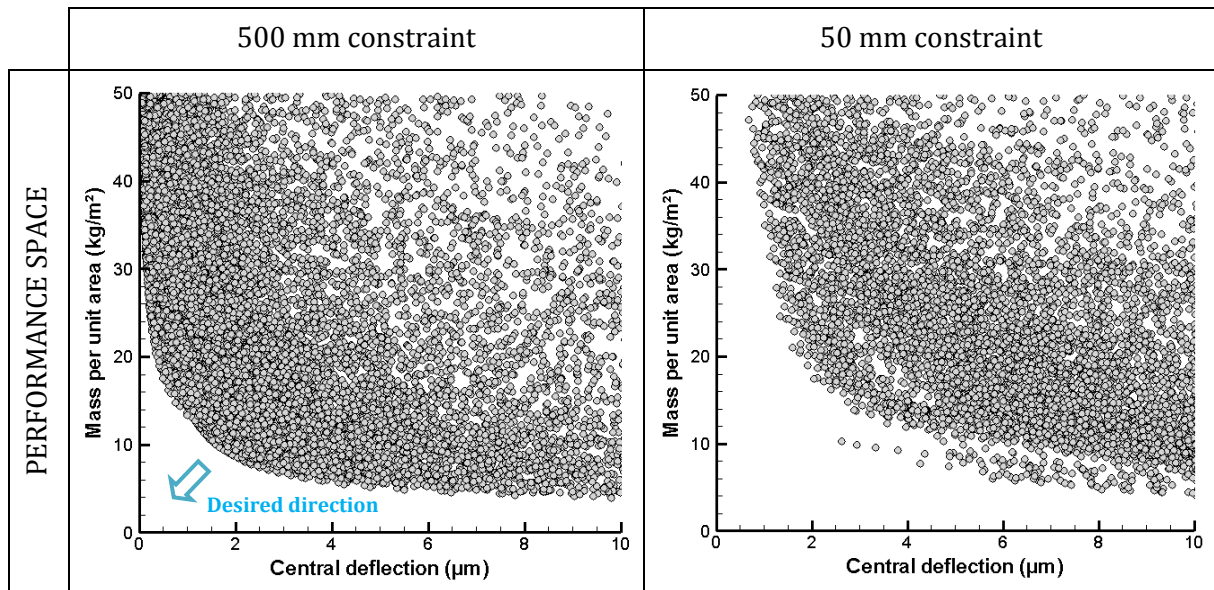


Figure 4.2: Performance space plotting the solutions generated by the optimization algorithm for flexural stiffness at minimal weight for two different size constraints.

Variability analysis

Figure 4.3 helps identify the most influent design variables by plotting their contour value on the performance space gathering the solutions generated by the genetic algorithm. In this figure, the first column corresponds to the influence of constitutive material and the second one corresponds to the influence of the geometry of the sandwich panel (thickness of the layer). The first line stands for the faces while the second one is for the core. This figure gathers the information on the influence of the four considered design variables.

As observed in this figure, the performance space can be divided into two sub-domains corresponding to two different core materials:

- One sub-domain gathers sandwich panels made of glass foam as core material, thus representing the stiffest obtained solutions.
- The other one gathers Polyvinylchloride (PVC) foam core sandwich panels with a core relative density of 0.0215.

The whole trade-off surface is the combination of Pareto fronts considering these two materials as core materials, which explains the split aspect of the trade-off surface.

The optimal choice for face material is Metal Matrix Composite (MMC). The trade-off surface is shared between an Al-60%C composite and a Mg-70%B one with no distinct advantage compared to the other.

Core thickness has an influence on the performances of the solutions. As shown in Figure 4.2, flexural stiffness increases as a function of core thickness. This is mainly observed for PVC foam core solutions. Glass foam core panels are thinner than PVC foam core ones as glass foam density is much higher than PVC foam one.

This change of optimal core materials is due to the size constraint. When the maximum thickness is reached, the only possibility to increase the flexural stiffness is to increase the stiffness of the core.

On the contrary, face thickness is minimal for both PVC and glass foam core panels in order to minimize panel mass.

Optimal design of architected sandwich panels for multifunctional properties

Pierre Leite

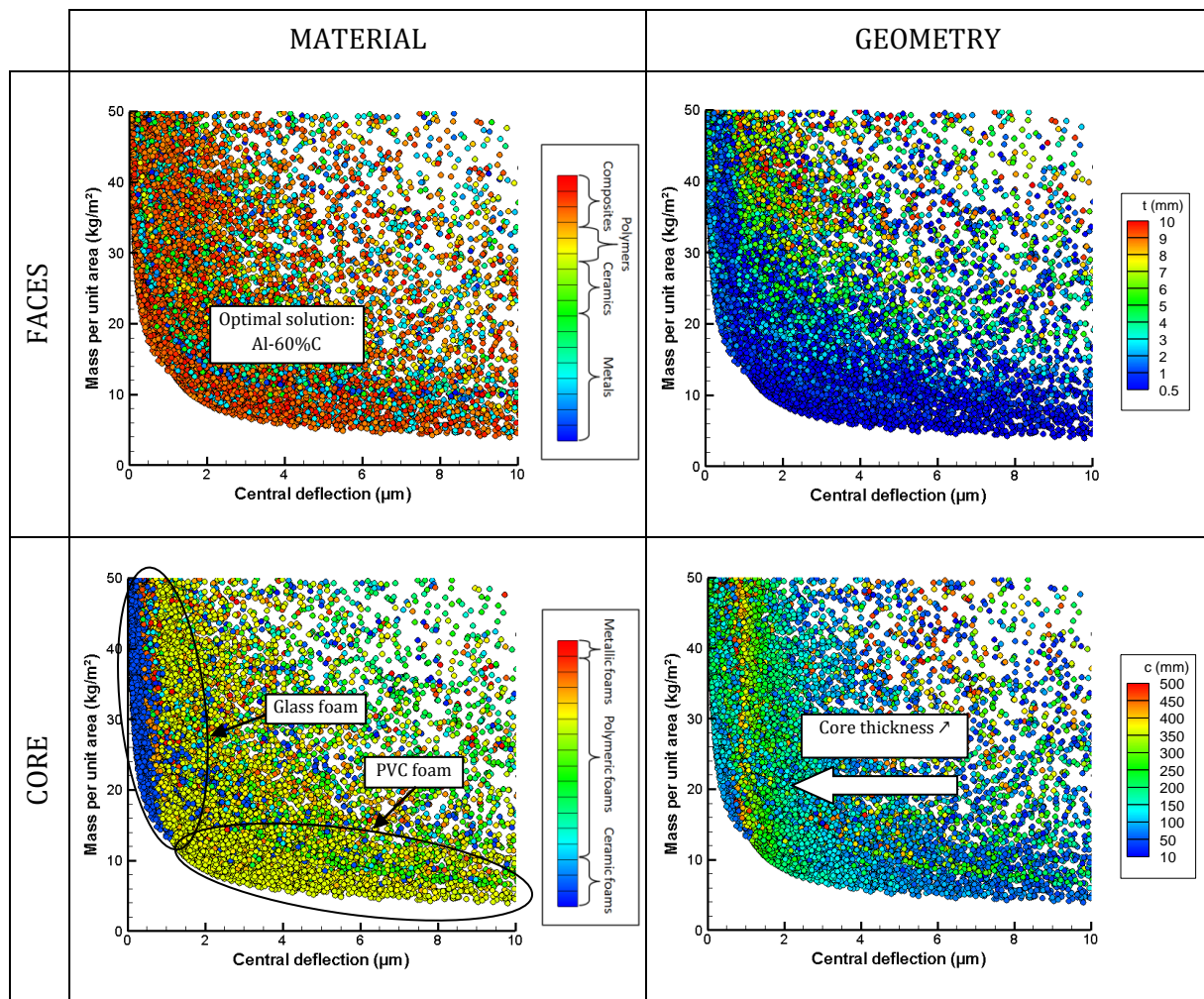


Figure 4.3: Influence of design parameters on the optimal design of a sandwich panel for flexural stiffness at minimal weight. The first column concerns the constitutive materials while the second one shows the influence of layer thickness. The first line concerns the face sheets while the second concerns the core.

Effect of size constraint

As shown in Figure 4.2, reinforcing the size constraint results in a displacement of the trade-off surface away from the previous one. If the minimum achievable mass is the same, the minimum achievable deflection increases from 0.15 to 0.69 μm . The optimal design also changes. When a thicker core is allowed, the main mechanism driving stiffness is the increased distance between the stiff faces and the neutral axis. In that case the core has to be light in order to ensure a constant distance between faces with a minor increase of mass. When this mechanism is constrained, the core also needs to be stiff. In this case, core material such as ceramic foams will overcome polymeric foams.

Advantage of sandwich solutions

As a comparison, Figure 4.4 plots the central deflection of a steel plate submitted to the same three-point bending test than the sandwich panels as a function of its mass per unit area for different thicknesses. The performances are not even comparable by comparing Figures 4.2 and 4.4. It is worthwhile noting that sandwich panels largely overcome monolithic plates at minimal

weight, but to the detriment of size. Monolithic plates would be thinner than a sandwich panel for a given stiffness.

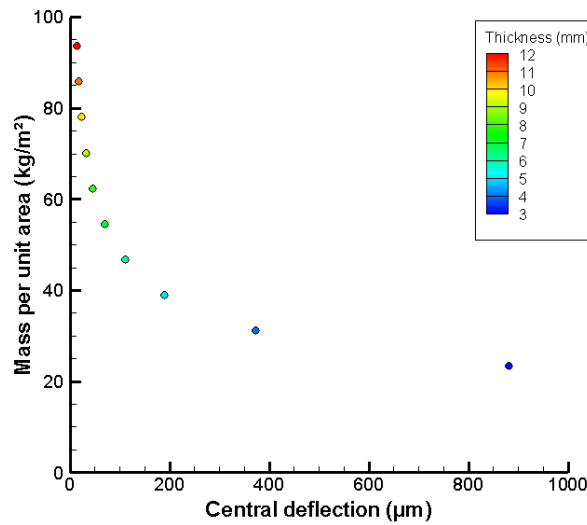


Figure 4.4: Central deflection of a steel plate of thickness t submitted to a three-point bending test as a function of its mass per unit area.

However, steel may not be the optimal choice for bending plates. In Figure 4.5 is plotted the property chart Young's modulus/density. The effective properties of PVC foam core sandwich panels made of Metal Matrix Composite faces have been plotted in order to compare the properties of such a panel to the ones of monolithic plates. Considering the optimal monolithic plate which would be a carbon fibre reinforced polymer, then the obtained sandwich panel is still about ten times stiffer at a given weight according to the guide lines.

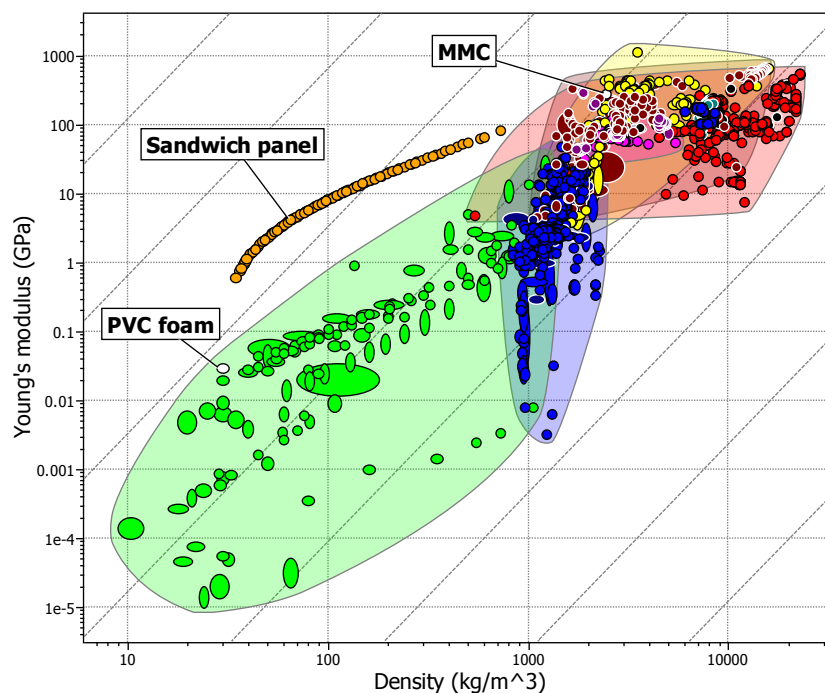


Figure 4.5: Property chart plotting Young's modulus against density. Dotted lines are guidelines representing the performance index corresponding to the design of panels for flexural stiffness at minimal weight.

2.2. Flexural strength

Design space:

- Face materials: Metals, Polymers, and Composites.
- Face thickness: from 0.5 to 10 mm.
- Core materials: Metal foams, Ceramic foams, Polymer foams.
- Core thickness: from 10 to 500 mm.
- Type of sandwich panel: symmetrical.

Objectives:

- Flexural strength: maximize the critical load corresponding to failure of a 1 m span sandwich beam submitted to a three-point bending test.
- Lightness: minimize the mass per unit area.

Constraints:

- Flexural strength > 2 kN.
- Mass per unit area < 50 kg/m².

Preliminary design: Performance index approach

The performance index corresponding to a strong panel at minimal weight is $\sigma^{1/2}/\rho$. The corresponding guide lines are drawn in the property charts given in Figure 4.6 for face material selection. Core is assumed to fail by indentation or by shear, thus leading to a different performance index. The appropriate one is σ/ρ and corresponding guide lines are drawn for core material selection.

According to the performance index approach, the optimal core material should be Polymethacrylimide (PMACR) foam even though many other solutions are close in terms of strength at minimal weight. Regarding the faces, the optimal material should be a Metal Matrix Composite (Al-60%C).

Advanced design

Compatibilities

The performance space generated by the genetic algorithm is shown in Figure 4.7. The trade-off surface is slightly concave with a very high radius of curvature. These two performances are compatible but except for an exchange constant of about 700 N/kg.m⁻², no interesting trade-off appears.

The two limit solutions are the most interesting ones: one with 7 kg/m² and a 2 kN strength (corresponding to the strength constraint) which is the lightest solution and another one with 44 kg/m² and a 28.5 kN strength which is the strongest one.

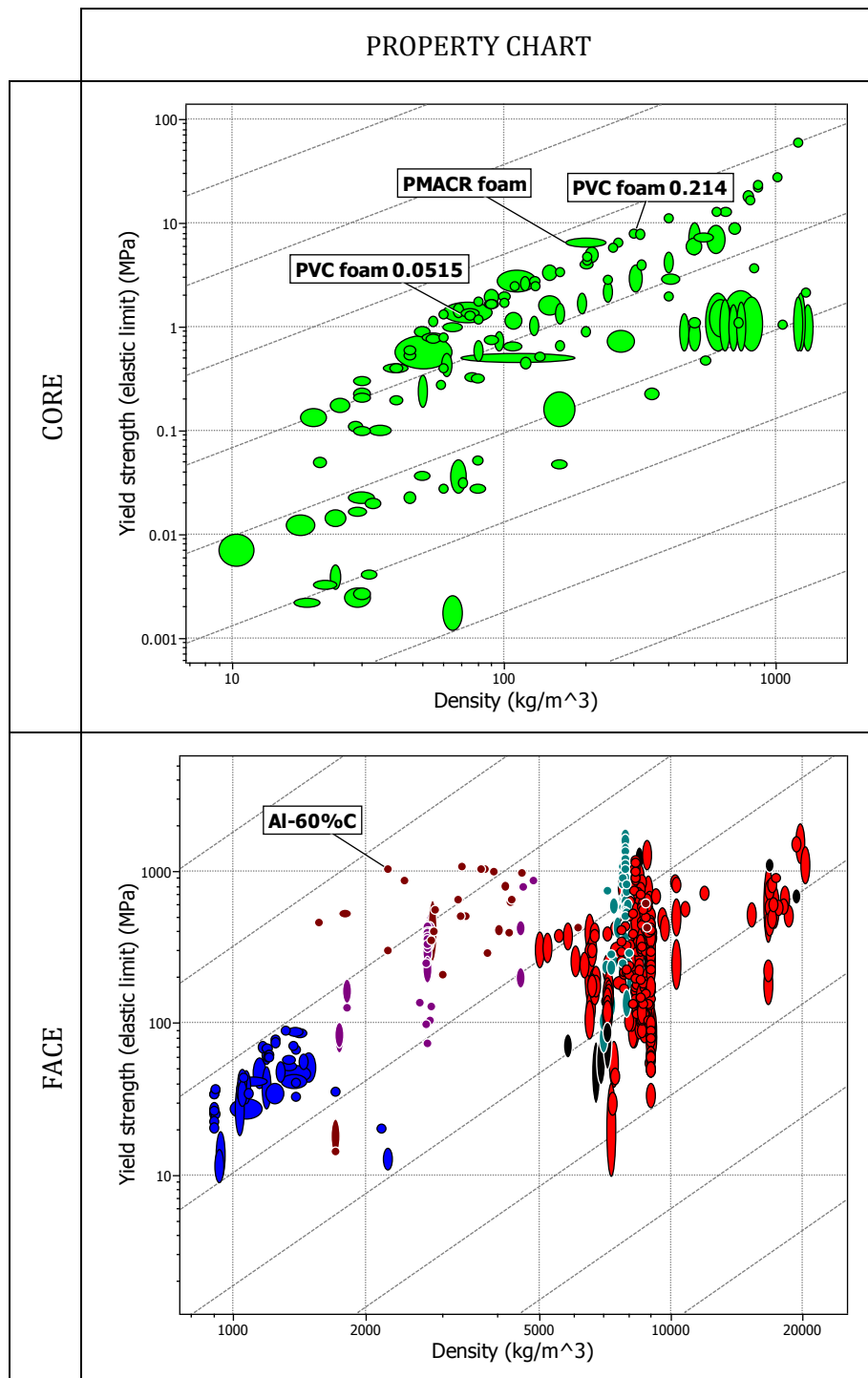


Figure 4.6: Property charts and guide lines corresponding to optimal material for flexural strength at minimal weight. Optimal core material is Polymethacrylimide (PMACR) foam while optimal face material is Al-60%C.

Optimal design of architected sandwich panels for multifunctional properties

Pierre Leite

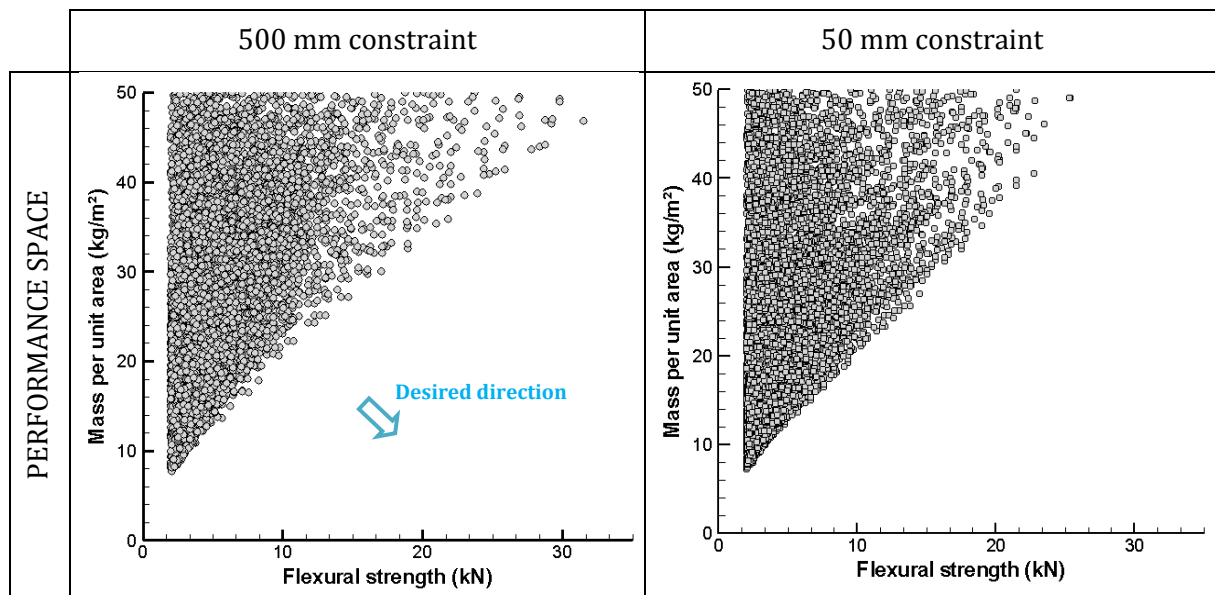


Figure 4.7: Performance space plotting the solutions generated by the optimization algorithm for flexural strength at minimal weight for two different size constraints.

Variability analysis

For flexural strength at minimal weight, the optimal choice for the face material is Carbon fibres reinforced Aluminium (Al-60%C MMC) as shown in Figure 4.8. An Aluminium alloy is competitive for low strength requirements but the reinforced Aluminium is the most represented face material in the Pareto front. This variable has a major influence, solutions made of other materials are quite distant from the trade-off surface.

Core material is also ranking influential as almost all the Pareto front is composed of PVC foam core sandwich panels. An increasing strength is achieved by increasing core strength which is done by increasing foam relative density. The lightest PVC foam core solutions are made of a foam with a 0.0515 relative density while the strongest ones are made of a foam with a 0.214 relative density. A few Polymethacrylimide (PMACR) foam core solutions are competitive for light and low strength requirements.

Face thickness mainly affects performances but not the ranking. Increasing face thickness will lead to an increase of mass and strength but if the constitutive materials and the core thickness are appropriately chosen, the obtained solution will be within the group of non-dominated solutions. On the other hand, core thickness has an optimal value of 40 mm for the PVC foam core sandwich panels.

The optimal design for flexural strength at minimal weight is a PVC foam core sandwich panels with Carbon reinforced Aluminium faces and a core thickness of 40 mm. Face thickness and core relative density can be used to obtain the required strength.

Effect of size constraint

There is a slight influence of size constraint. The Pareto front differs for high strength requirements, mainly because face thickness is limited to 5 mm. The optimal core thickness being found at 40 mm, which is below the 50 mm constraint, the performance space is nearly the same.

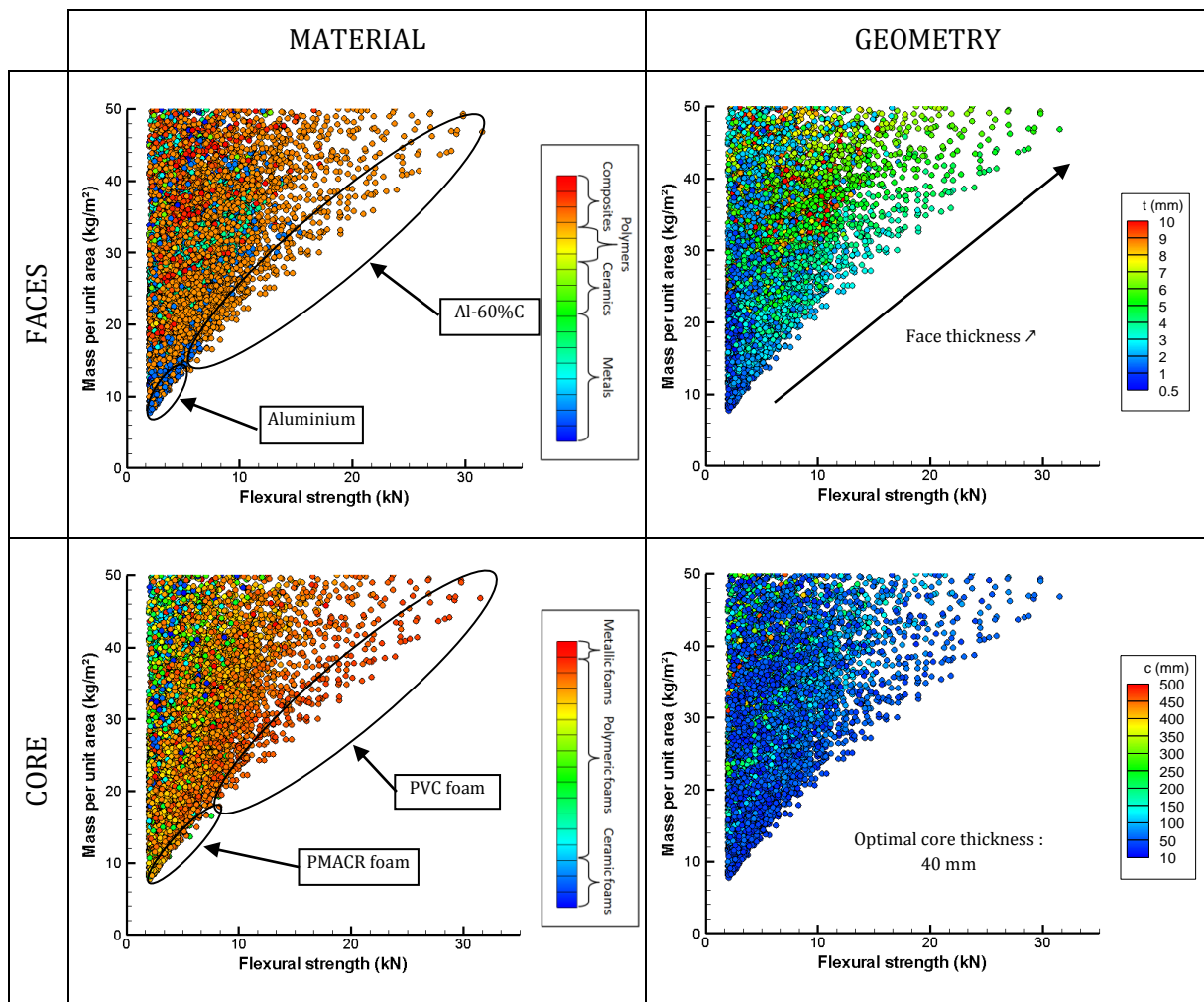


Figure 4.8: Influence of design parameters on the optimal design of a sandwich panel for flexural strength at minimal weight.

Advantage of sandwich solutions

Several studies were dedicated to the design of sandwich panels for flexural strength at minimal weight by using failure mode maps. They concluded that the path of optimal design follows limit contours of transition between failure modes as shown in Figure 4.9, taken from [DES01b]. This leads to trade-off surfaces as the one presented by Chen et al. [CHE01] and shown in Figure 4.9. The trade-off surface is divided into several parts corresponding to the competition between different failure modes.

The failure modes calculated for the obtained results are shown in Figure 4.10. For low strength, indentation and face wrinkling are the two failure modes in competition. For intermediate strength, core shear, face yielding and indentation are the occurring failure modes while for high strength, only indentation and core shear occur. A precise determination of the predominant failure modes would require further investigation with the creation of a failure mode map for a given type of sandwich panel.

The strength of a steel plate of thickness t as a function of its mass per unit area is given in Figure 4.10. Once again, sandwich panels are much more load bearing than monolithic solutions for the considered load conditions.

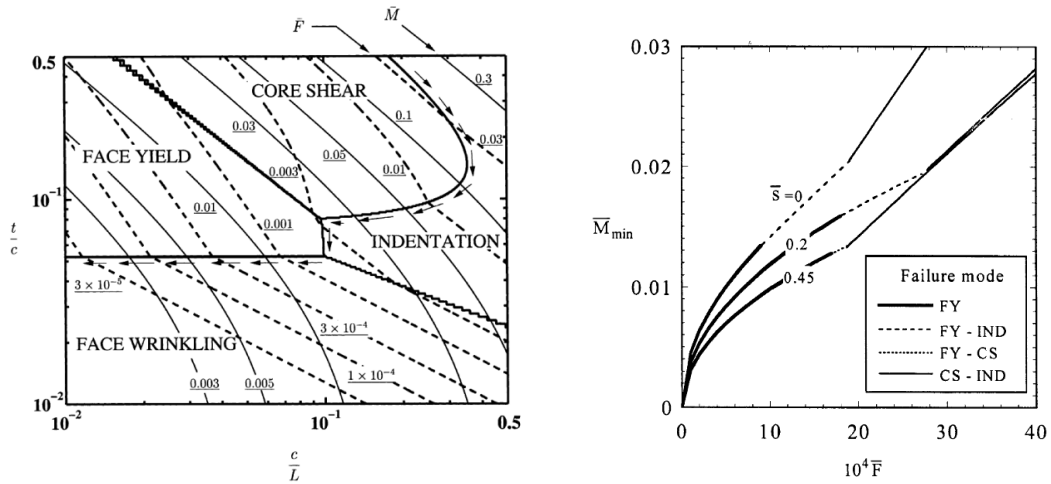


Figure 4.9: On the left hand side: failure mode map, taken from [DES01b]. The optimal path for strength design at minimal weight as a function of panel dimensions is indicated by arrows. This path follows the frontier between failure modes domains. The design variables are core thickness c and face thickness t . On the right hand side: influence of the failure mode on the shape of the trade-off surface between strength and mass, taken from [CHE01].

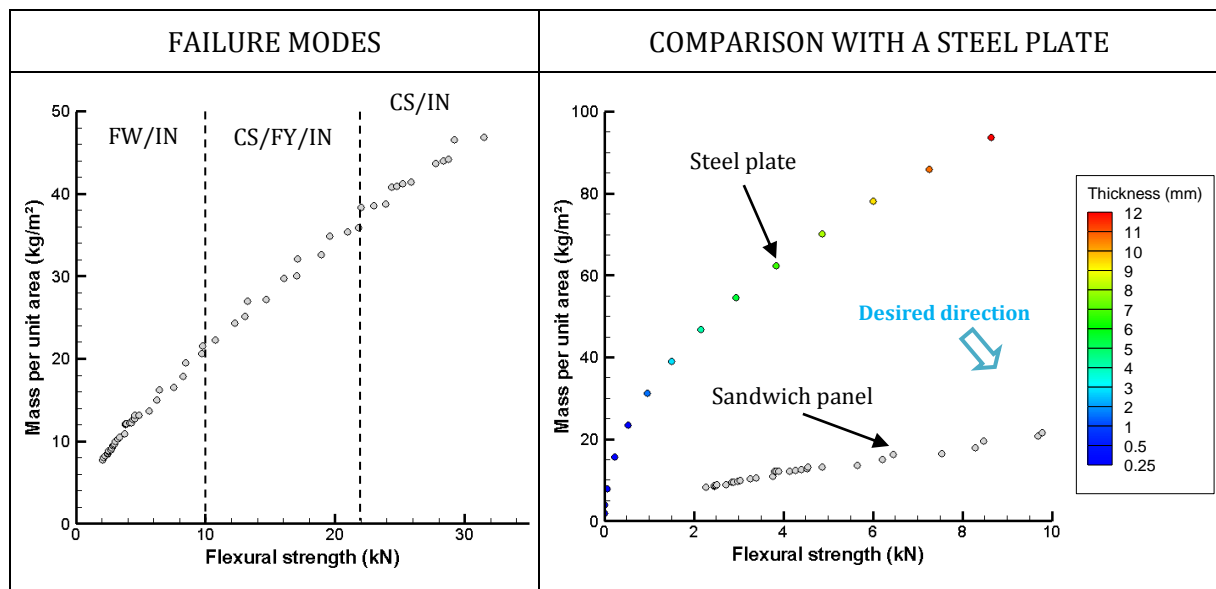


Figure 4.10: Evolution of the failure modes and comparison between sandwich panels and a steel plate (colour legend corresponds to the thickness of the steel plate). FY is face yielding, CS is core shear, IN is indentation and FW is face wrinkling.

Benefits of the present approach

The obtained results are consistent with a performance index approach in terms of material selection. The optimal face material determined by the genetic algorithm, which is Al-60%C, is the same than the one identified using a performance index.

In terms of core material selection, a simple approach based on performance indices fails to identify the whole set of optimal solutions. This is due to the competition between failure modes. Let us consider two sandwich panels made of the same face material but with different cores. For each solution, Figure 4.11 illustrates the evolution of properties of the optimal design in terms of dimensions. In the present case, the failure mode map is such that core thickness has an

optimal value of 40 mm in the whole range of observed performances. The curves can be split in two parts:

- At a low mass, face thickness is small, leading to face failure by face wrinkling or yielding. In this part of the curve, the Polymethacrylimide foam core panel is the optimal solution.
- For an increasing face thickness, comes a point for which failure mode switches from face to core failure. The slope of the curve changes, which means that the relative improvement of strength compared to the loss of lightness is lower than in the first part of the curve. A way to improve the panel properties is to increase core strength.

PVC foams are better solutions than Polymethacrylimide foams for high strength requirements because of a switch in the failure mode, given that no stronger Polymethacrylimide foams are present than the one identified in the database. PVC foams have a worse performance index but a better yield strength.

The optimal solutions are the ones that are at the intersection between face and core failures. This is consistent with the results obtained by several authors and discussed in Chapter 2 Section 3.2.

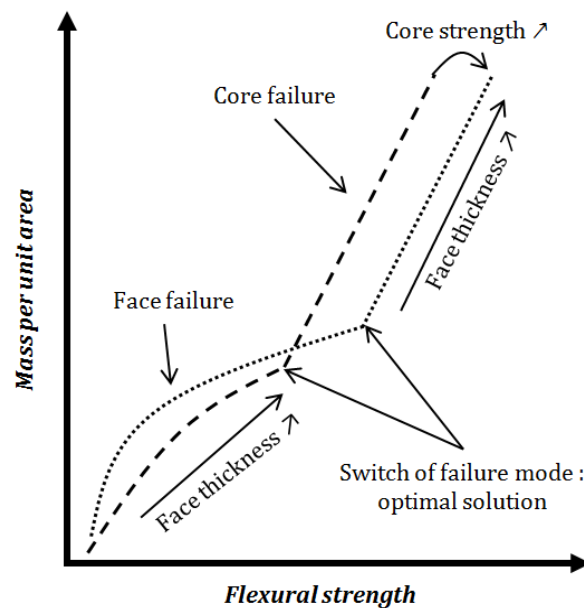


Figure 4.11: Schematic showing the evolution of the optimal properties for a sandwich. At a low mass, face failure is the dominant failure mode. Increasing strength is achieved by increasing face thickness. At a given point, failure mode switches from face to core failure. Then the optimal core material would change to a stronger one for which this switch occurs at a higher level of strength.

2.3. Acoustic damping

Design space:

- Face materials: Metals, Polymers, and Composites.
- Face thickness: from 0.5 to 10 mm.
- Core materials: Metal foams, Ceramic foams, Polymer foams.
- Core thickness: from 10 to 500 mm.
- Type of sandwich panel: symmetrical.

Objectives:

- Acoustic damping: maximize the mean value of the Acoustical Transmission Loss in the frequency range [1 000; 4 000] Hz.
- Lightness: minimize the mass per unit area.

Constraints:

- Acoustical Transmission Loss > 20 dB.
- Mass per unit area < 50 kg/m².

Preliminary design: Performance index approach

No dedicated performance index has been derived regarding the Acoustical transmission Loss at minimal weight. However, one should know that for sandwich panels, the two mechanisms that promote acoustic damping are the “mass law” and the “sandwich effect” (see Chapter 2, Section 3.4). The latter can be obtained when the core is sufficiently soft. So one could consider that an optimized sandwich panel in regard to acoustic damping would be made of heavy face sheets to promote the “mass law” and of very soft core to obtain a “sandwich effect”. The performance indices that are considered are then $1/E$ for the core material and ρ for the faces. The corresponding guide lines are drawn in the property charts in Figure 4.12.

According to the performance index approach, the optimal core material should be Polyurethane foam which is a popular solution for acoustic damping. Regarding the faces, the optimal material should be a Tungsten-Rhenium alloy.

Advanced design

Compatibilities

The performance space obtained for the optimization of a sandwich panel for acoustic damping at minimal weight is given in Figure 4.13. From this performance space, a convex trade-off surface can be obtained. The lightest solution has a mass of 1.05 kg.m⁻² for a 20 dB transmission loss while the heaviest one has a mass of 50 kg.m⁻² for a 96.8 dB transmission loss.

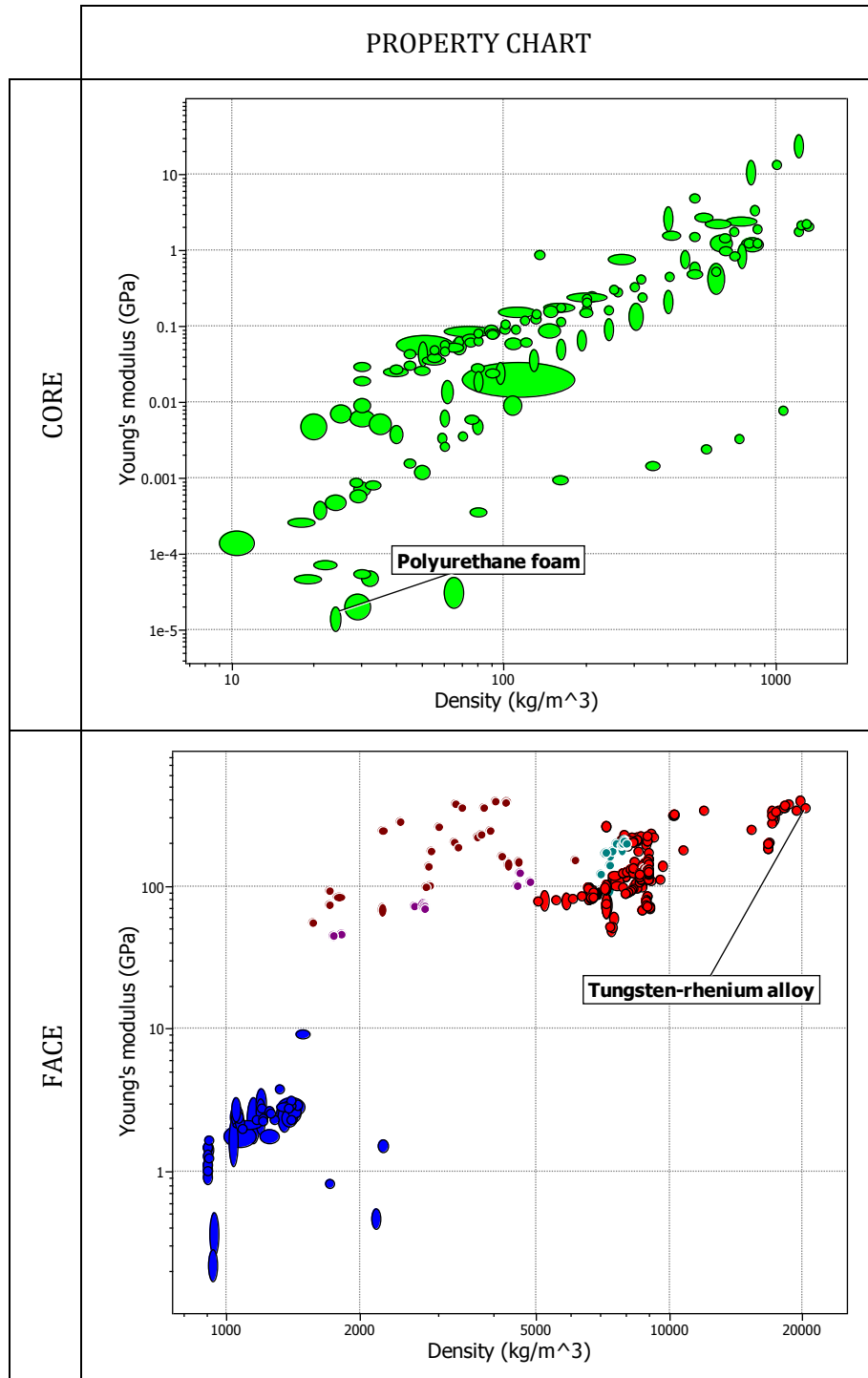


Figure 4.12: Property charts and guide lines corresponding to optimal material for acoustic damping at minimal weight. Optimal core material is Polyurethane foam while optimal face material is Tungsten-Rhenium alloy.

Optimal design of architected sandwich panels for multifunctional properties

Pierre Leite

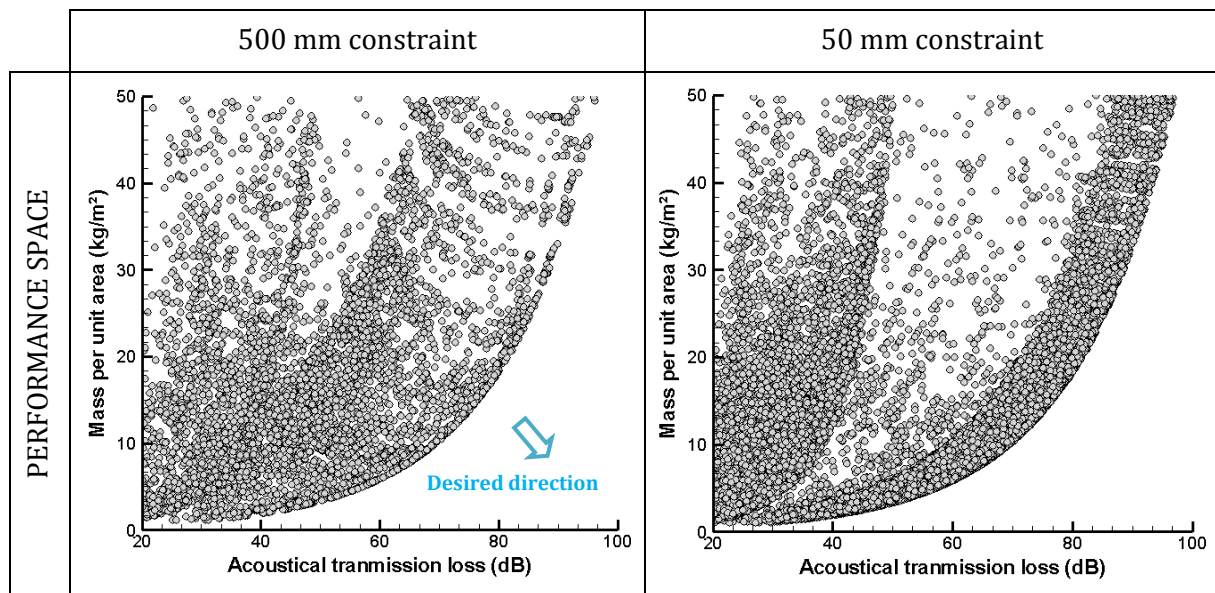


Figure 4.13: Performance space plotting the solutions generated by the optimization algorithm for Acoustical Transmission Loss at minimal weight for two different size constraints.

Variability analysis

The influence of design variables on the performance space is shown in Figures 4.14. It only takes a quick look at these plots to figure out that the core material is the most influential design variable. Solutions made of Polyurethane (PUR) foam as core material are gathered all along the Pareto front. This material has a relative density of 0.0175. Moreover, core thickness is significantly related to the rank of the solutions. Indeed the higher the thickness is, the more distant the solution is from the trade-off surface.

On the opposite, face material seems to have minor influence on the rank even though it has a significant influence on the performances. The only important parameter is face mass, whether it comes from the thickness or from the density.

The optimal core material has been perfectly predicted by the performance index approach. However, the optimal core thickness is counter-intuitive. Let us keep in mind that no mechanical requirements have been taken into account, so obtained solutions may have poor mechanical properties. Regarding face material selection, its impact is negligible on acoustic damping.

Effect of size constraint

The chosen values for size constraint do not allow the effects of this constraint to be monitored. Indeed, the two trade-off surfaces obtained with a 50 mm thick constraint and a 500 mm thick constraint are exactly the same as the optimal value for core thickness is 10 mm.

Advantage of sandwich solutions

Sandwich structures offer interesting possibilities in terms of acoustical insulation. As demonstrated by several authors, if correctly designed, sandwich panel can exhibit very high transmission loss compared to monolithic plates [DYM74, MUR98, SIM95, SIM04]. The “sandwich effect” is observed in Figure 4.15 in a particular case of a sandwich panel with 3 mm Aluminium Bronze faces and a 10 mm Polyurethane foam core. In this figure, the Acoustical Transmission Loss is plotted as a function of the frequency. The black dotted line represents the

obtained Acoustical Transmission Loss using a model which considers a possible transverse deformation in the soft core (allowing the occurrence of symmetric vibration modes) while the grey dotted line represents the Acoustical Transmission Loss using a model which considers no transverse deformation. The difference between these two curves shows the benefits from the presence of a soft core. The frequency range used for the assessment of the acoustical fitness of the solution, between 1 000 and 4 000 Hz, is the one that maximizes the difference between the two curves. The symmetric coincidence frequency is about 5 700 Hz.

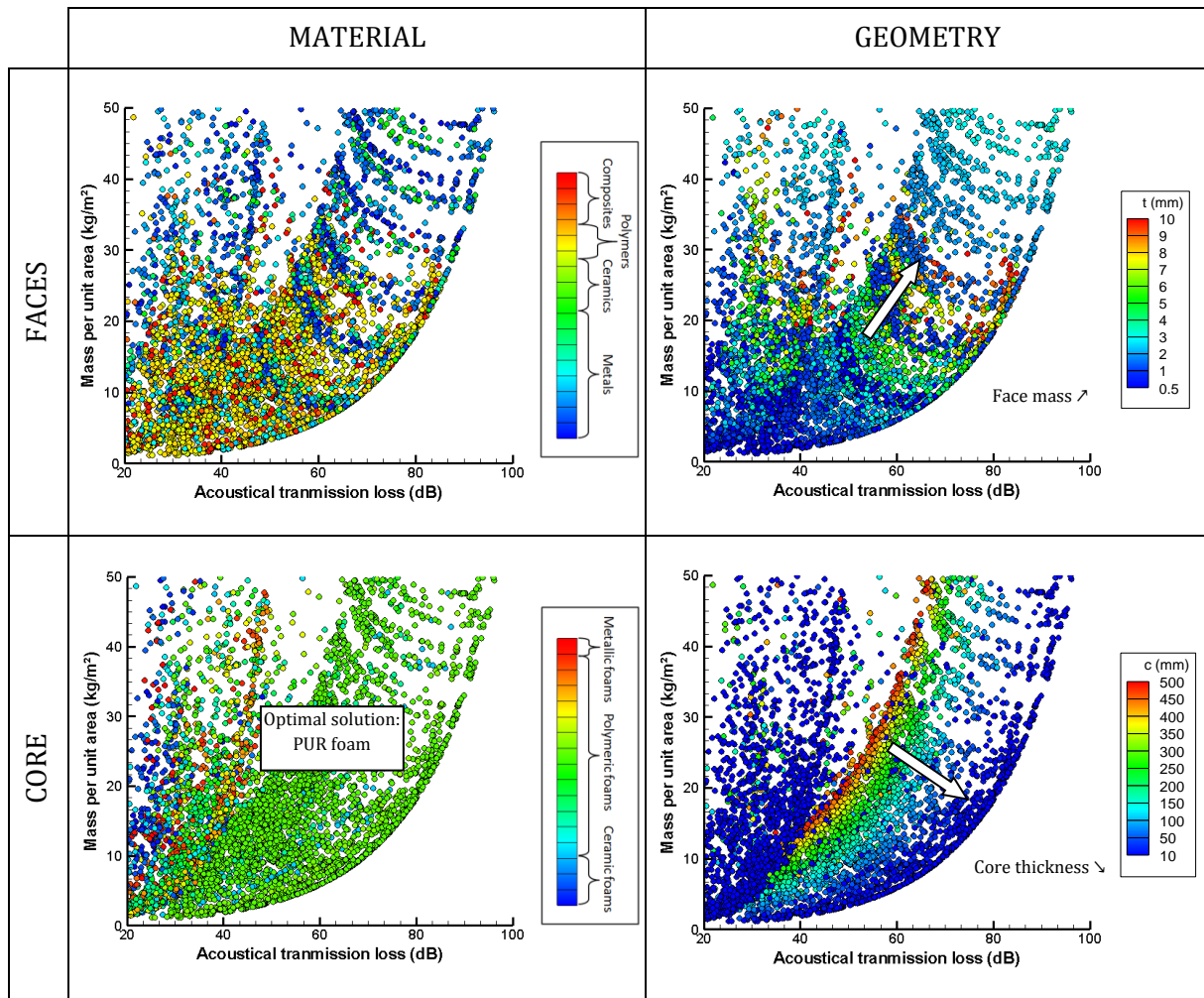


Figure 4.14: Influence of design parameters on the optimal design of a sandwich panel for Acoustical Transmission Loss at minimal weight.

Figure 4.16 shows that the symmetric coincidence frequency is related to the face thickness. Indeed, in this figure the Acoustical Transmission Loss is plotted as a function of frequency for six different sandwich panels made of the same constitutive materials than the previous example but with different thicknesses. Two core thicknesses are considered, 10 mm in black and 20 mm in grey. For face thickness, the considered values are 1, 2 and 3 mm. For 1 mm faces, the symmetric coincidence frequency is higher than 10 000 Hz and is out of the range of the plot. For other face thicknesses, this characteristic frequency is the same whatever the core thickness is. Nevertheless, core thickness has an influence on the peak value of Acoustical Transmission Loss and on the general shape of the curve. Panels with a 10 mm core exhibit a higher peak value of Acoustical Transmission Loss. However, ones with a 20 mm core exhibit a flatter curve than thinner panels with a higher Acoustical Transmission Loss at 500 Hz. No constraint has been set

Optimal design of architected sandwich panels for multifunctional properties

Pierre Leite

on the homogeneity of the Acoustical Transmission Loss but in some applications, having a flat evolution of the Acoustical Transmission Loss along a given frequency range can be required, changing the rank of the solutions. Even if the optimal design is counter-intuitive as one could have thought that better Acoustical Transmission Loss would have been obtained by having a thick core, this is explained by the frequency range chosen for the calculations. Considering a wider frequency range would lead to different results.

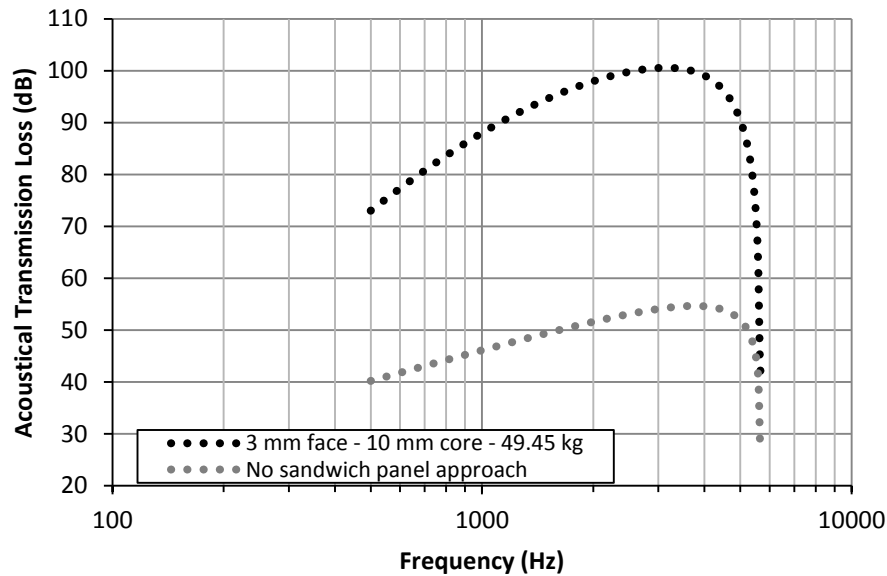


Figure 4.15: Illustration of the “sandwich effect” on the Acoustical Transmission Loss. The grey curve has been obtained using a model that considers no transverse core deformation while the black curve has been obtained with the appropriate model. The same materials and dimensions have been considered in both cases.

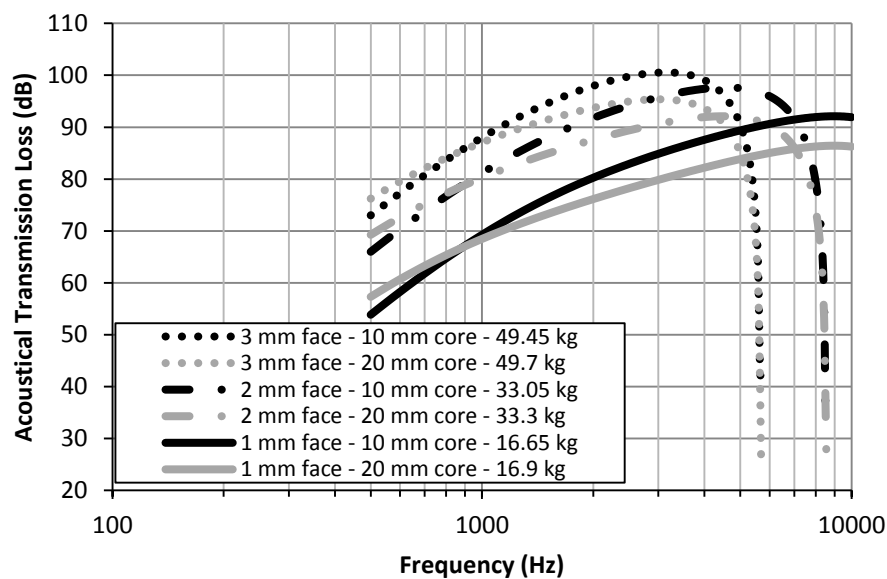


Figure 4.16: Evolution of the Acoustical Transmission Loss as a function of frequency for three different face thicknesses and two core thicknesses. Face thickness is related to the symmetric coincidence frequency while core thickness is related to the peak value of Acoustical Transmission Loss.

By plotting the performance space with the axis corresponding to mass in a log scale as in Figure 4.17, it appears that the optimal Acoustical Transmission Loss is proportional to the logarithm of the panel weight. This behaviour coincides with a classical “mass law”. Along the Pareto front, a higher Acoustical Transmission Loss is only achieved by increasing mass, i.e. by increasing either face thickness or face density. It can be assumed that the mean value of Acoustical Transmission Loss is the sum of two terms. The first one corresponds to the “mass law” contribution and is mainly dictated by face design while the second one corresponds to the “sandwich effect” and is dictated by core design.

Most noteworthy is the great difference for the Acoustical Transmission Loss between a steel plate of thickness t and the sandwich panel. For a monolithic solution, no sandwich effect occurs and then only the “mass effect” is observed (Figure 4.17).

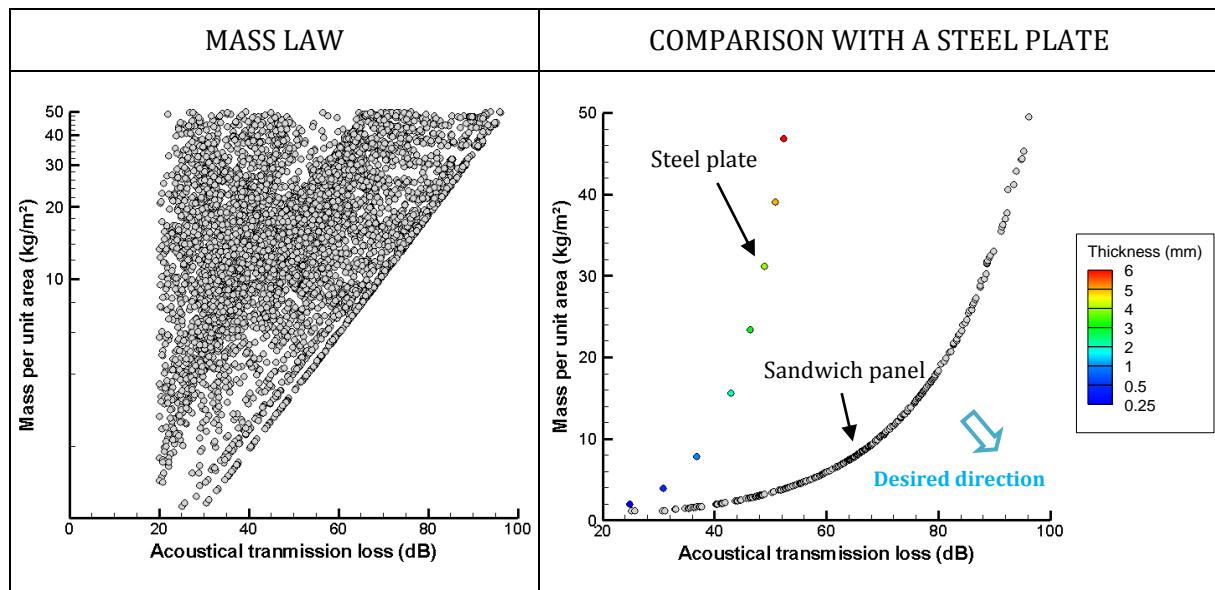


Figure 4.17: On the left hand side: performance space for Acoustical Transmission Loss at minimal weight in which mass is plotted in log scale. On the right hand side: the Acoustical Transmission Loss of a steel plate of thickness t is plotted as a comparison with the Pareto front obtained for sandwich panels.

2.4. Thermal resistance

Design space:

- Face materials: Metals, Polymers, and Composites.
- Face thickness: from 0.5 to 10 mm.
- Core materials: Metal foams, Ceramic foams, Polymer foams.
- Core thickness: from 10 to 500 mm.
- Type of sandwich panel: symmetrical.

Objectives:

- Thermal resistance: maximize the through-thickness thermal resistance.
- Lightness: minimize the mass per unit area.

Constraints:

- Thermal resistance $> 1 \text{ m}^2\text{K/W}$.
- Mass per unit area $< 50 \text{ kg/m}^2$.

Preliminary design: Performance index approach

The performance index regarding thermal conductivity in the through-thickness direction at minimal weight is directly linked to thermal conductivity and density. The performance index to be maximized is $1/k\rho$ for both face and core material with k the thermal conductivity.

As shown in the property charts of Figure 4.18, the optimal core material is Melamine foam and the optimal face material is Polypropylene.

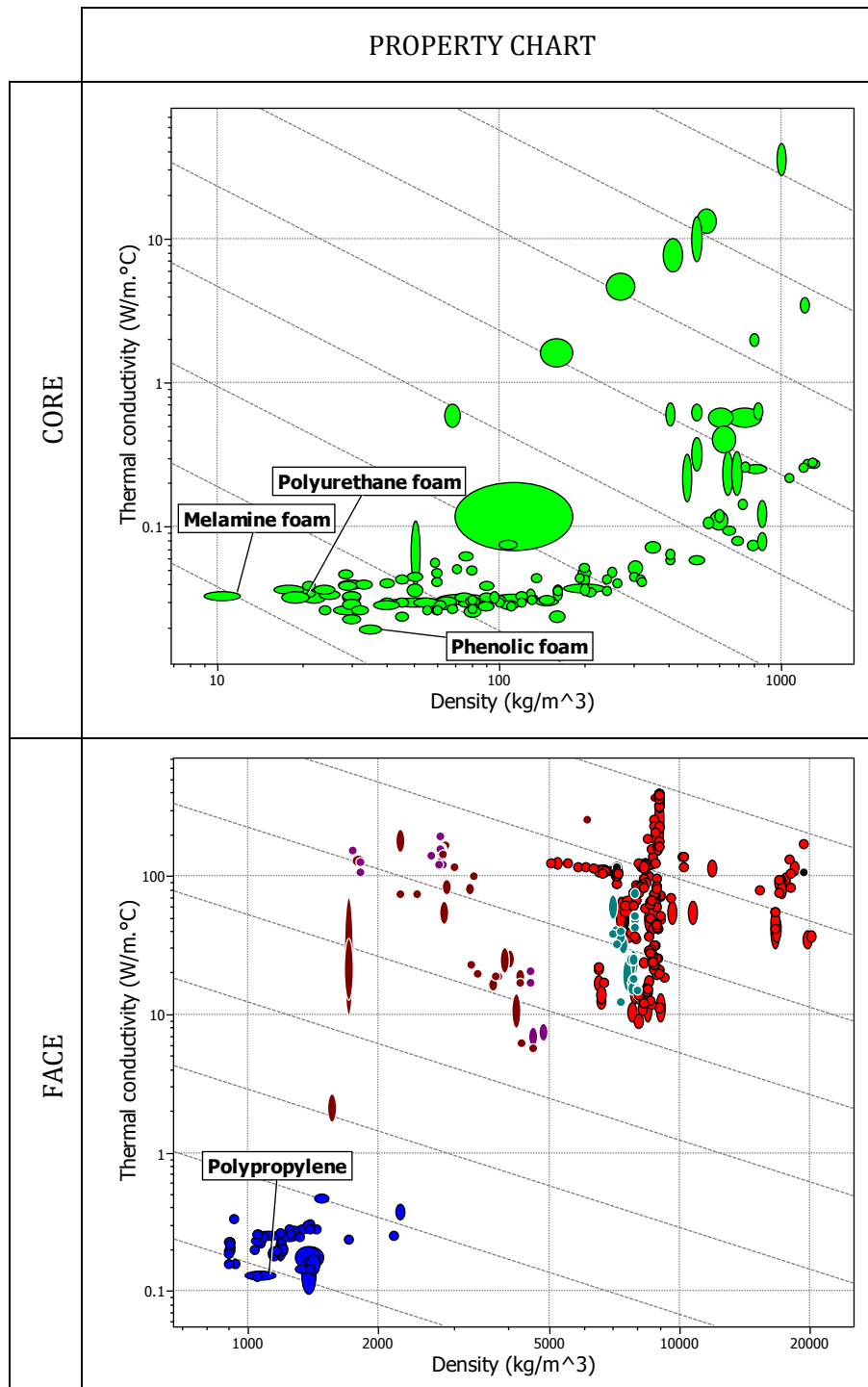


Figure 4.18: Property charts and guide lines corresponding to optimal material for thermal resistance at minimal weight. Optimal core material is Melamine foam while optimal face material is Polypropylene.

Advanced design

Compatibilities

The trade-off surface for thermal resistance against mass is composed of several parts with gaps between the different lines as shown in Figure 4.19. The Pareto-front is piecewise linear. Three sub-groups can be identified with corresponding exchange constants of $2.51 \text{ m}^2 \cdot \text{K} \cdot \text{W}^{-1} / \text{kg} \cdot \text{m}^{-2}$ for the first one, $1.78 \text{ m}^2 \cdot \text{K} \cdot \text{W}^{-1} / \text{kg} \cdot \text{m}^{-2}$ for the second one and $1.34 \text{ m}^2 \cdot \text{K} \cdot \text{W}^{-1} / \text{kg} \cdot \text{m}^{-2}$ for the last part of the Pareto front.

As the exchange constant decreases while increasing the mass of the solutions, there are several interesting solutions in terms of trade-off. Indeed, a total of four solutions can be considered as optimal solutions, mainly located at each gap in the Pareto front. They are marked by crosses in Figure 4.19.

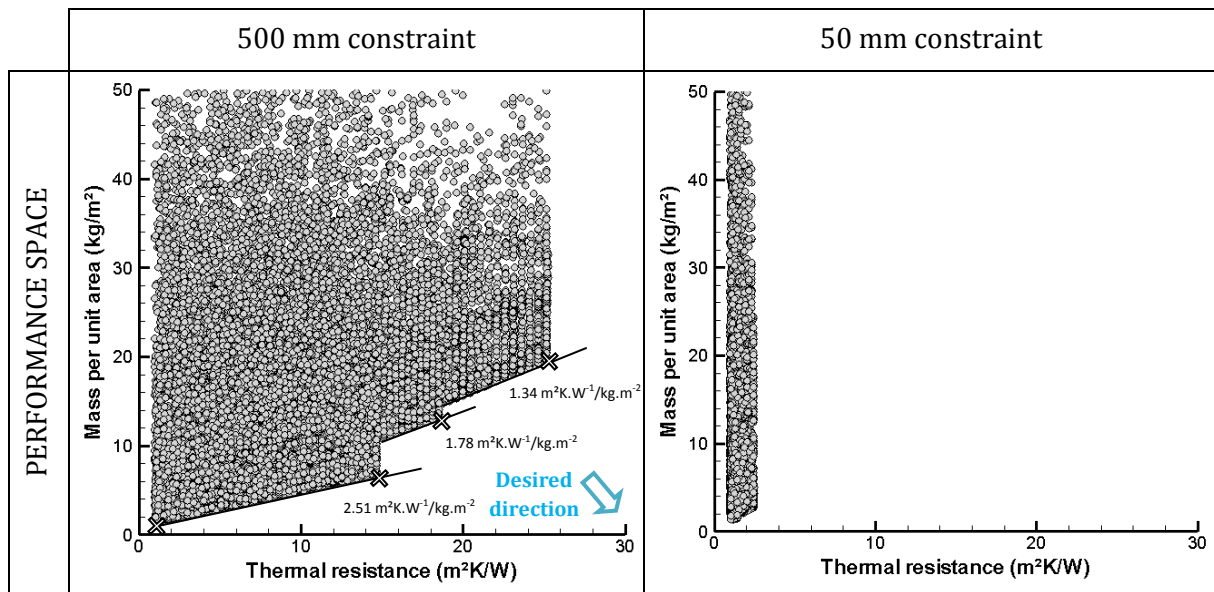


Figure 4.19: Performance space plotting the solutions generated by the optimization algorithm for thermal resistance at minimal weight for two different size constraints.

Variability analysis

The sub-groups identified in the performance space correspond to solutions with different core materials as shown in Figure 4.20:

- The first group represents panels with Melamine foam (Mel).
- The second one is the group of Polyurethane (PUR) foam core panels.
- The last one gathers the sandwich panels made of Phenolic foam core (Phe).

Among the four interesting solutions mentioned above, two are made of Melamine foam and are the lightest ones, one is made of Polyurethane foam and is an intermediate solution while the last one is composed of Phenolic foam as core material.

It is clear that this design variable has a major influence by completely dividing the performance space. The face material, on the other hand, influences the rank of the solutions. The best face material found in the used database considering these objectives is Polypropylene. Polyethylene and ABS (Acrylobutadienestyrene) come next in the ranking. These materials are the ones that minimize the product between thermal conductivity and density.

Optimal design of architected sandwich panels for multifunctional properties

Pierre Leite

In each sub-groups, increasing the core thickness leads to an increase of the thermal resistance and an increase of the mass. The gaps in the trade-off surface are due to the 500 mm thickness constraint. The gap occurs by reaching the maximum possible core thickness. Then, to further increase the thermal resistance, a material with lower thermal conductivity is selected. As shown in Figure 4.18, the optimal solutions are Melamine foam, Polyurethane foam and Phenolic foam in that order, confirmed by the obtained results.

The face thickness has a direct link with the rank of the solution as the Pareto front is exclusively composed of 0.5 mm thick faces. The higher the face thickness is, the further the solution is from the trade-off surface.

Foams are about ten times lighter and exhibit a thermal conductivity ten times lower than dense materials. Moreover, the core can be 10 times thicker than the faces. The major part of the thermal resistance is provided by the core while a big part of the mass can come from the faces. Then, the faces must be thin to reduce weight and the core must be thick to increase thermal resistance. The thermal resistance can then be tailored by adjusting the core thickness.

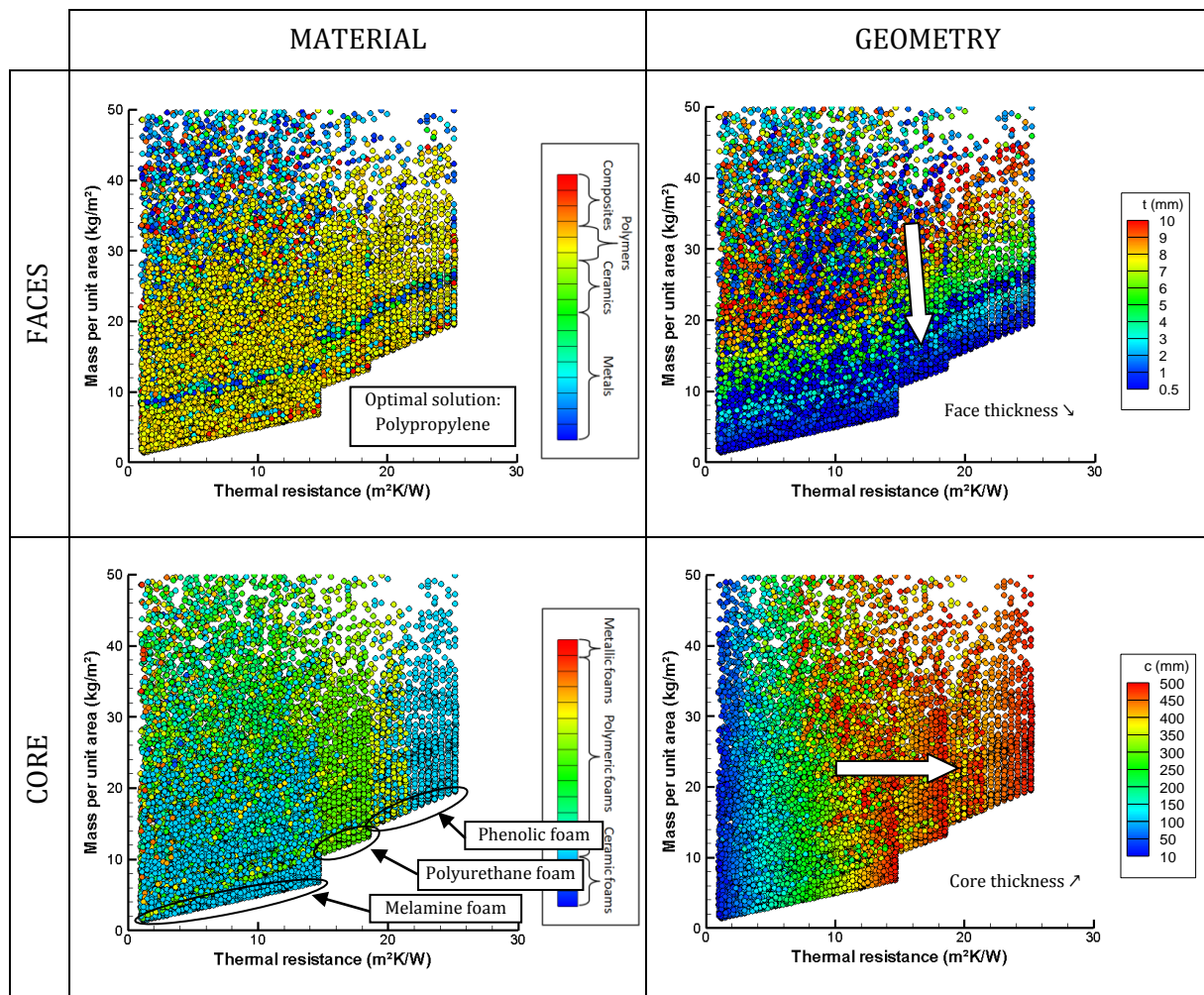


Figure 4.20: Influence of design parameters on the optimal design of a sandwich panel for thermal resistance at minimal weight.

Effect of size constraint

The size constraint has a major impact on the performance space as shown in Figure 4.19. The achievable thermal resistance with a 50 mm thick sandwich panel is about $2.5 \text{ m}^2 \cdot \text{K} \cdot \text{W}^{-1}$,

which is ten times less than the one for a 500 mm thick panel. The linear relationship between thickness and thermal resistance is quite plain, which can partly explain the linear shape of the trade-off surface.

Advantage of sandwich solutions

The main advantage of sandwich panel structures for thermal insulation at minimal weight is to integrate architected materials that are characterized by very low thermal conductivity and density as core material. As shown in Figure 2.21, foams exhibit a thermal conductivity which is ten times lower than the one for polymers. Faces do not strongly participate in thermal insulation, mainly because of the difference in the possible thickness.

2.5. Thermal insulation

Design space:

- Face materials: Metals, Polymers, and Composites.
- Face thickness: from 0.5 to 10 mm.
- Core materials: Metal foams, Ceramic foams, Polymer foams.
- Core thickness: from 10 to 500 mm.
- Type of sandwich panel: unsymmetrical.

Objectives:

- Thermal insulation: minimize the temperature at the inner face while the outer face is submitted to a 700 °C heat during 1 hour.
- Lightness: minimize the mass per unit area.

Constraints:

- Temperature at the inner face < 140 °C.
- Thermal shock resistance: $\max_{\forall x, \forall t} \left(\frac{\sigma(x, t)}{\sigma_y(x)} \right) < 1$.
- Temperature in the material < maximum service temperature of the material.
- Mass per unit area < 50 kg/m².

Preliminary design: Performance index approach

In regard to the specifications, three main properties are required: lightness, low thermal diffusivity and thermal shock resistance. It is assumed that the thermal gradient that will be experienced by face material is low enough for face thermal shock resistance not to be evaluated. The performance index corresponding to a plate with low diffusivity at minimal weight is $1/a\rho$ with a the thermal diffusivity and ρ the density.

On the other hand, core material is assumed to experience a high thermal gradient in order to minimize the temperature of the inner face of the panel. Then two performance indices are considered:

- A first one corresponding to a material with high thermal shock resistance at minimal weight $\sigma_y/(\alpha E \rho)$ with σ_y and α the yield strength and coefficient of thermal expansion respectively.
- A second one corresponding to a material with low thermal diffusivity at minimal weight $1/a\rho$.

Optimal design of architected sandwich panels for multifunctional properties

Pierre Leite

The appropriate guide lines are drawn in the property charts in Figure 4.21. A filter has been considered in order to discard the material having a maximum service temperature lower than 700 °C due to the constraint of service temperature.

According to the performance index approach, the optimal core material should be Carbon foam and the optimal face material should be Carbon fibre reinforced Carbon (Ceramic Matrix Composite).

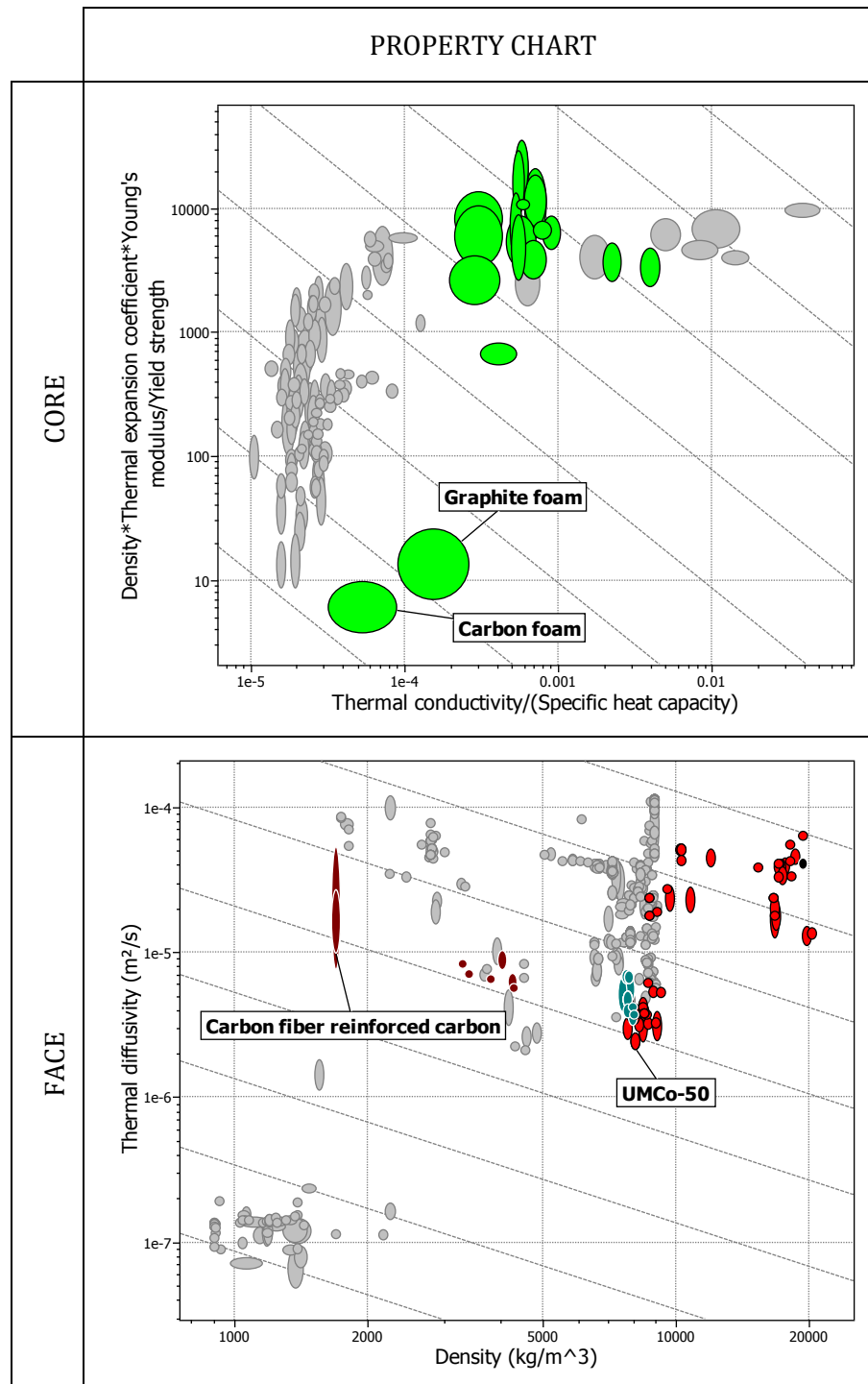


Figure 4.21: Property charts and guide lines corresponding to optimal material for thermal insulation at minimal weight. Optimal core material is Carbon foam while optimal face material is Carbon fibre reinforced Carbon.

Advanced design

Compatibility between performances

The performance space plotting the back temperature of a sandwich panel as a function of its mass per unit area is given in Figure 4.22 for a 500 mm constraint. Strictly speaking, a sufficient thermal resistance for a sandwich panel with a 50 mm constraint to protect from an external temperature of 700 °C is unattainable. The obtained Pareto front is convex. Solutions heavier than about 25 kg/m² have no real interest as the best solution with a 25 kg/m² mass per unit area offers a back temperature of 20.01 °C which is extremely close to the best possible value (20 °C). In this figure the maximum ratio between the thermal stress in the material and material yield strength is also represented. This value is quite relevant by being a constraint for the optimization process. The lower this ratio is, the more distant from the actual Pareto front the solution is.

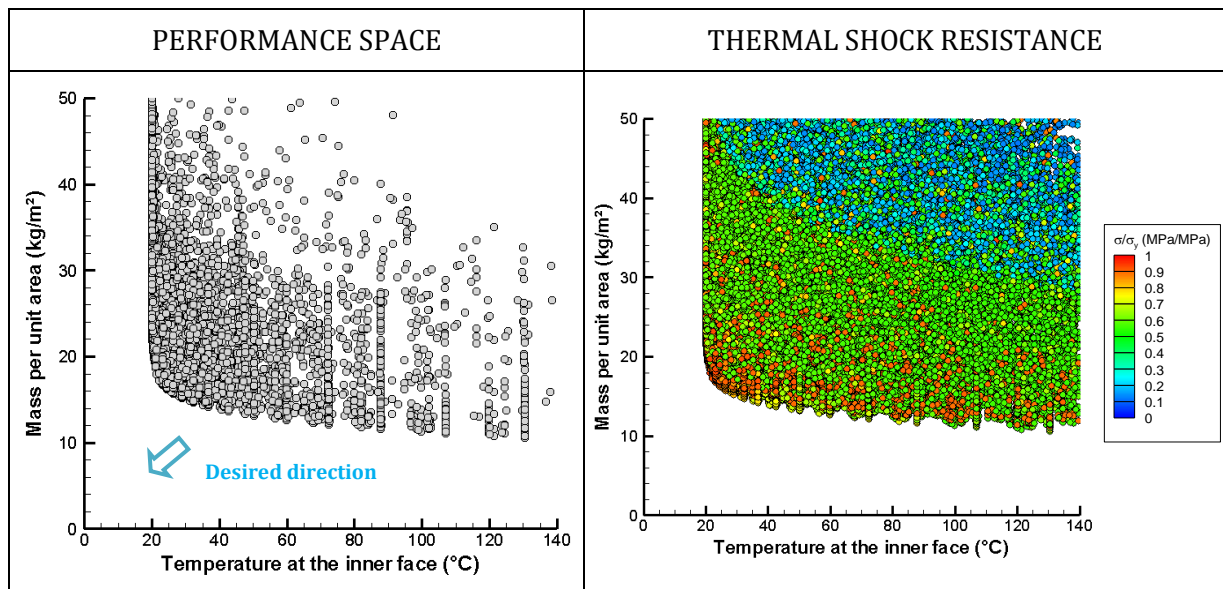


Figure 4.22: Performance space plotting the solutions generated by the optimization algorithm for thermal insulation at minimal weight. On the right hand side: contour values of the maximum value of the ratio between stress and yield strength are given by the colour legend.

Variability analysis

For thermal insulation problems, asymmetrical sandwich panels have been taken into account. There are then six design variables as shown in Figure 4.23. Material selection for the upper face and the core is very restrictive in terms of design. Only a few possibilities are present in the performance space. The optimal upper face material is a Ceramic Matrix Composite (CMC), carbon fibre reinforced carbon. The other materials present in the performance space are steel ASTM CF-20, Haynes alloy (Co-based superalloy), Inconel (Ni-based superalloy), Mo-30W alloy, Korloy (ZnCuTi alloy) and Tungsten alloys. Concerning the core material, ceramic foams are the only core material for which maximum service temperature is above 700 °C. Graphite foam overcomes Carbon foam for this application. Lower face material has a minor impact on performances since the thermal behaviour is mainly dictated by the core. The temperature in the lower face is between 20 and 140 °C. Then almost any material could fit. However, CMC raise as the optimal choice for their high thermal resistance and low density compared to metallic solutions.

Optimal design of architected sandwich panels for multifunctional properties

Pierre Leite

Face thickness has no strong effect on thermal performances but has a significant one on mass. For this reason, the optimal design is made of thin faces. On the opposite, core thickness has a major effect on the achievable temperature at the back side of the panel. For a core thickness of 150 mm, the temperature is about 140 °C while for a 300 mm thick panel, the temperature is about 20.8 °C.

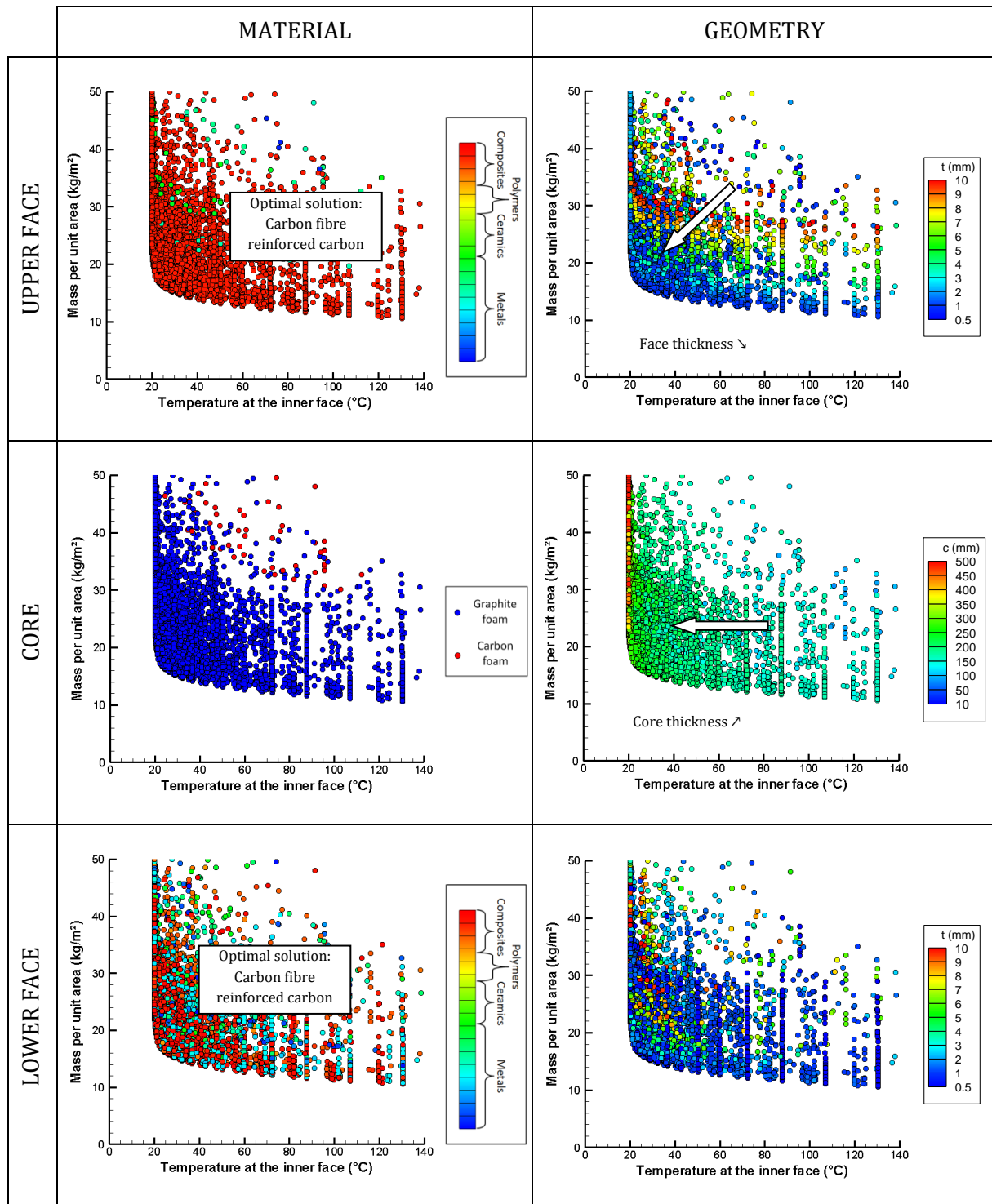


Figure 4.23: Influence of design parameters on the optimal design of a sandwich panel for thermal insulation at minimal weight.

The results obtained by the performance index approach are in good agreement with the one obtained by the genetic algorithm. The optimal face material is indeed Carbon reinforced Carbon. Nevertheless, the optimal core material is not Carbon foam but Graphite foam. This is due to the mismatch between the thermal expansion coefficients of Carbon fibre reinforced Carbon and carbon foam. As shown in Figure 4.24, the thermal expansion coefficient of Graphite foam is very similar to the one of Carbon fibre reinforced Carbon.

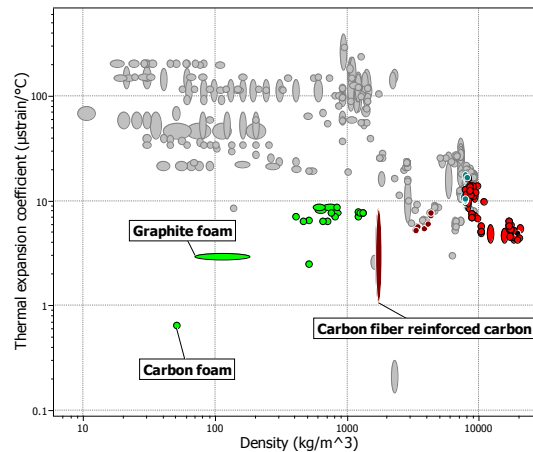


Figure 4.24: Property chart plotting the thermal expansion coefficient as a function of density. Graphite foam and Carbon fibre reinforced carbon have a similar thermal expansion coefficient.

Advantage of sandwich solutions

The main advantage of sandwich panels in this case, as for thermal insulation at minimal weight, is to integrate architected materials filled of air that have very low thermal conductivity and density. The main difficulty is to find out a core material capable of sustaining a temperature of 700 °C and with a sufficient strength to remain elastic despite the dramatic transverse thermal gradient.

2.6. Blast mitigation

Design space:

- Face materials: Metals, Polymers, and Composites.
- Face thickness: from 0.5 to 10 mm.
- Core materials: Metal foams, Polymer foams.
- Core thickness: from 10 to 500 mm.
- Type of sandwich panel: unsymmetrical.

Objectives:

- Blast resistance: minimize the normalized back deflection which is the central deflection of the back face normalized by the span of the panel when the panel is submitted to a blast impulse of 10^4 Nsm^{-2} .
- Lightness: minimize the mass per unit area.

Constraints:

- Normalized back deflection $< 0.2 \text{ m/m}$.
- No face failure.
- Mass per unit area $< 50 \text{ kg/m}^2$.

Preliminary design: Performance index approach

No specific performance index for selection of foam for blast resistance at minimal weight has been found in the literature. However, as face sheets are submitted to tensile loading, the performance index selected for face material selection is UTS/ρ with UTS the ultimate tensile strength and ρ the density. This corresponds to plates with high tensile strength at minimal weight.

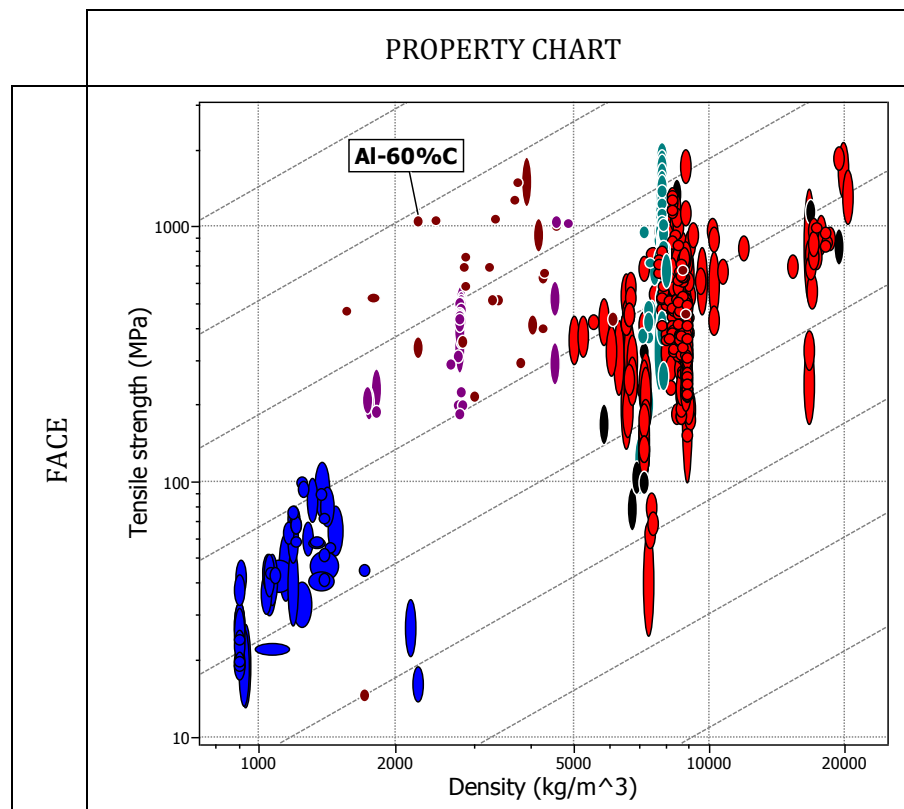


Figure 4.25: Property chart and guide lines corresponding to optimal face material for blast resistance at minimal weight. Optimal face material is Al-60%C.

According to the performance index approach (see Figure 4.25), the optimal face material should be Al-60%C (Metal Matrix Composite).

Advanced design

Compatibilities

For the assessment of the interactions between mass and blast mitigation, the mass constraint has been raised to 300 kg/m² in order to be sure that the performance space will be densely populated. The obtained results which are plotted in Figure 4.26 clearly show a Pareto front made of two distinct convex parts.

Solutions heavier than 212 kg/m² are not on the trade-off surface. At this level of weight, the normalized inner deflection after blast is 0.8 mm/m which is very low. Taking the corresponding solution as a starting point, decreasing the mass becomes possible with a minor loss of blast mitigation ability while it is possible to find out a solution allowing a normalized deflection of 5 mm/m for a mass of 84.7 kg/m².

At the other end, relatively light sandwich panels enable us to obtain quite satisfactory blast mitigating solutions as the lightest solution, with a mass of 23.4 kg/m^2 , thus leading to a normalized deflection after blast of 0.135 m/m , while the constraint was set to 0.2 m/m .

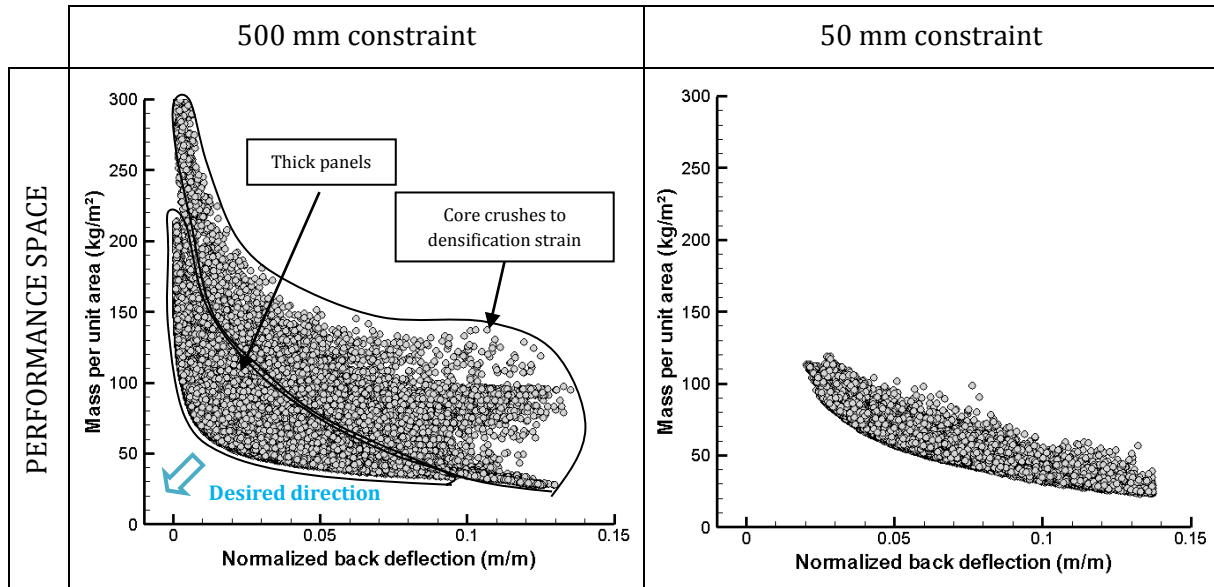


Figure 4.26: Performance space plotting the solutions generated by the optimization algorithm for blast mitigation at minimal weight for two different size constraints.

The performance space is composed of two different parts corresponding to two different behaviours:

- The first part is composed of thick sandwich panels with a good blast resistance at minimal weight.
- The second part is spread all over the performance space but is represented in the trade-off surface only for very light solutions. It is composed of sandwich panels for which the core compression strain during blast loading reaches core densification strain. In this case, the used model does not consider additional mechanisms to dissipate energy. Then, the performances of these solutions should not be taken for granted.

The transition between the two distinct groups can be observed as a shortage appears in the contour of the group of feasible solutions. The first group is the most interesting one in terms of trade-off, and variability analysis will be performed based on this class of solutions.

Variability analysis

As blast mitigation is one of the considered objectives, asymmetrical sandwich panels have been considered in this case. There are then six design variables.

The nature of face materials has a significant influence on the performance as shown in Figure 4.27. It appears that the optimal choice as face material is Al-60%C (Metal Matrix Composite), as predicted by the performance index approach. However, chromium steel AISI 5150 is also competitive as upper face material.

The influence of face thickness on blast resistance is not straightforward even though not negligible. When contour values of face thickness are plotted in the performance space, a banded pattern can be observed with bands oriented in the axis of normalized deflection. The blast resistance can be increased without increasing face thickness. Actually, the first design guide to

Optimal design of architected sandwich panels for multifunctional properties

Pierre Leite

increase blast resistance for a given set of constitutive materials is to increase core thickness. When maximal core thickness is reached, face thickness can be increased as a second design guide.

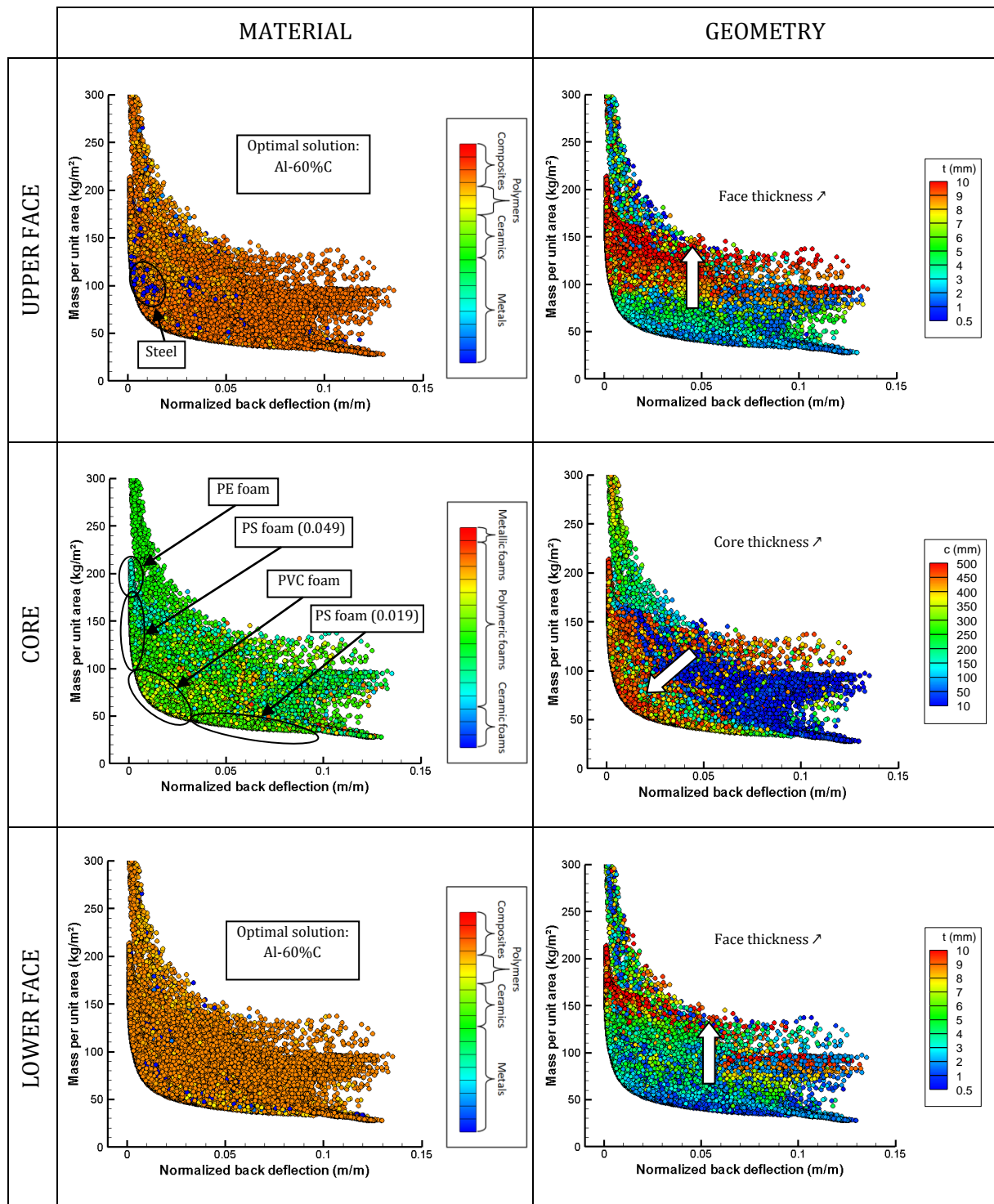


Figure 4.27: Influence of design parameters on the optimal design of a sandwich panel for blast resistance at minimal weight.

Both the rank and performances are sensitive to the core material dependence. Four different core materials are present in the trade-off surface but the transition from one to another is smooth and no shortage is observed. These materials, by decreasing resistance order, are a high

density Polyethylene (PE) foam (0.1095 relative density), a Polystyrene (PS) foam of 0.019 relative density, a PVC foam (0.0215 relative density) and a PS foam of 0.049 relative density.

Blast mitigation requires a thick core to absorb a maximum amount of energy. Decreasing core thickness becomes necessary when a mass under 43 kg/m^2 is needed and that the normalized deflection can be higher than 0.04 m/m . It appears that the thicker the core is, the most resistant the solution is.

Effect of size constraint

Size constraint can have a dramatic effect on blast resistance: this is indicative of the fact that the core material can reach its densification strain by reducing its possible thickness. Then, the main mechanism that dissipates energy is bending of the panel. As a consequence, the available performance space by considering a 50 mm thickness constraint is only limited to solutions for which no real interest is taken from the sandwich structure. The achievable resistance is reduced as well as the mass per unit area.

Advantage of sandwich solutions

The major point of interest arising from the use of a core material is emphasized by the discontinuity on the Pareto front. The group formed by the lightest solutions is composed of sandwich panels with 10 mm foam core. Under blast loading, the core of these solutions used to crush until densification. Most of the dissipated energy is due to bending of the sandwich panel. As an example, the blast resistance of a steel plate of thickness t is plotted in the performance space and compared to the performances obtained by sandwich panels in Figure 4.28. The change of convexity in the trade-off surface corresponding to sandwich solutions is indicative of the point at which core crushing starts to represent the major dissipative mechanism. In Figure 4.28, the evolution of the ratio between core compressive strain ε_c and core densification strain ε_d is plotted as a function of core thickness for a sandwich panel made of 3 mm Al-60%C faces together with a PMACR foam. In addition, the evolution of the ratio between the energy dissipated during crushing of the core U_{core} and the total dissipated energy U_{tot} is illustrated. For thin core values, the compressive strain is equal to the densification strain and the energy dissipated by the core material is very low. For thick core solutions, the amount of energy dissipated by core crushing is close to 80%.

The main results obtained in terms of geometrical design are summarized in Figure 4.29. The calculated deflection of the sandwich panel is drawn as a function of mass for different designs of solutions made of the same constitutive material. The results have been obtained for a solution with Chromium Steel faces and Polystyrene foam core. For this purpose, three different core thicknesses and six face thicknesses have been considered.

For the same constitutive material, increasing core thickness tends to bring the solution closer to the Pareto front. Meanwhile, increasing face thickness appears to lower the back deflection as the mass is increased. The different face thicknesses are noted in Figure 4.29 with the corresponding points for the 150 mm core solution. Quite noteworthy, the panels made of 1 mm faces suffered face failure. The one with a 150 mm core and 1 mm face is not represented.

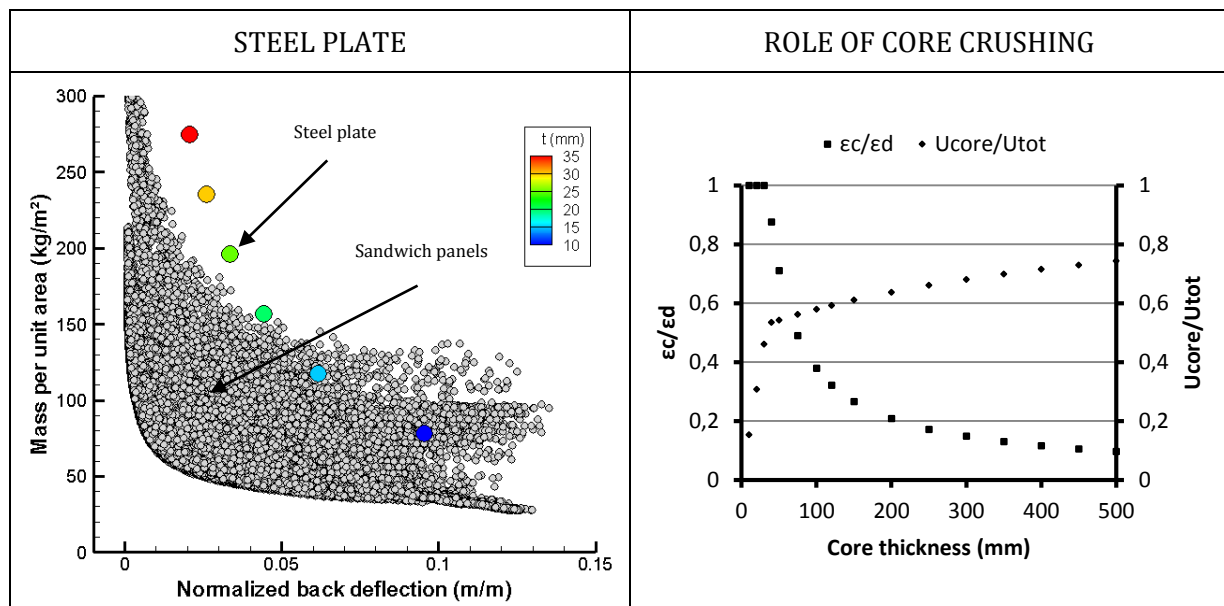


Figure 4.28: On the left hand side: comparison between the performance space of sandwich solutions and the obtained performances of a steel plate of thickness t . On the right hand side: evolution of core compression strain and energy dissipated by core compression as a function of core thickness.

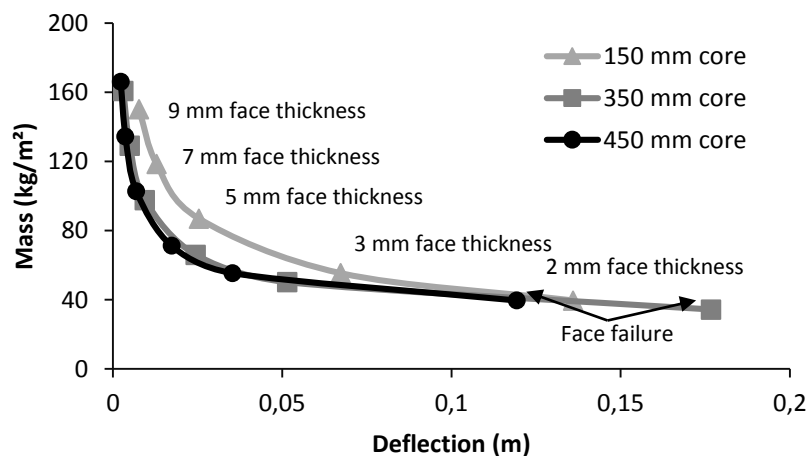


Figure 4.29: Evolution of mass and back deflection as a function of geometrical design for a symmetrical sandwich panel made of Steel faces and of a Polystyrene foam core.

As shown in the performance space in Figure 4.26, the normalized deflection of panels weighting less than 50 kg/m^2 ranges from 0.13 to 0.024 m/m which is quite acceptable. The next problems presented in this part involving blast mitigation will consider a weight constraint of 50 kg/m^2 instead of 300 kg/m^2 .

3. Design at minimal weight for multiple objectives

The previous optimization process was used to determine the optimal design at minimal weight for a single function. Two objectives were then considered including mass reduction. Now, architected sandwich panels are mainly dedicated to structural applications with multiple functions. Three-objective optimization problems are used to assess the capabilities of

such panels regarding multiple criteria. Four representative case studies have been selected, which reflect four typical situations that can be met in a multi-objective design.

First, a competition between the specifications can emerge. In this case, the competition can be qualified as advantageous if the trade-off surface is convex or disadvantageous if the trade-off surface is concave.

Second, if no competition occurs, the specifications can be either compatible or not. These four situations are illustrated using case studies which are representative of some typical industrial problems.

For each case, performances will be taken by pairs in order to evaluate the performance space and to obtain the trade-off surface between the two specifications. Mass is first constrained to be lower than 50 kg/m^2 . A tri-objective optimization is then used to assess the influence of mass constraint and of requirements on the performance space.

3.1. A case of beneficial competition between specifications: flexural stiffness and Acoustical Transmission Loss specifications

Design space:

- Face materials: Metals, Polymers, and Composites.
- Face thickness: from 0.5 to 10 mm.
- Core materials: Metal foams, Ceramic foams, Polymer foams.
- Core thickness: from 10 to 500 mm.
- Type of sandwich panel: symmetrical.

Objectives:

- Flexural stiffness: minimize the central deflection of a 1 m span sandwich beam submitted to a 1 N in a three-point bending test.
- Acoustic damping: maximize the mean value of the Acoustical Transmission Loss in the frequency range [1 000; 4 000] Hz.
- Lightness: minimize the mass per unit area.

Constraints:

- Central deflection $< 10 \text{ }\mu\text{m}$.
- Acoustical Transmission Loss $> 20 \text{ dB}$.
- Mass per unit area $< 50 \text{ kg/m}^2$.

Typical application

In the past decades, consistent efforts have been made to improve noise reduction in aeronautical aircrafts. One of the main issues addressed by helicopter makers concerns cabin noise reduction (see Figure 4.30). Some studies focused on active noise control methods while others investigate the acoustical possibilities offered by sandwich structures. Cabin noise reduction within helicopters can be achieved through the use of structural panels that also possess a good sound transmission loss in the desired frequency range. Quite often, the aimed frequency range for noise reduction is [1 000; 4 000] Hz which corresponds to a perceptive range in which mechanical devices within the helicopters produce high levels of noise. This range is considered as a mid-frequency range, and consequently low and high frequencies will not be addressed but could be treated by following the same approach. In addition to those requirements, reduction of weight is also sought in order to reduce fuel consumption, which is a recurrent objective in aircraft design.



Figure 4.30: Cabin noise reduction is a major issue for helicopter makers.

One of the main issues by designing a panel with both mechanical and acoustical properties is that it leads to contradictory geometrical and material requirements. On one hand, a way to improve the sound transmission loss of a panel is to increase its weight in order to use the inertial effect known as mass law. On the other hand, design guides for flexural stiffness have been developed in a minimum weight design approach. Then the improvement of one property can lead to the deterioration of the other one if the designer stands for these simple rules.

The solutions generated in what follows are designed for stiffness at minimal weight with increasing the Acoustical Transmission Loss as an additional objective.

Compatibilities

The performance space related to the present case is shown in Figure 4.31. The trade-off surface is partly convex but also presents a region with a pointed shape. These two sub-domains can be of interest but not in the same range of performances.

The convex sub-domain corresponds to solutions with a high acoustic damping but with a limited flexural stiffness although it represents a major part of the trade-off surface. The maximum Acoustical Transmission Loss obtained is 79 dB for a deflection of 10 μm . At the opposite, the minimum deflection obtained in this part of the trade-off-surface is 1 μm for a 48.3 dB Acoustical Transmission Loss. The convex shape indicates that there is a competition in terms of design between mechanical and acoustical specifications. These solutions take great advantage of the “sandwich effect” mentioned previously for the Acoustical Transmission Loss at minimal weight.

The second sub-domain exhibits interesting performances in a limited range of performance. It concerns very stiff sandwich panels. In view of the fact that a pointed shape is generated, the only optimal solution that is present in the trade-off surface corresponds to a 50.9 dB Acoustical Transmission Loss and a 0.1 μm deflection. The acoustic behaviour of these solutions is different from the first sub-domain. It follows a “mass law” and does not experience a “sandwich effect”.

In the performance space there is a particular solution which is isolated between the two mentioned sub-domains with a deflection of 0.65 μm and an Acoustical Transmission Loss of 53 dB, which represents a third sub-domain following a “mass law”. The other solutions belonging to this group are drawn in the convex sub-domain.

Through the variability analysis, the different mechanisms involved (“mass law” and “sandwich effect”) will be related to specific designs.

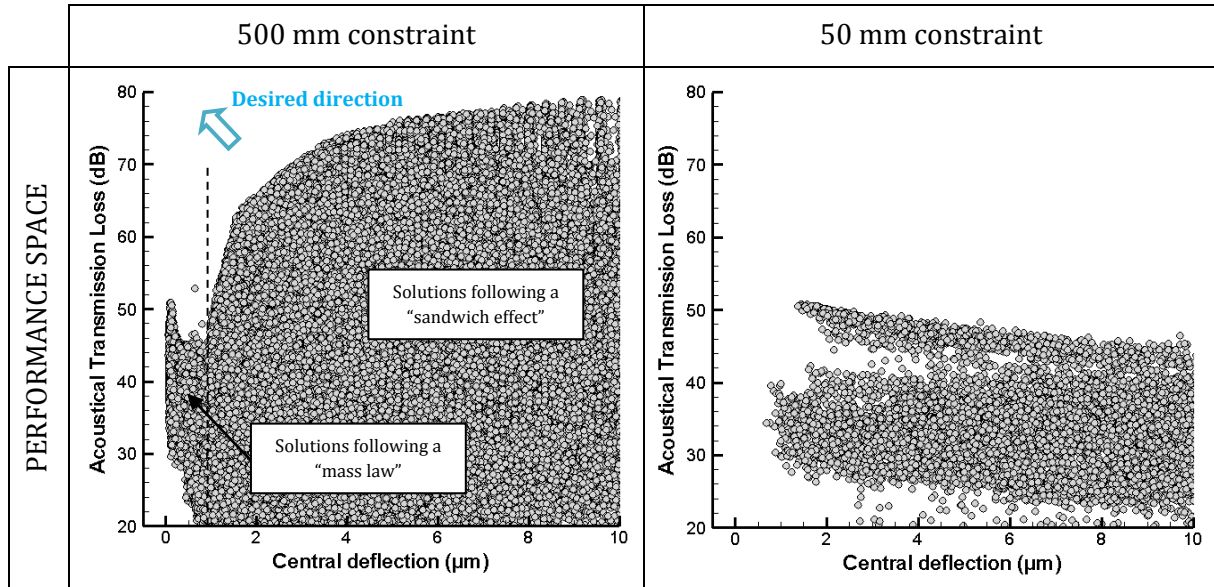


Figure 4.31: Performance space plotting the solutions generated by the optimization algorithm for flexural stiffness and Acoustical Transmission Loss at a mass of 50 kg/m^2 for two different size constraint.

Variability analysis

The three sub-domains are related to core material nature:

- The domain with a convex shape corresponds to sandwich panels with soft core such as Polystyrene foam. The softest solutions are made of Polystyrene foam of 0.019 relative density. Getting stiffer solutions is obtained, first by increasing the core thickness and second by increasing foam relative density when maximum core thickness is reached. As shown in Figure 4.32, the sub-domain can be divided into different domains with a gradient of thickness within it. The competition between mechanical and acoustical specifications is expressed in core thickness requirements. For acoustical specifications, a relatively thin core is required while for mechanical stiffness, a thick core is desired. Passing from a good acoustical panel to a stiff one with a Polystyrene foam as core material is done by increasing core thickness. For a deflection lower than $2 \mu\text{m}$, PVC foam core sandwich panels become competitive with Polystyrene foam solutions. The design guides corresponding to PVC foam are similar to the ones for Polystyrene foam.
- The second sub-domain, composed of the stiffest solutions, represents glass foam core sandwich panels. Glass foam is not soft enough to allow a transverse deformation sufficient to let symmetric vibration modes occur. In this case, the only mechanism used to increase Acoustical Transmission Loss is mass inertia. Then, increasing Acoustical Transmission Loss is done by increasing core thickness (and thus weight), which is consistent with the requirements for increasing flexural stiffness.
- The third sub-domain corresponds to structural Polypropylene foam core panels. This foam has a compressive modulus of 550 MPa which is very stiff for a foam (glass foam modulus is about 910 MPa and Polystyrene foam modulus is 5.2 MPa). Such as for glass foam solutions, the Acoustical Transmission Loss of Polypropylene foam panels follows a mass law.

Optimal design of architected sandwich panels for multifunctional properties

Pierre Leite

Face material choice depends on the acoustic behaviour of the panel, and thus depends on core material. With Polystyrene foams, heavy materials such as Bronzes, Tungsten and Copper alloys are preferred with an optimal thickness around 3 mm. For solutions following an acoustical mass law, a 4 mm thick metal matrix composite (Al-60%C) is the optimal choice.

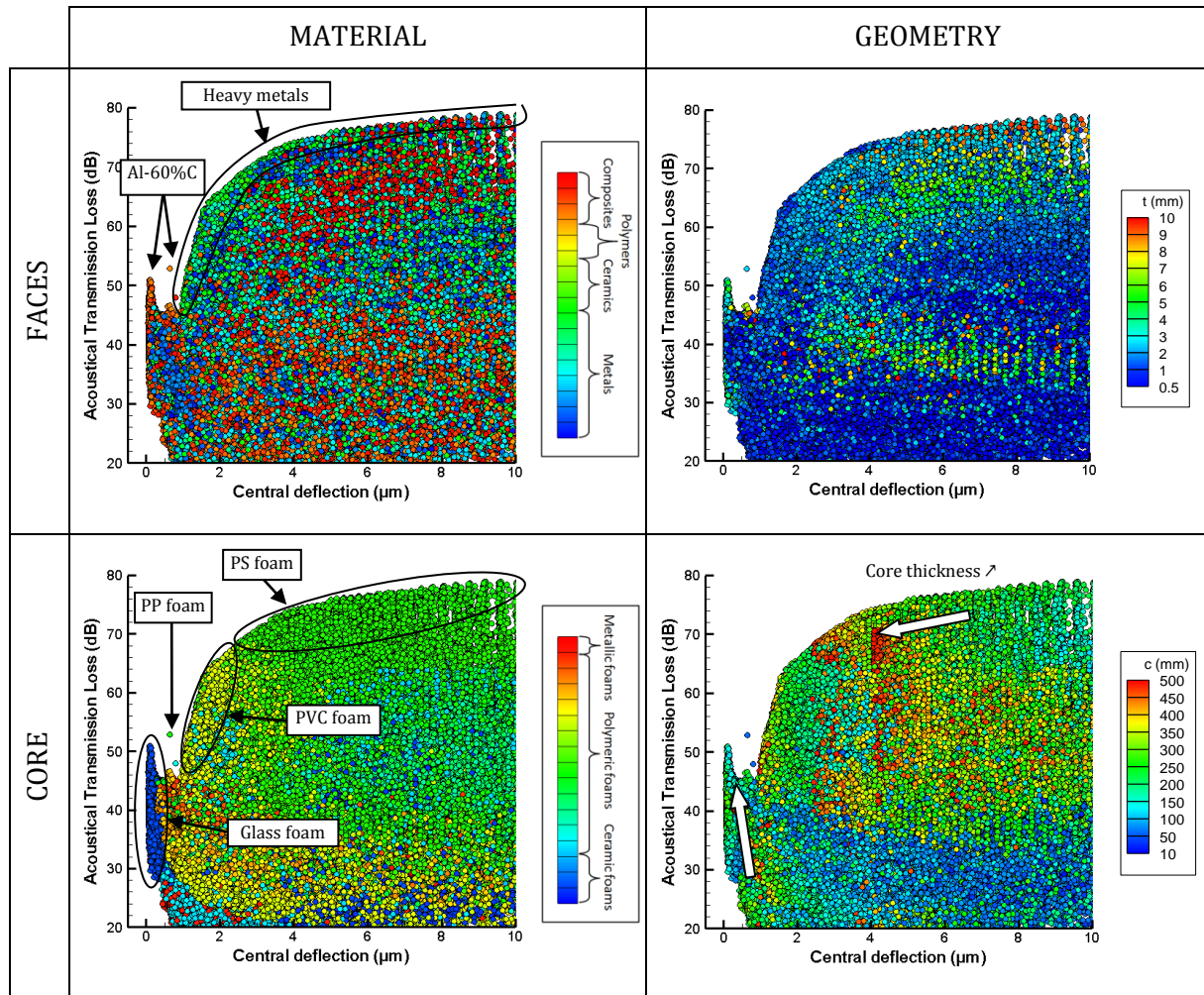


Figure 4.32: Influence of design parameters on the optimal design of a sandwich panel for flexural stiffness and Acoustical Transmission Loss at a mass of 50 kg/m^2 .

Competition between mechanisms

As mentioned, Acoustical Transmission Loss of sandwich panels can follow two different mechanisms:

- The “sandwich effect”, for which a sufficiently soft core is required, results in a convex shape in the performance space. This convex shape is due to the competition in terms of core thickness requirements. For example, the optimal core thickness regarding acoustic damping for a Polystyrene foam core panel is 200 mm. Then, the Acoustical Transmission Loss equals almost 80 dB. To increase flexural stiffness, an increase of core thickness is required. Then, by increasing core thickness and thus flexural stiffness, Acoustical Transmission Loss can be decreased. The performance space obtained for a Polystyrene foam core is given in Figure 4.33, illustrating the convex shape observed when “sandwich effect” occurs.

- The “mass law”, which is based on the inertial effect of mass such as for monolithic plates, results in a pointed shape. Then, increasing acoustic damping is achieved by increasing core and face thickness, thus leading to an increase of flexural stiffness. Figure 4.33 shows the performance space corresponding to Polypropylene foam core panels which follow a “mass law”.

Some types of core materials can exhibit a mixed behaviour, such as PVC foams for which a part of the performance space is convex and the other part is point-like as shown in Figure 4.33. This will depend on the relative density of the foam. Light foams will be soft enough to experience a sandwich effect while dense foams are too stiff to allow a transverse deformation to occur. This transition appears at a relative density of about 0.05 for PVC foams.

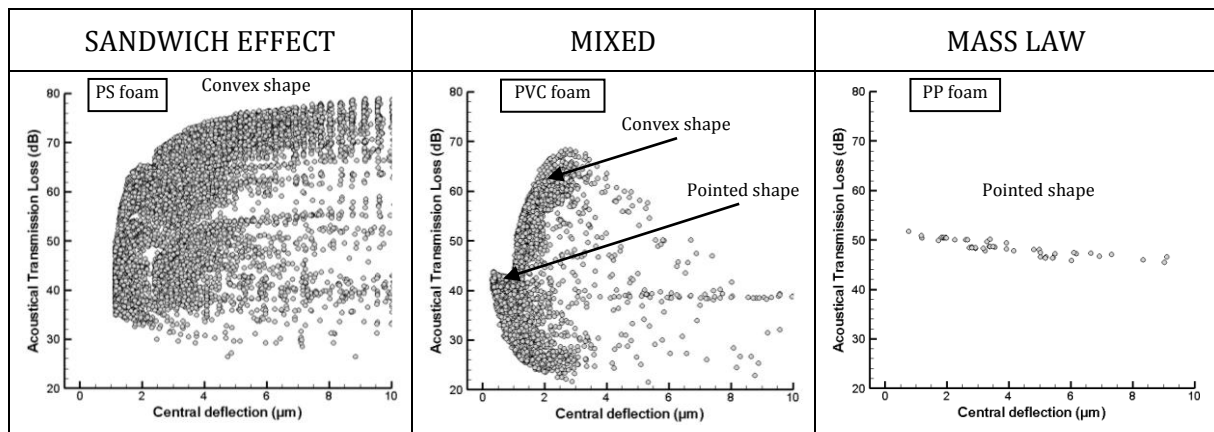


Figure 4.33: Different shapes of performance space depending on the acoustical behaviour.

Effect of size constraint

Changing the size constraint is found to dramatically impact the Acoustical Transmission Loss, passing its maximum from 79 to 50 dB as shown in Figure 4.31. Now by reducing the possible thickness of the panel the minimum deflection is also increased, even though the relative loss is less compared to the one of acoustical insulation. The shape of the performance space indicates that for thin panels, only acoustical mass law can be used to increase the Acoustical Transmission Loss. This is mainly because the limitations in size affect the core material selection for mechanical specifications. If flexural stiffness cannot be reached by increasing core thickness, one can succeed by increasing core stiffness. Then the core materials constituting the performance space are ceramic foams and stiff structural polymeric foams such as Polypropylene and PVC foams. Thus, a soft core sandwich panel of 50 mm thickness is not stiff enough to enter the group of feasible solutions.

Effect of mass as an objective

In Figure 4.34 is represented the performance space corresponding to the tri-objective optimization of a sandwich panel with flexural stiffness, acoustic damping and mass as objectives. An alternative view consists of plotting a performance space that considers Acoustical Transmission Loss and deflection as performances and mass as a constraint. Figure 4.34 gives the obtained performance space for three different values of mass constraint (10, 30 and 50 kg/m²).

The aspect of the trade-off surface slightly changes with the mass constraint but remains composed of both convex and point-like parts. The convex part is still composed of Polystyrene

Optimal design of architected sandwich panels for multifunctional properties

Pierre Leite

foam core solutions. For very light panels, PVC foam appears to be an optimal choice for high stiffness specifications while glass foam core solutions vanish from the performance space.

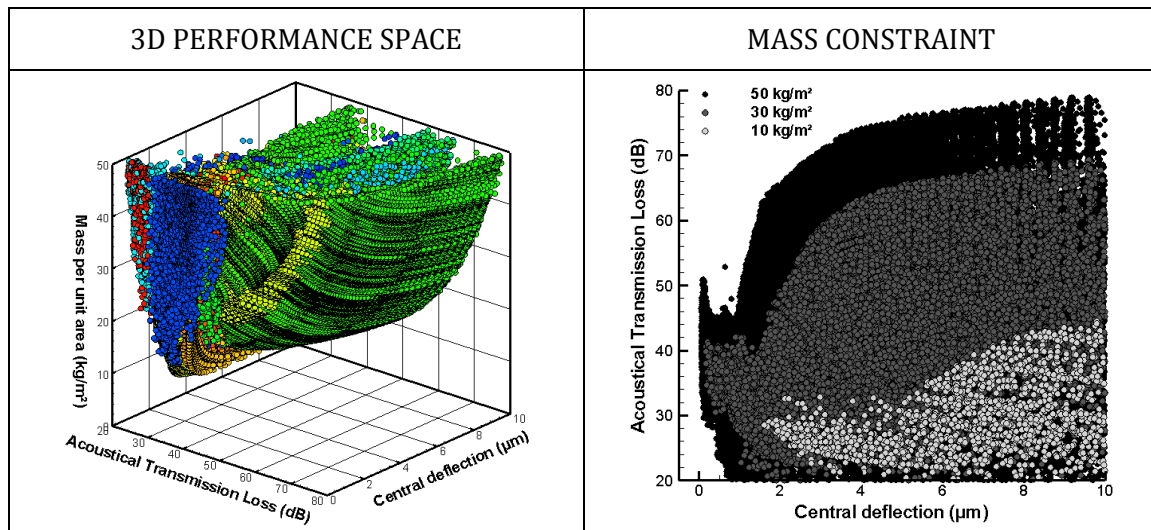


Figure 4.34: On the left hand side: performance space plotting the solutions generated by the optimization algorithm for stiffness and Acoustical Transmission Loss at minimal weight. Colour legend represents core material. On the right hand side: evolution of the performance space for stiffness and Acoustical Transmission Loss as a function of mass constraint.

Effect of functional constraints

In order to assess the effect of performance P_1 on performance P_2 , it is possible to plot the performance space by considering mass and P_2 as objectives and a constraint on P_1 . By taking different values of constraints, monitoring the change in the performance space gives graphical indication on how the performances interact. Figure 4.35 illustrates the corresponding effects for the present case study.

Stiffness requirements limit the Acoustical Transmission Loss as shown in Figure 4.35. The achievable values are far from the unconstrained trade-off surface composed of Polyurethane foam core panels. For high stiffness requirements, the form of the trade-off surface between Acoustical Transmission Loss and mass is transformed into the combination of two convex surfaces corresponding to different types of core materials (with the occurrence of PVC foam as optimal solution). These two shapes correspond to the two different mechanisms observed for the Acoustical Transmission Loss: sandwich effect and mass law.

As shown in Figure 4.35, a 20 dB constraint has no effect on the achievable stiffness. Even for a 40 dB constraint, high stiffness solutions are met although they are heavier. The trade-off surface is still the combination of two convex surfaces, corresponding to Polystyrene and glass foam. This is only for very high sound insulating requirements that stiffness is limited, as the only optimal core material satisfying all the requirements is Polystyrene foam. As far as the chosen specifications are concerned, this is due to the fact that high Acoustical Transmission Loss can only be achieved by the sandwich effect, and then by having a soft core.

Advantage of sandwich solutions

The competition between Acoustical Transmission Loss and flexural stiffness has been pointed out in a few studies including the one from Wang et al. addressing the optimal design of sandwich panels for both acoustical and mechanical properties [WAN09]. As shown in the

present study, flexural stiffness requires stiff and thick cores while Acoustical Transmission Loss requires thin and soft cores. Trade-off can be found by monitoring core density and core thickness.

As previously related, sandwich panels exhibit better flexural stiffness at minimal weight than monolithic plates. Moreover, the Acoustical Transmission Loss experiences a “sandwich effect” making sandwich panels better sound insulating solutions than monolithic ones. As these performances are somehow compatible though in competition, it can be deduced that a sandwich panel is a better choice for acoustical panels with good flexural stiffness at minimal weight than solid plates.

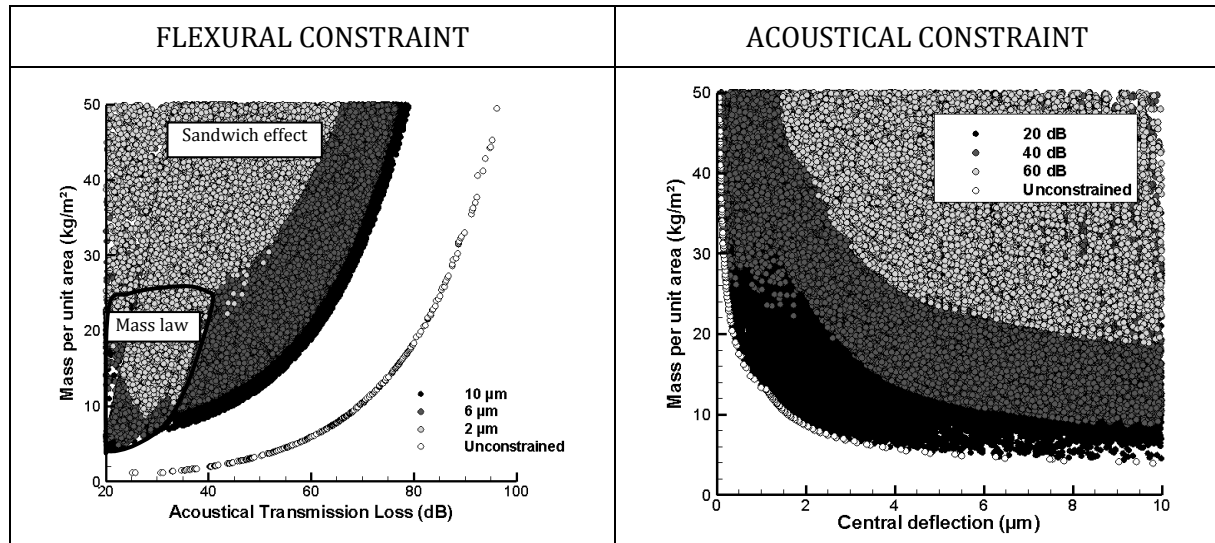


Figure 4.35: On the left hand side: evolution of the performance space for Acoustical Transmission Loss at minimal weight as a function of stiffness constraint. On the right hand side: evolution of the performance space for stiffness at minimal weight as a function of Acoustical Transmission Loss constraint.

3.2. A case of disadvantageous competition between specifications: flexural strength and thermal resistance specifications

Design space:

- Face materials: Metals, Polymers, and Composites.
- Face thickness: from 0.5 to 10 mm.
- Core materials: Metal foams, Ceramic foams, Polymer foams.
- Core thickness: from 10 to 500 mm.
- Type of sandwich panel: symmetrical.

Objectives:

- Flexural strength: maximize the critical load corresponding to failure of a 1 m span sandwich beam submitted to a three-point bending test.
- Thermal resistance: maximize the through thickness thermal resistance.
- Lightness: minimize the mass per unit area.

Constraints:

- Flexural strength > 2 kN.
- Thermal resistance > 1 m²K/W.
- Mass per unit area < 50 kg/m².

Optimal design of architected sandwich panels for multifunctional properties

Pierre Leite

Typical application

In some applications, panels with good mechanical properties and with high thermal resistance are required. This can be emphasized for example for cold storage facilities such as methane gas tanker reservoirs in which the walls have a structural role but also need to preserve the goods within the building at an adequate temperature. Another interesting example concerns refrigerated trucks for which it is important to minimize the weight in order to reduce fuel consumption or to increase trucks capacity. The last example has already been studied by Sirisalee et al. in an exchange constant approach [SIR06].

In these kinds of applications illustrated in Figure 4.36, sandwich panels are designed in strength at minimal weight, in addition to thermal resistance specifications.



Figure 4.36: On the left hand side: example of a cold storage room. On the right hand side: example of a refrigerated truck.

Compatibilities

The trade-off generated in the performance space shown in Figure 4.37 is made of two concave parts. The first one is the concave form corresponding to high insulating solutions with a thermal resistance higher than $21 \text{ m}^2\text{K/W}$. The other one is the concave form representing the major part of the trade-off surface. Still, the two interesting solutions in terms of trade-off are the ones at both ends of the Pareto front. The strongest solution has a thermal resistance of $1.33 \text{ m}^2\text{K/W}$ and a strength of 31.5 kN while the solution optimising thermal insulation has a $25.1 \text{ m}^2\text{K/W}$ thermal resistance and a 3.55 kN strength.

Variability analysis

In terms of design variables, Figure 4.38 shows that an optimal constitutive material has been found for the faces since every solution in the trade-off surface is made of the same face material. The latter, which is Carbon fibres reinforced Aluminium, largely dominates other possibilities. Indeed, the band corresponding to Aluminium matrix composite face sandwich panels is quite large compared to the size of the performance space. It corresponds to the optimal face material for flexural strength as emphasized in Section 2.2 of this chapter.

The Pareto front is divided in two parts corresponding to two different core materials:

- The first sub-group gathers Phenolic foam core sandwich panels which are the ones with the highest thermal resistance. Phenolic foam has been identified as one of the optimal core material regarding thermal resistance (see Section 2.4).
- The other sub-group is composed of PVC foam core sandwich panels with different core density. The strongest solutions are made of foams with a relative density of

0.214 while the ones with a high thermal resistance are made of a 0.0215 relative density foam. PVC foams are the best solutions for high flexural strength requirements as shown in Section 2.2.

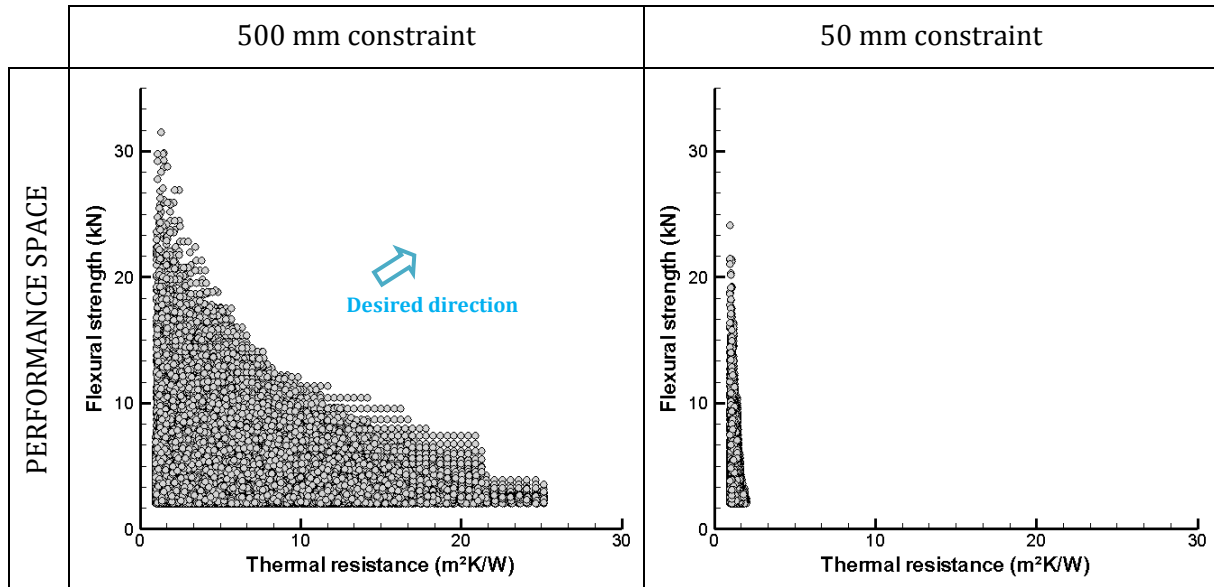


Figure 4.37: Performance space plotting the solutions generated by the optimization algorithm for flexural strength and thermal resistance at a mass of 50 kg/m^2 for two different size constraints.

As for the constitutive material, an optimal value has also been found for face thickness. This optimal value is between 5.5 and 6 mm while the possible range of thickness is from 0.5 to 10 mm.

The core thickness mainly affects the thermal resistance. The performance space has a banded structure regarding core thickness, with bands oriented vertically. The presence of two sub-groups in the performance space is due to the size constraint. A PVC foam core sandwich panel limited to a 500 mm core thickness cannot have a thermal resistance higher than $21.3 \text{ m}^2\text{K/W}$ while the thermal resistance of a 500 mm Phenolic foam core panel is $25.1 \text{ m}^2\text{K/W}$.

However, the shape of the trade-off surface is due to the mass constraint. To increase thermal resistance, the core thickness has to be increased. In order to keep the panel weight below 50 kg/m^2 , foam relative density is reduced, leading to a diminution of the flexural strength. The concave shape is due to the fact that foam compressive strength is proportional to the square power of relative density while thermal resistance is linearly proportional to the thickness. The relationship between thickness and relative density in the design of a panel at a constant weight is linear. Then, the relative advantage in terms of thermal resistance taken from an increase in thickness is lower than the relative loss in terms of strength due to the reduction of relative density.

The trade-off between thermal resistance and flexural strength is controlled by the relative density of the foam core. PVC foams are optimal in the major part of the observed performance range.

Effect of size constraint

The size constraint has a major influence on the range of achievable performances, particularly on the thermal resistance as shown in Figure 4.37. Once again, there is a direct link between the thickness of the solutions and their thermal resistance as a ten times increase in

Optimal design of architected sandwich panels for multifunctional properties

Pierre Leite

thickness leads to a ten times increase in thermal resistance. The flexural strength is less affected even though a slight decrease of the possible strength is observed, passing from 31.5 kN to 24.1 kN. Thermal resistance is affected by core thickness reduction while flexural strength is affected by face thickness reduction. However, the general shape of the trade-off surface is not modified by changing the size constraint.

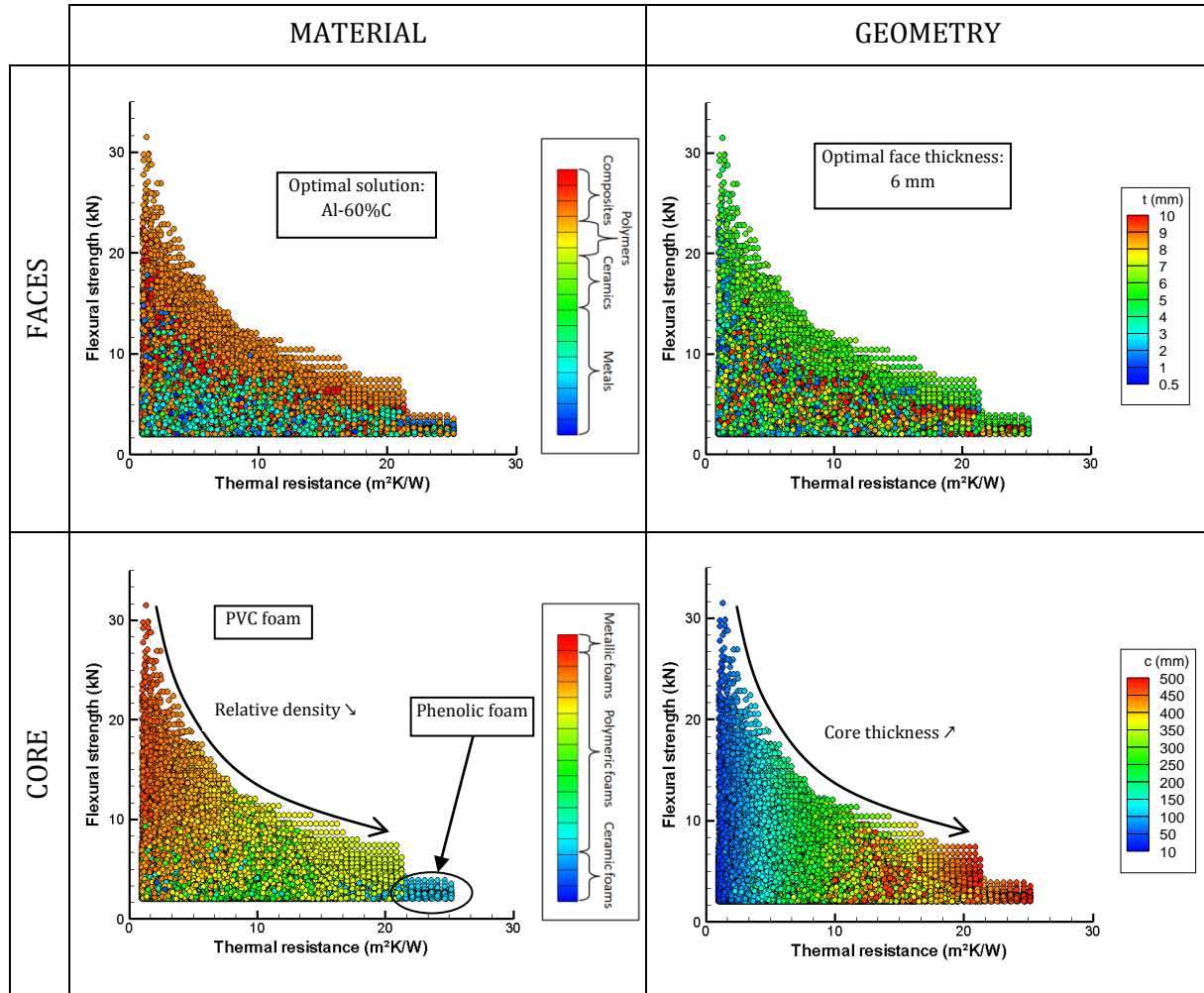


Figure 4.38: Influence of design parameters on the optimal design of a sandwich panel for flexural strength and thermal resistance at a mass of 50 kg/m².

Effect of mass as an objective

Similarly to the previous case study, the effect of mass is given by plotting the tri-objective performance space and the variation of the bi-objective performance by considering different values of mass constraint. As shown in Figure 4.39, the trade-off surface shape remains alike except that the sub-domain corresponding to Phenolic foam core panels vanishes for solutions with a mass lower than 30 kg/m².

Effect of functional constraints

Thermal resistance constraint has an effect on materials selection regarding the performance space corresponding to flexural strength at minimal weight. Higher thermal resistance is partly achieved by increasing the porosity of the foam, thus leading to a decrease of its strength. The

optimal design of sandwich panels for flexural strength at minimal weight has a thermal resistance higher than $1 \text{ m}^2\text{K/W}$ as shown in Figure 4.40.

On the other hand, strength requirements lead to a design with strong foams that exhibit a quite high relative density. As shown in Figure 4.40, increasing strength comes along with a decrease in thermal resistance. The optimal choice respecting every requirement is a PVC foam core sandwich panel. Foam relative density is a parameter that allows the trade-off between strength and thermal resistance to be adjusted.

For very high thermal resistance requirements, Phenolic foam overcomes other core materials due to size constraint but is limited to solutions with a mass higher than 30 kg/m^2 .

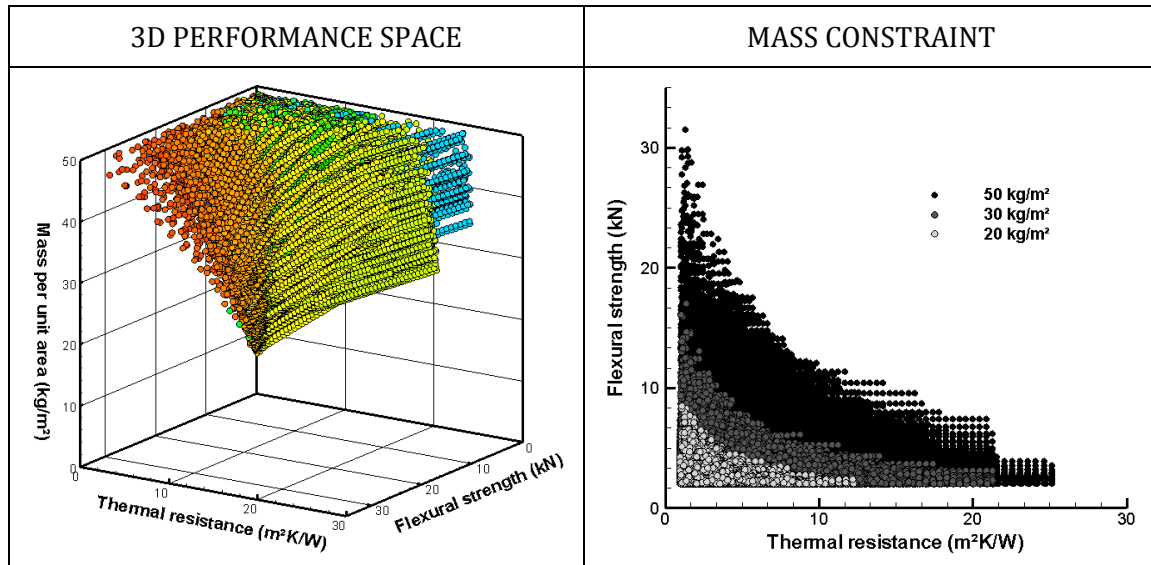


Figure 4.39: On the left hand side: performance space plotting the solutions generated by the optimization algorithm for strength and thermal resistance at minimal weight. Colour legend represents core material. On the right hand side: evolution of the performance space for strength and thermal resistance as a function of mass constraint.

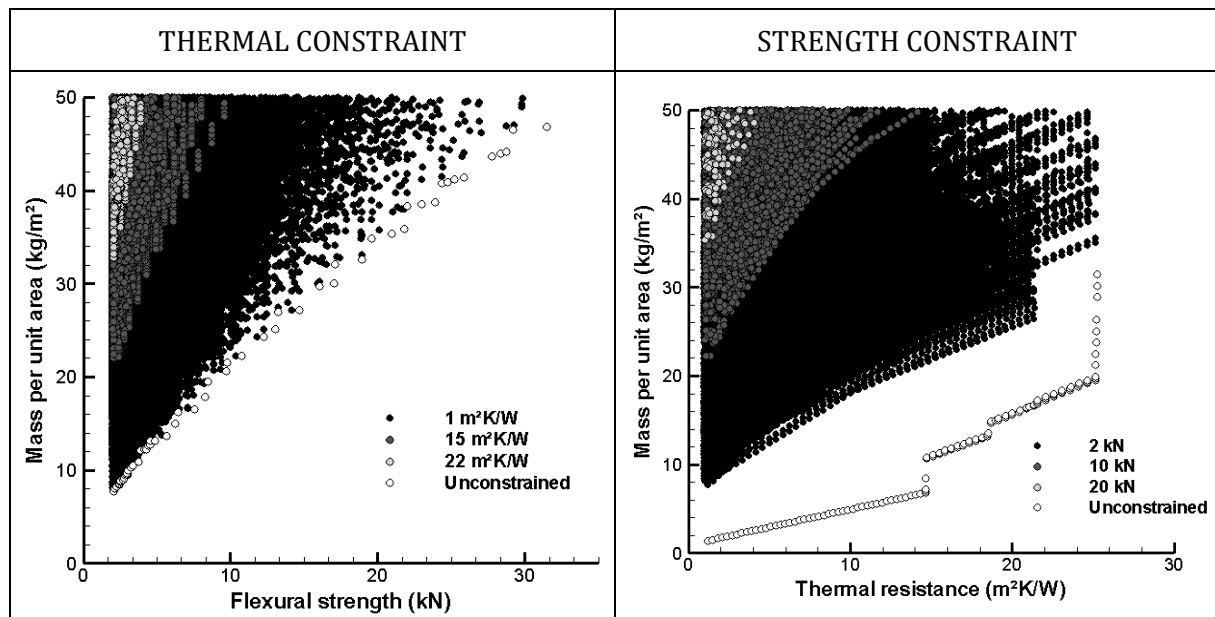


Figure 4.40: On the left hand side: evolution of the performance space for strength at minimal weight as a function of thermal resistance constraint. On the right hand side: evolution of the performance space for thermal resistance at minimal weight as a function of strength constraint.

Optimal design of architected sandwich panels for multifunctional properties

Pierre Leite

Advantage of sandwich solutions

Despite a concave Pareto front between thermal resistance and flexural strength, a sandwich structure will exhibit better performances than monolithic solutions. This can be accounted for by the better flexural strength at minimal weight obtained by a sandwich panel compared to a monolithic plate.

3.3. A case of compatibility between specifications: thermal insulation and blast mitigation specifications

Design space:

- Face materials: Metals, Polymers, and Composites.
- Face thickness: from 0.5 to 10 mm.
- Core materials: Metal foams, Polymer foams.
- Core thickness: from 10 to 500 mm.
- Type of sandwich panel: unsymmetrical.

Objectives:

- Thermal insulation: minimize the temperature at the inner face while the outer face is submitted to a 700 °C heat during 1 hour.
- Blast resistance: minimize the normalized back deflection which is the central deflection of the back face normalized by the span of the panel when the panel is submitted to a blast impulse of 10^4 Nsm^{-2} .
- Lightness: minimize the mass per unit area.

Constraints:

- Temperature at the inner face $< 140 \text{ }^{\circ}\text{C}$.
- Thermal shock resistance: $\max_{\forall x, \forall t} \left(\frac{\sigma(x,t)}{\sigma_y(x)} \right) < 1$.
- Temperature in the material $<$ maximum service temperature of the material.
- Normalized back deflection $< 0.2 \text{ m/m}$.
- No face failure.
- Mass per unit area $< 50 \text{ kg/m}^2$.

Typical application

Work conditions in offshore platforms can be described as extreme environments. In the case of fire, workers must take shelter somewhere to be safe from the extreme temperatures that can be experienced in these platforms. Usually, rescue services are about one hour away from the platforms. Then, protection cabins (see Figure 4.41) are often designed in order to protect people from a fire temperature (about 700 °C) during at least one hour. This means that the temperature inside the cabin should not exceed a critical level. It is considered that the temperature at the inside face of the panel should not reach 140 °C. Moreover, in the case of fire, risks of explosions should be taken into account and consequently, protection cabins should also be blast resistant. This case study is inspired by an actual industrial application from one of the partners of the MANSART project.

We will consider panels submitted to thermal and blast loads. The objectives in terms of design are threefold: decreasing the final temperature at the back side of the panel for a temperature of 700 °C after one hour, decreasing the back deflection of the panel submitted to blast load and decreasing its weight.



Figure 4.41: Protection cabin for offshore platforms.

Compatibilities

There is no relevant data in the performance space with the present specifications. On one hand, all core materials that can sustain such a high temperature are ceramic foams which are fragile and then do not sustain blast load. On the other hand, all the core materials that are blast resistant are not able to sustain the high temperature caused by conduction of fire temperature. However, for sake of example, the constraint set on material service temperature is removed, thus leading to a performance space filled of unrealistic solutions.

As shown in Figure 4.42, the Pareto front that can be extracted from the performance space is composed of a single point. This pointed shape indicates that design requirements between thermal and blast specifications are compatible and that increasing one property leads to the increase of the other one. This optimal solution is able to keep the temperature at the back of the sandwich panel at the initial temperature with a deflection after blast of 3.6 mm.

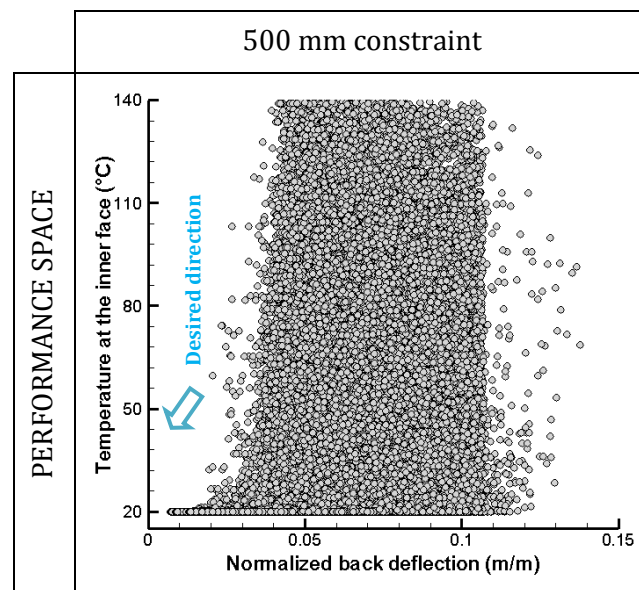


Figure 4.42: Performance space plotting the solutions generated by the optimization algorithm for blast mitigation and thermal insulation at a mass of 50 kg/m^2 . All solutions on the performance space are not feasible as the considered temperature exceeds their maximum service temperature.

Optimal design of architected sandwich panels for multifunctional properties

Pierre Leite

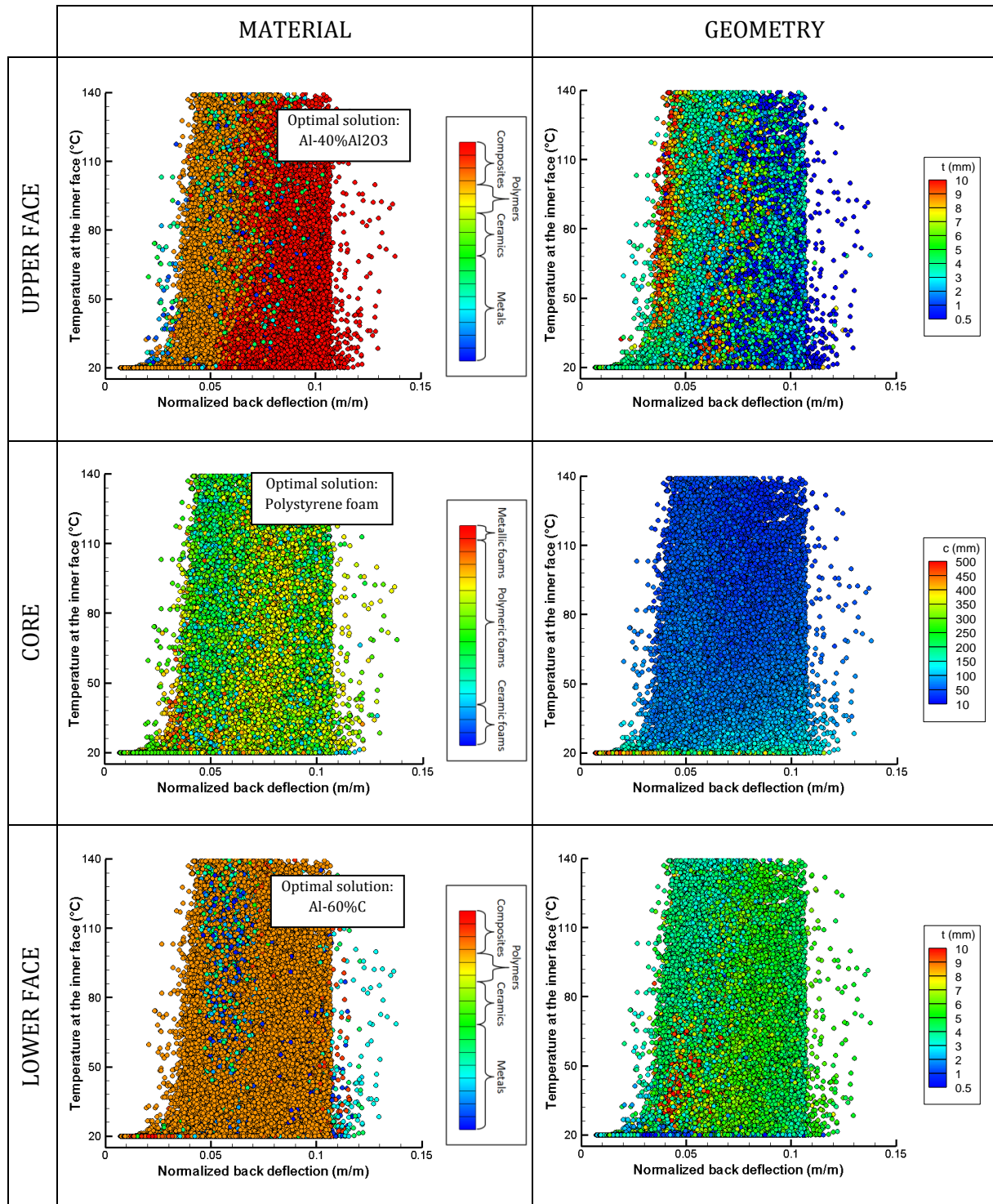


Figure 4.43: Influence of design parameters on the optimal design of a sandwich panel for thermal insulation and blast resistance at a mass of 50 kg/m².

Variability analysis

In Figure 4.43, the contour values of design variables are given in the performance space. The optimal solution is made of a Polystyrene foam core of 440 mm thick with MMC faces (Al-40%Al₂O₃). Upper face is 4.5 mm thick while the lower face thickness is 3.5 mm. As no constraints are considered on service temperature, polymeric foams such as PS foams are the optimal choice as good blast resistant materials having a low thermal diffusivity. Face material optimal choice is a metal matrix reinforced by ceramic fibres. Its thermal conductivity is reduced compared to a metal alloy due to the presence of ceramic fibres, but it also exhibits good mechanical properties such as a relatively good tensile strength.

Both blast and thermal specifications require high core thickness. As shown in Figure 4.43, the best solutions are made of thick core while a large part of the performance space is filled by thin panels. Face thickness value depends on face material and core thickness.

Effect of mass as an objective

Mass acts like a constraint as by reducing the acceptable value of mass, the thermal and blast properties are also reduced. But this does not change the overall aspect of the 2D performance space as shown in Figure 4.44. The Pareto front is still composed of a single solution. However, for light structures, below about 25 kg/m², the performance space shape is very close to a rectangle. These solutions correspond to thin panels for which the blast behaviour is different as their core reaches densification strain during blast. As it has been discussed in Section 2.6, the behaviour is then different and the results are not as reliable.

Effect of functional constraints

As the design requirements are compatible, constraints on one property have no effect on the other one.

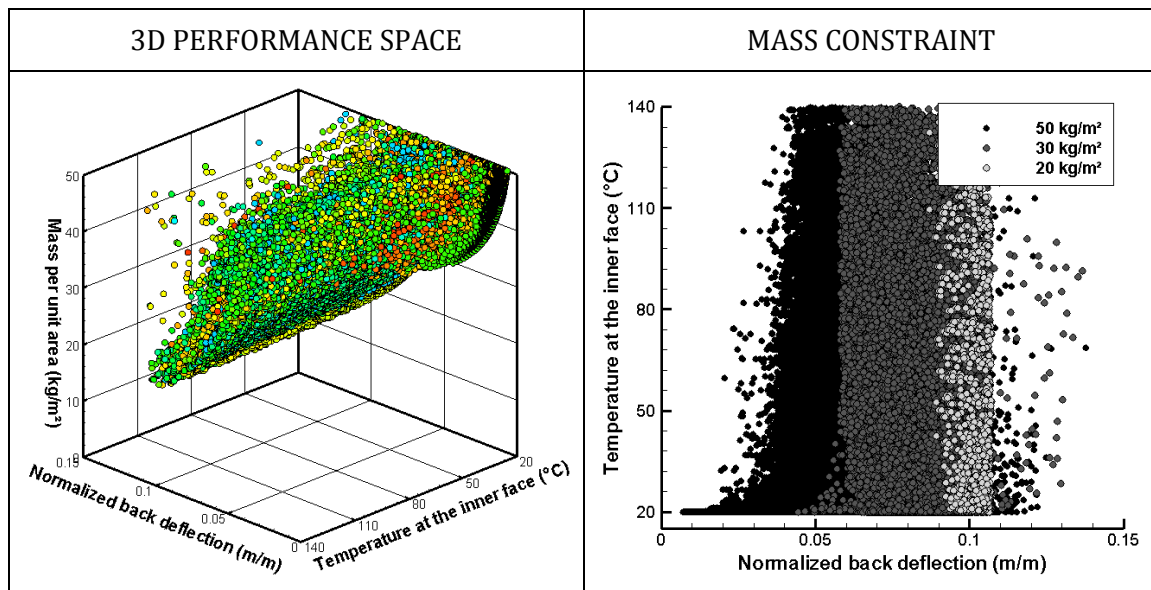


Figure 4.44: On the left hand side: performance space plotting the solutions generated by the optimization algorithm for thermal insulation and blast resistance at minimal weight. Colour legend represents core material. On the right hand side: evolution of the performance space for thermal insulation and blast resistance as a function of mass constraint.

3.4. A case of incompatibility between specifications: Acoustical Transmission Loss and blast mitigation specifications

Design space:

- Face materials: Metals, Polymers, and Composites.
- Face thickness: from 0.5 to 10 mm.
- Core materials: Metal foams, Ceramic foams, Polymer foams.
- Core thickness: from 10 to 500 mm.
- Type of sandwich panel: unsymmetrical.

Objectives:

- Acoustic damping: maximize the mean value of the Acoustical Transmission Loss in the frequency range [1 000; 4 000] Hz.
- Blast resistance: minimize the normalized back deflection which is the central deflection of the back face normalized by the span of the panel when the panel is submitted to a blast impulse of 10^4 Nsm^{-2} .
- Lightness: minimize the mass per unit area.

Constraints:

- Acoustical Transmission Loss > 20 dB.
- Normalized back deflection < 0.2 m/m.
- No face failure.
- Mass per unit area < 50 kg/m^2 .

Typical application

In some industrial fields, particularly critical devices need to be closed in a reinforced room. This can be the case of power plants, chemical and oil production plants, where devices could explode (Figure 4.45). These devices often produce a large amount of noise that can be unpleasant for workers or people nearby the plant in general. For that reason, panels with good blast resistance and good Acoustical Transmission Loss are required. The objectives in terms of design are minimizing back deflection after blast, increasing Acoustical Transmission Loss and minimizing mass, even though the latter is not of major importance in this kind of applications.



Figure 4.45: Example of power plant.

Compatibilities

The performance space corresponding to a bi-objective optimization involving blast mitigation and acoustical insulation ends to a very special Pareto front as shown in Figure 4.46.

The considered performances seem to have very little interactions between each other as the performance space can nearly be divided into two rectangular sub-domains as if one can be optimized regardless of the other one.

Then, only two solutions can be considered as of great potential in terms of trade-off, intermediate solutions being disadvantageous compared to them. The first one maximizes acoustical insulation with a decent deflection after blast, while the other one maximizes blast mitigation with a minimal deflection.

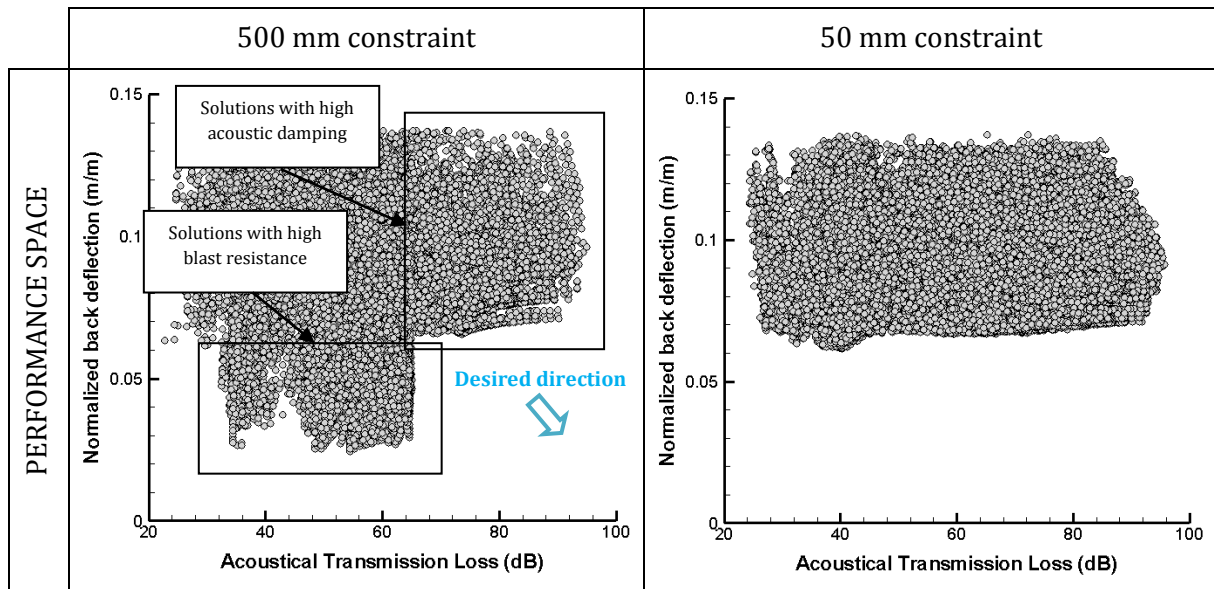


Figure 4.46: Performance space plotting the solutions generated by the optimization algorithm for blast mitigation and acoustic damping at a mass of 50 kg/m^2 for two different size constraint.

Variability analysis

The performance space is mainly populated of Al-60%C composite face sandwich panels. It seems that no advantage can be taken from a dissymmetry in terms of face material. However, some solutions on the Pareto front are made of Chromium Steel (AISI 5150).

Almost all the solutions sitting on the Pareto front are made of composite faces. Moreover, face thickness is between 2 and 3 mm for both the upper and lower faces.

The two blocs in the performance space correspond to two different types of core materials:

- The first one corresponds to the most blast resistant solutions and is characterized by a 0.05 relative density Polystyrene foam. From Figure 4.47, it is observed that decreasing the core thickness helps increase the transmission loss but it is limited to a maximum value of 65 dB. An optimal solution can be identified with a 64.6 dB transmission loss and a 0.029 mm/m normalized deflection after blast. This solution is made of 2.5 mm composite faces and a 260 mm Polystyrene foam core. These solutions are made of thick core materials with a good absorption capacity, which is required for blast resistance specifications as shown in Section 2.6.
- In the second group, several core materials can be found in the Pareto front. Some Polyethylene and Melamine foam core sandwich panels are localized along the Pareto front but the most interesting core material is the one that occupies a large vertical band at the right end of the performance space, which is a Polyurethane foam. This core material is the best candidate for acoustic damping (see Section 2.3). Once again, decreasing the core thickness leads to an increase in the transmission loss. If high

Optimal design of architected sandwich panels for multifunctional properties

Pierre Leite

transmission loss of 95 dB can be achieved by a Polyurethane foam core sandwich panel, the minimum normalized deflection is limited to 0.066 m/m. An optimal solution can be identified here with a 90.2 dB transmission loss and a normalized deflection of 0.07 m/m. This solution is made of 3 mm composite faces and a 10 mm Polyurethane foam core. These solutions are made of thin and soft core materials, which is required for Acoustical Transmission Loss specifications. As mentioned previously, the foam core reaches densification strain during blast loading.

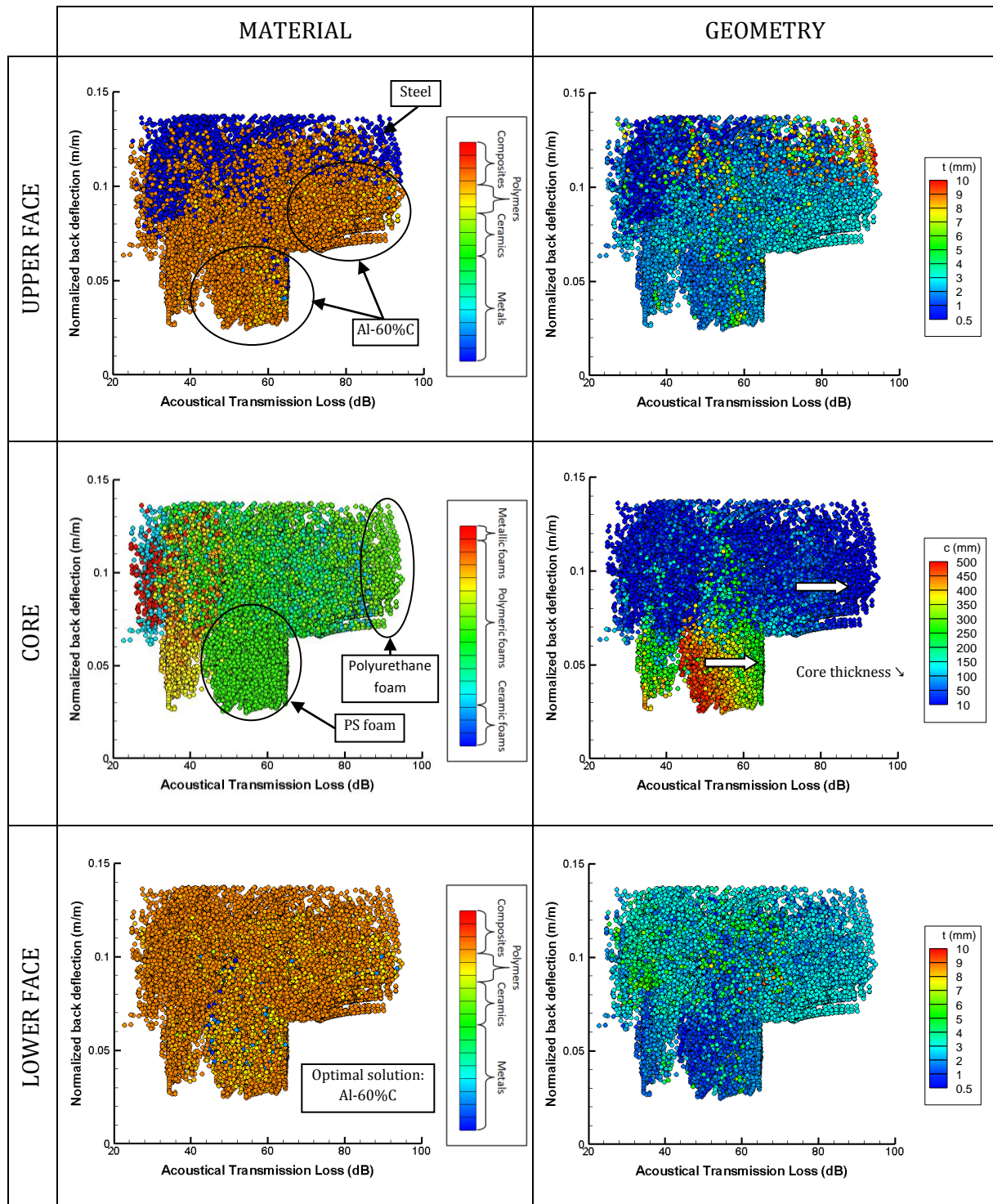


Figure 4.47: Influence of design parameters on the optimal design of a sandwich panel for blast resistance and Acoustical Transmission Loss at a mass of 50 kg/m^2 .

Effect of size constraint

Size constraint mainly disturbs the achievable performances of blast mitigation as shown in Figure 4.46. Indeed, optimal design of an acoustical panel does not dictate a panel thicker than 50 mm. This is why the maximum Acoustical Transmission Loss obtained with a 50 mm constraint is the same than the one obtained with a 500 mm constraint. However, the minimum normalized deflection after blast which is achievable by a 50 mm thick panel is only 0.06 m/m against 0.029 m/m for a 500 mm thick one. One of the two blocks in the performance space vanishes even if a small hump can be observed.

Effect of mass as an objective

Figure 4.48 shows the influence of mass constraint on the performance space between blast mitigation and sound insulation. Decreasing mass is mainly done by decreasing core thickness for Polystyrene foam core solutions and by decreasing face thickness for Polyurethane foam core ones. While mass is upper than 35 kg/m², the performance space is composed of two blocs corresponding to Polystyrene and Polyurethane foams as core materials. In view of the fact that “sandwich effect” is no longer observed for blast mitigation in the case of lighter panels, the performance space is limited to a rectangle with a tight range of blast deflection while the Acoustical Transmission Loss ranges up to about 87 dB.

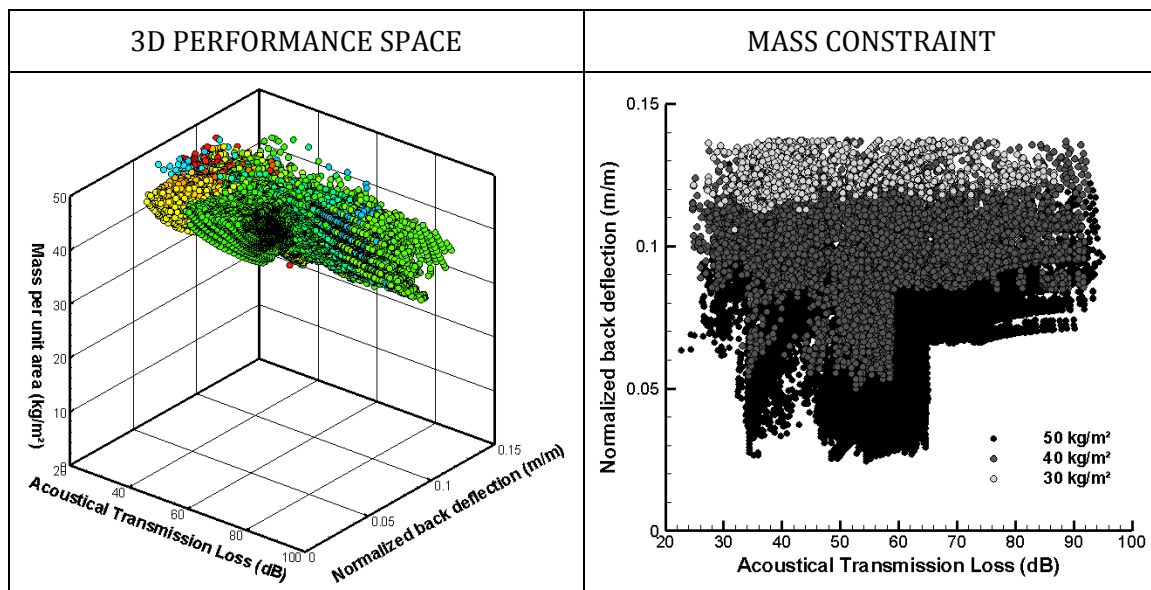


Figure 4.48: On the left hand side: performance space plotting the solutions generated by the optimization algorithm for blast mitigation and Acoustical Transmission Loss at minimal weight. Colour legend represents core material. On the right hand side: evolution of the performance space for blast mitigation and Acoustical Transmission Loss as a function of mass constraint.

Effect of functional constraints

As shown in Figure 4.46, for a normalized back deflection upper than 0.07 m/m, the achievable Acoustical Transmission Loss is very large. This is translated in Figure 4.49 in which the performance space between Acoustical Transmission Loss and mass is observed to reach the unconstrained Pareto front for constraint on the normalized deflection of 0.1 and 0.15 m/m. However, as already observed, panels with a mass lower than 25 kg/m² cannot sustain the blast load. Thus, the performance space is truncated. For a better blast mitigation, thicker and

Optimal design of architected sandwich panels for multifunctional properties

Pierre Leite

stronger core is required. As mentioned for the design of acoustical panels, thick and strong cores exhibit a poor Acoustical Transmission Loss.

Figure 4.49 also shows that Polystyrene foam core sandwich panels have an Acoustical Transmission Loss that can exceed 65 dB. This is only for higher Acoustical Transmission Loss that thin panels with a Polyurethane foam core are required. In Figure 4.49 the constrained performance space is also plotted against the blast resistance as a function of mass for different values of Acoustical Transmission Loss constraints. The thin Polyurethane foam core panels follow a path corresponding to panels for which core reaches densification strain, and then exhibit worse performances than thick panels.

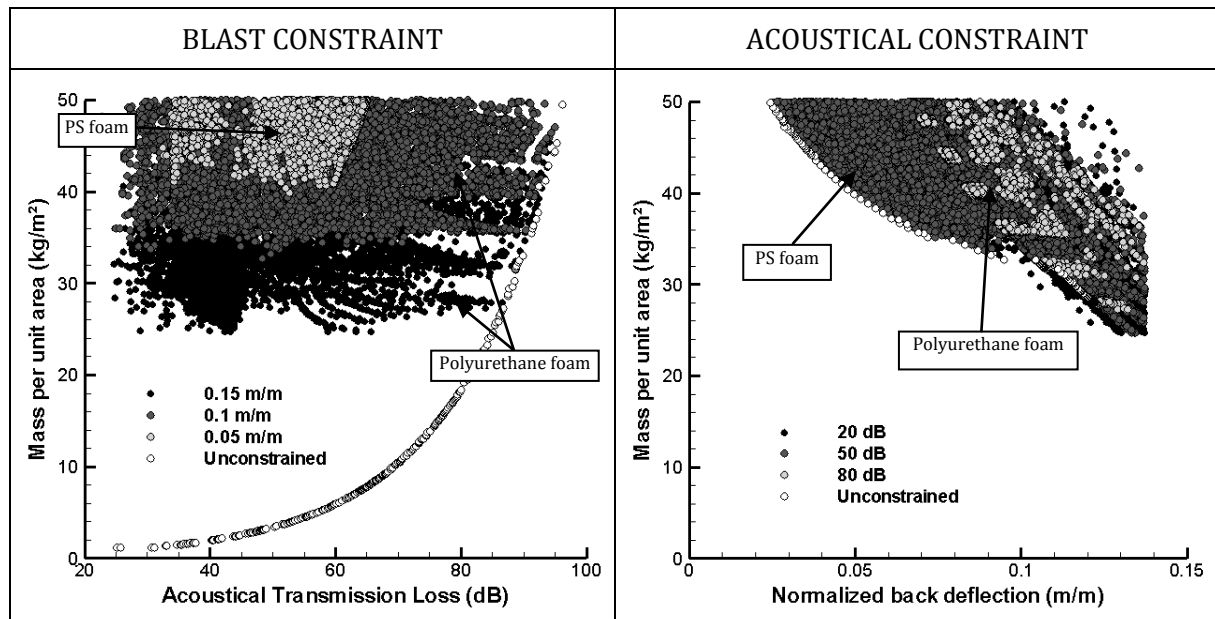


Figure 4.49: On the left hand side: evolution of the performance space for Acoustical Transmission Loss at minimal weight as a function of mitigation constraint. On the right hand side: evolution of the performance space for blast mitigation at minimal weight as a function of Acoustical Transmission Loss constraint.

Advantage of sandwich solutions

The evolution of the back deflection of a Polyurethane foam core sandwich panel as a function of the core thickness is presented in Figure 4.50. For a core thickness higher than 150 mm, the deformation of the upper face implied by the crushing of the soft core results in failure of face material. The Polyurethane foam is not strong enough to absorb energy while limiting the deformation of the upper face. For this reason, normalized deflection is limited to 0.066 m/m for this kind of solutions. The observed evolution of deflection as a function of core thickness is consistent with prior observations obtained by FE simulations on solid plates [XUE03]. Compared to monolithic solutions, these panels undergo a far better Acoustical Transmission Loss while the blast resistance remains satisfactory.

Figure 4.51 represents the Acoustical Transmission Loss as a function of the frequency for Polystyrene foam core sandwich panels with different core thickness but with the same face sheets (3 mm Steel faces). In the section dedicated to the optimal design of acoustic panels at a minimum weight, it has been demonstrated that the optimal design was a thin Polyurethane foam core sandwich panel. In the case of Polystyrene foam core solutions, when core thickness

decreases, the peak value of Acoustical Transmission Loss in the range [1 000; 4 000] Hz increases whereas the Acoustical Transmission Loss decreases at the boundaries corresponding to 1 000 and 4 000 Hz. Then, the averaged Acoustical Transmission Loss in the frequency range reaches its maximum at a core thickness around 200 mm as shown in Figure 4.51. It has also been demonstrated that the symmetric coincidence frequency was linked to face thickness. Decreasing face thickness leads to an increase of this frequency. A good balance should be found between the peak value and the sharpness of the curve. The optimal Polystyrene solution for the considered constraints (mass below 50 kg/m²) is then a 2.5 mm Aluminium matrix composite faces with a 260 mm core sandwich panel. Even though their Acoustical Transmission Loss is not as good as Polyurethane foam core solutions, a 64 dB Acoustical Transmission Loss is quite satisfactory compared to monolithic plates given that the blast resistance of the Polystyrene panel largely overcomes the one of Steel plates.

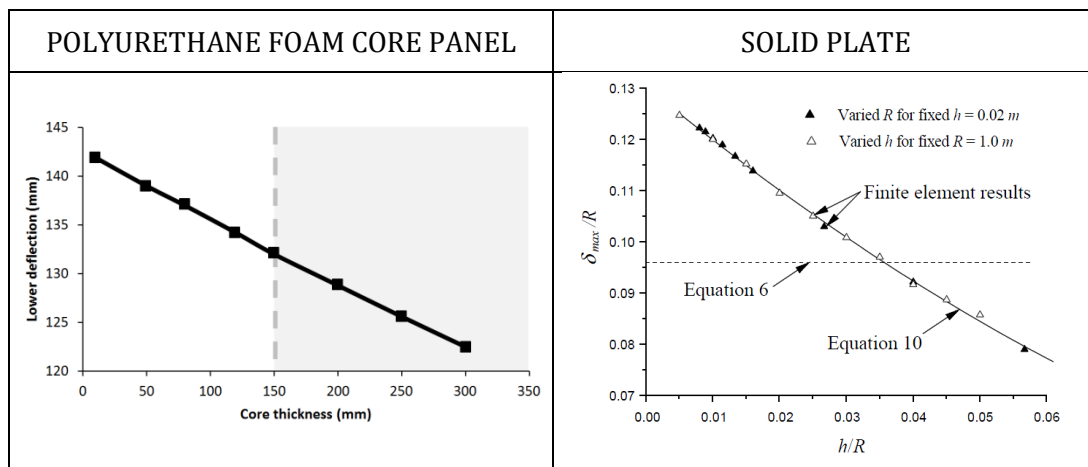


Figure 4.50: On the left hand side: Evolution of back deflection as a function of core thickness for a Polyurethane foam core panel with Steel faces. The dotted line marks the onset of face failure. Failure occurs for core thickness higher than 150 mm. On the right hand side: Evolution of back deflection as a function of core thickness normalized by plate length for a solid plate. Taken from [XUE03].

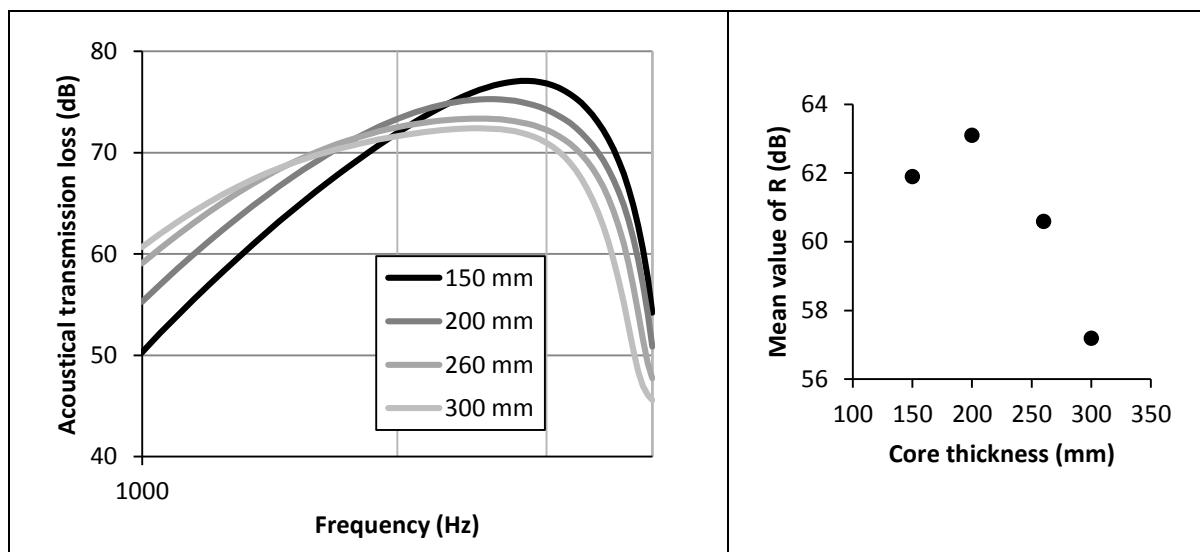


Figure 4.51: On the left hand side: Influence of core thickness on the Acoustical Transmission Loss curve as a function of frequency for a Polystyrene foam core panel made of 3 mm Al-60%C faces. On the right hand side: Corresponding mean value of Acoustical Transmission Loss as a function of core thickness.

The trade-off between Acoustical Transmission Loss and blast resistance is mainly driven by core material choice. A Polystyrene foam will be the best choice for blast mitigation, with a quite good Acoustical Transmission Loss somehow. A Polyurethane foam will be the best choice for Acoustical Transmission Loss (see Figure 4.52 for a comparison) with a not so poor blast resistance.

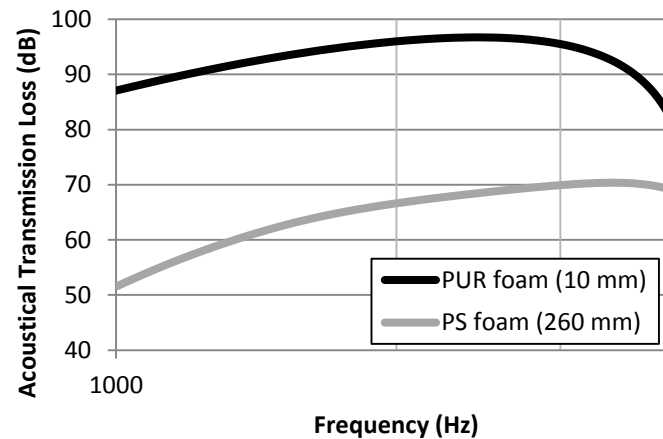


Figure 4.52: Comparison between the optimal design of a Polyurethane foam core sandwich panel and a Polystyrene foam core one regarding acoustical insulation. The Polyurethane foam core solution is made of a 10 mm thick core while Polystyrene foam thickness is 260 mm.

4. Overview of the results of multi-objective design by “real path”

The main results obtained in this chapter are summarized in Table 4.2 for optimal design at minimal weight for a single other objective and Table 4.3 for optimal design at minimal weight for a multiple function.

Firstly, optimization problems have been carried out by using the presented design process on the minimal weight design for a single other function. For each case, the shape of trade-off surface gives an indication on the possible compatibility between the specifications.

By analysing the contour values of the design variables in the performance space, optimal design can be identified in terms of material selection and geometry. It is also possible to identify the possible interactions between the design variables. For example, due to size limitations, the optimal material can change. In a few cases such as for thermal insulation, a match between materials properties is required modifying the rank of the candidates. For instance, Graphite foam is a better core material than Carbon foam for thermal insulation mainly because Graphite foam has a thermal expansion coefficient similar to the one of the face material.

A performance index approach has been used for a preliminary material selection. The optimal solutions identified by using performance indices often concurs with the optimal solutions identified by using the optimization algorithm. However, this kind of approach can hardly deal with the interactions mentioned above. For example, this cannot easily handle a ratio between core and face thickness, or core and face stiffness. For simple cases, flexural stiffness or thermal resistance for instance, the performance index approach is clearly sufficient to select the optimal material. For more complex cases such as flexural strength (change of failure mode) or thermal insulation (match of Coefficient of Thermal Expansion between face and core material), the present method is preferable.

For every case study, the properties of the optimal solutions generated by the genetic algorithm have been compared to the properties of a Steel plate, which is a classical solution in transportation applications. In every case, sandwich panels are better than Steel plates without forgetting that Steel plate could be better solutions for space required. In general, sandwich panels need a relatively thick core.

Table 4.2: Results overview regarding functional design.

Objectives	Shape of the trade-off surface	Optimal face material	Optimal core material	Most influential variable
<ul style="list-style-type: none"> Flexural stiffness 	Convex	MMC (Al-60%C)	PVC, Glass	<ul style="list-style-type: none"> Core material Face material
<ul style="list-style-type: none"> Flexural strength 	Concave	MMC (Al-60%C)	PVC	<ul style="list-style-type: none"> Core material Face material
<ul style="list-style-type: none"> Acoustic damping 	Convex	None	Polyurethane	<ul style="list-style-type: none"> Core material Core thickness
<ul style="list-style-type: none"> Thermal resistance 	Linear	Polypropylene	Melamine, Polyurethane, Phenolic	<ul style="list-style-type: none"> Core material
<ul style="list-style-type: none"> Thermal insulation 	Convex	CMC (C/C)	Graphite	<ul style="list-style-type: none"> Core material Face material
<ul style="list-style-type: none"> Blast mitigation 	Convex	MMC (Al-60%C)	Polystyrene, PVC, Polyethylene	<ul style="list-style-type: none"> Core thickness Face material

Secondly, tri-objective optimization cases have been solved corresponding to two different properties optimized at minimal weight. Four case studies, representative of the four different types of compatibility have been presented. These four cases can be divided into two groups:

- A first group for which a competition occurs between the two considered properties, mass being the third one. The competition is beneficial if the trade-off surface is convex, whereas the competition is non-beneficial if it is concave.
- A second group for which there is no competition. The properties can be either compatible or not.

For each case, a similar analysis as the ones performed for the first cases have been conducted. The optimal designs have been identified as well as the interactions between performances.

As a conclusion, from Tables 4.2 and 4.3, it comes out that the part of the sandwich panel which has the main influence on properties is the core. In a functional design, core material is the most influential parameter. Core material selection is then of top priority for the design of sandwich panels. In a multifunctional design, incompatibility often comes from an incompatibility in terms of design guides for core material selection or core geometrical design. However, face material and thickness can also have a major influence on some performances such as blast resistance or acoustical insulation.

Optimal design of architected sandwich panels for multifunctional properties

Pierre Leite

Table 4.3: Results overview regarding multifunctional design.

Objectives	Compatibility	Optimal core material	Variable influencing the trade-off
<ul style="list-style-type: none">• Flexural stiffness• Acoustic damping	Beneficial competition	<ul style="list-style-type: none">• Stiffness: glass• Acoustic damping: PS	<ul style="list-style-type: none">• Core thickness• Core relative density
<ul style="list-style-type: none">• Flexural strength• Thermal resistance	Non-beneficial competition	<ul style="list-style-type: none">• Strength: PVC• Thermal resistance: Phenolic	<ul style="list-style-type: none">• Core thickness• Core relative density
<ul style="list-style-type: none">• Blast mitigation• Thermal insulation	Compatibility	<ul style="list-style-type: none">• PS	NA
<ul style="list-style-type: none">• Blast mitigation• Acoustic damping	Incompatibility	<ul style="list-style-type: none">• Blast mitigation: PS• Acoustic damping: Polyurethane	<ul style="list-style-type: none">• Core material

Chapter 5

Influence of core architecture: “optimization by virtual path”

The previous chapter pointed out that the most influent design variable in the design of architected sandwich panels is the core material. In the present chapter, for each case studies treated in Chapter 4 by a “real path” approach, a design process is conducted using a “virtual path” approach.

The core material is no longer considered as a discrete variable. It can rather be described by a semi-continuous variable, with discrete information for material selection and continuous information for the geometry.

Three core architectures are examined: foams, honeycombs and truss structures. A comparison between these topologies helps identify the optimal core topology regarding the investigated functions.

The emphasis is laid upon the core design in terms of material selection, geometrical design and core architecture selection.

The structure of Chapter 5 is similar to the one of Chapter 4. Section 2 is dedicated to minimum weight design with a single other objective while Section 3 deals with multifunctional requirements of three objectives including mass reduction.

Finally, Section 4 provides an overview of the results, displaying the optimal core architecture for the considered functions.

Chapter contents

1. Introduction	173
2. Design at minimal weight for a single objective.....	175
2.1. Flexural stiffness	175
2.2. Flexural strength.....	179
2.3. Acoustic damping.....	183
2.4. Thermal resistance	189
2.5. Thermal insulation	192
2.6. Blast mitigation	197
3. Design at minimal weight for multiple objectives	199
3.1. A case of beneficial competition between specifications: flexural stiffness and acoustic damping specifications.....	200
3.2. A case of non-beneficial competition between specifications: flexural strength and thermal resistance specifications.....	203
3.3. A case of compatibility between specifications: thermal insulation and blast mitigation specifications	206
3.4. A case of incompatibility between specifications: acoustic damping and blast mitigation.....	211
4. Overview of the results of multi-objective design by “virtual path”	214

1. Introduction

In Chapter 4, it has been demonstrated that core material has a major impact on the performances of sandwich panels. The advantage of sandwich solutions over monolithic ones often comes from architected materials specificities, particularly the fact that it includes a certain pattern of the constitutive material. The influence of design variables at the length scale of the layers has been assessed: effect of material and effect of thickness. Compatibility between specifications has also been investigated. This chapter is focussed on core architecture. Previously, only foam core sandwich panels were considered, as foam materials are present in materials database. In order to assess the influence of core architecture, three different patterns have been selected, including foam as reference architecture. These three “patterns” are foams, honeycombs and truss structures. In Chapter 4, they were considered as “existing core materials”, i.e. for instance two foams with different densities were considered as two different materials in the database. In the present chapter, a virtual approach is taken where the architected core is described by the constitutive material and by continuous variables (density, angle, aspect ratio) related to the geometry. By using an optimization by “virtual path”, a comparison between the performances of the panels made of these different architectures will be performed. Each case treated in Chapter 4 will be explored with these three architectures. A variability analysis performed on core design (material and geometry) will also help monitor the differences between the three patterns. Face material and thickness remain free variable and are also optimized. Nevertheless, as the optimal face design identified in Chapter 5 are unchanged compared to the results obtained in Chapter 4 for almost all the case studies, no details will be provided concerning these design variables.

More information on the specificities of architectures and on “virtual path” optimization parameters is provided below.

In Figure 5.1, the three core architectures are introduced with a picture, a schematic representative unit cell and the design space in terms of geometrical design variables.

- The first architecture corresponds to the foam which is considered as an isotropic material for which the effective behaviour can be described from the constitutive material properties and the relative density ρ^* . The latter is the ratio between the volume occupied by the material in a representative unit cell and the volume of this unit cell. It has also been demonstrated using Maxwell criterion that this pattern is bending-dominated [DES01a]. In this chapter, foams are considered in a “virtual path” optimization using scaling laws presented in Chapter 3.
- Regular hexagonal honeycomb is the second core architecture considered in this chapter. Like foams, this pattern is bending-dominated [GIB97]. However, it is not an isotropic material, and its performances in the out-of-plane direction are excellent and can be assimilated to a stretching-dominated behaviour in this direction. Its effective properties can be calculated using scaling laws involving materials properties and the ratio between wall thickness and wall length as defined in Figure 5.1. Like for foams, the honeycomb architecture can be tailored by monitoring only one geometrical parameter. Honeycomb relative density is directly linked to the ratio t/l as presented in Chapter 3.
- The last architecture under investigation is the tetrahedral truss structure. Besides being stretching-dominated [DES01b], its effective properties are given by scaling laws depending on two different geometrical parameters in addition to materials properties.

Optimal design of architected sandwich panels for multifunctional properties

Pierre Leite

The two geometrical parameters are the trusses aspect ratio (a/l with a the radius and l the length of the struts) and the angle ω between struts and face sheets.

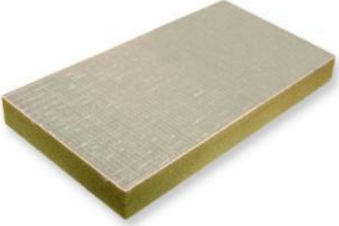

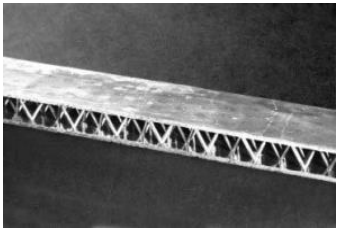
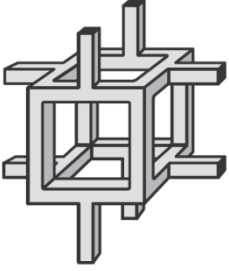
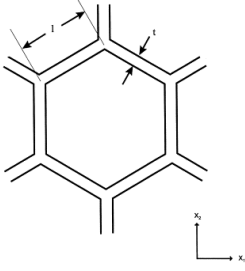
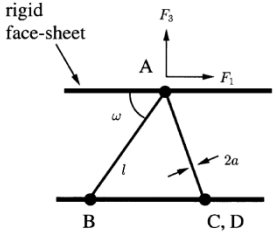
	FOAM	HONEYCOMB	TRUSS
PICTURE			
UNIT CELL			
DESIGN SPACE	$\rho^* \in [0,005; 0,4]$	$\frac{t}{l} \in [0,01; 0,2]$	$\omega \in [35^\circ; 75^\circ]$ $\frac{a}{l} \in [0,02; 0,05]$

Figure 5.1: Presentation of the three architectures considered for core material.

The optimization problems consider classical sandwich panels composed of three layers made of different core material. For each specification, three optimization problems involving each core architecture are analysed successively.

Concerning foams and honeycombs, the design space of a symmetrical sandwich panel is composed of five variables: two are the materials, two are the thicknesses and the last one describes the core geometry.

In the case of the truss structure as core material, there are not one but two variables describing the core geometry: the aspect ratio of trusses and the angle ω . In the case of asymmetric panels, an additional thickness and material are considered.

When appropriate, a more realistic size constraint has been set with a maximum size constraint of 200 mm. In this case, face thickness can vary from 0.5 to 5 mm and core thickness can vary from 10 to 200 mm. Concerning the other constraints, except for blast resistance, the same values as in Chapter 4 have been chosen. The case of blast resistance will be discussed in the section dedicated to the optimal design of panels for blast resistance at a minimum weight.

The design space in terms of constitutive material changes accordingly to a “virtual path” approach. The possible constitutive materials for the core are metals and polymers. Ceramics have not been considered for practical reasons, since some of the used models are not compatible with a brittle material behaviour.

2. Design at minimal weight for a single other objective

This section is dedicated to bi-objective optimization problems involving mass as an objective. Each function is treated successively. For each case, the trade-off surface extracted from the performance space obtained for each architectures is presented in order to rank the different architectures. For each architectures this performance space is used to perform a variability analysis which is focused on the core. The optimal design of each architectures is then obtained. A preliminary design process based on performance indices is used to predict the optimal core material.

2.1. Flexural stiffness

Design space:

- Face materials: Metals, Polymers, and Composites.
- Face thickness: from 0.5 to 5 mm.
- Core materials: Metals, Polymers.
- Core thickness: from 10 to 200 mm.
- Type of sandwich panel: symmetrical.

Objectives:

- Flexural stiffness: minimize the central deflection of a 1 m span sandwich beam submitted to a 1 N in a three-point bending test.
- Lightness: minimize the mass per unit area.

Constraints:

- Central deflection < 10 μm .
- Mass per unit area < 50 kg/m^2 .

“Real path” results:

- Optimal foam core material: PVC foam/Glass foam.

Preliminary core design: Performance index approach

The performance index displaying the optimal material for a plate submitted to bending at minimal weight is $E^{1/3}/\rho$, irrespective to the type of core material. However, it has been underlined that architected materials can be either bending or stretching dominated (see Chapter 2, Section 2.2).

Consequently, the effective mechanical properties should be evaluated using different performance indices. Bending-dominated patterns such as foams require performance indices dedicated to beams under bending while stretching-dominated patterns such as truss structures require performance indices dedicated to ties under tension.

Then, the performance index for core material selection is $E^{1/2}/\rho$ for foams and E/ρ for honeycombs and truss structures. The corresponding guidelines are drawn in the property chart plotting Young’s modulus E as a function of density ρ in Figure 5.2 for bending or stretching-dominated architectures.

The optimal foam core material is Magnesium. The optimal core constitutive material for honeycombs and truss structures is Chromium, followed by Aluminium and Magnesium.

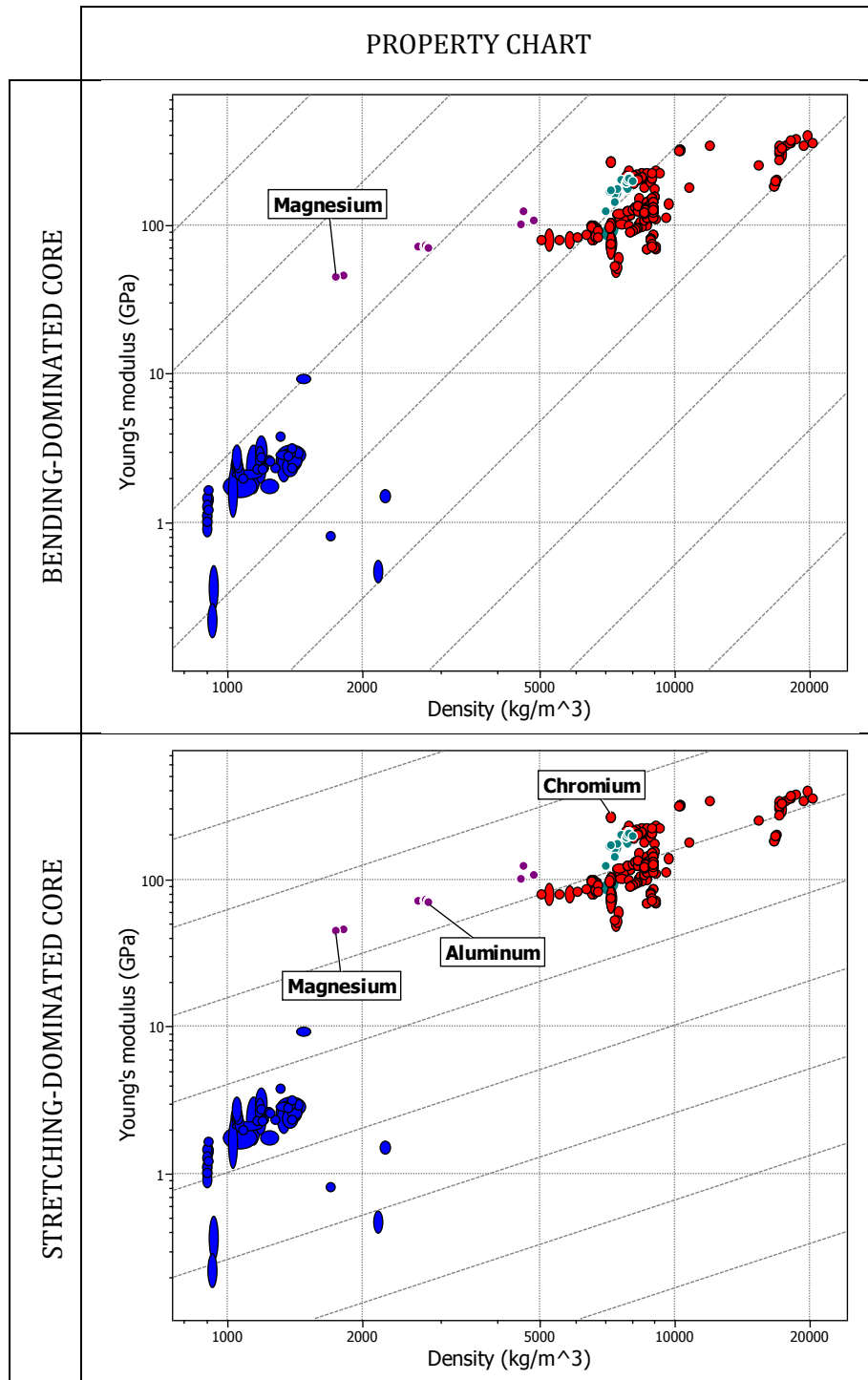


Figure 5.2: Property charts and guide lines corresponding to core constitutive optimal material for flexural stiffness at minimal weight according to core local loading. Optimal core material is Magnesium for foams and Chromium for honeycombs and truss structures.

Advanced core design

Comparison between architectures

In Figure 5.3 the Pareto fronts corresponding to the three different architectures are given by considering flexural stiffness at minimal weight. As expected from the results obtained in Chapter 4, the optimal design is composed of minimal face thickness and of a core thickness

which is increased when required stiffness is increased. Honeycombs and truss structures largely overcome foams for lightweight stiffness applications as expected, as they are stretching-dominated. Even though for a high value of mass, the difference between the performances of the three architectures becomes negligible, the advantage of stretching-dominated solutions is really obvious for lighter solutions. For a mass per unit area of 10 kg/m^2 , the deflection of the optimal foam core sandwich panel is $2.2 \mu\text{m}$ while for stretching-dominated core panels, it is also between 0.2 (honeycombs) and $0.3 \mu\text{m}$ (truss structure). Honeycombs are then slightly better than truss structures.

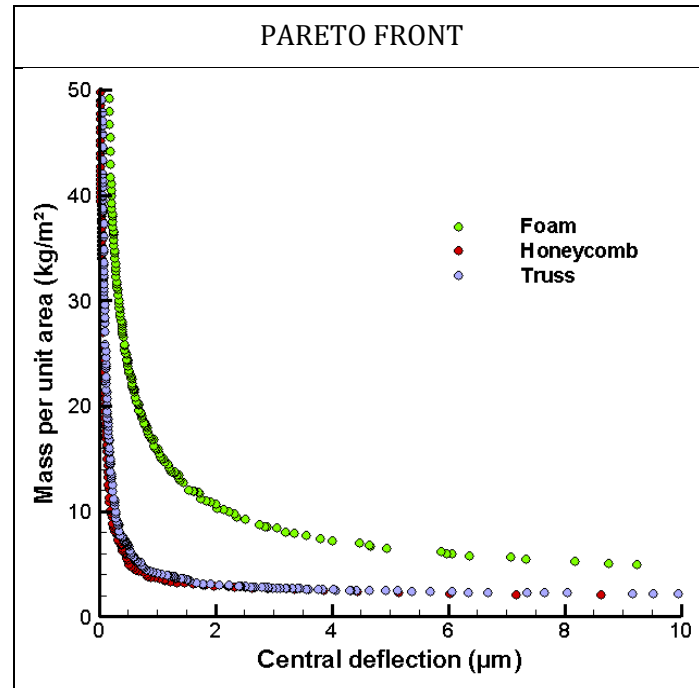


Figure 5.3: Pareto fronts corresponding to the three architectures for flexural stiffness at minimal weight.

Variability analysis of core design

Figure 5.4 shows the performance space corresponding to the three selected architectures. In the first column is represented the influence of core constitutive material while the second one represents the influence of core relative density. Magnesium alloys are the optimal choice for a foam core sandwich panel as core constitutive material. Regarding both honeycomb and truss structures, Magnesium is also an optimal solution for light solutions with a deflection higher than $1.2 \mu\text{m}$. For a deflection between 0.4 and $1.2 \mu\text{m}$, the optimal core constitutive material is Aluminium alloys while for stiffer solutions Chromium alloys are the best choice.

In terms of relative density, foam core sandwich panels are much denser than stretching-dominated core solutions. As expected, an increase in stiffness is partly achieved by increasing foam relative density in order to increase foam stiffness. The relative density of the foam core solutions on the Pareto front varies from 0.06 to 0.1 from the lighter to the stiffer respectively. The same behaviour is observed for honeycomb core materials but at different levels. The optimal relative density for a magnesium honeycomb is 0.005 . By reaching the maximum allowed core thickness, Aluminium is the optimal choice with a relative density ranging from 0.005 to 0.01 . Once again, due to size limitation, optimal core material changes to Chromium with a relative density ranging from 0.005 to 0.023 . The optimal relative density of truss core solutions follows the same trend than for honeycomb core panels. The value of the optimal angle

Optimal design of architected sandwich panels for multifunctional properties

Pierre Leite

ω for stiffness specifications is around 50° . The change of relative density is mainly achieved by a decrease of struts aspect ratio, the angle being reduced when very light specifications are required.

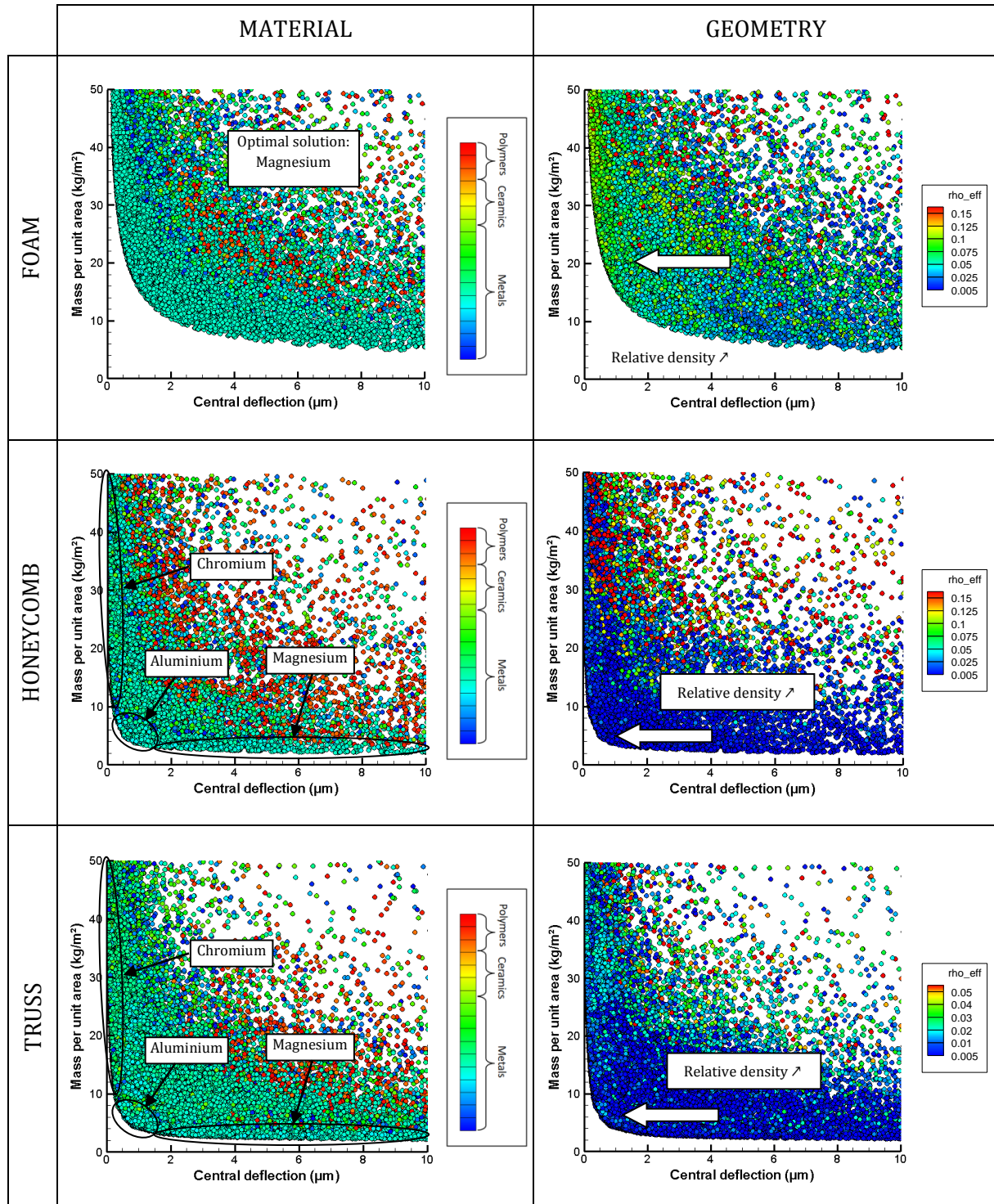


Figure 5.4: Influence of core constitutive material and relative density as a function of core architecture on the performances of the sandwich solution. The first column corresponds to constitutive material while the second one corresponds to relative density. The first line is for foam, the second one for honeycomb and the last one for truss structure.

The performance index approach succeeded in predicting the optimal core materials. For stretching-dominated structures, honeycombs and trusses, the stiffest solutions are made of Chromium. It is of interest to highlight that trade-off between mass and stiffness is tailored by changing core constitutive material but also by varying the relative density. This can explain the change of material selection. A Chromium truss structure of 160 mm thickness and 0.005 relative density has similar density and elastic modulus as an Aluminium truss structure of 190 mm and 0.01 relative density.

Comparison to the “real path” approach

No Magnesium foam is referenced in the database. It seems that Magnesium foams would be more efficient than the PVC foam proposed as optimal solution in the previous chapter. A few studies pointed out the possible interests of these Magnesium foams against other metal foams [GUP12]. However, additional work should be produced in order to validate the effective properties of such foams. A positive point is that manufacturing processes already exist but fire and corrosion resistance are certainly an issue.

The fact of using Magnesium and Aluminium as constitutive materials for both honeycomb and truss structures is already common [DES01b]. On the contrary, using Chromium as constitutive material is not usual. Except for Nickel-Chromium alloy, no reference to such architected materials has been found, probably because of the toxicity of Chromium.

2.2. Flexural strength

Design space:

- Face materials: Metals, Polymers, and Composites.
- Face thickness: from 0.5 to 10 mm.
- Core materials: Metals, Polymers.
- Core thickness: from 10 to 200 mm.
- Type of sandwich panel: symmetrical.

Objectives:

- Flexural strength: maximize the critical load corresponding to failure of a 1 m span sandwich beam submitted to a three-point bending test.
- Lightness: minimize the mass per unit area.

Constraints:

- Flexural strength > 2 kN.
- Mass per unit area < 50 kg/m².

“Real path” results:

- Optimal foam core material: PVC foam.

Preliminary design: Performance index approach

The performance index corresponding to the strength of a plate at minimal weight is $\sigma^{1/2}/\rho$. This is translated into a performance index for the core constitutive material considering that it is composed of struts loaded in bending or stretching. The corresponding performance indices are then $\sigma^{2/3}/\rho$ for bending-dominated architectures (foams) and σ/ρ for stretching-dominated ones (honeycombs and truss structures). The property chart plotting the yield strength as a

Optimal design of architected sandwich panels for multifunctional properties

Pierre Leite

function of density is used to identify the optimal solutions for each case (Figure 5.5). Aluminium is the optimal choice for bending load while Steel is the best one by considering stretching.

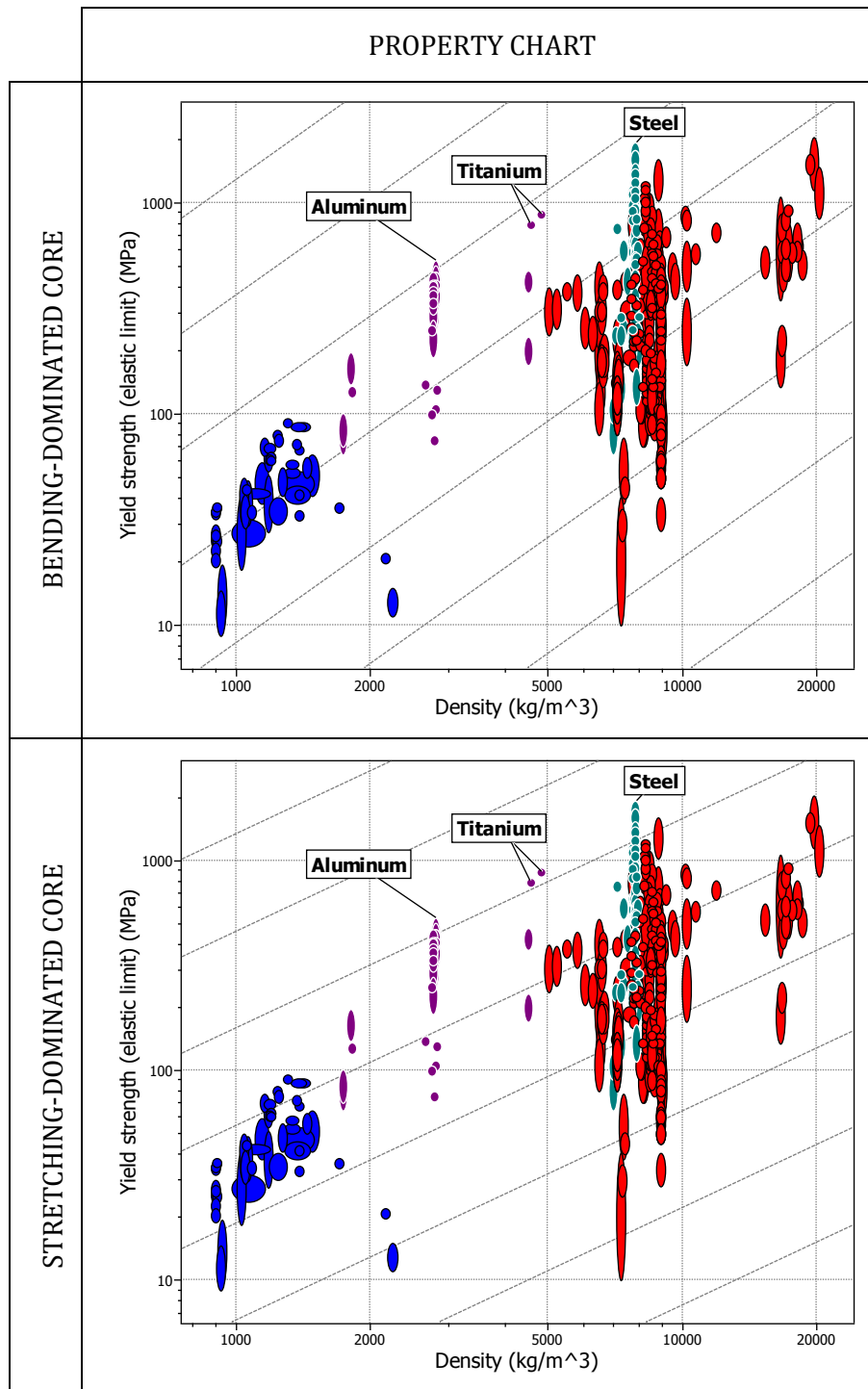


Figure 5.5: Property charts and guide lines corresponding to core constitutive optimal material for flexural strength at minimal weight according to core local loading. Optimal core material is Aluminium for foams and Steel for honeycombs and truss structures.

Comparison between architectures

As expected, stretching-dominated core materials are more weight efficient than bending-dominated ones for flexural strength as shown in Figure 5.6. The size constraint has been set at

200 mm but the optimal core thickness is smaller than this value. For foam core, it ranges between 30 and 50 mm. For honeycomb, it varies from 30 to 90 mm and for truss structure its range is almost the same, between 30 and 80 mm.

Honeycomb is a more efficient core material than truss structure but their performances are close. As an example, for a mass per unit area of 30 kg/m^2 , the strength of the optimal foam core panel is 17 kN against 52 kN for the optimal truss core solution. This value reaches 59 kN for the optimal honeycomb core panel.

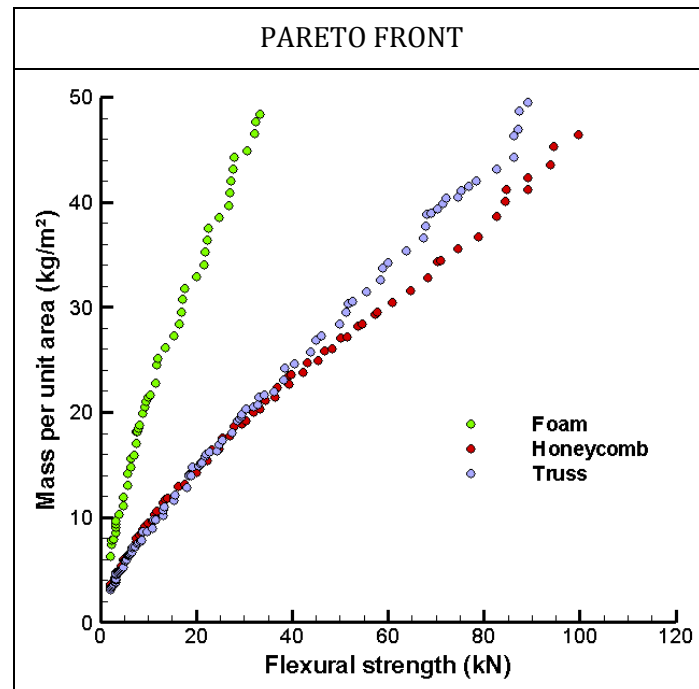


Figure 5.6: Pareto fronts corresponding to the three architectures for flexural strength at minimal weight.

Variability analysis of core design

For flexural strength at minimal weight, Aluminium is among the best constitutive core material as shown in Figure 5.7. This is the optimal choice for designing foam and honeycomb cores. This is also among the optimal choice for light truss core panels (mass under 16 kg/m^2 corresponding to a strength of 24 kN). The other optimal constitutive core materials for truss core structures are Titanium until a mass of 33 kg/m^2 and a strength of 58 kN. For more resistant solutions, Steel trusses are used. The corresponding Steel is a Carbon Steel (AISI 1340).

Regarding relative density, foam core panels require denser cores than stretching-dominated core solutions. The relative density of optimal foam panels ranges from 0.07 to 0.3. As a comparison, optimal honeycomb relative density only varies from 0.02 to 0.1.

Optimal truss core structures have a relative density varying between 0.02 and 0.05. The difference between truss structures and honeycombs is that the relative density of the former depends on two independent variables, the aspect ratio of trusses and the angle ω while for the latter it only depends on the ratio t/l . The limitations on the aspect ratio of trusses seem to be the limiting design variable as the optimal constitutive material changes when the aspect ratio reaches its maximum allowed value. An optimal angle value is found around 50° . As a consequence, an increase of relative density of the truss structure by increasing the angle above 50° results in a decrease of core strength. At relatively high relative density, honeycombs are then stronger than truss structure for a given material.

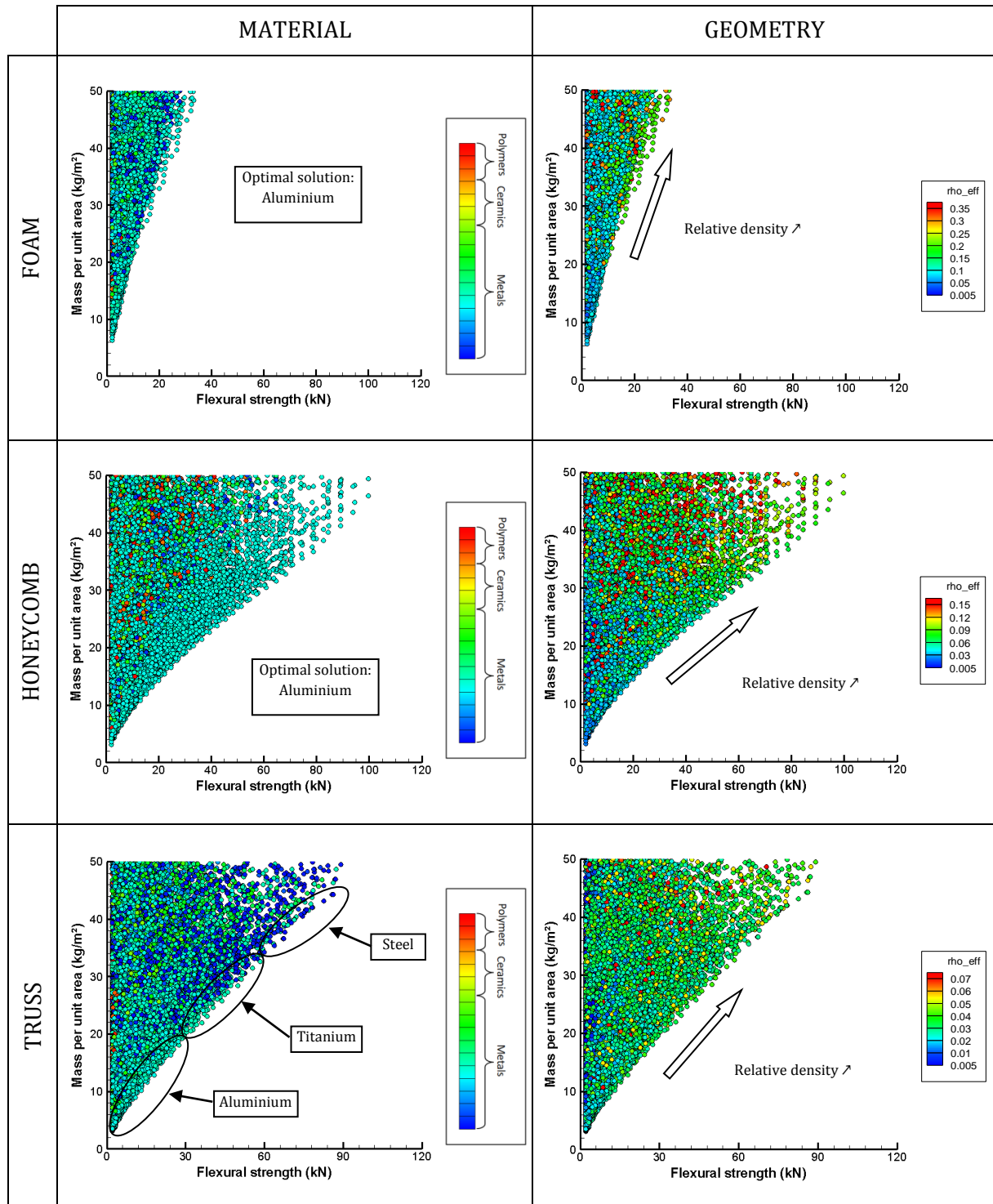


Figure 5.7: Influence of core constitutive material and relative density as a function of core architecture on the flexural strength at minimal weight of the sandwich solutions.

The results obtained by the performance index approach are consistent with the results obtained using the genetic algorithm. The optimal foam material is Aluminium.

Regarding truss structures, the strongest solutions are made of Steel. Then, lightening the solutions is achieved by changing to Titanium and to Aluminium for low strength requirements. The same ranking is identified using the performance index as shown in Figure 5.5.

For honeycomb core panels, the structure of the performance shape should be the same as for truss structure. However, the transition between Steel and lighter materials should occur at higher strength than the observed range, then only Aluminium solutions are present as optimal solution.

2.3. Acoustic damping

Design space:

- Face materials: Metals, Polymers, and Composites.
- Face thickness: from 0.5 to 5 mm.
- Core materials: Metals, Polymers.
- Core thickness: from 10 to 200 mm.
- Type of sandwich panel: symmetrical.

Objectives:

- Acoustic damping: maximize the mean value of the Acoustical Transmission Loss in the frequency range [1 000; 4 000] Hz.
- Lightness: minimize the mass per unit area.

Constraints:

- Acoustical Transmission Loss > 20 dB.
- Mass per unit area < 50 kg/m².

“Real path” results:

- Optimal foam core material: Polyurethane foam.

Preliminary design: Performance index approach

No performance index has been found in the literature for Acoustical Transmission Loss at minimal weight as already mentioned in the previous chapter. However, in a first approximation, by considering that the core should be soft to promote symmetric vibration modes, the performance index for core material selection is simply E which is to be minimized. This one stands for both bending and stretching-dominated architectures. The property chart given in Figure 5.8 shows that the softest material available in the considered database is Polyethylene (MDPE).

Comparison between architectures

It has been demonstrated that a soft core, by allowing a transverse deformation, is a good choice as core material in a sandwich panel for Acoustical Transmission Loss [SIM95, LAN60, WAN09]. The mass law is another mechanism allowing the Acoustical Transmission Loss to be increased and is based on inertial effects. Then a promising candidate for core material in an acoustic panel is a soft and heavy architected material. From the literature and the results above, stretching-dominated materials are more weight efficient for mechanical purpose [DES01a, ASH11]. Thus, for a given weight and the same constitutive material, the stiffness of a stretching-dominated material will be higher than that of a bending-dominated one. It seems intuitive that bending-dominated materials such as foams should be better candidates for acoustic damping than stretching-dominated ones such as honeycombs and truss structures.

Optimal design of architected sandwich panels for multifunctional properties

Pierre Leite

Results obtained in Figure 5.9 show that this trend is followed as core architectures are ranked from foam as the best candidate to honeycomb as the worst one.

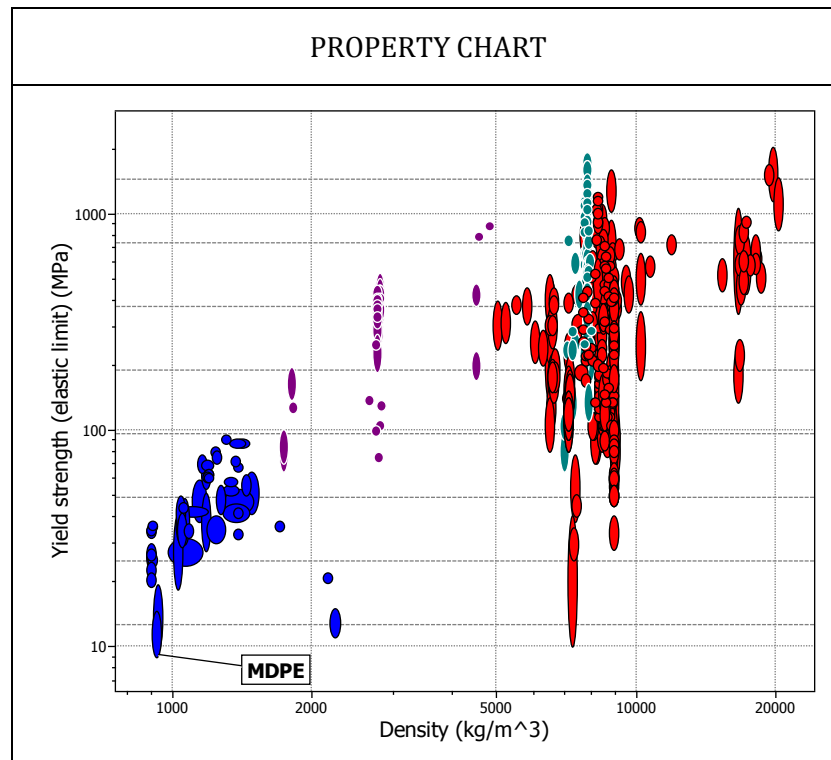


Figure 5.8: Property chart and guide lines corresponding to core constitutive optimal material for acoustic damping at minimal weight. Optimal core material is Polyethylene (MDPE) for every core architectures considered.

It is worthwhile noticing that the performances of truss core sandwich panels are not far from the ones of foam core solutions. Contrary to flexural properties (both stiffness and strength), the truss structure is closer to foam than to honeycomb even though it is a stretching-dominated architecture.

The Pareto fronts are also plotted in log scale in order to illustrate the mass law. Honeycomb core panels exhibit a specific behaviour. There is a major part of the curve that approximately exhibits the same slope than the curves corresponding to foams and truss structures. In this part, the involved mechanisms are the “mass law” and the “sandwich effect” as mentioned in Chapter 2 and Chapter 4. But the beginning of the curve has a completely different slope, where mass law is the dominant mechanism. The relative increase of acoustic damping for a unit increase of mass is lower in this part of the curve. This illustrates the fact that the most advantageous mechanism for acoustic damping is the “sandwich effect” coming from a soft core.

Variability analysis of core design

Like for the optimization by “real path” (Chapter 4), a lead design variable is the core constitutive material. As polyurethane is not in the database as possible constitutive material, the optimal choice is a Medium Density PolyEthylene (MDPE) as predicted by the performance index approach, whatever the architecture, as shown in Figure 5.10.

Regarding relative density, all optimal solutions for every architectures have a 0.005 relative density which is the minimum possible value in the design space. This results from the fact that a soft core is required. Indeed, a direct link occurs between relative density and core stiffness through the scaling laws given in Chapter 3. Let us note that, for the optimal truss structures, the angle ω has its minimum possible value (35°) and the aspect ratio is also minimal (0.02).

As already observed in Chapter 4 in terms of face sheets, the higher the acoustic damping, the larger the face mass.

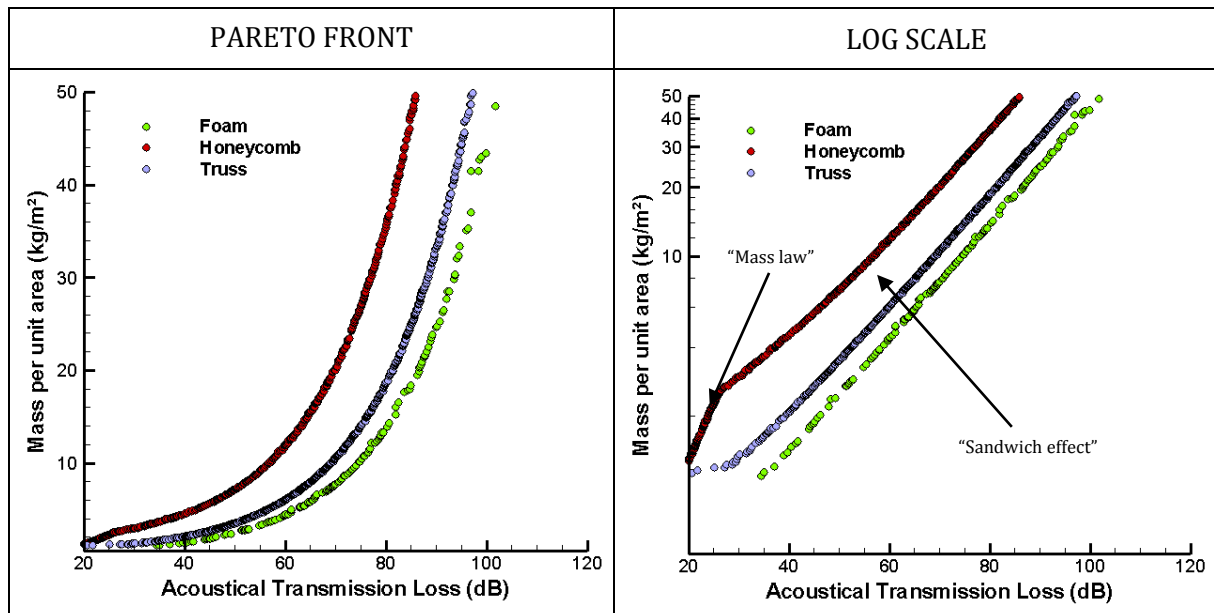


Figure 5.9: Pareto fronts for Acoustical Transmission Loss at minimal weight. The same Pareto fronts are plotted in a log-scale in order to illustrate the logarithmic mass law.

The main difference in terms of design is the optimal core thickness. In Figure 5.11, the influence of core thickness on the performance space is plotted as a function of core architecture. In Chapter 4, it has been shown that the optimal design was a Polyurethane foam core sandwich panel with a core thickness of 10 mm which is the minimum allowed value. As emphasized in Figure 5.11, the same trend is followed for foam core solutions as the optimal solutions are thin core panels of 30 mm, whereas for stretching-dominated architectures, the behaviour is completely different. For honeycomb core panels, the optimal core thickness is 190 mm, leading to a 200 mm thick solution. Similarly, the optimal core thickness of a truss core panel is 100 mm.

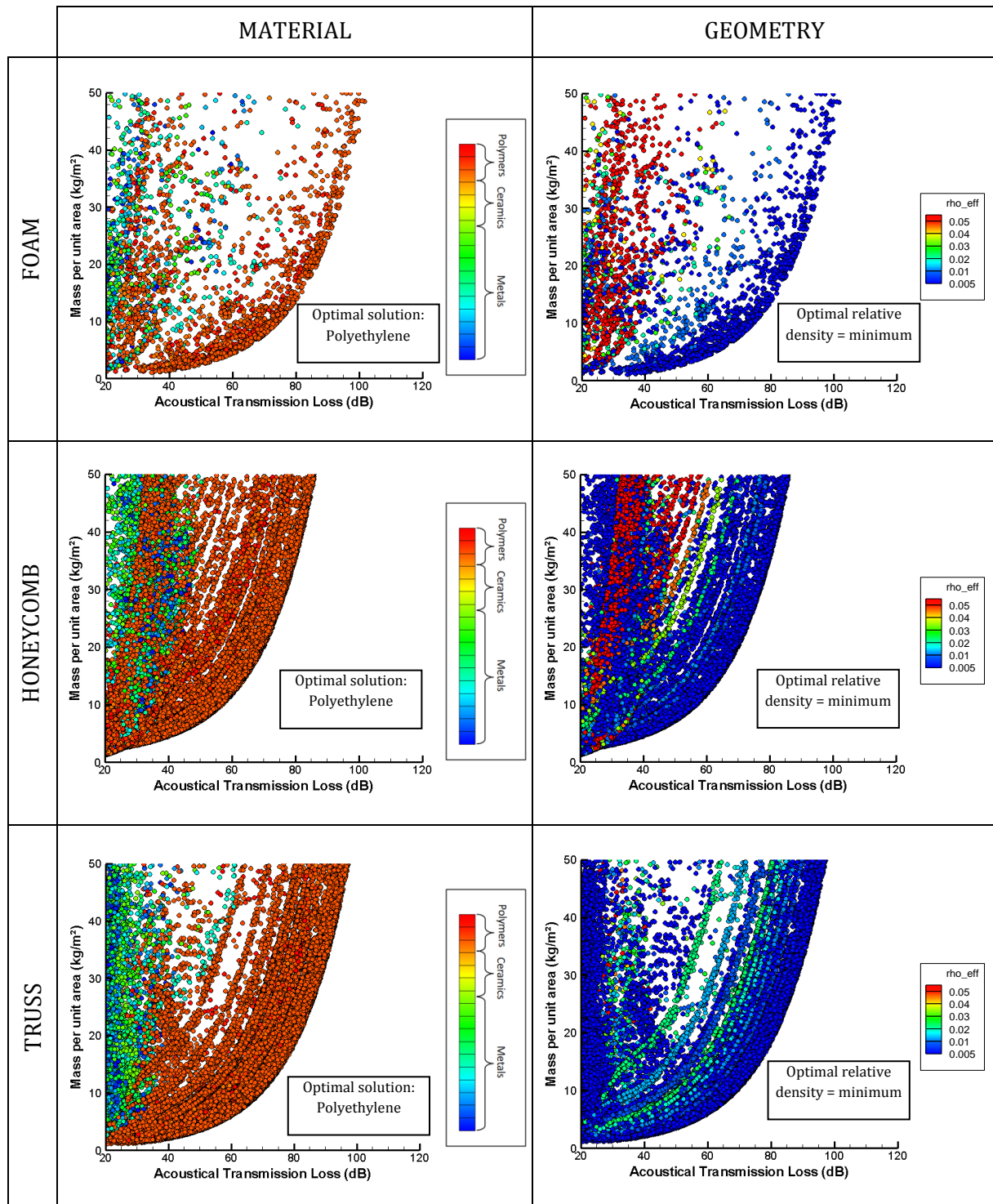


Figure 5.10: Influence of core constitutive material and relative density as a function of core architecture on the Acoustical Transmission Loss at minimal weight of the sandwich solutions.

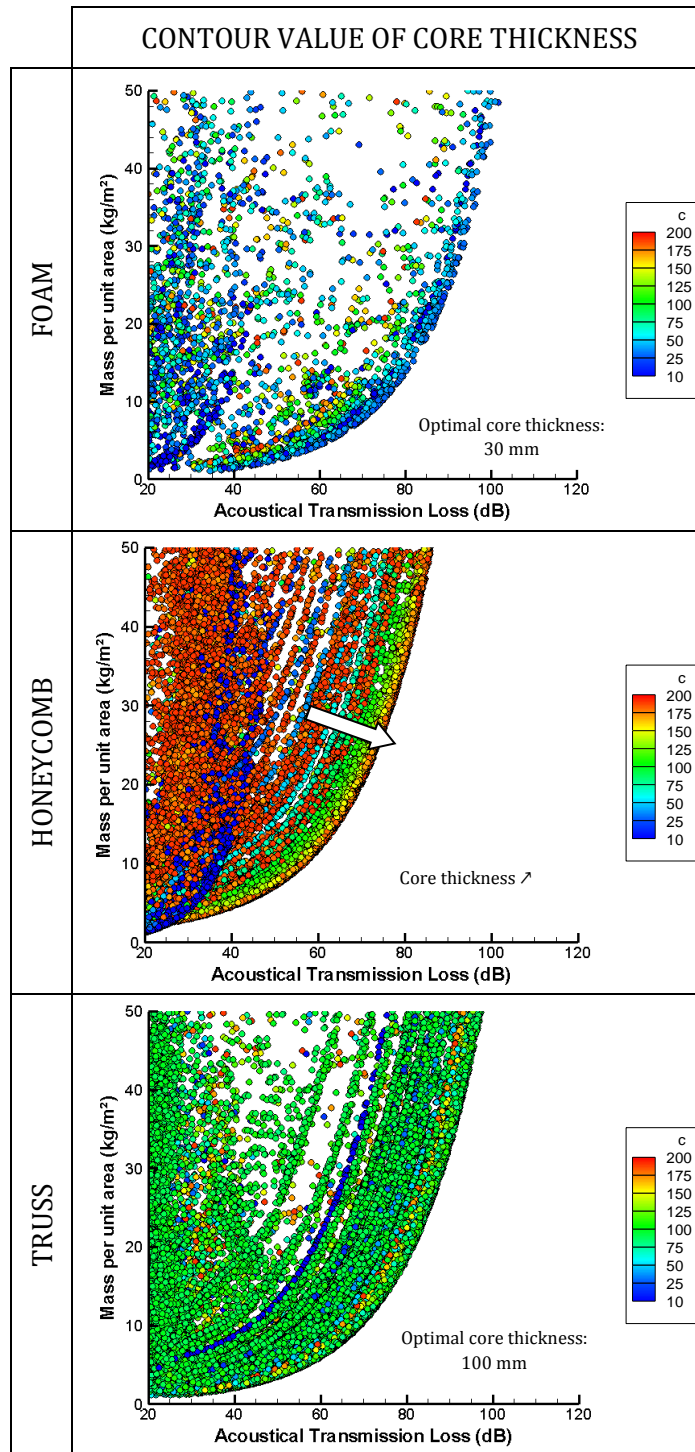


Figure 5.11: Influence of core thickness on the optimal design of the sandwich panel as a function of the architecture of the core material.

The evolution of the Acoustical Transmission Loss as a function of the frequency for different core thicknesses is plotted in Figure 5.12 for honeycomb core and truss core panels. The honeycomb core panel is made of 1.25 mm Babbitt metal⁷ faces and a Polyethylene honeycomb of 0.005 relative density. The truss core panel is made of 3.25 mm Babbitt metal and a

⁷ The considered Babbitt metal is a Tin-based alloy with a relatively low Young's modulus for a density close to the one of Steel. Babbitt metals are usually used for bearing surfaces.

Optimal design of architected sandwich panels for multifunctional properties

Pierre Leite

Polyethylene truss structure of 0.005 relative density.

The shape of the curve corresponding to a honeycomb core panel follows the one obtained for a foam core. Decreasing core thickness induces an increase in the peak value of the Acoustical Transmission Loss but it also induces a decrease in the Acoustical Transmission Loss at low frequencies. The shape of the curve corresponding to a truss core is different from the others. A hump is observed between 1 000 and 2 000 Hz. At higher frequencies, the Acoustical Transmission Loss increases with frequency in a regular manner. Relating the mean value of R with the corresponding curve, the importance of Acoustical Transmission Loss at low frequencies is quite clear. This comes from the calculation of the mean value of the Acoustical Transmission Loss R :

$$R = -10 \log \left(\frac{\sum P_{tr}^2(f)}{\sum P_{inc}^2(f)} \right) \quad (5.1)$$

with $P_{tr}^2(f)$ the sum of the transmitted quadratic pressure as a function of frequency f and $P_{inc}^2(f)$ the sum of the incident quadratic pressure. High values of transmitted pressure, as in low frequencies, will have a high relative weight in the sum. Then, good value of Acoustical Transmission Loss at the low frequencies has a major weight in the mean value R . However, these curves show that the optimal solution could change if another criterion was chosen. Nevertheless, truss structure still overcomes honeycomb as core material for Acoustical Transmission Loss.

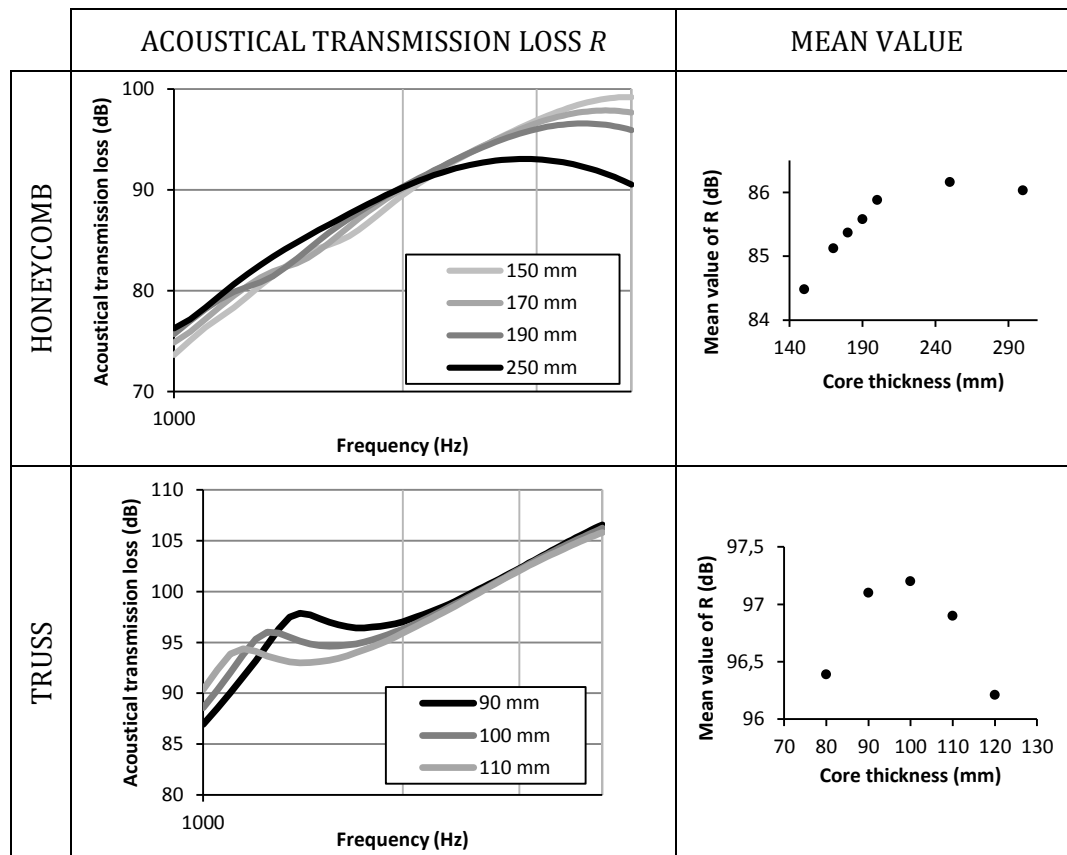


Figure 5.12: On the left hand side: Influence of core thickness on the Acoustical Transmission Loss curve as a function of frequency for a panel made of Babbitt metal faces and Polyethylene core. On the right hand side: Corresponding mean value of Acoustical Transmission Loss as a function of core thickness.

2.4. Thermal resistance

Design space:

- Face materials: Metals, Polymers, and Composites.
- Face thickness: from 0.5 to 5 mm.
- Core materials: Metals, Polymers.
- Core thickness: from 10 to 200 mm.
- Type of sandwich panel: symmetrical.

Objectives:

- Thermal resistance: maximize the through thickness thermal resistance.
- Lightness: minimize the mass per unit area.

Constraints:

- Thermal resistance $> 1 \text{ m}^2\text{K/W}$.
- Mass per unit area $< 50 \text{ kg/m}^2$.

“Real path” results:

- Optimal foam core material: Melamine foam.

Preliminary core design: Performance index approach

The performance index for thermal resistance at minimal weight is very simple as the requirements are to minimize the thermal conductivity and the density of the material. Then, the index is $1/k\rho$. The property chart plotting the thermal conductivity as a function of density is given in Figure 5.13 and guidelines corresponding to the performance index are drawn in dotted lines. The optimal choice is Polypropylene.

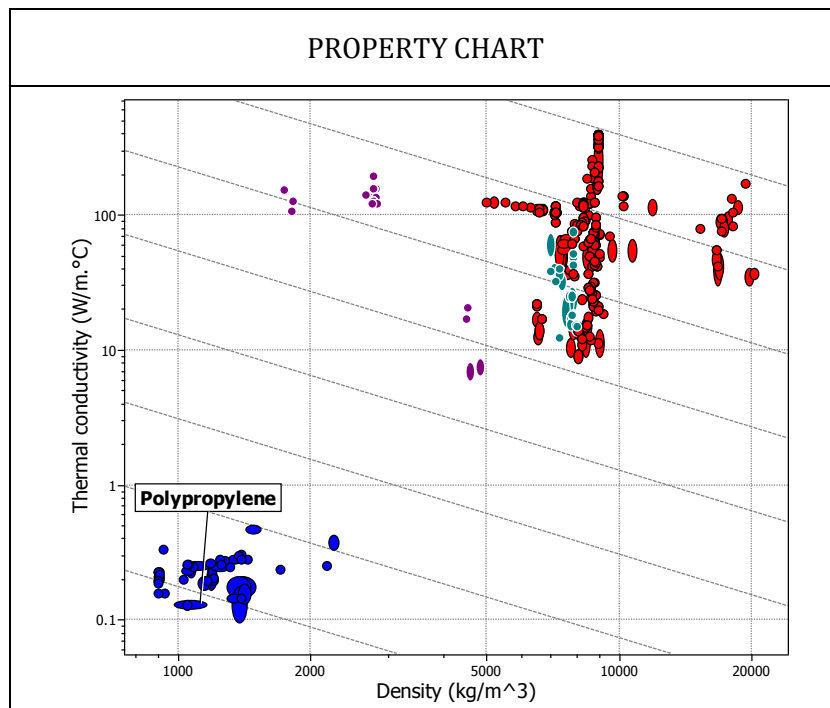


Figure 5.13: Property chart and guide lines corresponding to core constitutive optimal material for thermal resistance at minimal weight. Optimal core material is Polypropylene for every core architectures considered.

Optimal design of architected sandwich panels for multifunctional properties

Pierre Leite

Comparison between architectures

Figure 5.14 displays the Pareto fronts for the three core architectures corresponding to the optimal design of sandwich panels for thermal resistance at minimal weight. The only parameters that influence thermal resistance are both thickness and thermal conductivity. As the effective thermal conductivity of each architectures only depends on relative density, no real differences appear in the optimal solutions of both architectures.

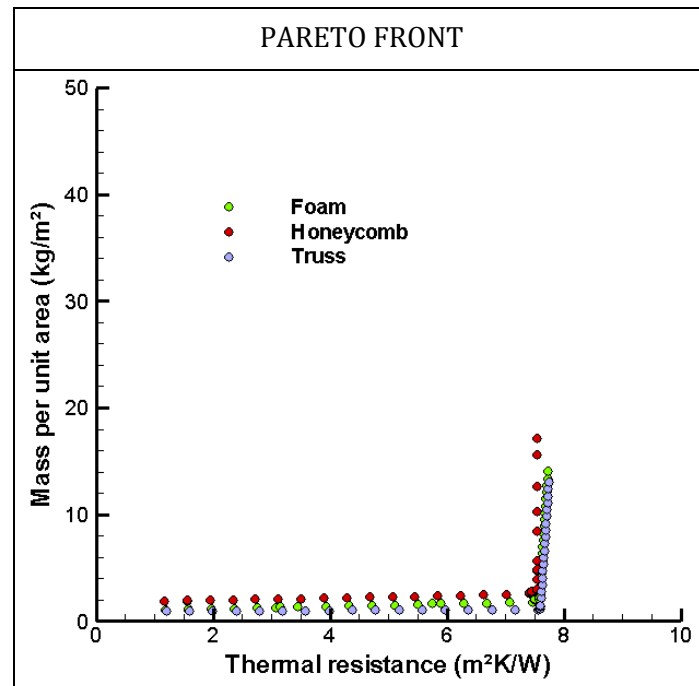


Figure 5.14: Pareto fronts for thermal resistance at minimal weight.

Variability analysis of core design

The optimal design is then the one that minimizes thermal conductivity. The optimal core relative density is 0.005 and the optimal core constitutive materials are Polypropylene and Polystyrene which achieve similar performances regarding thermal resistance (see Figure 5.15).

The obtained results are better than the ones obtained by a “real path” approach. This is mainly due to the fact that the relative density of the Melamine foam (which is the best real foam candidate for this application) is 0.006 with a core density of 12 kg/m². As a comparison, the proposed Polypropylene foam has a relative density of 0.005 and a core density of 4.55 kg/m². The real issue is the manufacturability of this kind of foams. However, in a multiple function design, the poor mechanical properties of such a core material could lead to more realistic solutions.

Once again the results obtained by the performance index approach are consistent with the ones obtained by the optimization algorithm in terms of material selection. Let us note that Polypropylene and Polystyrene have very similar properties, thus being both in the trade-off surface.

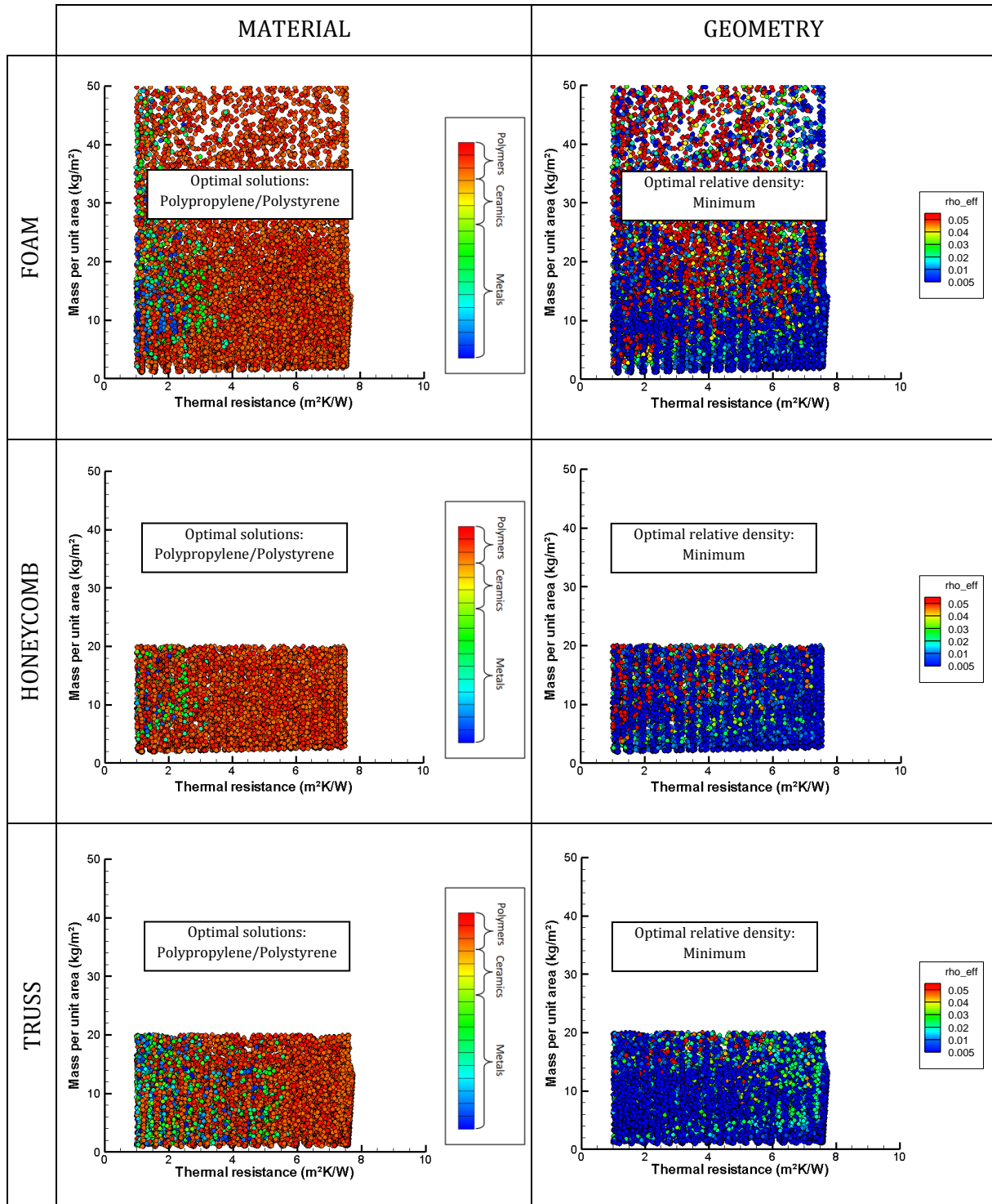


Figure 5.15: Influence of core constitutive material and relative density as a function of core architecture on the thermal resistance at minimal weight of the sandwich solutions.

2.5. Thermal insulation

Design space:

- Face materials: Metals, Polymers, and Composites.
- Face thickness: from 0.5 to 10 mm.
- Core materials: Metals, Polymers.
- Core thickness: from 10 to 500 mm.
- Type of sandwich panel: unsymmetrical.

Objectives:

- Thermal insulation: minimize the temperature at the inner face while the outer face is submitted to a 700 °C heat during 1 hour.
- Lightness: minimize the mass per unit area.

Constraints:

- Temperature at the inner face < 140 °C.
- Thermal shock resistance: $\max_{\forall x, \forall t} \left(\frac{\sigma(x, t)}{\sigma_y(x)} \right) < 1$.
- Temperature in the material < maximum service temperature of the material.
- Mass per unit area < 50 kg/m².

“Real path” results:

- Optimal foam core material: Graphite foam.

Preliminary design: Performance index approach

Regarding the case of thermal insulation, the optimal material at minimal weight can be identified using the performance index a/ρ with a the thermal diffusivity. Corresponding guidelines are drawn on the property chart plotting thermal diffusivity as a function of density in Figure 5.16. Due to maximum service temperature, which is constrained to be upper than 700 °C, several materials have been discarded from the selection. The optimal choice is the cobalt-based superalloy UMC0-50.

Comparison between architectures

In Chapter 4, only two core materials were identified in the performance space as feasible solutions. This is mainly due to the lack in the database of metal foams dedicated to high temperature applications such as superalloys based foams. Let us remind that for this specification, the objective is to minimize the temperature at the back of the panel. In addition, two constraints must be filled:

- The temperature within the material should not reach the maximum service temperature (for example, a stainless steel with a melting point at about 1500 °C has a maximum service temperature of 250 °C).
- The stress within the material should not reach the yield strength. As described in Chapter 3, the thermal stress calculated is in-plane. As a consequence, the in-plane yield strength should be considered.

Figure 5.17 illustrates the Pareto fronts corresponding to the different core architectures. In this case, the size constraint of 500 mm has been kept. For panels with a mass per unit area above 30 kg/m², the difference is negligible. The temperature of the back is approximately 20 °C

which is the initial temperature. However, below this mass value, truss core panels are the optimal choice while honeycombs are less effective as core candidate for weight saving purpose. The overall shape of the curve is similar for every architectures and is also similar to the one obtained by a “real path” in Chapter 4.

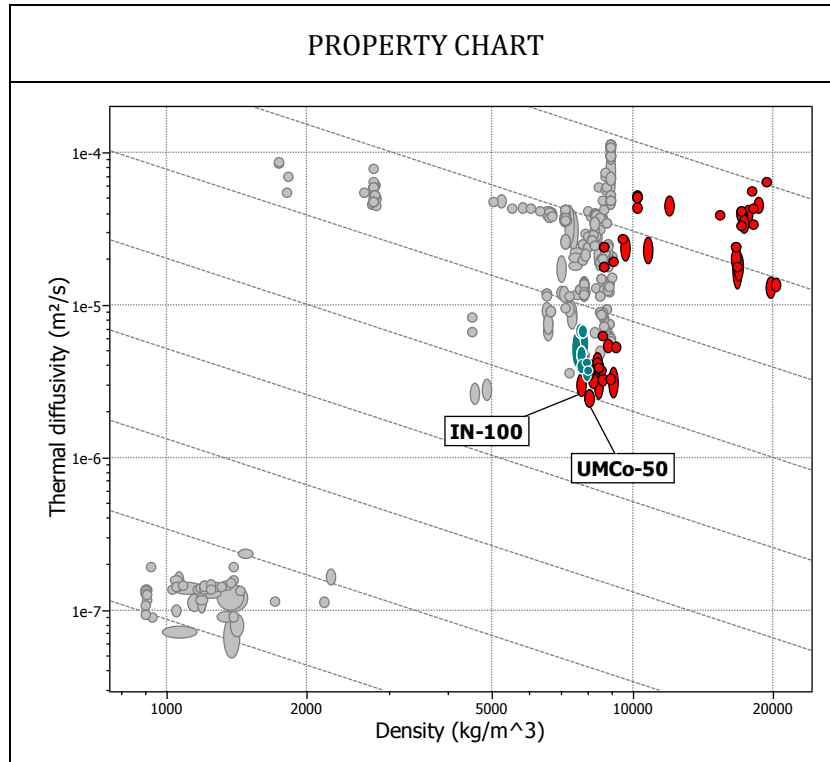


Figure 5.16: Property chart plotting the thermal diffusivity as a function of density with guidelines corresponding to the optimal design for thermal insulation at minimal weight. The cobalt-based superalloy UMCo-50 is the optimal solution, followed by the nickel-based IN-100.

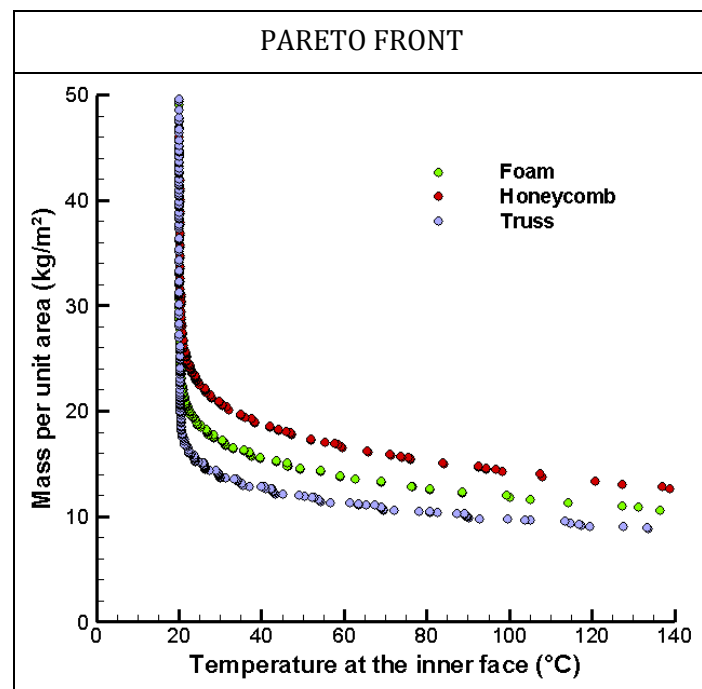


Figure 5.17: Pareto fronts corresponding to the three architectures for thermal insulation at minimal weight.

Variability analysis of core design

The optimal core constitutive material, as shown in Figure 5.18, is a Cobalt-based superalloy UMCo-50 which is well known for its outstanding thermal shock resistance. For foam core panels, a Nickel-based superalloy, IN-100, is competitive for light panels, with a mass under 23 kg/m^2 . In general, performances of UMC0-50 based structures are very similar to the ones of IN-100 based solutions.

In order to decrease the core thermal diffusivity, the relative density might be decreased, thus leading to an optimal relative density of 0.005. The main difference between the three architectures in terms of thermal properties is the efficiency factor used in the scaling laws for the thermal conductivity. For foams and truss structures, an efficiency factor of $2/3$ has been considered while for honeycombs the efficiency factor is 1. Then, the thermal resistance of foams and truss structure for the same core material and the same relative density is higher than the one of honeycombs. This explains why honeycombs are the less promising candidate. The fact that truss structures overcome foams comes from the Thermal Shock Resistance which is higher for truss structures than for foams, as emphasized in Figure 5.19.

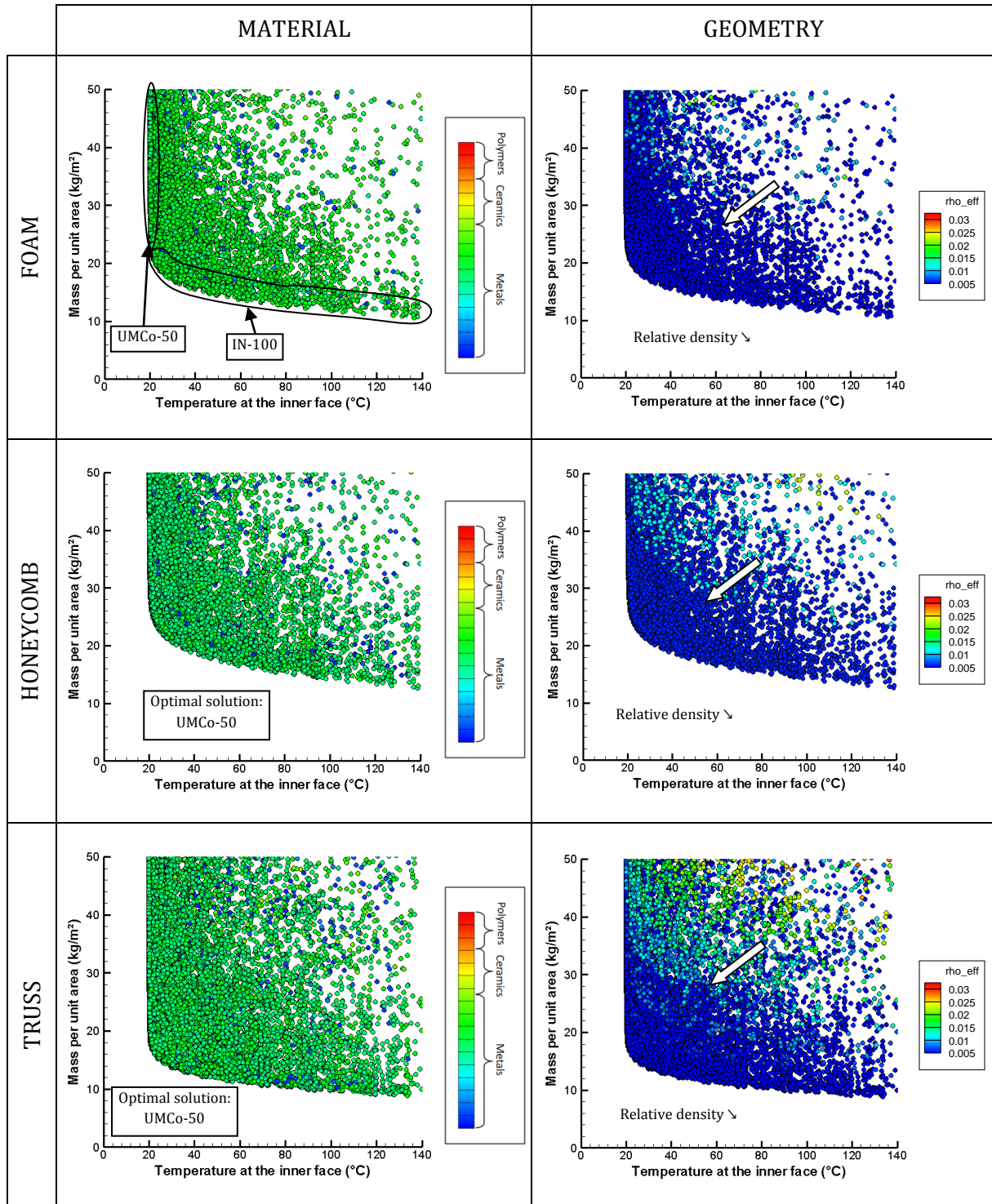


Figure 5.18: Influence of core constitutive material and relative density as a function of core architecture on the thermal insulation at minimal weight of the sandwich solutions.

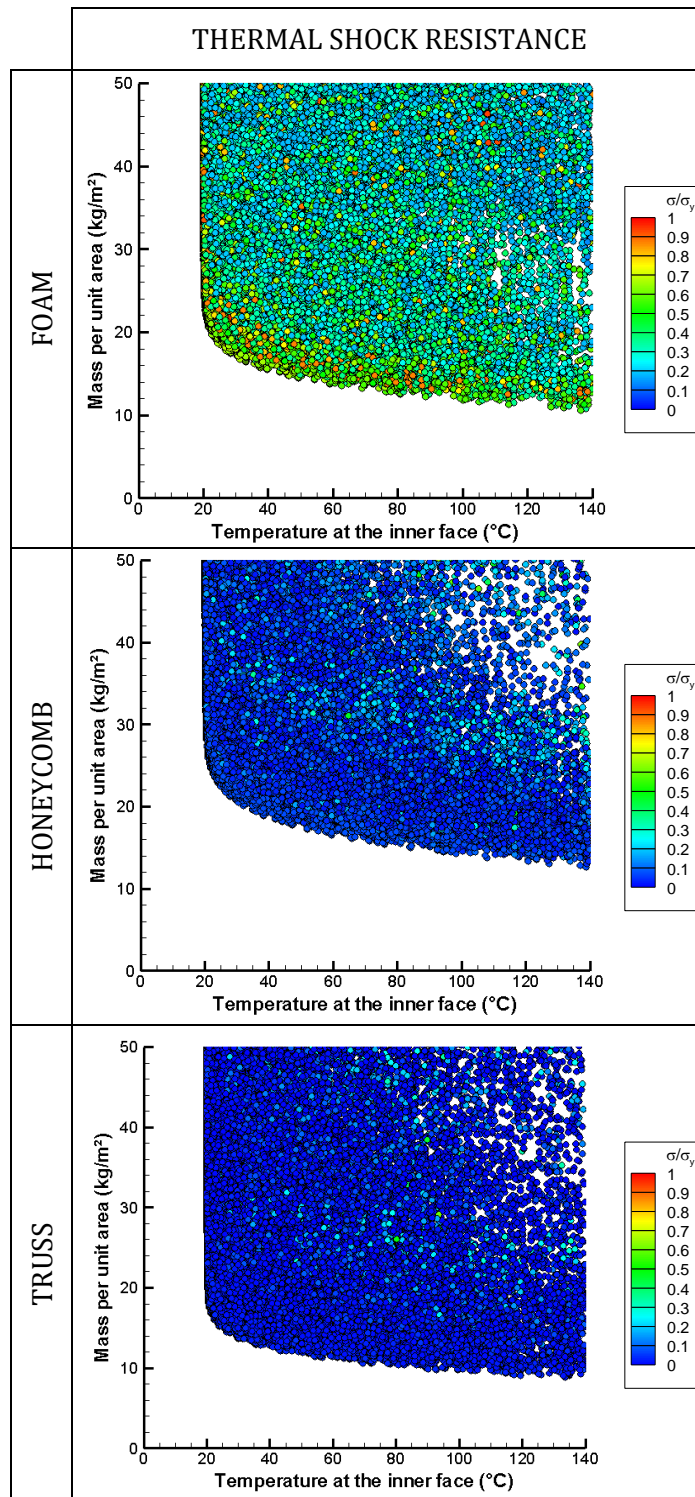


Figure 5.19: Influence of core constitutive material and relative density as a function of core architecture on the thermal insulation at minimal weight of the sandwich solutions.

2.6. Blast mitigation

The optimization of sandwich panels for blast mitigation at minimal weight by a “real path” was performed using a size constraint of 500 mm and a peak pressure value of 50 MPa. For the approach by “virtual path”, the size constraint is unchanged but the peak pressure value has been modified to 10 MPa. The reason of that change is discussed further in this section.

Design space:

- Face materials: Metals, Polymers, and Composites.
- Face thickness: from 0.5 to 10 mm.
- Core materials: Metal foams, Polymer foams.
- Core thickness: from 10 to 500 mm.
- Type of sandwich panel: unsymmetrical.

Objectives:

- Blast resistance: minimize the normalized back deflection which is the central deflection of the back face normalized by the span of the panel when the panel is submitted to a blast impulse of $2 \cdot 10^3 \text{ Nsm}^{-2}$.
- Lightness: minimize the mass per unit area.

Constraints:

- Normalized back deflection $< 0.2 \text{ m/m}$.
- No face failure.
- Mass per unit area $< 50 \text{ kg/m}^2$.

Comparison between architectures

The Pareto front used to compare the three core architectures regarding blast specification is given in Figure 5.20. Stretching-dominated core architectures clearly overcome foams, which is consistent with the results found in the literature [FLE04, XUE04]. Truss structure shows better weight efficiency than honeycomb one. As in the previous chapter, two different behaviours are observed. One part of the curve corresponds to designs for which core compression leads to a core strain equal to the densification strain while the other part corresponds to designs for which core thickness is sufficiently high to allow a large amount of energy dissipated during core compression. For more details on that issue, the reader is referred to the previous chapter.

It is assumed that, when core reaches densification during core compression, the main dissipation mechanism is bending of the sandwich panel. In this case, core architecture has practically no effect as shown in Figure 5.20. The Pareto fronts are very close in the part corresponding to this mechanism.

Variability analysis of core design

As the core material has an influence only in the part of the curve for which core has not reached densification, the variability analysis will specifically focus on that part (see Figure 5.21).

The optimal core constitutive material depends on the core architecture. For foam core panels, Aluminium 7075 is the best candidate that can be found in the database. For honeycomb and truss core panels, Magnesium is by far the optimal choice. For honeycomb, this corresponds to a QE22 Magnesium alloy while for truss core, QE22, ZE41 and pure Magnesium lie on the trade-off surface.

Optimal design of architected sandwich panels for multifunctional properties

Pierre Leite

The relative density of the core material slightly differs from an architecture to another but remains low. As a reminder, in the “real path” approach, one of the best solutions was a PS foam with a 0.019 relative density. The obtained values with a “virtual path” approach are very close. The optimal relative density for foam core solutions varies from 0.02 to 0.03. For honeycomb structures the optimal value is 0.023 while for truss cores it is between 0.005 and 0.02. For foams and truss structures, the variation of the relative density is inversely proportional to the blast resistance. The maximum relative density is observed for the maximum value of deflection.

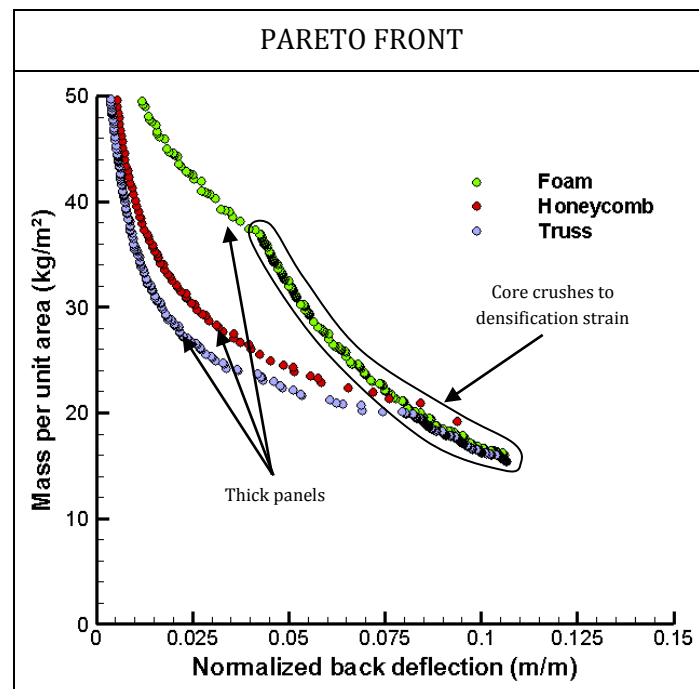


Figure 5.20: Pareto fronts corresponding to the three architectures for blast resistance at minimal weight.

Comparison with optimization by “real path” – scaling laws issues

The main reason why the peak pressure has been reduced is that the scaling laws that have been used seem to underestimate core mechanical properties. For example, for a Polystyrene foam of 0.019 relative density extracted from the database, the densification strain is 0.95 and the compressive strength (plateau stress) is 0.13 MPa. By using the scaling laws presented in Chapter 3, then the calculated densification strain is 0.972 and the calculated compressive strength is 0.099 MPa. As the calculated compressive strength is 25% lower than the measured value, the core compression is higher than it should be. As a consequence, some solutions that would not have reached core densification in a “real path” approach are discarded by using a “virtual path” approach. This also results in an increase of the calculated deflection for a solution at a given weight and a given design.

However, a performance space could still have been filled with feasible solutions considering a peak pressure of 50 MPa. On the other hand, no feasible solution has been found in the optimization problem involving thermal insulation specifications with blast resistance ones (this case study is discussed further). In order to be able to estimate the impact from adding another specification in the optimization problem on the design of the sandwich panels, the present optimization problem has been resolved using a peak pressure value of 10 MPa.

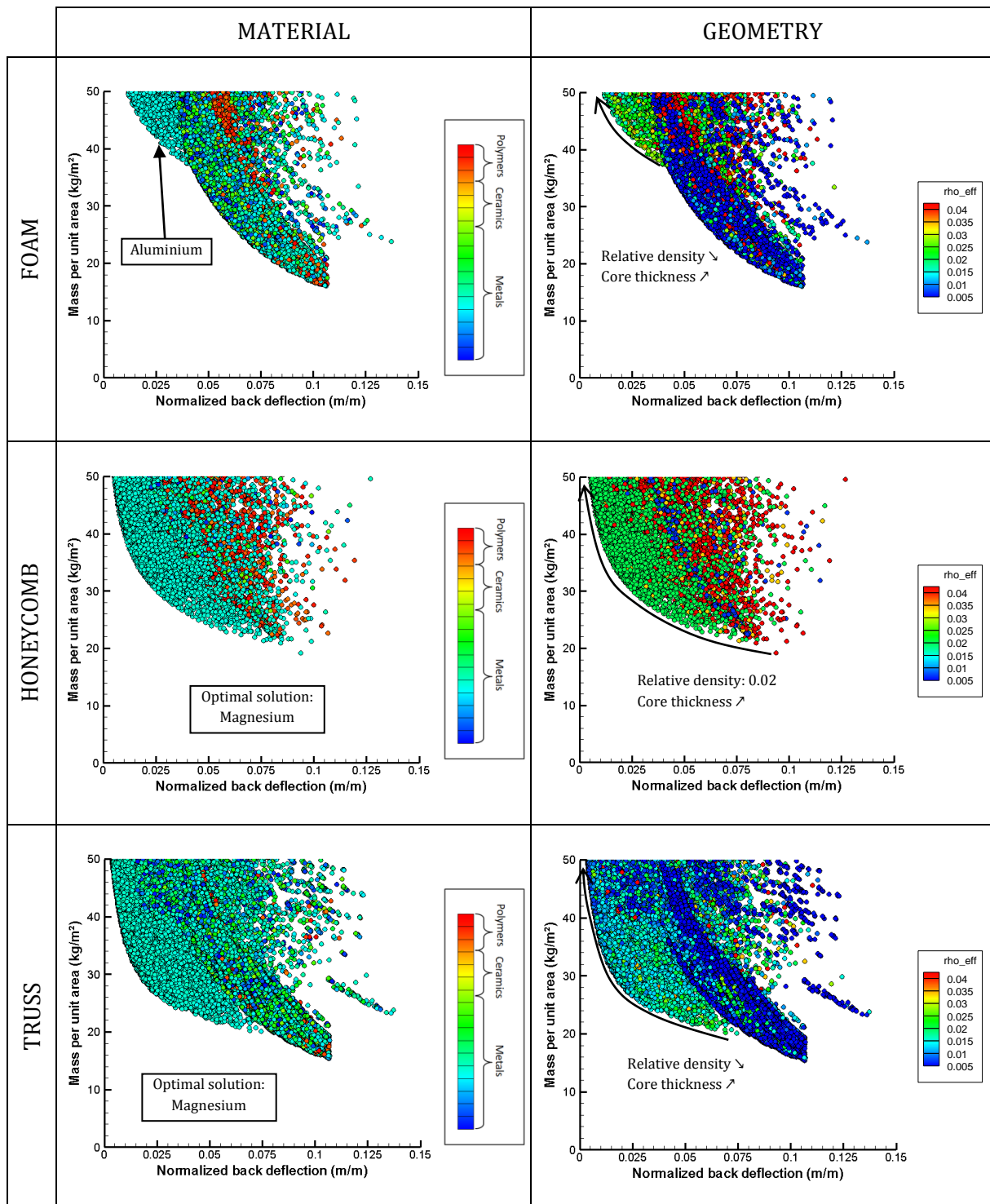


Figure 5.21: Influence of core constitutive material and relative density as a function of core architecture on the blast resistance at minimal weight of the sandwich solutions.

3. Design at minimal weight with multiple objectives

The four case studies treated in a “real path” approach in the previous chapter are treated underneath using a “virtual path” approach. The core architecture has no influence on the compatibility between the specifications. But in some cases, some architectures are better than

Optimal design of architected sandwich panels for multifunctional properties

Pierre Leite

others due to their geometrical specificities. For each case, a comparison between the different architectures is made. A variability analysis on the core design is performed.

In the particular case of the panel designed for thermal insulation and blast resistance at minimal weight, a more detailed analysis is performed since no feasible solution was found in the previous chapter.

3.1. A case of advantageous competition between specifications: flexural stiffness and Acoustical Transmission Loss specifications

Design space:

- Face materials: Metals, Polymers, and Composites.
- Face thickness: from 0.5 to 5 mm.
- Core materials: Metals, Polymers.
- Core thickness: from 10 to 200 mm.
- Type of sandwich panel: symmetrical.

Objectives:

- Flexural stiffness: minimize the central deflection of a 1 m span sandwich beam submitted to a 1 N in a three-point bending test.
- Acoustic damping: maximize the mean value of the Acoustical Transmission Loss in the frequency range [1 000; 4 000] Hz.
- Lightness: minimize the mass per unit area.

Constraints:

- Central deflection < 10 μm .
- Acoustical Transmission Loss > 20 dB.
- Mass per unit area < 50 kg/m^2 .

Comparison between architectures

In the previous chapter, the trade-off surface obtained by considering Acoustical Transmission Loss and flexural stiffness specifications consisted of two parts corresponding to two different core materials involving two different mechanisms in terms of acoustical behaviour. In the present case, size constraint has been reduced to 200 mm. The non-dominated solutions obtained using a “virtual path” approach for the three architectures are given in Figure 5.22. For the sake of clarity, the contour of the performance spaces are drawn by coloured lines in order to determine more precisely the rank between the three architectures. As in Chapter 4, the solutions with a high flexural stiffness have an Acoustical Transmission Loss following a “mass law”, meaning that flexural stiffness and acoustic damping can increase simultaneously. For these solutions, increasing both Acoustical Transmission Loss and stiffness is possible by increasing core thickness.

The optimal core architecture is the tetrahedral truss core which exhibits a better Acoustical Transmission Loss for a given stiffness. Between foam and honeycomb, the ranking is non-decisive. For high stiffness, honeycomb is a better core architecture as it is stretching-dominated, whereas for higher Acoustical Transmission Loss, of about 60 dB, foam is a better candidate.

The overall shape of the trade-off surface for honeycomb and truss architectures is similar to the one observed in Chapter 4 with a first part corresponding to the “mass law” and the second

one corresponding to a competition between design requirements. The shape of the trade-off surface corresponding to foam core panels is different as it is composed of several regions in which the Acoustical Transmission Loss follows a “mass law”. This difference is partly due to the size limitation which has been reduced from 500 to 200 mm but also to the material selection. In the present approach, Aluminium foams with a low relative density can be considered. Then, they are more weight efficient in flexural stiffness but also relatively soft to exhibit a better Acoustical Transmission Loss than polymeric foams.

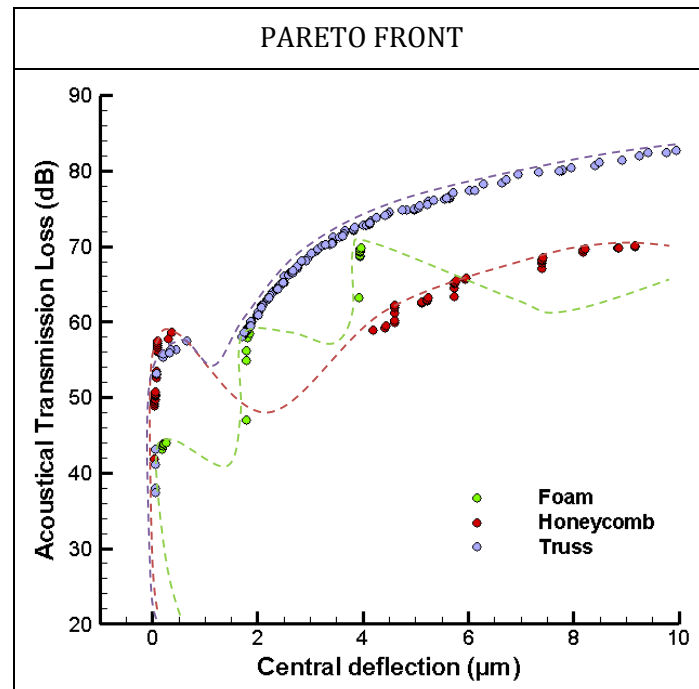


Figure 5.22: Pareto fronts corresponding to the three architectures for flexural stiffness and Acoustical Transmission Loss specifications at a mass of 50 kg/m^2 .

Variability analysis of core design

As shown in Figure 5.23, the optimal foam core sandwich panels are exclusively made of Magnesium as core constitutive material, which is the best candidate for flexural stiffness specifications. Three different relative densities enable to change the trade-off between Acoustical Transmission Loss and stiffness. With a 0.1 relative density foam core, the Acoustical Transmission Loss is of 44 dB and the deflection is of $0.22 \mu\text{m}$. For a 0.03 relative density the Acoustical Transmission Loss increases up to 58.5 dB while the deflection is increased up to $1.8 \mu\text{m}$. The solution made of a 0.01 relative density foam exhibits the best achievable Acoustical Transmission Loss at 69.6 dB but with a deflection of $3.95 \mu\text{m}$.

The performance space corresponding to honeycomb is composed of a group of metal honeycomb solutions and of another one composed of polymeric cores. The group of metal honeycombs represents the solutions with the highest stiffness and an Acoustical Transmission Loss following a “mass law”. It is mainly composed of Molybdenum honeycombs in the Pareto front but a large number of metals are present inside the performance space. Heavy materials are preferred in order to increase inertial effects for acoustic damping. The stiffest solution is characterized by an Acoustical Transmission Loss of 57.5 db and a $0.1 \mu\text{m}$ deflection.

The group of polymeric honeycombs is dominated by PC and PBT solutions. In order to increase the Acoustical Transmission Loss, relative density is decreased from 0.023 at a 52 dB

Optimal design of architected sandwich panels for multifunctional properties

Pierre Leite

Acoustical Transmission Loss to a 0.01 relative density at a 70 dB Acoustical Transmission Loss. The core thickness is at its maximum allowed value. Compared to the results of Chapter 4, only core relative density can be used as a design variable to adjust the trade-off between stiffness and Acoustical Transmission Loss.

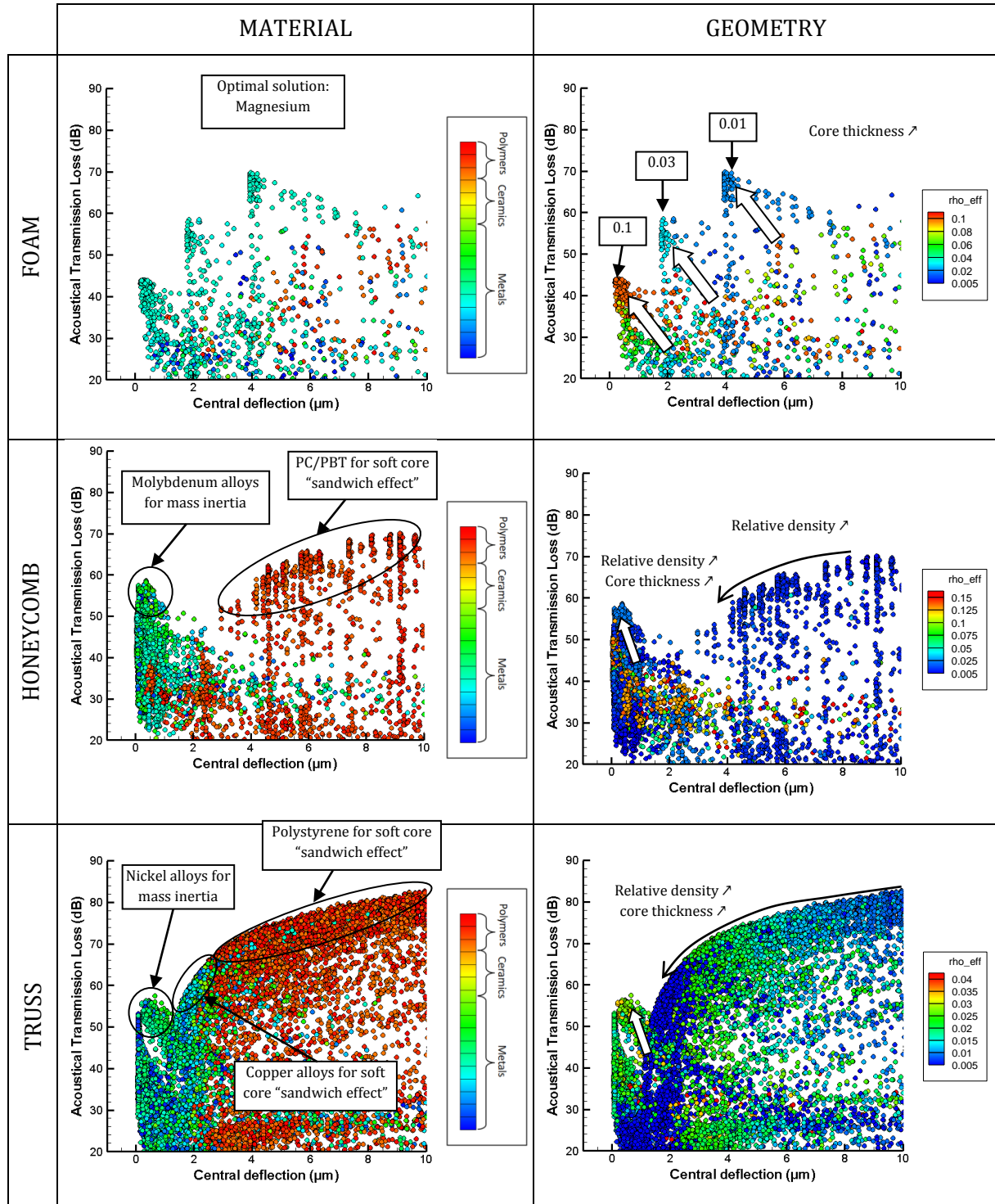


Figure 5.23: Influence of core constitutive material and relative density as a function of core architecture on the flexural stiffness and acoustic damping performances at a mass of 50 kg/m^2 .

The performance space corresponding to truss structure as core material is similar to the one corresponding to honeycomb. A part corresponds to metallic trusses with Nickel alloys as

optimal candidates and is translated into a pointed part of the performance space. The other part corresponds to polymeric trusses with Polystyrene as the optimal solution and results in a convex shape in the performance space. However, in the part where the Acoustical Transmission Loss follows a “sandwich effect, i.e. the convex part, Brasses and Bronzes are also optimal solutions but at a lower Acoustical Transmission Loss than Polystyrene solutions even though there is a continuity between these two kinds of panels in terms of performances. As for honeycombs, the optimal sandwich panel thickness is 200 mm. Then, to tailor the trade-off between the two specifications, in the case of Polystyrene trusses, the relative density varies from 0.025 at an Acoustical Transmission Loss of 66 dB to 0.008 at an Acoustical Transmission Loss of 82.6 dB. The Cu-based truss structures (made of Brasses and Bronzes) that are located on the Pareto front have a relative density of 0.005, which is the minimal value. The trade-off between the specifications is then tailored by changing the alloy.

3.2. A case of disadvantageous competition between specifications: flexural strength and thermal resistance specifications

Design space:

- Face materials: Metals, Polymers, Composites.
- Face thickness: from 0.5 to 5 mm.
- Core materials: Metals, Polymers.
- Core thickness: from 10 to 200 mm.
- Type of sandwich panel: symmetrical.

Objectives:

- Flexural strength: maximize the critical load corresponding to failure of a 1 m span sandwich beam submitted to a three-point bending test.
- Thermal resistance: maximize the through-thickness thermal resistance.
- Lightness: minimize the mass per unit area.

Constraints:

- Flexural strength > 2 kN.
- Thermal resistance > 1 m²K/W.
- Mass per unit area < 50 kg/m².

Comparison between architectures

In Chapter 4, it has been demonstrated that the trade-off surface between flexural strength and thermal resistance specifications is concave. In this chapter, the size constraint has been reduced to 200 mm. The Pareto fronts obtained for the three considered architectures are shown in Figure 5.24. Different concave parts are noticeable. The more weight efficient architecture is the honeycomb, followed by the truss structure. Foam is largely overcome by the stretching-dominated architectures regarding mechanical requirements as shown previously. At high thermal resistance specification, however, the three architectures exhibit similar performances.

Variability analysis of core design

The performance space gives additional information on the differences between the architectures. Indeed, the shape of the performance space for foam and honeycomb is very

Optimal design of architected sandwich panels for multifunctional properties

Pierre Leite

similar even though the achievable flexural strength of honeycomb core solutions is much larger. The shape of the performance space corresponding to truss core panels is slightly different.

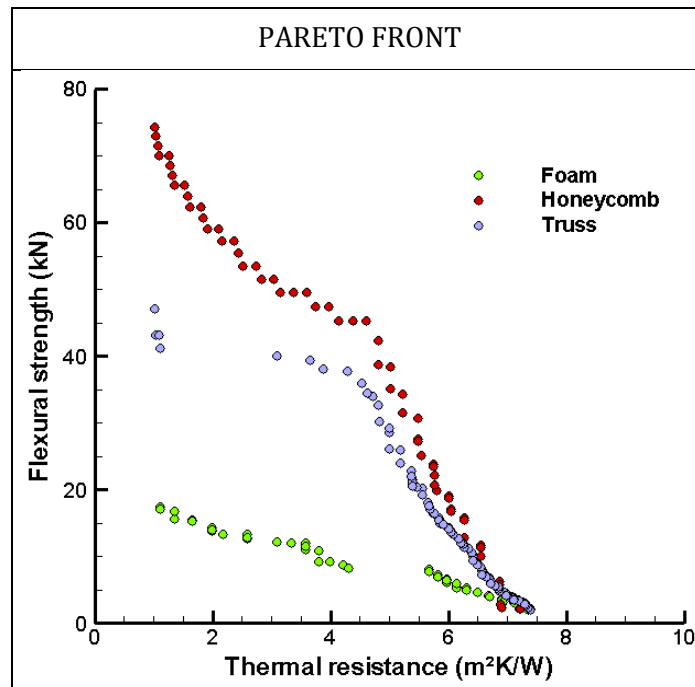


Figure 5.24: Pareto fronts corresponding to the three architectures for flexural strength and thermal resistance specifications at a mass of 50 kg/m^2 .

In terms of material selection, PMMA emerges as the best core constitutive material for both foam and honeycomb architectures. However, for honeycomb core solutions, Polystyrene is competitive at high thermal resistance specifications. The performance space corresponding to truss core structures is composed of two different parts corresponding to two different types of core constitutive materials. A first group, which represents the major part of the trade, corresponds to polymeric trusses with PMMA and Polystyrene as the optimal candidates just like for honeycombs. The second group is made of Titanium truss core sandwich panels. These solutions can exhibit a better flexural strength than polymeric core panels but are limited to low thermal resistance specifications.

The split aspect of the trade-off surface is due to size limitations. For foam and honeycomb core structures, the part of the trade-off surface corresponding to high flexural strength specifications is not limited by size constraint. Then, the variation between strength and thermal resistance along the Pareto front is achieved by increasing core thickness and decreasing relative density, as shown in Figure 5.25, in order to keep the mass of the panel at a constant value. The core thickness corresponding to the highest value of flexural strength is 70 mm for both foam and honeycomb. When core thickness reaches its maximum allowed value, about 190 mm, the only way to increase thermal resistance is by decreasing relative density at a constant core thickness. This mechanism corresponds to the second part of the trade-off surface.

For truss core panels, the situation is different. For each part corresponding to the different core materials, the trade-off surface has a concave shape. But unlike for foam and honeycomb, decreasing core thickness of polymeric core panels does not lead to an increase in strength. To remain at a constant weight, the decrease in thickness should be compensated by an increase in core strength, which is usually achieved by an increase in relative density. In the case of truss

structures, increasing relative density is achieved by both increasing the aspect ratio of the struts and the angle between the faces and the struts. The optimal strength is reached at an angle of approximately 55° , which does not coincide with the maximum value of relative density. In such a case, the optimal relative density corresponding to the maximum achievable core strength is already reached at the maximum core thickness.

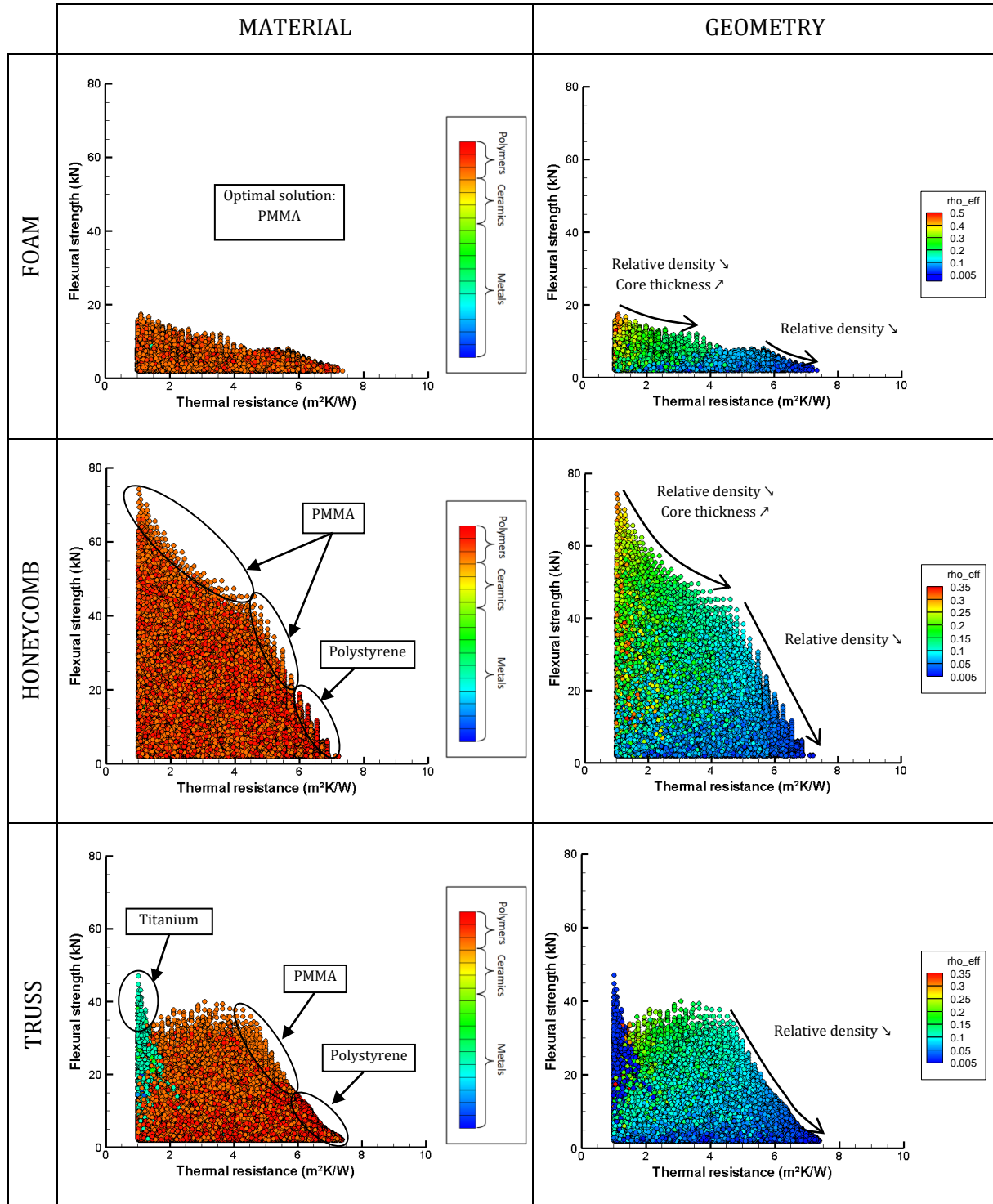


Figure 5.25: Influence of core constitutive material and relative density as a function of core architecture on the flexural strength and thermal resistance performances of the sandwich solutions at a mass of 50 kg/m^2 .

3.3. A case of compatibility between specifications: thermal insulation and blast mitigation specifications

Design space:

- Face materials: Metals, Polymers, and Composites.
- Face thickness: from 0.5 to 10 mm.
- Core materials: Metals, Polymers.
- Core thickness: from 10 to 500 mm.
- Type of sandwich panel: unsymmetrical.

Objectives:

- Thermal insulation: minimize the temperature at the inner face while the outer face is submitted to a 700 °C heat during 1 hour.
- Blast resistance: minimize the normalized back deflection which is the central deflection of the back face normalized by the span of the panel when the panel is submitted to a blast impulse of 2.10^3 Nsm^{-2} .
- Lightness: minimize the mass per unit area.

Constraints:

- Temperature at the inner face $< 140 \text{ °C}$.
- Thermal shock resistance: $\max_{x,t} \left(\frac{\sigma(x,t)}{\sigma_y(x)} \right) < 1$.
- Temperature in the material $<$ maximum service temperature of the material.
- Normalized back deflection $< 0.2 \text{ m/m}$.
- No face failure.
- Mass per unit area $< 100 \text{ kg/m}^2$.

In Chapter 4, an optimization problem involving thermal insulation and blast mitigation specifications has been addressed. No feasible solution emerged from the calculations. The only core materials able to sustain the thermal load were ceramic foams, which are not suited for blast mitigation. However, the performance space has been filled with solutions fulfilling all the constraints except the one on the maximum service temperature. This enabled us to observe the shape of the trade-off surface. The specifications were characterised as compatible as the trade-off surface was composed of a single solution. With the present approach, metals specifically designed for high temperature applications can be used as core constitutive material, leading to high temperature core architectures with potentially interesting blast resistance. The size constraint has been kept as 500 mm and the mass constraint has been set at 100 kg/m^2 .

Comparison between architectures

Ranking the architectures in this case is not obvious. Indeed, they exhibit very close performances as shown in Figure 5.27.

In absolute terms, truss structure overcomes honeycomb and foam in both thermal insulation and blast resistance with an optimal solution characterized by a temperature at the back of the panel of 20.01 °C and a normalized deflection of 2.2 mm/m . Regarding honeycomb, this is a better structure than foam in terms of blast requirements while foam is better than honeycomb for thermal insulation.

The performances of the three architectures may be very close as shown in Figure 5.26 but these values correspond to solutions with a mass per unit area close to 100 kg/m^2 . The influence of the mass constraint is discussed further.

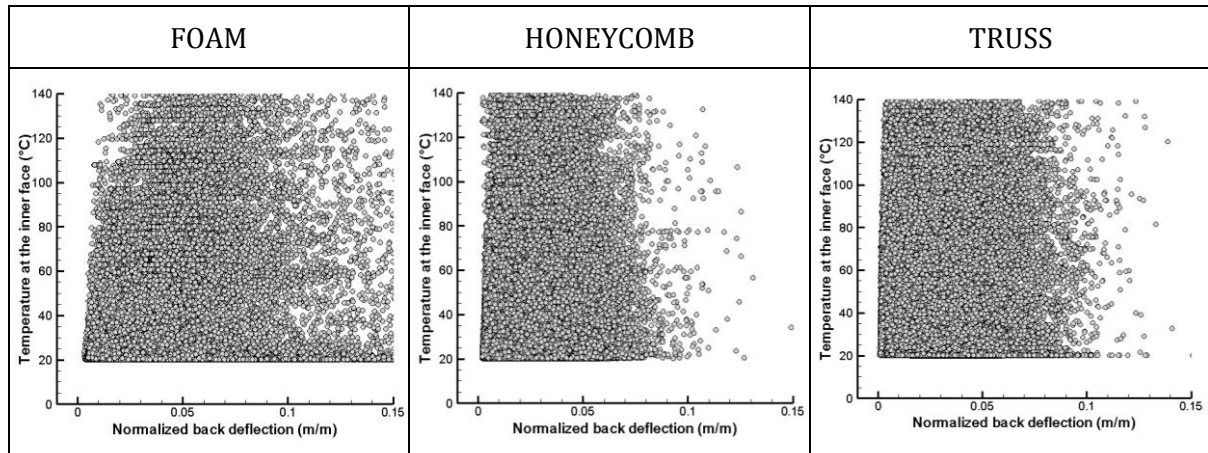


Figure 5.26: Performance space plotting the solutions generated by the optimization algorithm for each core architecture regarding thermal insulation and blast resistance specifications at a mass of 50 kg/m^2 .

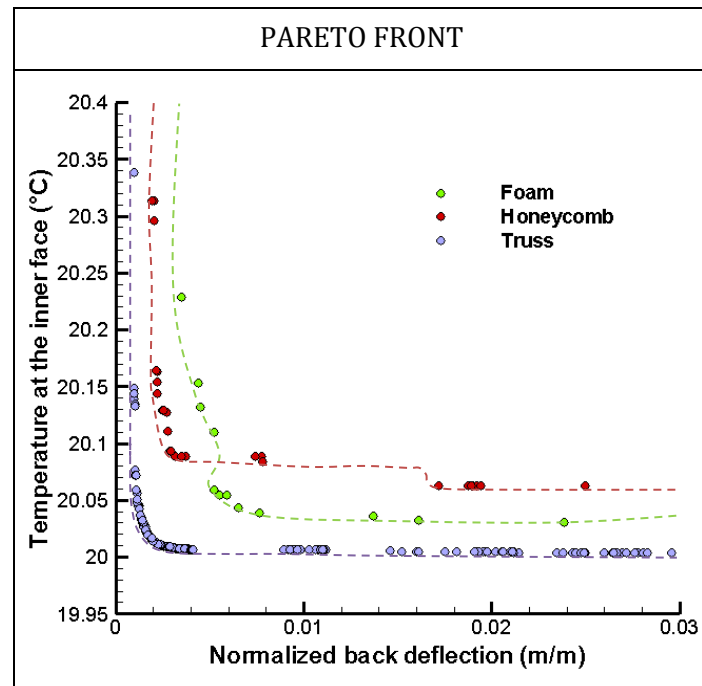


Figure 5.27: Pareto fronts corresponding to the three core architectures for thermal insulation and blast resistance specifications at a mass of 50 kg/m^2 .

Variability analysis of core design

The performance space corresponding to foam core panels is filled by solutions with three main different core constitutive materials as shown in Figure 5.28. For thermal insulation the best material is the Ni-based superalloy IN-100 (see also Section 2.5). On the other hand, the best candidate for blast resistance specifications is the Ni-W alloy MAR-M200. Between these two possibilities, the material which offers the best trade-off is a Ni-based superalloy, Inconel 713. The optimal core relative density is 0.01, even though a relative density of 0.005 can be

Optimal design of architected sandwich panels for multifunctional properties

Pierre Leite

required for blast resistance since an increase of core thickness has a higher impact than an increase of strength.

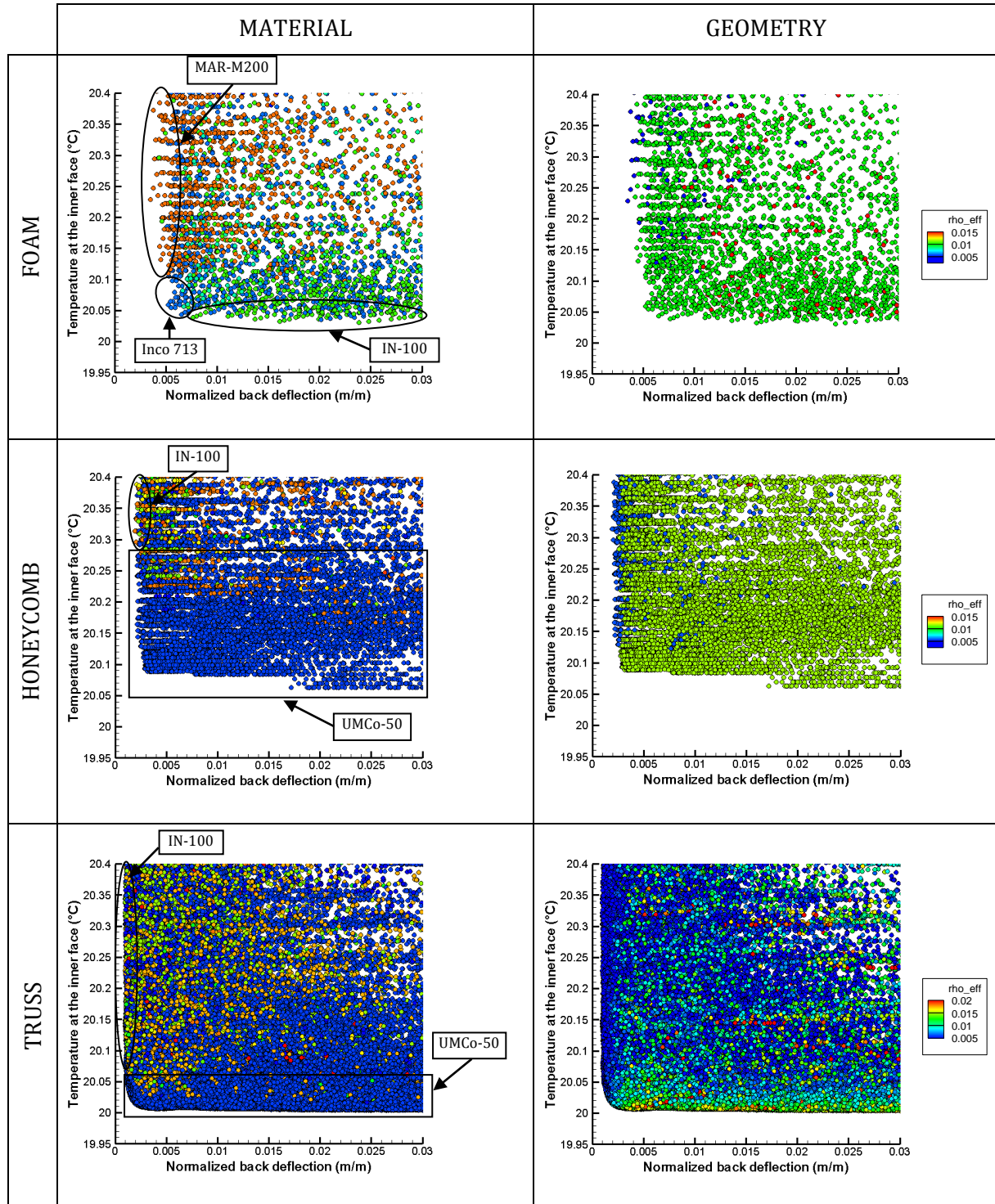


Figure 5.28: Influence of core constitutive material and relative density as a function of core architecture on the thermal insulation and blast resistance performances at a mass of 50 kg/m^2 .

The optimal core constitutive material for a honeycomb core panel is the Co-based superalloy UMCo-50, already identified as optimal solution for thermal insulation in Section 2.5. For a normalized deflection below 0.002, IN-100 shortly overcomes UMCo-50 despite a very tight difference. The optimal relative density is 0.0115 except for very high blast resistance

requirements for which the optimal design is made of honeycomb core with a 0.005 relative density.

The case of truss core solutions is similar to the one of honeycomb structures as the optimal candidate is UMCo-50 except for a temperature above 20.13 °C for which IN-100 is slightly better. Some other materials appear in the performance space such as Inconel alloys or some Stainless Steels but are not on the Pareto front. The optimal relative density varies from 0.005 for blast resistant specifications to 0.015 for thermal insulation ones.

Effect of functional constraints

In Figure 5.29 are plotted several performance spaces corresponding to the different core architectures. A projection of the three dimension performance space is carried out in order to assess the impact of the multiple specifications on the optimal design at minimal weight. In the first column, the solutions are given as a function of their mass and blast performance. The colour legend gives information on the influence of the thermal insulation specification. All the available solutions in this performance space do satisfy to the thermal insulation constraint. The second column, on the other hand, provides the solutions as a function of mass and thermal performance with a colour legend corresponding to the blast performance. All the solutions contained in these spaces satisfy to the blast resistance constraint. For a comparison, the unconstrained trade-off surface is also plotted in these figures.

For foams with a mass of about 100 kg/m², the impact of thermal specifications on the blast resistance is negligible. But below this value of mass, the blast resistance is quite affected. For example, for a mass of 60 kg/m², the deflection over half-length passes from 0.0031 to 0.042. While the mass constraint remain above 60 kg/m², the sandwich panel follows a behaviour in blast loading in which core does not reach densification strain. In this case, the thermal performance is not too much reduced as the temperature at the back of the panel is 54 °C in the case of a 60 kg/m² panel with a normalized deflection of 0.042 m/m. For a mass below 60 kg/m², the thermal performance is more dramatically reduced even though it remains below the set constraint. This mass value marks the transition between two blast mitigation behaviours. Above, the optimal panel is made of a thick Stainless Steel foam core which does not reach densification strain. Below, the optimal panel is made of a thin MAR-M200 foam core which reaches densification during core crushing.

The performance space of thermal performance as a function of mass is composed of two parts corresponding to two different core materials. The first group is dominated by solutions made of IN-100 foam core and corresponds to the best thermal insulating panels. The solutions of this group are characterized by thermal and mass properties close to the ones of the unconstrained problem. However, for a mass between 60 and 70 kg/m², the normalized deflection of the solutions on the Pareto front is quite high. The second group is composed of solutions made of UMCo-50 foam. The transition between the two groups occurs at a temperature of 36.6 °C and a mass of 60 kg/m². These solutions exhibit a medium blast resistance with a normalized deflection around 0.08. There is no feasible solution with a mass below 24 kg/m².

For honeycombs, the influence is less dramatic. The blast resistance is notably affected only for a mass below 85 kg/m². Until a mass of 57 kg/m², the thermal performances of the optimal solutions are still qualified as good with a temperature of 40 °C. At this point, the optimal normalized deflection is 0.015. Below this mass value, the thermal performances decrease until the lightest possible solution appears at a mass of 33.6 kg/m², a temperature of 135 °C and a

Optimal design of architected sandwich panels for multifunctional properties

Pierre Leite

normalized deflection of 0.07 m/m. For a comparison, for this value of normalized deflection, the lightest unconstrained solution was at 22 kg/m². This performance space is dominated by three different core materials. For a mass between 100 and 75 kg/m², the optimal core material is a IN-100 honeycomb with a relative density of 0.005. For a mass between 75 and 56 kg/m², a Stainless Steel dominates other materials while for a mass under 56 kg/m², the IN-100 with a relative density of 0.01 is again the optimal material.

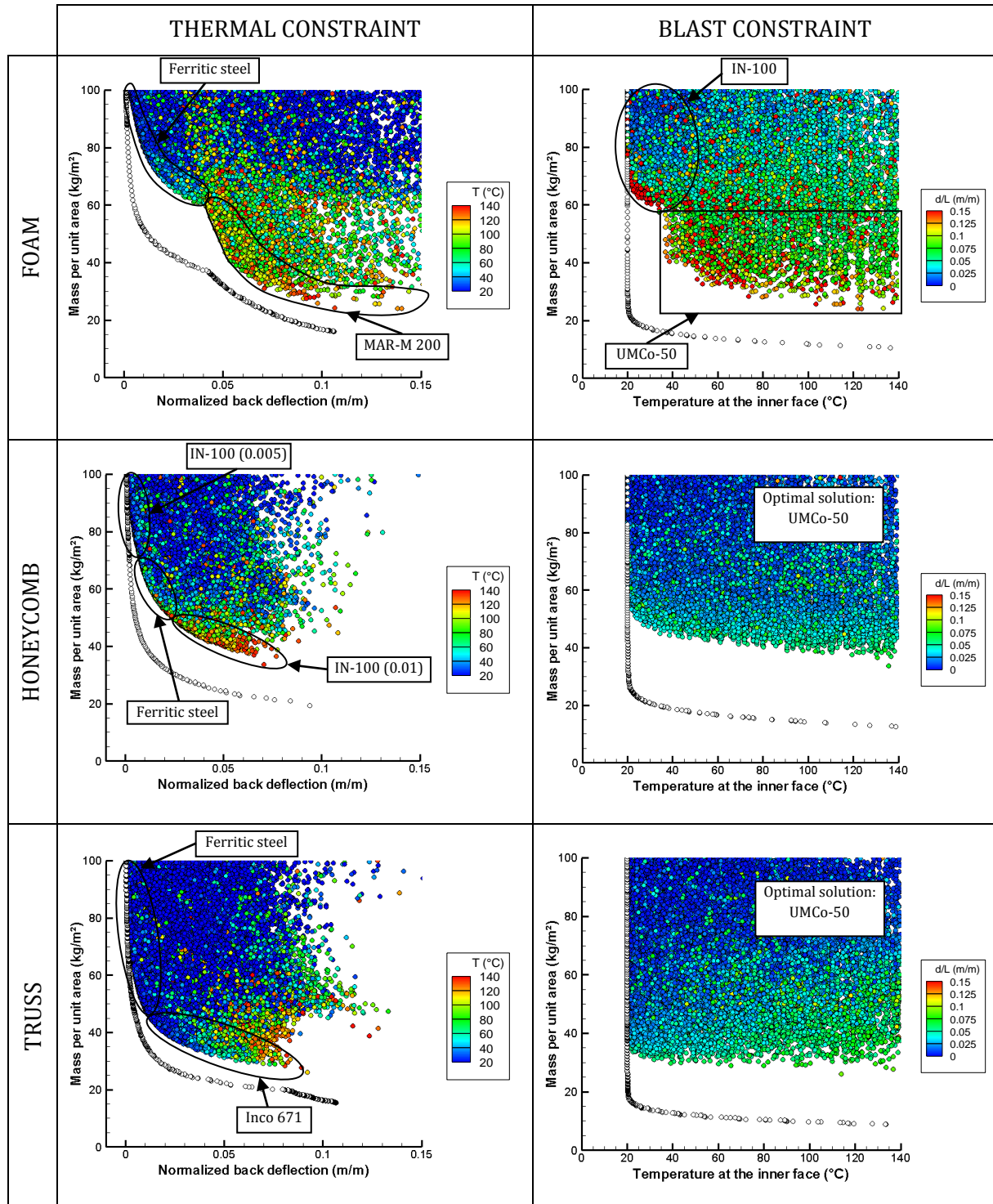


Figure 5.29: 2D performance spaces. These projections of the 3D performance space are used to assess the impact of the multiple criteria on the optimal design at minimal weight regarding each performance. The unconstrained Pareto fronts are also plotted as a comparison.

Regarding the thermal performances at minimal weight, the blast specifications mainly impact the minimal achievable mass which passes from 12.8 to 33.6 kg/m². The performance space is dominated by UMCo-50 honeycomb core solutions.

The behaviour of truss structure is similar to the one of honeycomb. The blast resistance at minimal weight is affected as the mass specification reaches 68 kg/m². For example, at a normalized deflection of 0.08, the mass passes from 20.1 kg/m² for the unconstrained problem to 28.2 kg/m² in the present case. The thermal performance of the optimal solutions can be qualified as “good”, even at a mass of 31 kg/m² and a normalized deflection of 0.057, and a temperature at the back of the panel of 44 °C.

The thermal performance at minimal weight is not affected except that the minimal achievable mass passes from 9.2 kg/m² to 26 kg/m² by adding the blast constraint. The performance space is dominated by UMCo-50 truss core panels.

Let us remind that UMCo-50 has been identified as the optimal core material for thermal insulation applications in Section 2.5.

3.4. A case of incompatibility between specifications: Acoustical Transmission Loss and blast mitigation specifications

To be consistent with the results previously presented for blast resistance, the optimization problem involving blast resistance and Acoustical Transmission Loss as objectives is treated by considering a size constraint of 500 mm and a peak pressure of 10 MPa for the blast load.

Design space:

- Face materials: Metals, Polymers, and Composites.
- Face thickness: from 0.5 to 10 mm.
- Core materials: Metals, Polymers.
- Core thickness: from 10 to 500 mm.
- Type of sandwich panel: unsymmetrical.

Objectives:

- Acoustic damping: maximize the mean value of the Acoustical Transmission Loss in the frequency range [1 000; 4 000] Hz.
- Blast resistance: minimize the normalized back deflection which is the central deflection of the back face normalized by the span of the panel when the panel is submitted to a blast impulse of 2.10³ Nsm⁻².
- Lightness: minimize the mass per unit area.

Constraints:

- Acoustical Transmission Loss > 20 dB.
- Normalized back deflection < 0.2 m/m.
- No face failure.
- Mass per unit area < 50 kg/m².

Comparison between architectures

Ranking the three architectures in terms of blast resistance and Acoustical Transmission Loss specifications is tricky. As in Chapter 4, the performance space is composed of two blocks, one

Optimal design of architected sandwich panels for multifunctional properties

Pierre Leite

gathering the blast resistant solutions, the other one gathering the solutions with a high Acoustical Transmission Loss. Only the performance space corresponding to honeycomb core solutions is composed of one block, which is the one gathering blast resistant solutions. Architectures should be compared regarding both specifications separately.

Concerning Acoustical Transmission Loss, truss structure is the best candidate by exhibiting an Acoustical Transmission Loss of 92.8 dB for a normalized deflection of 0.07 m/m as shown in Figure 5.30. Foam core panels are competitive for a good Acoustical Transmission Loss but result in a less attractive blast resistance. On the contrary, honeycomb core solutions are limited to an Acoustical Transmission Loss of 59.3 dB at a normalized deflection of 0.048 m/m.

Regarding blast resistance, truss structure is also the best candidate as the minimum normalized deflection achieved by truss core panels is 0.015 m/m while the best value reached by a honeycomb core solution is 0.019 m/m, against 0.038 m/m for foam core panels. However, for an Acoustical Transmission Loss between 46 and 60 dB, honeycomb core solutions are better than truss core ones with a deflection over half-length after blast varying between 0.019 and 0.066 m/m. Foam is overcome by both truss structure and honeycomb regarding blast resistance with a normalized deflection limited to 0.038 m/m corresponding to an Acoustical Transmission Loss of 57.5 dB.

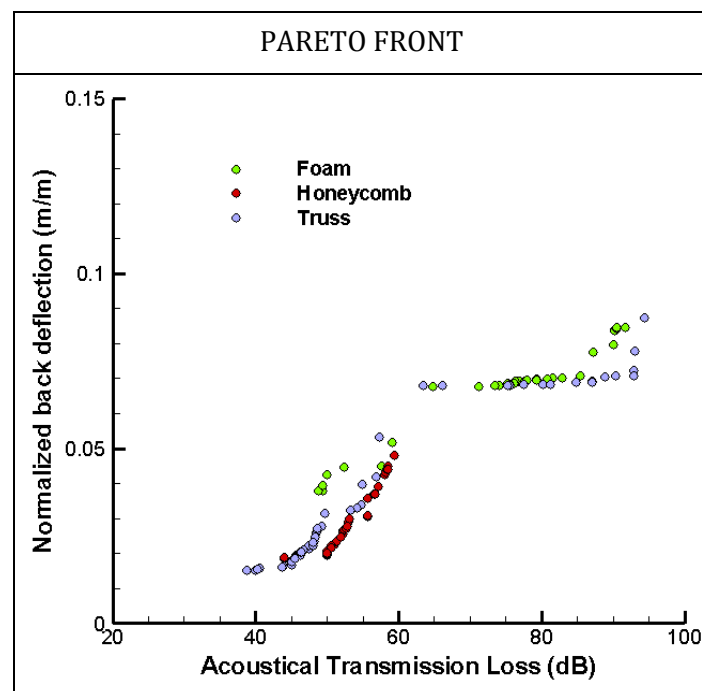


Figure 5.30: Pareto fronts corresponding to the three core architectures for blast resistance and Acoustical Transmission Loss specifications at a mass of 50 kg/m^2 .

Variability analysis of core design

The performance space of each architecture is shown in Figure 5.31 as a function of core constitutive material and of core relative density. In regard to foam, two main materials emerge as optimal depending on the trade-off between the specifications:

- For blast resistant solutions, Aluminium is the optimal candidate as demonstrated in Section 2.6. The optimal relative density of Aluminium foam for blast resistance is 0.02.

- On the other hand, for a good Acoustical Transmission Loss, Polyethylene foam is the best choice as emphasized in Section 2.3. The optimal core relative density is then 0.005.

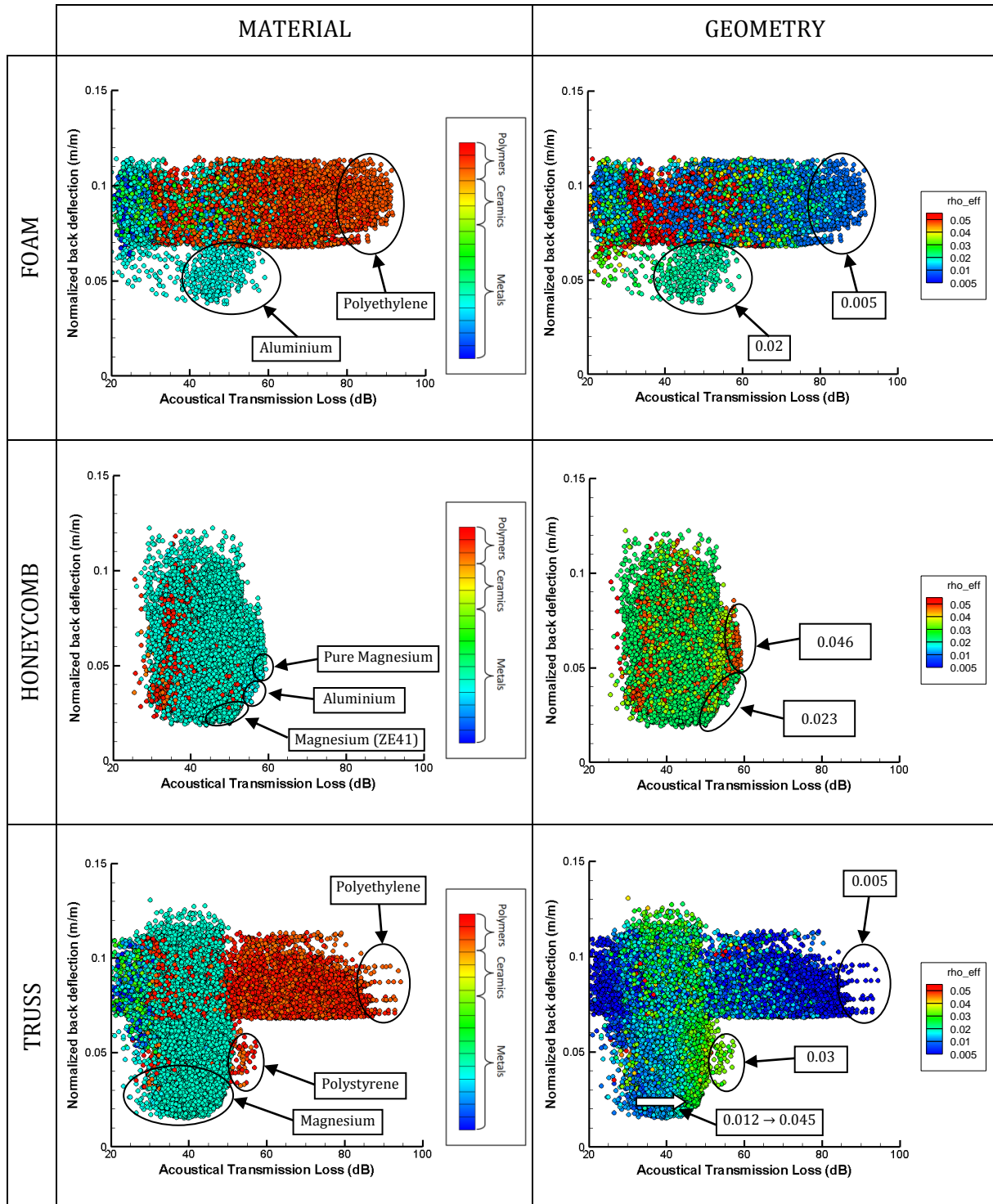


Figure 5.31: Influence of core constitutive material and relative density as a function of core architecture on the Acoustical Transmission Loss and blast resistance performances at a mass of 50 kg/m².

The performance space of honeycomb core panels is only composed of one block filled by blast resistant solutions. In Section 2.6, Magnesium was found to be the optimal core constitutive material. For the present specifications, Magnesium is still on the trade-off surface but so does

Optimal design of architected sandwich panels for multifunctional properties

Pierre Leite

Aluminium. In the range 52.8 to 58 dB of Acoustical Transmission Loss, which corresponds to a normalized deflection of 0.029 and 0.043 m/m respectively, the solutions on the Pareto front are made of Aluminium honeycombs as core part. For best blast resistant solutions, the optimal core material is pure Magnesium and for better acoustic damping solutions, the better candidate is a Magnesium alloy (ZE41). Except for pure Magnesium honeycombs, the optimal relative density is 0.023. For pure Magnesium core solutions, it is twice this value.

The case of truss core panels is similar to the one of foam core solutions: the performance space is constituted of two blocks, one for metal core blast resistant solutions and the other one for polymeric core sound insulating panels. But an additional group of solutions has emerged and the performances achieved by truss core panels are better than the one achieved by foam core panels.

- The group of blast resistant solutions gathers Magnesium truss core panels with a relative density between 0.012 and 0.045, which is consistent with the results of Section 2.6.
- The group of sound insulating solutions are principally dominated by Polyethylene truss core structures of 0.005 relative density.
- Contrary to foams, an intermediate group of solutions has emerged and is composed of Polystyrene truss core panels with a core relative density around 0.03.

Truss structures take great advantage of the possibility to tailor the ratio between stiffness and density by changing the angle between struts and faces. The higher the angle is, the stiffer the structure is (in the transverse direction). Actually, the optimal angle value for blast resistance is 55° while for Acoustical Transmission Loss it is 35°.

4. Overview of the results of multi-objective design by “virtual path”

By using a “virtual path” approach, an objective classification between three different architectures is possible. These architectures are representative of the different architected materials that can be used as core with a stochastic bending-dominated architecture, the foam, a 2D extruded pattern, the honeycomb, and a 3D stretching-dominated architecture, the tetrahedral truss structure. These three architectures have different advantages and drawbacks and are then dedicated to different applications. The results obtained in Section 2 are summarized in Table 5.1. When soft core is required, which is the case for acoustic damping, bending-dominated structures are better than stretching-dominated ones at a given weight. On the contrary, when good mechanical properties are required, like for stiffness, strength or blast resistance, stretching-dominated are the optimal choice. The case of thermal insulation is particular as the constraint on the thermal shock resistance is a mechanical constraint.

In some instances, core constitutive material selection can be performed by using a performance index approach adapted to the core architecture. For mechanical specifications, the performance indices corresponding to ties or beams can be used. For bending-dominated architectures, the beam is considered as submitted to bending, such that the performance index is the one for stiff beams in bending at a minimal weight. For stretching-dominated, the argument is the same considering a tie in tension. However, for blast resistance no performance index has been found.

As already mentioned in the previous chapter, performance indices are perfectly suited for simple applications. When complex behaviours are involved, a more refined method such as the present one is required.

Table 5.1: Results overview of optimizations that include mass reduction and one other objective. For each case, ranking between the core architectures is set. The corresponding optimal constitutive material is given from the most efficient one to the lightest one. The topology of the optimal local loading (bending or stretching) is also given. In the last column are referenced the performance indices that could be used for core material selection for each architecture. NA indicates that no ranking has emerged.

Function	Ranking	Optimal core material	Optimal local loading	Corresponding PI
Stiffness	1) Honeycomb 2) Truss 3) Foam	- Cr/Al/Mg - Cr/Al/Mg - Mg	Stretching	- E/ρ - E/ρ - $E^{1/2}/\rho$
Strength	1) Honeycomb 2) Truss 3) Foam	- Al - Steel/Ti/Al - Al	Stretching	- σ/ρ - σ/ρ - $\sigma^{2/3}/\rho$
Acoustic damping	1) Foam 2) Truss 3) Honeycomb	- MDPE - MDPE - MDPE	Bending	$1/E$
Thermal resistance	NA	PP/PS	NA	$1/k\rho$
Thermal insulation	1) Truss 2) Foam 3) Honeycomb	- UMCo-50 - UMCo-50 /IN-100 - UMCo-50	Stretching	$1/a\rho$
Blast mitigation	1) Truss 2) Honeycomb 3) Foam	- Mg - Mg - Al	Stretching	-

The case studies chosen in Chapter 4 to illustrate the optimal design at minimal weight for multiple functions have been treated in this chapter using a “virtual path” approach. In a general manner, the shape of the Pareto fronts is not dependent of the architecture. The only exception is the honeycomb core sandwich panel designed for blast resistance and Acoustical Transmission Loss.

The ranking between architectures as well as the optimal core constitutive materials are given in Table 5.2 for each case. In some instances, an optimal solution emerges but the ranking of the two others changes as a function of the performances. For each performance is associated its second best solution.

Truss structure is not far from being the top architecture for every case. This is mainly due to the fact that its topology is defined by two parameters. Then, the range of properties that can be reached in a controlled manner by a truss structure is wider than for a foam or a honeycomb. In particular, the angle ω between the faces and the struts can be used to pass from a very stiff material in the out-of-plane direction (as close as possible to 90°) to a very soft one (as close as possible to 0°). This is why in some instances the truss structure is close to a honeycomb one and in some others it is close to a foam one.

Optimal design of architected sandwich panels for multifunctional properties

Pierre Leite

Table 5.2: Results overview for optimal design with multiple functions. For each case, ranking between the core architectures is set. The corresponding optimal constitutive material is given.

Functions	Ranking	Optimal core material
<i>Stiffness and acoustic damping</i>	1) Truss Stiffness → Honeycomb Acoustic damping → Foam	- Ni/Cu/PS - Mo/PC/PBT - Mg
<i>Strength and thermal resistance</i>	1) Honeycomb 2) Truss 3) Foam	- PMMA/PS - Ti/PMMA/PS - PMMA
<i>Thermal insulation and blast mitigation</i>	1) Truss Thermal insulation → Foam Blast mitigation → Honeycomb	- UMC0-50/IN-100 - IN-100/Inco713/MAR-M200 - UMC0-50/IN-100
<i>Acoustic damping and blast mitigation</i>	1) Truss Acoustic damping → Foam Blast mitigation → Honeycomb	- MDPE/PS/Mg - MDPE/Al - Mg/Al

A comparison can be made between the “real” and “virtual path” approaches as foam core sandwich panels have been treated by the two methods. Table 5.3 summarizes the results in terms of material selection for each optimal design at minimal weight for a single function. There is no coincidence between the results obtained by a “real path” approach and those obtained by a “virtual path” one. This could be explained by two different points.

First, the foams contained in the materials database are mainly polymeric. On the contrary, the number of 85 metallic materials considered as constitutive materials for the “virtual path” approach largely exceeds the one of polymeric materials (16 polymers). As a consequence, metal foams can be considered as not sufficiently represented in the database for the “real path” approach while polymers are not sufficiently represented for the “virtual path” approach.

The second point is that, in some cases, the used scaling laws are not appropriate. For instance, the scaling law giving the plateau stress of foams corresponds to a plastic behaviour while many polymeric foams have an elastomeric behaviour. This can be a cause of error in the effective properties of the architected materials which could be greater for a given type of core material.

In some cases, optimal results obtained by “virtual path” exhibit better performances than the optimal results obtained by “real path”. This occurs when the calculated virtual material corresponding to the optimal solution is not listed in the database. On the contrary, optimal results obtained by “real path” can exhibit better performances than the optimal solutions obtained by “virtual path” when the constitutive material of the optimal “real” solution is not in the database as constitutive material for “virtual” materials.

The “virtual path” approach becomes really effective if every possible constitutive material is taken into account. Among the possible materials that have not been taken into account in the present work, one can mention:

- Phenol like for Phenolic foams.
- Melamine like for Melamine foams.
- Impregnated paper like for honeycombs.

These materials have not been taken into account because they cannot be processed as trusses for a truss structure, then the comparison between architectures could have been disadvantageous for the truss structure.

Table 5.3: Comparison between the real and virtual path approach for material selection. For each case of optimal design at minimal weight for a single function, the optimal constitutive material of the foam core is given for the real and virtual path.

Function	Real path	Virtual path
Stiffness	Glass/PVC	Mg
Strength	PVC/PMACR	Al
Acoustic damping	PUR	MDPE
Thermal resistance	Phe/PUR/Mel	PP/PS
Thermal insulation	Graphite	UMCo-50/IN-100
Blast mitigation	PE/PS/PVC	Al

In general, whether it is for single or multiple functions, the design guides obtained in Chapter 4 for the face sheets and core thickness are still valid whatever the architecture is. The only exception is the value of the optimal core thickness when Acoustical Transmission Loss is an objective. Indeed, as shown in Figure 5.12, the optimal core thickness depends on the stiffness of the core architecture. Foams being softer than honeycombs and truss structures, its corresponding optimal core thickness is lower than the one for honeycombs and truss structures.

The advantage of using scaling laws is that they are convenient to run the calculations. The main critical point is that the error made on the effective properties could lead to false results, especially in the ranking of architectures. In order to overcome this difficulty, additional results should be produced to confirm the ranking and the calculated performances. For example, a few numbers (three or four) of solutions from the Pareto fronts could be selected and Finite Element Modelling could be used to assess with more precision the desired performances. And, *in fine*, an experimental investigation has to be performed to validate the optimal solutions.

To conclude, the results obtained using a “virtual path” approach depends dramatically on the materials present in the database. For example, theoretically, the optimal core constitutive material for mechanical applications could have been reinforced polymers. However, the manufacturing process of foam or truss structures made of reinforced polymers still remains a critical issue. Nevertheless, a generalized performance index approach gives information on the type of properties required for the considered functions depending on the local loading. It should be pointed out that the results of an optimization process depend on the design space.

Chapter 6

Improvement of the optimization process: mixed methods

The design process used in the previous chapters exploits simple convenient models to evaluate the performances of the solutions generated by the genetic algorithm. However, more accurate models should advantageously be used if the design process directly concerns industrial applications. Nevertheless, the computational cost of such models appears to be incompatible with the computational cost of the present design process. Then, mixed methods should be relevant to tackle this issue.

This chapter aims at giving some perspectives in order to improve the design process. In Section 1, the value of mixed methods in a general manner is discussed. Two different approaches, inspired by principles of materials science, are presented and tested on a case study.

The first approach, presented in Section 2, tends to couple a Branch & Average approach (inspired from the Branch & Bound algorithm) with the genetic algorithm in order to take advantage of the particularity of the design space with the idea that materials can be classified in an arborescence.

In a second approach, Design Of Experiments is used to create an approximated performance index built from numerical simulations.

A conclusion on the effectiveness of such approaches closes this chapter.

Chapter contents

1. Value of mixed methods	221
1.1. Link between optimization method, analysis and models complexity	221
1.2. Behaviour of the genetic algorithm – presentation of a reference case.....	223
2. Coupling genetic algorithm with a branch and average approach	226
2.1. Principles: branch-average-rank-select-delete.....	226
2.2. Mixed method applied to the reference case.....	228
2.3. Mixed method applied for the design of sandwich panels for stiffness and acoustic damping at minimal weight.....	232
2.4. Conclusion/Recommendations	235
3. Using Design Of Experiments to create performance indices	236
3.1. Determination of the approximated performance index.....	236
3.2. Using approximated performance index for the design of sandwich panels for stiffness and acoustic damping at minimal weight.....	238
3.3. Conclusion/Recommendations	240
4. Conclusion on the value of mixed methods	240

1. Value of mixed methods

1.1. Link between optimization method, analysis and models complexity

So far, a multi-objective problem involving material selection and geometrical design has been solved by using a genetic algorithm. Now, one of the main difficulties was to deal simultaneously with discrete and continuous variables. Moreover, the goal was to obtain the trade-off surfaces in order to assess the compatibility between performances and to determine some guidelines based on the analysis of the performance space. Only a Pareto set approach seemed to be relevant to achieve this goal. MOGA has been used as the optimization algorithm, being particularly suited for this kind of problems. However, one of the main difficulties with MOGA and genetic algorithms in general is that a large number of evaluations is required in order to converge to the Pareto front.

A summary of the performances of the genetic algorithm (number of evaluations, number of generations, population size, etc...) on the cases presented in Chapters 4 and 5 is given in Appendix B. The number of evaluation which is needed to converge ranges from about 8000 to more than a million. For that reason, the models that have been used for the calculations are simple ones. These are based on analytical developments or in the case of thermal insulation on a 1D finite difference scheme. The computing time needed to solve one problem is very short. The most sophisticated analyser is the PIAMCO software which needs about 30 seconds to give an answer. The aim of this chapter is to explore simple ways to improve the optimization process. The design problems considered here are treated in a “real path”, i.e. with an explicit database of materials.

In order to increase the model and analysis complexity, optimization complexity should be reduced. As stated by Venkataraman and Haftka, due to limitations in computer power, complexity of model, analysis and optimization method in an optimization problem are linked, as shown in Figure 6.1 [VEN04]. Basically, if high complexity of one of these three components is required, the complexity of the two others should not be too high in order to obtain a satisfactory computing time.

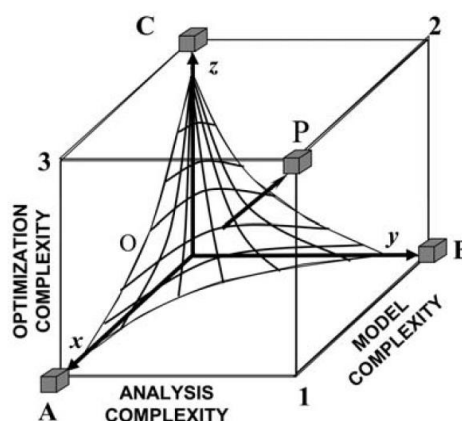


Figure 6.1: Venkataraman and Haftka represent the relationship between optimization, analysis and model complexity towards a plot in which each axis corresponds to one of the aforementioned domain. The limitations in computational capacity imply that any structural optimization problem can be placed on a surface in which, increasing the complexity on one direction requires a reduction in the two other directions. Figure taken from [VEN04].

Based on the applications that are in the scope of the present study, more refined models and analysis could be necessary. More specifically, Finite Element Modelling could be used to obtain more accurate results regarding the mechanical performances of the sandwich panels (flexural stiffness and strength, but also blast resistance and thermal shock resistance). This means using 3D modelling in a non-linear analysis. According to Venkataraman and Haftka, it is the worst case in terms of model and analysis by resulting in the most complex one. Such an analysis can last hours to be performed, and even weeks. Compared to the computing time of the analysis used in Chapters 4 and 5 (between one second and half a minute), this would lead to a dramatic increase of computational cost. Then, the number of evaluations needed to converge would have to be reduced to its minimum. My objective is to reduce the computational cost of the optimization process without reducing its complexity. The present chapter gives some examples of methods that can be beneficial in that way. However, our claim is not to make a complete review of all the possible manner for reducing the computational cost of the optimization process.

Three different tracks can be explored:

1. Reducing the size of the design space.
2. Modifying the optimization algorithm.
3. Improving the analysis tools by using surrogate models.

1. In terms of material selection, filtration methods can be used to reduce the number of materials considered in the design space. As presented by Giaccobi et al., it is possible, by using simple expressions as performance indices, to express the constraints of the optimization problem as a function of the free variables of the design problem [GIA10]. Then, solving the system of equations gives the bounds of materials that fulfil the requirements and that should be considered as potential materials. This method can be used for monolithic solution design but also for multi-material design.

Filtration methods have not been investigated here. However, in order to save substantial computing time, the analysis tools were ranked. This means that the less expensive models in terms of computing time are run first. At any time, if a constraint is violated, the calculations stop. The objective functions of the solution are given penalty values which ensure that the solution is not in the performance space.

2. Improving the optimization algorithm can be achieved by two means. First, an appropriate calibration of the algorithm can improve its efficiency. This can be obtained by refining the optimal population size, cross-over and mutation rates and other typical parameters of the genetic algorithm. As these optimal values depend on the case that is treated, no great efforts have been made to find them, even though they can have a significant importance. They have mainly been chosen in order to ensure the representativeness of the calculation. In some cases, genetic operators can also be modified in order to incorporate the working knowledge of the user. The efficiency of this approach depends on the match between the solved problem and the additional modifications. LeRiche and Haftka successfully modified a genetic algorithm for the optimal design of composite laminates at a minimum thickness [LeR94].

Second, it can be achieved by coupling the genetic algorithm with another optimization algorithm. Several coupling can be considered. A coupling between stochastic and deterministic algorithms can provide interesting results in dealing with discrete and continuous variables. A coupling between two stochastic algorithms can also be used in a

strategy where one of the algorithms performs a global search while the other one is focused on a local area of the design space [HEI12]. A particular approach, inspired from the Branch & Bound algorithm, is proposed in Section 2 of this chapter.

3. Finally, the last track is by modifying the analysis. If it is possible to obtain a high-fidelity analysis with a very short computing time, there will be no need to reduce the number of evaluations of the genetic algorithm. This is the field of surrogate based models. The main idea is to transfer the computational efforts on building an approximated model which is often analytical. Once obtained, this model gives very quick and rather accurate results. There are many ways to determine a surrogate model. Among them, one can mention the kriging approach, the neural networks or the polynomial reduction.

Similarly, an interesting approach has been proposed by Castillo et al. [CAS09]. Using Design Of Experiments (DOE) techniques, the authors determined an approximated performance index. This explicit analytical expression, built from Finite Element Modelling, gives a direct link between materials properties and the performance required.

Based on their work, an example is given in Section 3 of this chapter. An approximated performance index is determined and introduced as a fitness assessor by the genetic algorithm in a multi-objective design problem.

1.2. Behaviour of the genetic algorithm – presentation of a reference case

Presentation of the reference case

In some applications, such as thermal protection systems for spacecrafts, the external panel can experience a severe increase in temperature at one side of the panel while the other side should remain at an acceptable temperature. The main issues are that the induced thermal gradient causes thermal stresses to appear. In addition to protect from heat, the panel should be designed in order to preserve its mechanical performances. Let us then consider an unsymmetrical sandwich panel of length L , height l and thickness b , submitted to an increase in temperature of 1 600 °C at one side. The objectives of the optimization problem are threefold: the minimization of the temperature at the back of the panel after 180 seconds, the minimization of the thermal stress and the minimization of the panel thickness.

The objective functions to minimize are:

- $T(x = b; t = t_{end})$, the temperature at the inner face of the panel.
- $\max_{\forall x, \forall t} \left(\frac{\sigma(x, t)}{\sigma_y(x)} \right)$, the maximum ratio between stress and yield strength in the material.
- b , the total thickness.

And the constraints are:

- $\max_{\forall x, \forall t} \left(\frac{\sigma(x, t)}{\sigma_y(x)} \right) < 1$.
- $b < 35$ mm.

Design space

In the present case, honeycomb materials have been added in the database as possible core material. A number of 85 different honeycombs, metallic, polymeric and organic ones, have been added to the 107 referenced foams. All types of face materials have also been taken into account.

Optimal design of architected sandwich panels for multifunctional properties

Pierre Leite

This includes metals, polymers and composites but also ceramics and natural materials for a total of 166 different possibilities.

Face thickness can vary from 0.1 to 4 mm while core thickness is included between 2 and 25 mm.

Results

The optimization process took 780 328 evaluations and 199 generations to converge to the trade-off surface shown in Figure 6.2. The colour legend on the left hand side of Figure 6.2 corresponds to the core material. Only two different possibilities have emerged: carbon and graphite foams. The optimal face material is a ceramic sheet, made of carbon or graphite. A projection of this trade-off surface on the plane by plotting the temperature at the back of the panel as a function of the total thickness is also given in Figure 6.2, with the contour values of the thermal shock resistance displayed in a colour scale. The relation between the back temperature and the total thickness is translated into a convex shape. For a given temperature, decreasing the ratio between stress and yield strength involves an increasing total thickness of the panel. Let us note that the best obtained design in terms of thermal insulation results in a moderate increase of the back temperature of 10 °C.

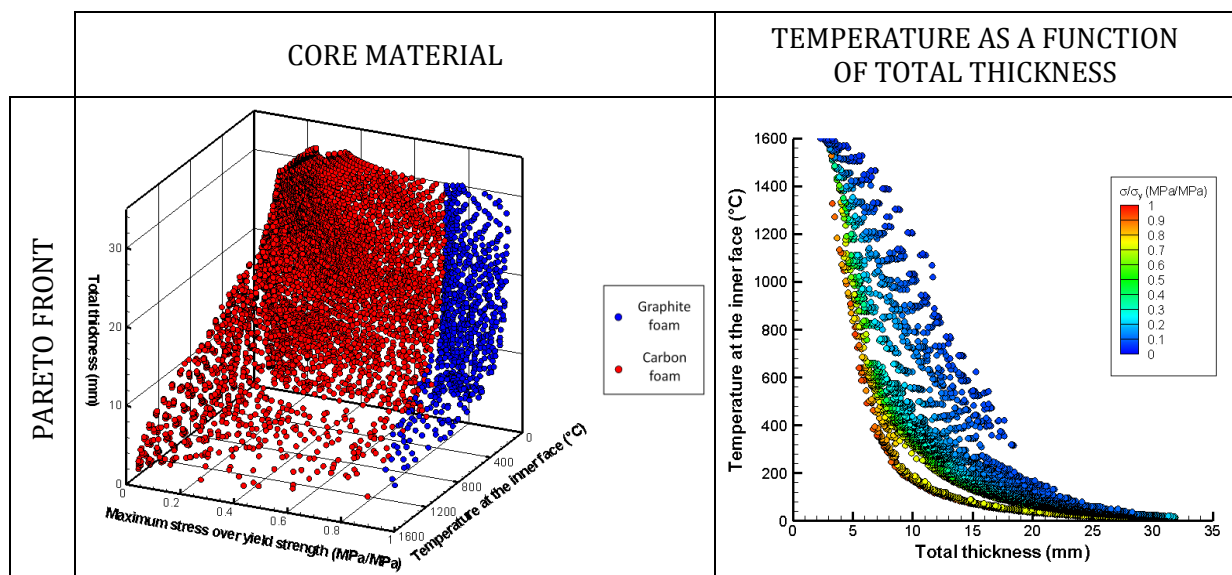


Figure 6.2: Pareto front between the temperature at the back of the panel, the ratio between maximal stress and yield strength and total thickness. On the left hand side: 3D view with colour legend representing the core material. On the right hand side: projection of the Pareto front with the temperature as a function of the total thickness. The colour displays the contour value of the ratio between maximal stress and yield strength.

Analysis of the optimization process

The feasible region of the design space is very small. Only two core materials out of the 192 possible ones are present in the feasible performance space. During the exploration stage, the genetic algorithm has to detect this feasible region. In Figure 6.3, the evolution of the number of individuals on the population is drawn. This curve can be divided in two different parts, a decrease in the population size until the 37th generation followed by an increase.

- In the first generations, no feasible solution has been detected. The first feasible solution emerged at the 15th generation. During this stage, the number of selected

solutions decreases while getting closer to the feasible region. Once the first feasible solution has been reached, then the population size still decreases during a few numbers of generations. During these generations, the non-feasible designs are discarded until reaching a population composed exclusively of feasible solutions.

- At this point, cross-over between two solutions has a great opportunity to lead to a feasible design. The population size will grow, supplied by feasible solutions obtained due to cross-over. Mutation can also contribute to that growth, but its purpose is to continue the exploration of the design space. At the end of the optimization, the population size has passed from 5 000 for the initial population to about 8 400 for the last one.

In spite of this increasing number, it is recalled that during the optimization process, only the fittest solutions are selected to remain in the population.

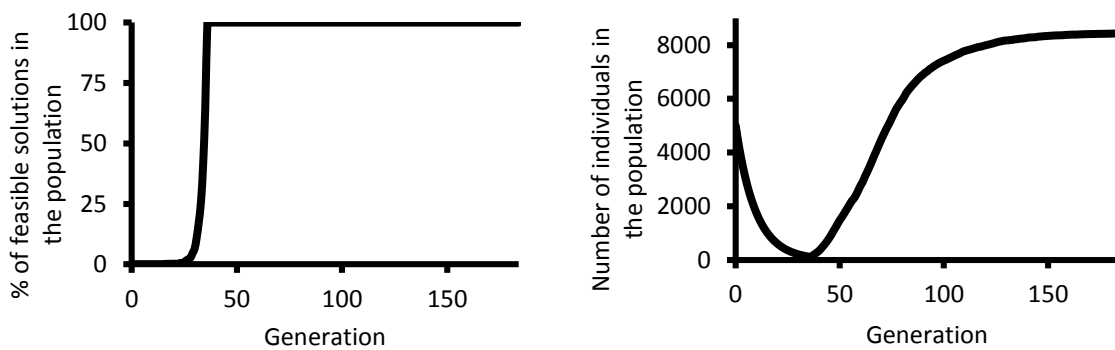


Figure 6.3: Evolution of the solutions along the different generations. On the left hand side: the first populations are only composed of non-feasible solutions. Between the 15th and 37th populations, feasible solutions are found. After the 37th population, all solutions selected in the population are feasible ones. On the right hand side: evolution of the number of individuals in the population. The population size decreases until the overall population is composed of feasible solutions. Then, the population grows and is filled with feasible solutions.

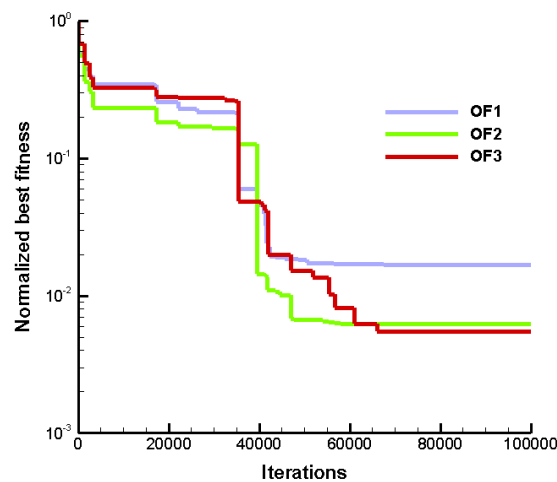


Figure 6.4: Evolution of the best fitness. Each curve corresponds to the best value of an objective function normalized by the fitness of the first solution evaluated as a function of the number of evaluations. The evolution of these curves shows the improvements of fitness for each objective.

Optimal design of architected sandwich panels for multifunctional properties

Pierre Leite

The evolution of the best value for the objective functions is given in Figure 6.4. It is observed that the best value for each objective is reached quite early in the optimization process. At about 68 000 evaluations, in the 55th generation, the best values of the objective functions have been reached and will never be improved. It is worthwhile mentioning that these values are not obtained for the same solution as the trade-off surface is not limited to a single point. The three solutions corresponding to these three values are limit solutions. During the rest of the optimization process, the performance space included between the solutions related to the three limit values is filled by intermediate solutions. The duration of this filling phase depends on the number of objectives and on the shape of the trade-off surface.

2. Coupling genetic algorithm with a branch and average approach

In this part, a specific approach based on the principle of the Branch & Bound algorithm and on a hierarchical classification of the materials in the database is presented and tested on two examples. A first section introduces the principles of this approach and the two following sections present the results obtained using this approach.

2.1. Principles: branch-average-rank-select-delete

The world of materials can be divided into different families. The most adopted classification is the one presented in Figure 6.5 in which the families are: metals, polymers, elastomers, ceramics, glasses and hybrids. The materials included in these families have some specific features in common, making sense to this classification. Within these families, the materials are ranked in a hierarchical manner defining classes, sub-classes and members as shown in Figure 6.5 in the case of Aluminium alloy 6061. This classification provides an effective structure for computer-aided material selection and management. A similar classification exists for material process. More details on the common features between the materials within each family can be found in the following references [ASH99, ASH07].

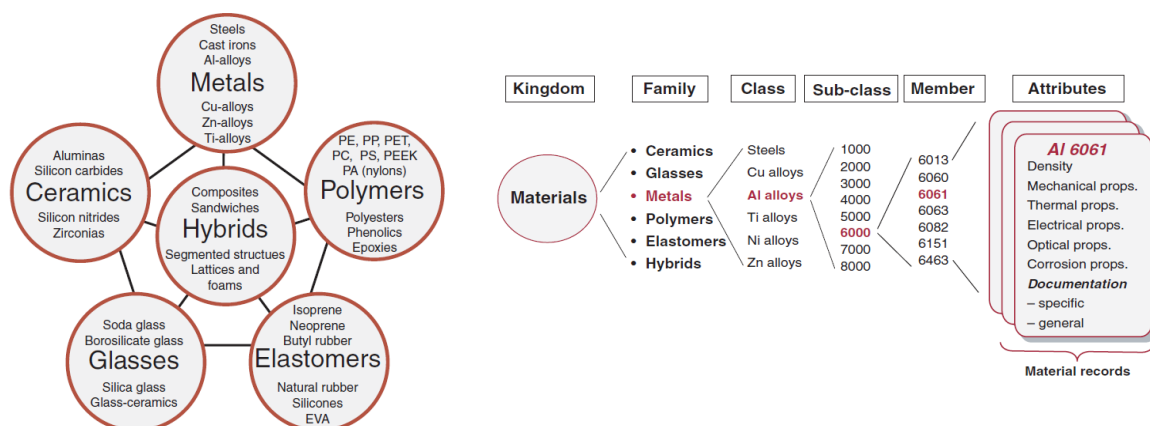


Figure 6.5: Classification of materials. On the left hand side: the materials can be classified by families. Five main families are classified: metals, ceramics, glasses, polymers and elastomers. Hybrids are a particular case as they correspond to a combination of materials. On the right hand side: families can be divided hierarchically in classes and sub-classes containing the materials. This kind of classification is used for data management in materials database. Figures taken from [ASH07].

This classification can be used in order to speed up the exploration stage in terms of material selection. As all the materials within a family or each sub-category of the classification tree have common features, their properties are also similar. Instead of directly selecting a material, the idea is then to select first a family and to go through the tree by selecting the appropriate branch at each step. This is the main philosophy of the Branch & Bound algorithm as presented in Chapter 2. Owing to the material classification, the design space is already wisely branched. But in the present case, the designed object is a sandwich panel. It is not one but the combination of three different materials that has to be selected. The main difficulty is then to bound the performances obtained in each branch. Moreover, the selection is based on multiple criteria while the Branch & Bound algorithm is dedicated to mono-objective optimizations.

In order to deal with multiple criteria in a Pareto set approach, a genetic algorithm is used, combined with a Branch & Average approach. As shown in Figure 6.6, the properties of the materials within a family are close. Instead of trying to bound the performances, the materials within a category of the materials tree will be represented by a “standard” representative material. For example, metals will be represented by a material having a density which is the mean value of all metals density, and so on for the other properties.

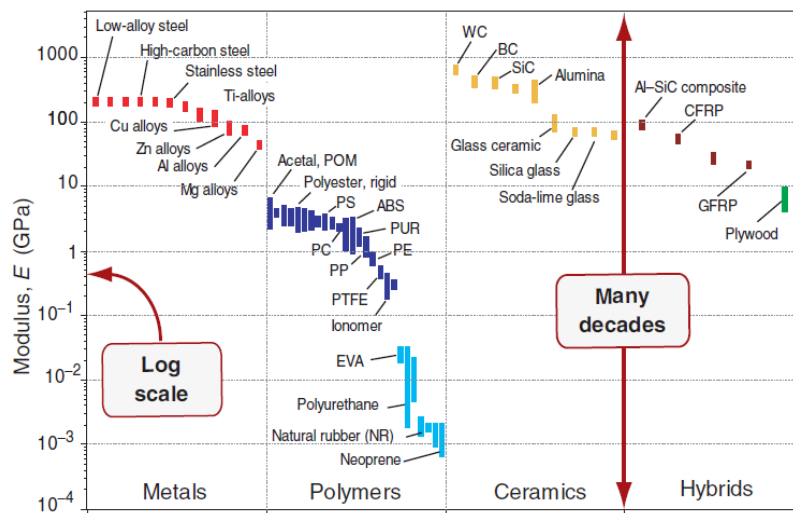


Figure 6.6: Example of bar chart showing the stiffness of representative materials classed by family. It can be observed that each family occupies a different range of Young's modulus.

As illustrated in Figure 6.7, the new optimization process steps are:

1. Create a new database composed of standard materials representing the first level of material by averaging the material properties.
2. Run the genetic algorithm using the design space obtained with the database created in the previous step.
3. Identify the standard materials present in the Pareto front.
4. Delete the branch corresponding to the standard materials that are not on the Pareto front.
5. Return to step 1 and continue the sequence on the sub-level considering the branches that have not been deleted in the previous step.

Due to the size of the database used for the present work, only three levels have been considered. The materials have only been classified by considering their family and class, the last

Optimal design of architected sandwich panels for multifunctional properties

Pierre Leite

level being the instances themselves. Then, the total optimization process is composed of three stages. The first stage deals with materials family while the second one deals with materials class. The last one considers all the instances that correspond to the classes that have not been deleted during the two previous stages.

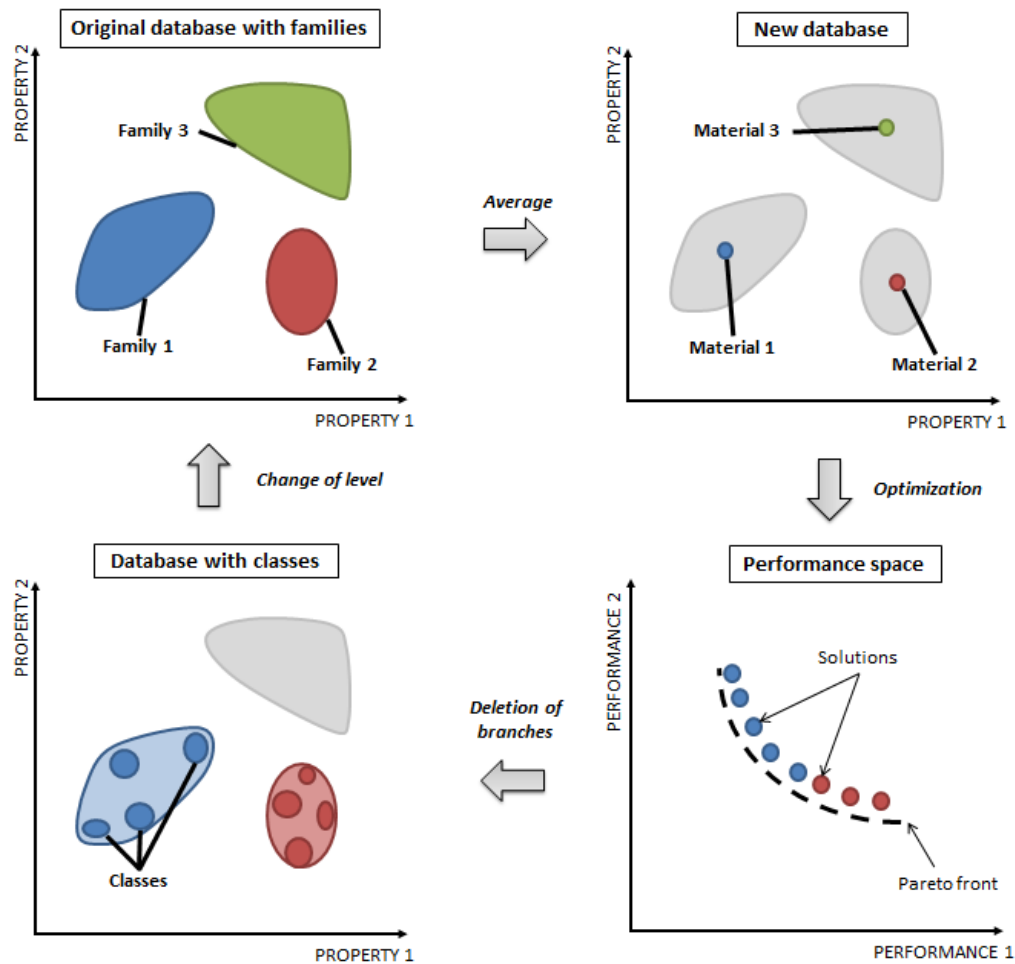


Figure 6.7: Steps of the mixed method. First step: a representative of each family is created by calculating the mean value of materials properties. Second step: Using this new design space, the genetic algorithm performs a first run of optimization. Third step: the promising families are identified along the Pareto front. The families that are not in the Pareto front are deleted from the design space. Fourth step: families are divided into classes and another cycle is done using classes instead of families.

2.2. Mixed method applied to the reference case

Schematically, the design space in terms of material selection can be illustrated by the tree presented in Figure 6.8. All the instances of the materials database can be listed in this tree. The design problem introduced in section 1.2 of this chapter is newly treated using the presented approach, called mixed method (GA+B&A). The resolution of the problem is described in three stages corresponding to the different classification levels.

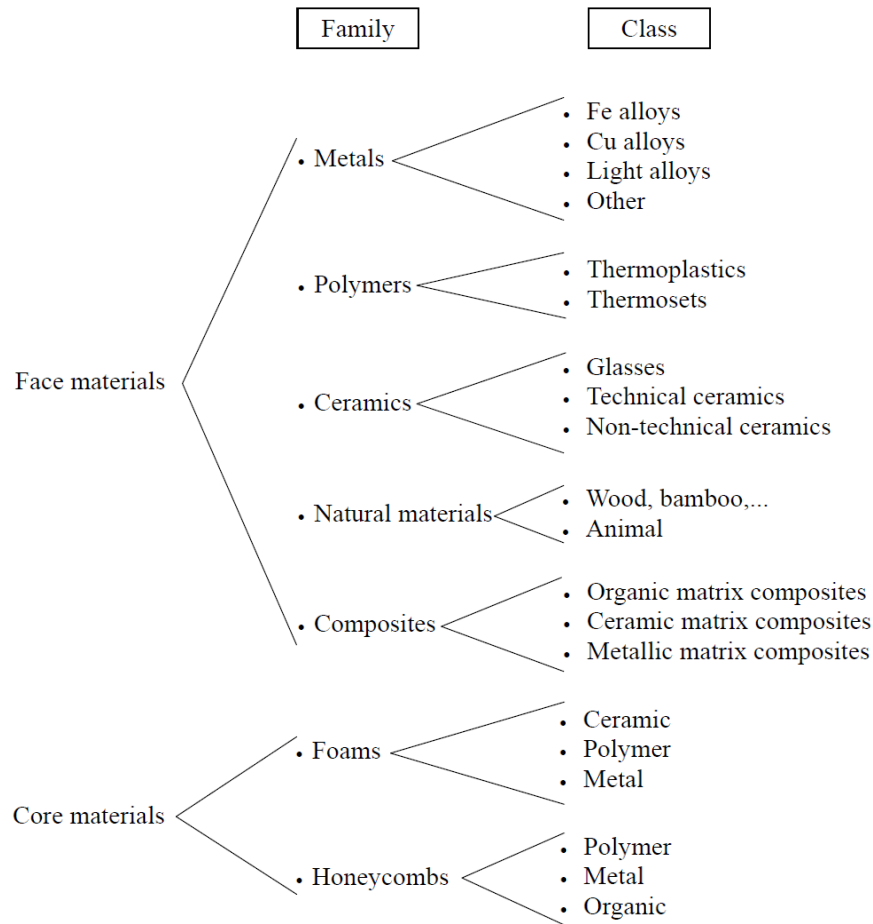


Figure 6.8: Materials classification used for the present work.

1st stage: family level

In this first stage, materials family selection is considered. The number of possible face material is 5: metal, polymer, ceramic, natural material and composite. There are two possible cores, either foam or honeycomb. Face and core thickness possibilities are also reduced. Only three different values are considered for each layer. The faces can be characterized by a thickness of 0.1, 2 or 4 mm and core thickness can have the value of 2, 10 or 25 mm. The main goal of this phase is to identify the most promising materials family and to reach the region of feasible solutions. So, the objective of minimizing panel thickness is set apart during this phase, the limiting performances being thermal insulation and thermal shock resistance. In order to be sure to obtain solutions in the performance space, no constraint is considered on the thermal stress nor on the maximum service temperature.

The initial population size is 10. The Pareto front has been obtained after 515 evaluations in 51 generations. The ratio between thermal stress and yield strength of the evaluated solutions varies from 4.6 and 15.9 which is far from the constraint (the thermal stress should be lower than the yield strength). From the performance space shown in Figure 6.9, it is observed that foams are more promising than honeycombs. The comparison between face materials is more complex, as no material really overcomes the others. All face materials except natural material are represented in the Pareto front.

As a conclusion for this first stage, honeycombs and natural materials can be deleted from the search space.

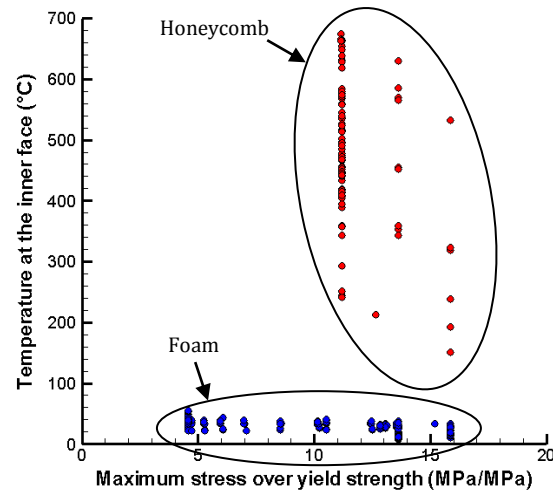


Figure 6.9: Performance space corresponding to the first stage. Foam largely overcomes honeycomb as core material. No feasible solution is met as all solutions have a thermal stress higher than the yield strength.

2nd stage: class level

The next stage deals with material class selection. The design space is larger than for the first stage. The number of possible face materials increases to 12 while the number of possible core materials is 3. The same approach as in the first stage is used. No constraint on the thermal stress and maximum service temperature is set and the objectives consist of minimizing the ratio between thermal stress and yield strength and of minimizing the temperature. The same thickness values are used.

This time, the initial population size is 20 and the genetic algorithm only took 128 evaluations in 20 generations to converge. As shown in the performance space presented in Figure 6.10, ceramic foams are the most promising class of materials for the considered specifications. Regarding face materials, only the three ceramic materials are on the Pareto front. Thus, the materials design space for the next level is composed of ceramic materials for the face sheets and ceramic foam for the core. Let us note that the constraints have not been respected yet.

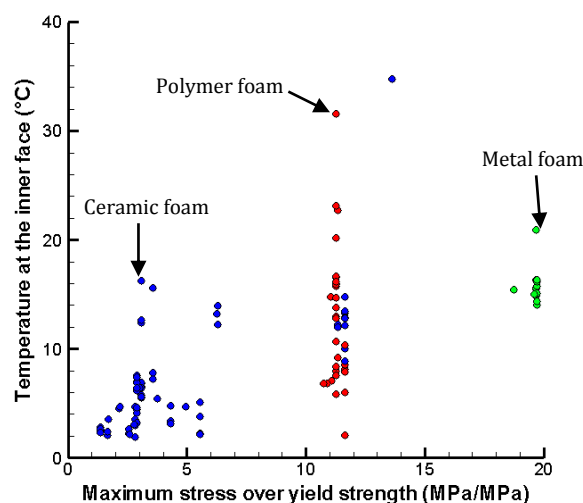


Figure 6.10: Performance space corresponding to the second stage. Ceramic foam largely overcomes the other types of foams as core material. Feasible solutions have not been found yet.

3rd stage: member level

The last stage takes up the actual material selection. The design space is composed of all the ceramic materials - there are 30 of them - and of the ceramic foams which are 20 in the used database. For this run, the same parameters than for the reference case have been chosen. The third objective, minimizing the panel thickness is considered as a third objective and the constraints are also taken into account. The thicknesses are defined as in Section 1.2.

With an initial population size of 100, the genetic algorithm needed 152 941 evaluations and 126 generations to found the trade-off surface shown in Figure 6.11. The comparison between the obtained Pareto front and the reference front is very satisfactory.

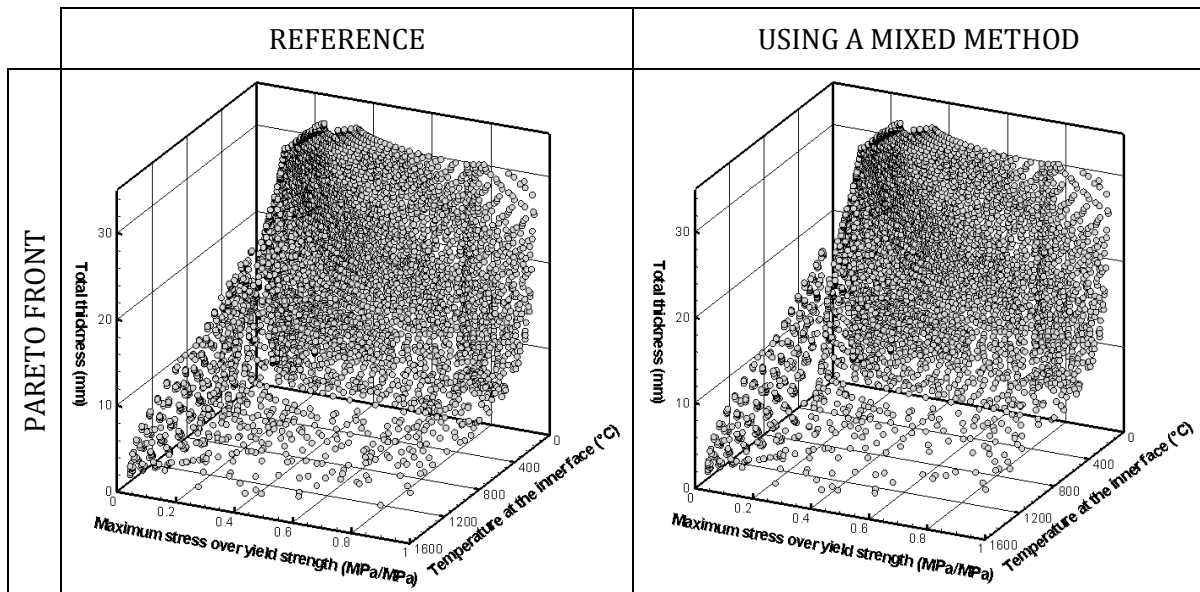


Figure 6.11: Comparison between the Pareto fronts obtained with the original method (genetic algorithm) and with a mixed method (genetic algorithm and Branch & Average). Except for a few solutions, the match is very satisfactory.

Adding the number of evaluations at each stages, a total of 153 584 evaluations have been performed using this approach, which represents a 80 % cut-off. The obtained Pareto front is slightly less populated than the reference one. The curves in Figure 6.12 show the difference between the genetic algorithm and the genetic algorithm + Branch & Average approach in terms of speed. The best fitness values are found after about 16 300 evaluations in the case of the “GA + B&A” approach while it took 68 000 evaluations in the case of the genetic algorithm alone. It is worthwhile noting that to properly compare the performances of the two approaches, statistical data should be obtained as genetic algorithm is based on stochastic phenomenon. Here, the comparison is made on only one run.

Even though the number of evaluations needed to converge is still too high to consider using Finite Element Analysis in the optimization process, the number of evaluations needed to find the region of feasible solutions has been greatly reduced. This kind of approach could be used as a preliminary stage to reach this region. One of the main characteristics of the present case study is that material selection is the most limiting design. Only two core materials have the appropriate properties regarding the specifications, and the trade-off surface is composed of very few face materials. This can explain why this approach works so well. In order to test their

results in a different type of design problem, one of the case studies presented in the previous chapters is treated using this approach.

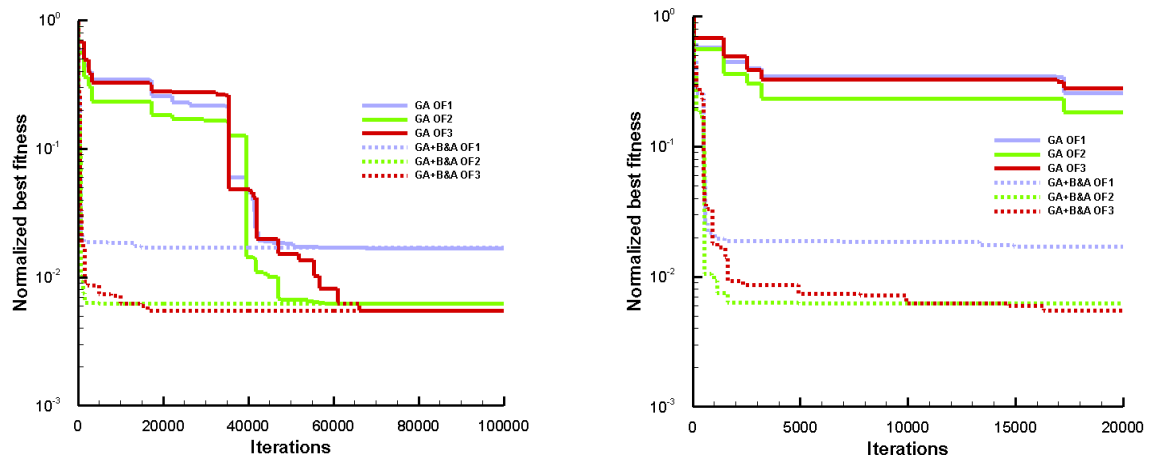


Figure 6.12: Comparison between the original approach and the mixed method. Each curve corresponds to the best value of an objective function normalized by the fitness of the first solution evaluated as a function of the number of evaluations. Solid lines correspond to the optimization process run with the genetic algorithm while the dotted lines correspond to the one run with the mixed method. On the left hand side: at the end, the two approaches have the same best fitness. On the right hand side: for the mixed method, the best fitnesses for the three objectives are reached after about 16 300 evaluations while for the original method it took about 68 000 to do so.

2.3. Mixed method applied for the design of sandwich panels for stiffness and Acoustical Transmission Loss at minimal weight

Presentation of the case

In the previous case study, the design was mainly limited by material selection. In the case of the sandwich panel designed for flexural stiffness and Acoustical Transmission Loss at minimal weight, both material selection and geometry imposes their limitations. In this section, the optimal design of a sandwich panel is considered using the mixed method “GA + B&A”.

The objectives are:

- Minimize G the central deflection of the panel submitted to a three-point bending test, in μm .
- Maximize R the mean value of the Acoustical Transmission Loss in the frequency range [1 000; 4 000] Hz, in dB.
- Minimize M the mass per unit area of the panel, in kg/m^2 .

And the constraints are:

- Central deflection $< 10 \mu\text{m}$.
- Acoustical Transmission Loss $> 20 \text{ dB}$.
- Mass per unit area $< 50 \text{ kg}/\text{m}^2$.

The initial results are presented in Chapter 4, Section 3.1.

Design space

For this application, only metals, polymers and composites have been regarded as face material for the design of foam core sandwich panels in a “real path” approach. Face thickness ranges between 0.5 and 10 mm while core thickness can vary from 10 to 500 mm.

1st stage: family level

The size of the design space regarding material selection for this first stage is quite small as only three face materials are possible and foam is the only core material. This means that reaching the region of feasible solutions is not difficult in this case. In order to obtain a representative performance space, the design space in terms of thickness has not been branched.

The constraints have been released for this stage. The population size has been set to 100 for the initial step. After 659 evaluations, the performance space has been filled as shown in Figure 6.13. The Acoustical Transmission Loss ranges between 24 and 65 dB, the deflection between 0.03 and 100 μm and the mass between 6.6 and 610 kg/m^2 . The behaviour observed in the performance space is a mass law behaviour in terms of Acoustical Transmission Loss. Increasing the stiffness and the acoustical damping comes with an increase of the mass of the panel. In terms of material selection, polymer is not in the trade-off surface, unlike metal and composite. Thus, polymers are deleted from the search space.

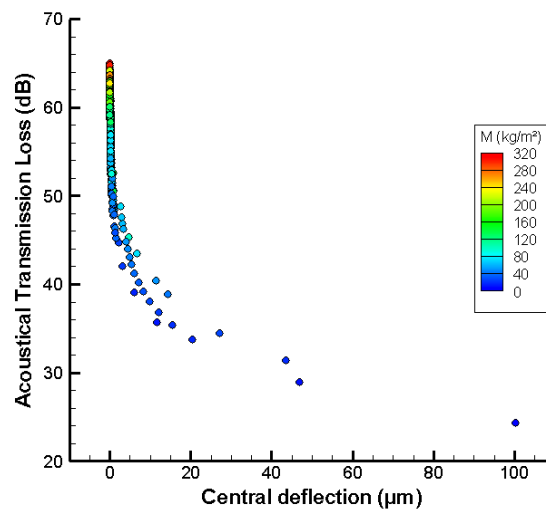


Figure 6.13: Performance space obtained after the first stage of the mixed method. The Acoustical Transmission Loss is plotted as a function of the deflection with contour values of mass per unit area as colour scale. The shape of the group of solutions in the performance space is typical from an acoustic mass law behaviour.

2nd stage: class level

For the materials class level, three classes of foams are considered while seven classes of face materials are still in the design space (4 metals and 3 composites). Initial size population is still 100 but this time a mass constraint has been set at 50 kg/m^2 .

The trade-off surface has been obtained after 1 376 evaluations. The evaluated solutions still follow a mass law. Projections of the performance space are displayed in Figure 6.14 with the nature of core materials class shown in colour legend. Polymer foam overcomes ceramic and

Optimal design of architected sandwich panels for multifunctional properties

Pierre Leite

metal foams for both stiffness and Acoustical Transmission Loss at minimal weight. Regarding face material, Fe and Cu alloys are deleted as they are not in the trade-off surface.

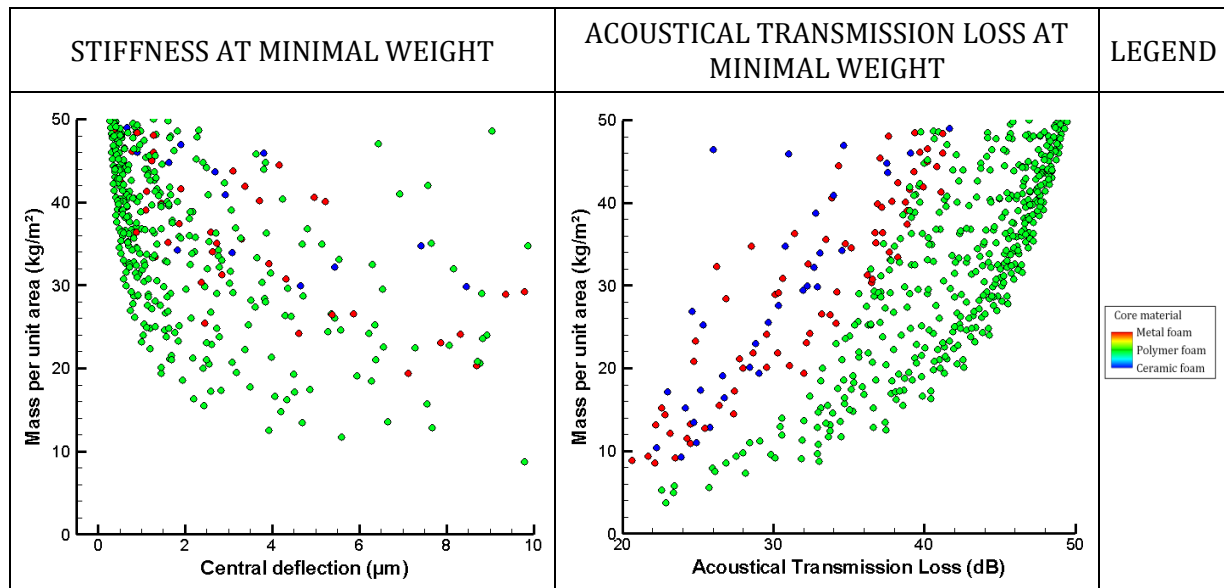


Figure 6.14: Performance space plotting the solutions generated by the optimization algorithm obtained after the second stage of the mixed method. The plots correspond to projections of the performance space in order to observe the deflection and the Acoustical Transmission Loss as a function of mass per unit area. The colour legend represents the three possible core materials: metal, polymer and ceramic foams. Polymer foam overcomes the other candidates in both stiffness and Acoustical Transmission Loss at minimal weight.

3rd stage: member level

For this last stage, a total of 79 face materials and 84 polymer foams are taken into account, reducing the possible materials from 234 to 164. All constraints are set such as for the results presented in Chapter 4, section 3.1.

The initial population size is unchanged. After 287 546 evaluations, the performance space shown in Figure 6.15 has been obtained. The performance space should be divided in two parts corresponding to two different acoustic behaviours as already observed in the previous chapters. For the part corresponding to solutions with an acoustical behaviour experiencing a “sandwich effect”, a perfect agreement is found between the reference performance space and the present one.

For the solutions following an acoustic mass law, the optimal designs are different between the two performance spaces. In the reference case, the optimal core material is a glass foam and its best performances at 50 kg/m² are 0.1 µm and 51 dB for the deflection and the Acoustical Transmission Loss respectively. In the present case, using a Branch & Average approach, ceramic foams have been deleted from the search space during the second stage. Then, the optimal core material in this part is a PP foam with a 0.0235 relative density. The best performances achieved by such a panel are 0.29 µm and 45.2 dB for the deflection and the Acoustical Transmission Loss respectively. By using the mixed method, a complete group of optimal solutions has been lost. It appears that averaging the properties instead of bounding the performances has been a misleading approach in this case.

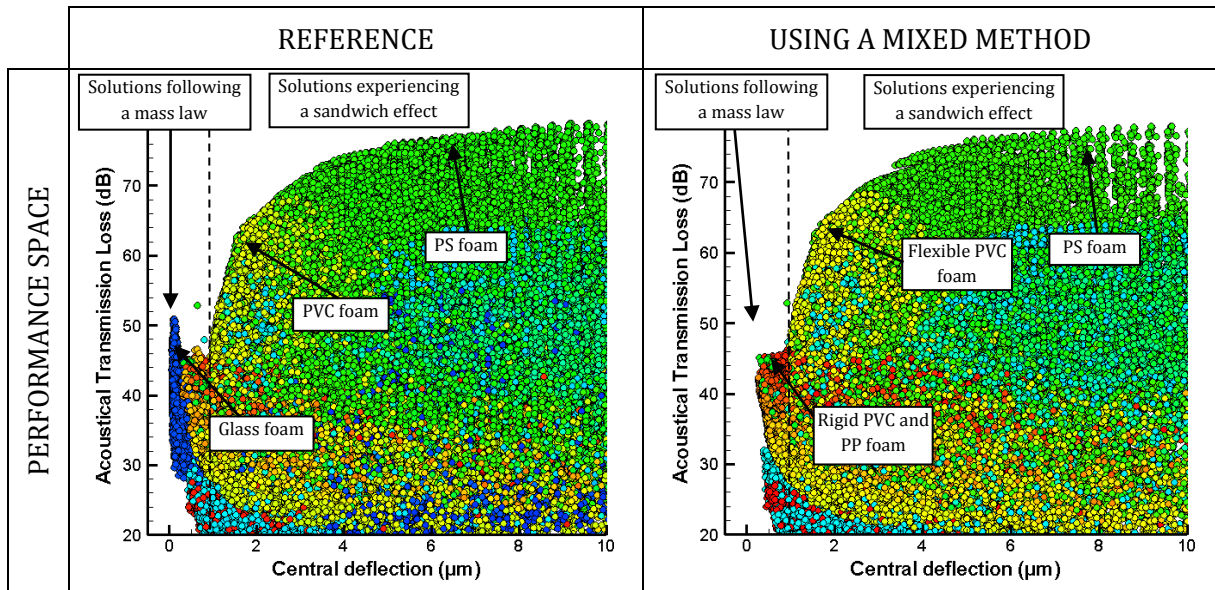


Figure 6.15: Comparison between the reference performance space obtained in Chapter 4 and the one obtained using the mixed method. The multi-modal behaviour is reproduced even though polymer foam core panels do not strongly take advantage of a mass law. The match between the two performance spaces is really satisfactory in the region dominated by the sandwich effect. On the contrary, glass foam solutions have been ruled out during the optimization process.

Adding the number of evaluations of each stages, a total of 289 581 evaluations have been performed in order to obtain a better performance space than the original one which took 867 042 evaluations to run. As a comparison, it represents a 66 % cut-off of the number of evaluations.

2.4. Conclusion/Recommendations

The results obtained using the mixed method are satisfactory in the capacity to efficiently fill up the performance space with optimal solutions in a limited number of evaluations. In the first treated case, as material selection was the limiting design, the method shows its best performances with a 80 % reduction of the number of evaluations. However, in this kind of situation, filtration methods could be sufficient to eliminate the materials that cannot fulfil the requirements in terms of constraints.

In the second case, material selection is not so limiting and filtration methods would potentially not be able to reduce the design space as for the first case. The reduction of the number of evaluations is less impressive but still promising. However, the multi-modal behaviour of the acoustic transmission loss has not been caught by the method. It seems that a Branch & Average approach is not appropriate for catching this type of non-linearity. A Branch & Bound approach could potentially lead to better results.

The efficiency of this mixed method depends on the relative importance of material selection over geometrical design. It could also be improved by taking a fully branched material classification divided into families, classes, sub-classes and members. However, this classification is only efficient if the database is representative of the diversity of all types of materials.

Branching the thicknesses can be efficient as for the first presented case. But in some instances, geometrical design is deeply linked to material selection, and solutions could be unfairly discarded if geometrical variables have not sufficient freedom.

3. Using DOE to create performance indices

The previous mixed method is not suited when complex non-linear behaviours are involved. In addition, from the results obtained in Chapter 5, it has been observed that the performance index method could be used to deal with the material selection in the design of sandwich panels.

In this part, another approach inspired from Castillo's work [CAS09] is presented. The authors used DOE techniques coupled with Finite Element Analysis to determine an approximated performance index. This analytical performance index is used as a replacement of the Finite Element Modelling to assess the fitness of the candidates in a material selection approach. The authors treated a mono-objective problem with two constraints.

The present work being dedicated to multi-objective design problems, the treated case is an example of multi-objective design. The DOE approach is used to determine an analytical performance index to be treated by the genetic algorithm as a fitness assessor. The algorithm still leads to a performance space in which it is possible to extract the trade-off surface, the difference being the computational cost of the analysis.

The case study chosen for this part is the design of a sandwich panel for both stiffness and Acoustical Transmission Loss specifications as treated in Chapter 4 Section 3.1 and in Chapter 6 Section 2.3. This case is multi-modal as solutions can follow two different behaviours that are translated into two different shapes in the performance space. Given that the Acoustical Transmission Loss assessor (PIAMCO software) is the most expensive analysis tool, the DOE approach is used to find out an analytical expression to replace it.

3.1. Determination of the approximated performance index

Mass and deflection of a sandwich beam submitted to a three-point bending test are already evaluated using analytical expressions. This is not the case for the Acoustical Transmission Loss. As a symmetrical sandwich panel is considered, the main parameters influencing the Acoustical Transmission Loss are:

- t_f, ρ_f and E_f , the thickness, density and Young's modulus of the face sheets respectively
- t_c, ρ_c and E_c , the thickness, density and Young's modulus of the core respectively

The Acoustical Transmission Loss is a non-linear phenomenon. As shown in Chapter 4, the evolution of the Acoustical Transmission Loss as a function of core thickness appears to be parabolic. For that reason, a design with three levels has been chosen, i.e. the Box-Behnken design with 6 factors. This particular design is able to consider quadratic effects. For more details on the Box-Behnken design, please refer to [BOX60].

As the Acoustical Transmission Loss can either follow a mass law or experience a sandwich effect, these two cases are considered. An approximation of the Acoustical Transmission Loss R resulting from a mass law is given by the formula [FAH85]:

$$R = 20 \log(fM) - 47 \quad (6.1)$$

with f the frequency and M the mass per unit area of the panel.

It is known that the "sandwich effect" is due to the possible transverse deformation of the soft core of the sandwich panel. So the transition between a mass law and a sandwich effect depends

on the softness of the core. In order to get more precise results, the range of variation of the input variables should not be too large [CAS09]. Only foams with a Young's modulus lower than 100 MPa is considered as soft enough to result in a sandwich effect. Then, the foam density is considered as ranging from 10 to 100 kg/m³. Panels made of other foam will be assessed using the mass law. Regarding the face sheets, Young's modulus varies from 1 to 350 GPa and the density from 1 000 to 12 000 kg/m³.

The results obtained in Chapter 4, Section 2.3 on the optimal design of sandwich panels for Acoustical Transmission Loss at minimal weight showed that the optimal solutions are thin panels. The optimal core thickness depends on the core material but this optimal value tends to be low. The variation range of thicknesses has been reduced to [0.5; 5] and [10; 200] for the faces and the core respectively.

DOE has been performed using the Minitab® software. The main effects and interactions plots are given in Appendix C. The DOE includes 90 experiments. The linear and quadratic effects and interactions between factors are given in Table 6.1:

Table 6.1: Effects and interactions between the different factors. Cells coloured in yellow denote the 7 most influential effects and interactions.

	Effects	Interactions					
		t_f	t_c	ρ_f	ρ_c	E_f	E_c
t_f	9.34	-6.42	-2.44	1.22	-1.76	-12.92	3.38
t_c	3.50		-3.22	-5.48	2.74	0.80	12.22
ρ_f	21.86			-3.28	-3.16	-5.42	-8.48
ρ_c	-2.04				-3.16	0.50	4.82
E_f	-11.62					-2.90	11.40
E_c	-6.80						13.68
Constant	51.08						

These effects and interactions can be used to evaluate an approximation of the Acoustical Transmission Loss. By considering the 7 most influential effects only, an approximate value, noted R^* , can be calculated by the following equation:

$$R^* = 51.1 + 4.7t_f^* + 10.9\rho_f^* - 5.8E_f^* + 6.8E_c^* \times E_c^* - 6.5t_f^* \times E_f^* + 6.1t_c^* \times E_c^* + 5.7E_f^* \times E_c^* \quad (6.2)$$

The exponent * denotes the use of coded variables. Passing from non-coded variables to coded ones is made using:

$$V^* = \frac{2V - (V_{max} + V_{min})}{V_{max} - V_{min}} \quad (6.3)$$

with V_{min} and V_{max} the minimal and maximal values of the variable in its variation range respectively. During the optimization process, the calculations of the approximated value of the Acoustical Transmission Loss have been performed with an expression involving all terms and coefficients. The most influential factor is the face density. This is consistent with a mass law approach. The heavier the face, the higher the transmission loss. The core Young's modulus has also a significant influence as in the 7 most influential terms, 3 are related to it. The comparison between the Acoustical Transmission Loss calculated for the experiments and the approximated values calculated using equation (6.2) is shown in Figure 6.16.

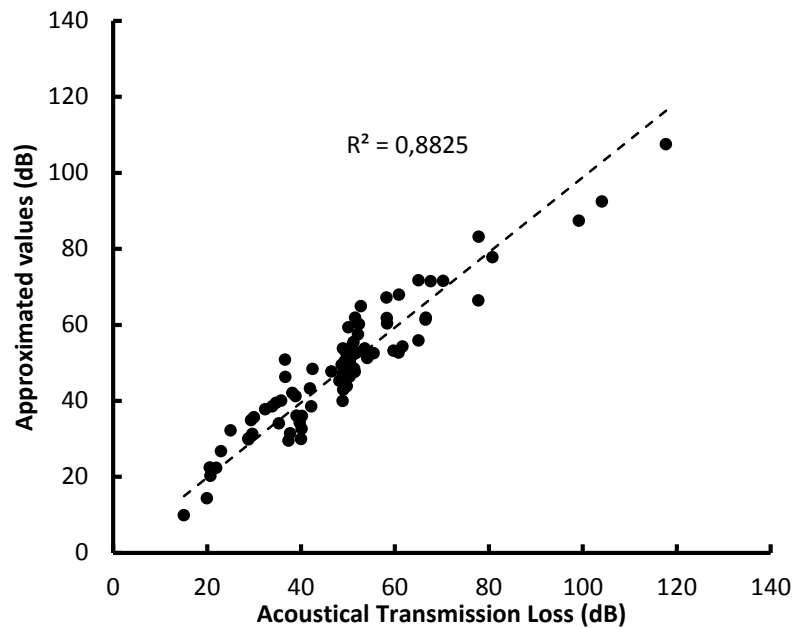


Figure 6.16: Approximated values of the Acoustical Transmission Loss as a function of the actual values used in the Design Of Experiments. This plot gives the relative error made with the approximation. The dotted line represents the equation $y = x$.

3.2. Using approximated performance index for the design of sandwich panels for stiffness and Acoustical Transmission Loss at minimal weight

The design problem has been solved by using the approximated expression of the Acoustical Transmission Loss obtained in the previous section and the mass law of equation (6.1) as analysis tool in the optimization process. During the optimization process, if the core material has a Young's modulus higher than 100 MPa used as limit value in DOE, the mass law is used to evaluate the Acoustical Transmission Loss. If Young's modulus is lower than 100 MPa, then the approximated expression is used.

The performance space obtained using this reduced model for the assessment of the Acoustical Transmission Loss is shown in Figure 6.17 along with the reference one. The multi-model approach is effective to reproduce the multi-modal aspect of the performance space. In the region corresponding to solutions following a mass law, there are two groups of solutions. The first one gathers rigid PVC foam core panels while the second one gathers glass foam core panels. The mass law does not properly reproduce the performances of the solutions, even though the right tendencies are found. Then, the expression which has been used should be revised.

In the region where the solutions experience a sandwich effect, there are once again two main groups of solutions. The first one gathers PS foam core panels and the second one gathers flexible PVC foam core panels. The performances calculated for the flexible PVC foam core solutions are slightly overestimated in terms of Acoustical Transmission Loss. Compared to the original performance space, a solution taken along the Pareto front with a deflection of $1.5 \mu\text{m}$ has a 58 dB Acoustical Transmission Loss according to the original performance space and a 64 dB transmission loss according to the one obtained with an approximated model. On the other hand, the performances calculated for the PS foam core solutions match with very good accuracy the one of the original performance space.

Even though the performances are overestimated for some types of solutions, the general shape of the performance space is consistent with the original results. In terms of material selection, the optimal solutions determined in Chapter 4 have been found again.

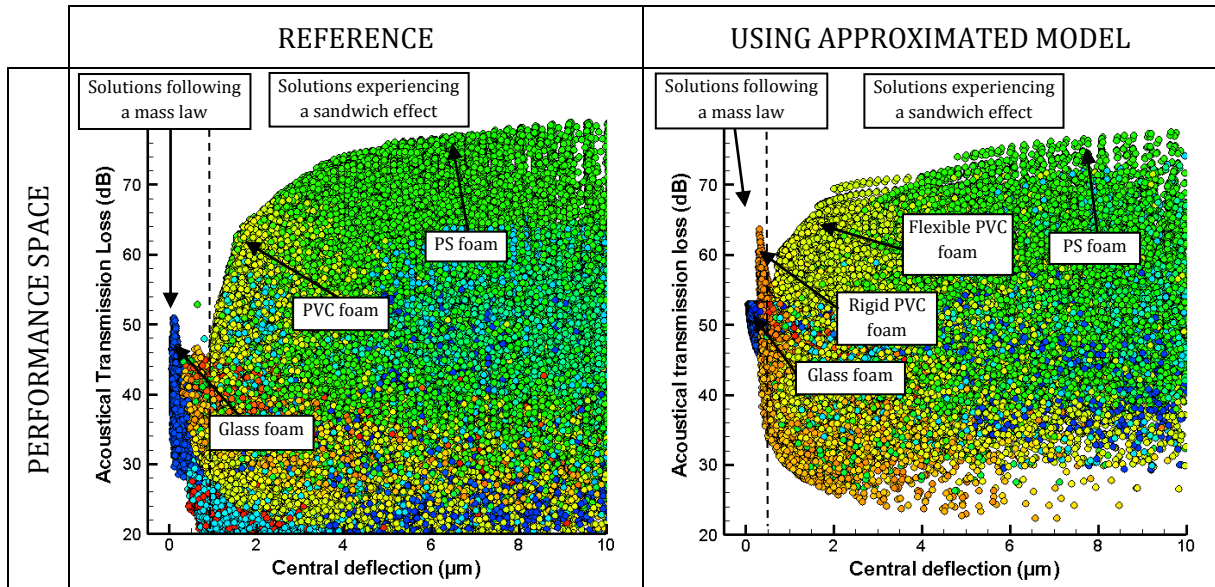


Figure 6.17: Comparison between the reference performance space and the one obtained using the approximated model. The multi-modal behaviour is reproduced thanks to the use of two separate models to evaluate the solutions. The range corresponding to the two different behaviours is satisfactorily determined. The approximated mass law on the Acoustical Transmission Loss makes a noticeable error on the results. It completely overestimates the acoustic performances of rigid PVC foam core panels. The approximated model on the sandwich effect is quite satisfactory even though the acoustic performance of the flexible PVC foam core solutions is overestimated. The performances of the PS foam core panels are perfectly reproduced. In terms of material selection, all core materials that have been identified as optimal ones have been found again with the approximated models.

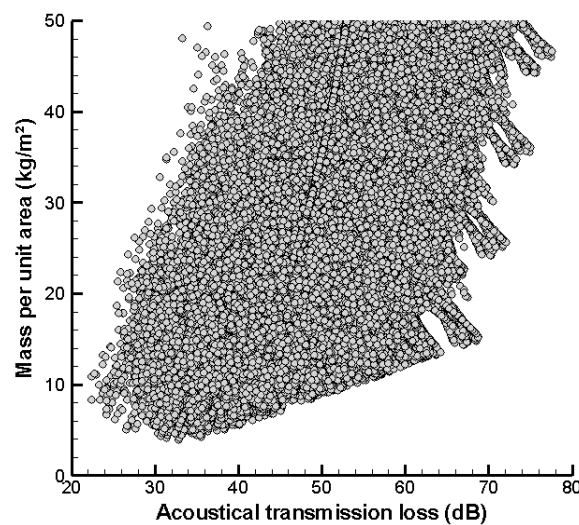


Figure 6.18: Performance space plotting the Acoustical Transmission Loss of the solutions as a function of their mass per unit area using the approximated model. This figure can be compared with Figure 4.28. There is a bi-linear relationship between the approximated Acoustical Transmission Loss and the mass per unit area while it should be logarithmic (see Figure 4.13).

The approximated expression could be improved by taking the logarithm of the factors instead of the factors themselves. As shown in Chapter 4, the Acoustical Transmission Loss has a logarithmic relationship with mass. Using the Box-Behnken three level design, the obtained expression fails to reproduce the logarithmic behaviour. As shown in Figure 6.18, the evolution of the approximated Acoustical Transmission Loss as a function of the mass is bi-linear.

3.3. Conclusion/Recommendations

Using optimization methods in order to obtain an approximated expression of performance index or fitness assessor is quite effective. Indeed, the computational effort is made before the optimization process and can be largely reduced. As a comparison, getting the approximated expression with the used design, a Box-Behnken three-level design, only takes 90 calculations, while during the optimization process, more than 800 000 calculations have been performed. However, obtaining a reduced model can be difficult and the method to be employed depends on the model to be reduced. The Acoustical Transmission Loss is a quite complex performance to assess. Its behaviour is non-linear and multi-modal. A more refined methodology should be used to obtain better results than the one presented in this part. More specifically, the approximated mass law should be revised.

Another difficulty can come from the number of factors to take into account in DOE. A six factors case has been presented as the sandwich panel is symmetrical. But in some instances, unsymmetrical panels are more likely to be used and then the number of factors can be increased. Moreover, some performances depend on many different factors. For example, thermal insulation, if thermal shock resistance is considered, depends on density, thermal conductivity, specific heat capacity, thickness, but also on Young's modulus, Poisson's ratio, coefficient of thermal expansion and yield strength. This makes 8 factors per layer. The DOE can dramatically grow due to this number of factors.

As stated by Castillo et al., other regression methods can be used such as neural networks. Model reduction is a wide field of research that has not been explored in the present work. Though, this is a widespread approach for structural optimization [IRI11b, MER08, BAU11].

4. Conclusion on the value of mixed methods

The accuracy of the results obtained in optimization process depends on the optimization algorithm when it comes to rank the solutions, but it depends on the analysis tools when it comes to the performances evaluation. A good optimization algorithm can lead to wrong solutions if the analysis tools are not representative enough of the reality. For that reason, it is preferable to use more accurate models to assess the fitness of the solutions. Nevertheless, the computational cost of the optimization process mainly comes from the fitness assessor. Unfortunately, high-fidelity models often require expensive computational means. This is why it is important to explore the possible ways to reduce the optimization costs.

Different ways to improve the optimization process have been mentioned. Among them, two different approaches have been presented and tested as an example of what can be expected from these techniques. If more results are needed to completely characterize the presented approaches, specifically for statistical reasons, some conclusions can be made.

One of the specificities of the design problems addressed by this work is that the design space can be represented as an arborescence. Using material classification to guide a Branch & Average approach helps reduce the number of evaluations needed to identify the region of feasible solutions and the region of the design space corresponding to the optimal solutions in

the performance space. However, the efficiency of this approach depends on the linearity of the models. As shown by the second example, the method fails to reproduce a multi-modal behaviour, especially when it is translated by the presence of two groups made of different kinds of materials in the Pareto front. Then, in some cases, averaging the properties instead of bounding the performances can be misleading.

Even though the number of evaluations is greatly reduced by improving the optimization algorithm, the computational cost remains expensive. This is why model reduction represents a promising approach. Turning a high-fidelity model into an explicit approximated performance index is in line with the principles of genetic algorithm. Indeed, the genetic algorithm uses a fitness assessor to rank the solutions. Performance indices are a practical way to evaluate the fitness of a solution. As simple models have been selected for the case studies, using this approach was mainly a matter of demonstration. However, the example of the Acoustical Transmission Loss is very interesting as its behaviour is non-linear and multi-modal. It shows that, in this case, it could be of interest to consider multiple reduced models according to different regions of the search space. The obtained reduced model has not been optimized. Better solutions can be obtained using the appropriate methods. However, it has been effective in finding the optimal solutions in terms of material selection, although the value of the performances is not perfectly right for a group of solutions.

This approach seems to be ideal but building a surrogate model can be difficult. The main difficulty is to sufficiently reduce the variation range of the considered factors in order to improve the accuracy of the reduced model as stated by Castillo et al. [CAS09].

Chapter 7

Conclusion

Chapter contents

1. Summary	244
2. Further work.....	246

1. Summary

This thesis was dedicated to the optimization process of architected sandwich panels for multiple design criteria. A classical material selection method has been introduced in Chapter 2, based on material performance indices. This method is suited for simple geometries and simple loading cases but is not adapted to the design of sandwich panels and architected materials in general.

Then a first optimization process has been presented and tested in Chapter 4. It is based on a discrete database in which face and core materials are referenced. This is a “real path” optimization in the sense that every potential material is listed as a material in a database.

Simple models presented in Chapter 3 are used in order to evaluate the properties of the solutions regarding the considered applications. The set of optimal solutions is determined using a genetic algorithm in a Pareto set approach.

Chapter 4 focused on foam core sandwich panels as foams are satisfactorily represented in the material database.

Sandwich panels have been optimised in a minimum weight design considering a single additional function. Three possible cases in terms of trade-off emerged in this part:

- In some cases, for instance flexural stiffness, acoustical damping, thermal insulation and blast mitigation, the trade-off surface is convex. There is a competition between mass and the other property in the sense that increasing one property requires to reduce the other one. This competition can be qualified as beneficial. Indeed, between two solutions S_1 and S_2 along the trade-off surface lie intermediate solutions with properties that can be better than the mean value of the properties of S_1 and S_2 .
- On the contrary, the trade-off surface between mass and flexural strength is concave. There is still a competition between these properties but in this case, it is non-beneficial. This means that an intermediate solution between two solutions S_1 and S_2 along the trade-off surface will have less interesting properties than the mean value of the properties of S_1 and S_2 .
- The last possible case concerns thermal resistance at minimal weight for which the trade-off surface is piecewise linear. This case is the intermediate state between the two other possibilities mentioned before.

Optimal design at minimal weight for multiple functions has been addressed. Four representative case studies have been presented. In terms of compatibility between requirements the four cases are:

- Beneficial competition, as for instance when flexural stiffness and acoustical damping at minimal weight are required.
- Non-beneficial competition, as encountered for flexural strength and thermal resistance at minimal weight specifications.
- Compatibility, such as for thermal insulation and blast resistance specifications at minimal weight. In this case, the trade-off surface between thermal insulation and blast resistance at a given weight has a square shape. It is possible to increase both properties until reaching the optimal design.
- Incompatibility, which has been encountered when acoustical damping and blast resistance at minimal weight are required. The trade-off surface can be divided into two different groups of solutions, one gathering solutions adapted for blast resistance

and the other one gathering the solutions adapted for acoustical damping. There is no solution with intermediate properties.

Core material is one of the most important design variables. The ability of a sandwich panel to exhibit multifunctional properties is often due to the presence of the core and to its effective properties. For that reason, the optimization process has been modified in order to pass from a discrete database to a semi-continuous one where the core material is described using a continuous variable. This is called a “virtual path” optimization.

Each case study treated by a “real path” optimization has been analysed using this new approach. As far as possible, material selection using material performance indices is performed in order to obtain preliminary results. The appropriate performance index depends on the application but also on the considered architecture and finally on either it is bending or stretching dominated.

The shape of the trade-off surface is not modified by a change of core topology, whereas the achievable performances are. Among the three studied patterns, one is bending-dominated which is the foam, while the two others are considered as stretching-dominated. Stretching-dominated patterns are more weight-efficient structures for high stiffness and strength requirements.

Indeed, the obtained results place honeycomb and truss structures ahead of foam as weight efficient core architectures for the following functions: flexural stiffness, flexural strength, blast mitigation and thermal insulation (due to thermal shock resistance requirements). On the contrary, bending dominated structures are better than stretching dominated ones for acoustical damping. The case of thermal resistance is different as the effective thermal conductivity is considered as only dependent of the relative density of the core.

For multiple functions in addition to the minimization of the mass per unit area, core material and architecture selection should not be separated from the geometrical design. Depending on the requirements and on the trade-off, the optimal local loading in core material can pass from bending to stretching or from stretching to bending. Then, it becomes difficult, or even impossible to determine an optimal architecture.

Nevertheless, truss structures exhibit particular properties compared to foams and honeycombs. It is a stretching-dominated pattern, but by varying the angle between the face and truss directions, the core can pass from very stiff in the out-of-plane axis to very soft. If the struts are oriented in the out-of-plane direction, the core stiffness is maximal.

The variability range of the effective properties of such a structure is larger compared to foams and honeycombs for which there is only one design variable describing the geometry. Foam can be seen as a limit case of soft core material and honeycomb as a limit case of stiff out-of-plane one. Truss structures are an intermediate solution, lying between the two limit cases while being able to move from one to the other regarding the situation. For acoustic damping, truss structures are close to foams in terms of properties whereas for flexural stiffness they are close to honeycombs.

The accuracy of the optimization process in terms of performances is dependent of the precision of the analysis tools used to evaluate the solutions. In the present work, simple models have been utilized, based on the effective properties of the materials constituting the sandwich panel. In an optimization by “virtual path”, the precision of the analysis tools is also impacted by the quality of the present scaling laws. For industrial design, very accurate models are preferred to simple models. It is then preferable to handle with numerical simulations than with analytical

expressions to assess the performances of the solutions in complex situations. Still, the complexity of the optimization process cannot be reduced in the present case. The design space is filled with local optima. Using an optimization algorithm capable of identifying the global optimum enables to ensure an objective ranking of the solutions.

However, there is an incompatibility between using complex models and complex optimization methods due to computational power limits. It is important to find out a trade-off and therefore mixed methods can be relevant in this case.

Some possible mixed methods have been presented:

- Using a Branch & Average approach coupled with the genetic algorithm is in line with the usual methods of materials science in which materials are classified by families, classes and sub-classes.
- The other approach, based on a work found in the literature, consisting of coupling DOE and numerical simulation to create an approximated performance index is consistent with material selection techniques based on performance indices.

This is just short examples of what can be achieved using simple methods based on principles from the world of material science. More investigations should be made to fully assess the possibilities of mixed methods. Nevertheless, the results obtained in Chapter 6 are promising.

To conclude, optimization by “real path” stands for a practical method for industrial purpose. This approach encompasses material selection and pre-dimensioning to determine the optimal solution made of existing materials from a set of requirements. The fact that the constitutive materials are existing ones is important, especially as decision-makers can use their own database gathering the materials already available for them. Collaborations with industrial partners of the MANSART project prove that this approach could be popular for designing sandwich solutions.

2. Further work

The present work focused on minimum weight design of sandwich panels. Issues such as size or cost requirements have not been taken into account. The chosen size constraints are not always representative of industrial problems, even though there is a practical advantage of keeping a certain freedom in size. A simple way to reconsider the size constraint is to filtrate the obtained solutions regarding their total thickness, although the results may not be optimal ones. In order to obtain optimal solutions for a new size constraint, a new optimization should be performed.

Consequently, an immediate evolution of this work would be to consider cost and size as objectives in the design process. Industrial components are often optimized in cost and weight with a constraint on the size. This implies an increase of the number of objectives but this increase seems not to be too prohibitive. The main difficulty will be to display the results in a manner that allows clarity in terms of graphical view and analysis of the results.

As presented in the literature review, there are many architected materials that can be integrated as core material in a sandwich panel. Increasing the number of possible core architectures can be an interesting evolution. Core topology should become a design variable in the optimization process. It is not the case in the present work in which three optimizations were performed corresponding to the three selected topologies.

Including core topology as a design variable would be more efficient since the less promising topologies could be discarded during the optimization process. The optimal core topology would then be identified according to the set of requirements.

Based on the presented results, a potential design process can be summarized as follows:

- A first step in the design process for sandwich panels in a minimum weight approach could be to determine whether a stiff or a compliant core material is required.
- A second step is to determine the optimal material using the appropriate performance index. For bending-dominated structures, the most relevant performance indices are the ones corresponding to a beam in bending. For stretching-dominated structures, performance indices corresponding to a beam in tension are the most relevant ones.
- When core architecture and material are determined, the only core design variables to optimise are geometrical ones. Material selection and geometrical design could be separated using this approach. The advantage of doing so is to use more efficient optimization algorithm for the geometrical design and to reduce the size of the design problem by determining some design variables before running the calculations.

In another respect, the method has been developed for planar sandwich panels, which is an easy geometry to evaluate. The use of architected sandwich material, i.e. the integration of an architected material within two dense materials, is not only narrowed to planar geometries. As shown by Banhart and Seeliger for Aluminium foam, architected sandwich panels can be manufactured in 3-D complex shapes [BAN08]. There is no doubt that architected sandwich solutions can present a great interest in plenty of industrial applications involving components that do not exhibit a planar geometry.

However, to be able to run the optimization process on this kind of industrial applications, two main issues should be addressed: the manufacturability and the possibility to efficiently analyse the performances of the solution.

- In terms of manufacturability, layered materials with a complex 3-D shape can be difficult to bound. Banhart and Seeliger do present an interesting review of the possible ways to manufacture and form the sandwich panels. In-situ bonding techniques seem to be an efficient method to bond the faces to the core material. However, it implies that the face and core materials are chemically compatible for bonding and this technique is only possible for foam core panels.
Ex-situ bonding techniques such as using adhesive layers are common for sandwich panels. The main issue for these techniques is to be able to form the component without breaking the bound.
Beyond this, manufacturing core architectures like honeycombs and truss structures in another form than a planar geometry constitute a real challenge. Taking manufacturability into account could lead to optimal design made of easy-to-manufacture solutions such as foam core solutions. For real life applications, it seems of crucial interest to be able to take into account the manufacturability of the evaluated solutions. A manufacturing process which seems promising for the breakthrough of architected sandwich solutions with complex shapes is the additive manufacturing.
- Analysing the performances of heterogeneous components with a complex shape is hardly achieved by analytical expressions. More efficient tools are required such as

numerical simulations based on Finite Element Modelling (FEM). As presented in Chapter 6, using FEM requires special care in the optimization process. A promising outlook resides in homogenization techniques. Basically, homogenization consists of the determination of the effective properties of the core material in order to replace it by a dense homogenized material. Then, the complex inner geometry of the architected material is replaced by a block of material that possesses the same properties than the initial structure. Simplifying the geometry of the component is a key point to reach acceptable computational costs. The study of homogenization of architected materials is currently in progress [DIR12b].

Homogenization techniques could be coupled to Finite Element Modelling and used in a multi-level optimization process. A high-level would correspond to the component description with a Homogeneous Equivalent Medium replacing the architected material. The low-level would correspond to the architected material assessed using homogenization techniques in order to display the equivalent effective properties in the high-level.

For the present work, several classical specifications addressed by sandwich panels have been selected: flexural stiffness and strength, acoustic damping, thermal resistance, thermal insulation and finally blast mitigation. Sandwich panels could be emerging solutions for other applications. It has been demonstrated that sandwich panels are promising solutions for resistance against impact loading. This topic has been extensively studied in Kolopp's Ph.D. work [KOL12]. In a completely different field, Bollen et al. investigated the electromagnetic properties of sandwich panels. The authors developed a honeycomb core sandwich structure filled with a carbon nanotube reinforced polymer foam and glass fibre reinforced composite faces in order to combine high electromagnetic absorption and high flexural stiffness [BOL13].

The presented design method could be adapted and used for the optimization of such structures, although advanced dedicated numerical tools are required to evaluate the performances that would be considered. For instance, a dedicated model to predict the impact resistance of a sandwich panel submitted to impact loading is being developed based on Finite Element Analysis (in collaboration with the DADS department at ONERA) and could be used in the design process.

To conclude, the appropriate design technique for industrial purpose would certainly involve a multi-level approach. The first stage would be to use simple representative models in order to determine the most promising core topology and materials. Using these results, surrogate models can be built in order to perform a more accurate analysis on a reduced design space. A verification of the performances of the obtained optimal solutions can finally be performed using advanced numerical simulations or direct experiments as far as possible. Using this scheme, the cost of the analysis is inversely proportional to the size of the design space while the accuracy of the analysis is constantly increased.

Glossary

Acoustical Transmission Loss: Measurement of the capability of a panel of not transmitting an incident acoustic wave.

Performance space: Space displaying the performance of the solutions generated by the optimization algorithm.

Trade-off surface, Pareto front: Group of non-dominated solutions.

Symmetric coincidence frequency: Frequency at which the impedance of the symmetric motion matches the air impedance.

Sandwich effect (acoustic behaviour): This refers to a particular behaviour of soft core sandwich panels that take advantage of the softness of the core to exhibit a high Acoustical Transmission Loss in a given frequency range.

Mass law (acoustic behaviour): The mass law refers to the dependence of the Acoustical Transmission Loss on the mass of the panel.

Design space: Set of possible solutions in an optimization problem.

Pareto set optimization: Optimization using a dominance notion in order to rank the solutions according to their fitness.

Constraint: Limiting value for the optimization.

Objective: In an optimization problem, the objective defines the entity to be optimized.

Design variables: Set of variables that describe a solution.

Evolutionary algorithm: Optimization technique that mimics Darwin's theory of evolution. It is based on a fitness assessment and reproduction steps to create new individuals with advanced properties.

Genetic algorithm: Particular type of Evolutionary Algorithm using strings of number to code the genotype of individuals.

Design Of Experiments (DOE): Method for decreasing the number of experiments and for determining the effects and interactions of parameters on the observed property via combinatorial analysis.

LU decomposition: Mathematical method utilized in order to solve a problem of the form $Ax = y$ with A a square matrix.

Finite Element Modelling (FEM): Numerical technique for finding approximate solutions to boundary value problems.

Appendices

Contents

A. Additional case studies.....	252
B. Performance of the genetic algorithm.....	271
C. Design Of Experiments for acoustic damping.....	274

A. Additional case studies

a. A case of compatibility between specifications leading to a convex trade-off surface: flexural stiffness and thermal resistance specifications

Design space:

- Face materials: Metals, Polymers, and Composites.
- Face thickness: from 0.5 to 10 mm.
- Core materials: Metal foams, Ceramic foams, Polymer foams.
- Core thickness: from 10 to 500 mm.
- Type of sandwich panel: symmetrical.

Objectives:

- Flexural stiffness: minimize the central deflection of a 1 m span sandwich beam submitted to a 1 N in a three-point bending test.
- Thermal resistance: maximize the through thickness thermal resistance.
- Lightness: minimize the mass per unit area.

Constraints:

- Central deflection $< 10 \mu\text{m}$.
- Thermal resistance $> 1 \text{ m}^2\text{K/W}$.
- Mass per unit area $< 50 \text{ kg/m}^2$.

Compatibilities

The performance space plotting flexural stiffness as a function of thermal resistance is a borderline case. The whole Pareto front can be seen as a convex shape trade-off surface but locally it has a pointed shape which is due to compatibility between specifications. However, three main solutions arise from this trade-off surface. These solutions correspond to three different sub-domains. In each sub-domain, increasing stiffness is compatible with increasing thermal resistance until the boundaries of the sub-domain are reached. Even though the trade-off surface is rough, these two performances are compatible.

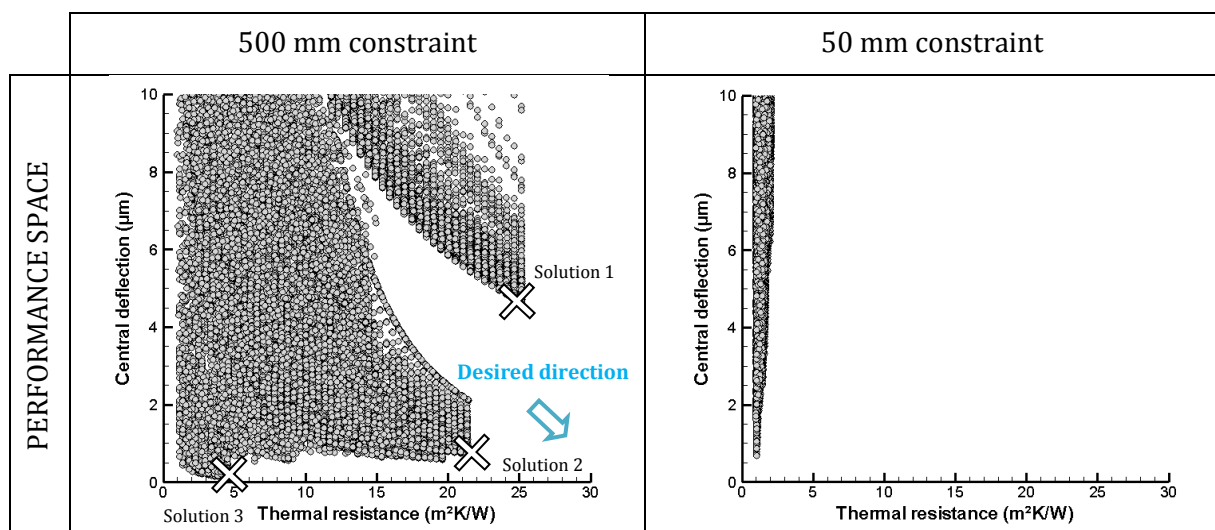


Figure A.1: Performance space for flexural stiffness and thermal resistance for two different size constraints.

Variability analysis

The performance space is clearly divided into three different parts corresponding to three different types of core materials as shown in Figure A.2:

- Phenolic foam (0.027 relative density) is the best one for thermal insulation. The best solution within this group is solution 1 which is made of a 490 mm thick Phenolic foam core with 2 mm silicon carbide faces. The obtained performances are a 25.14 m²K/W thermal resistance and a 4.65 µm deflection. This material has been identified as a promising material for thermal resistance in Chapter 4 Section 2.4.
- A second part of the performance space is composed of PVC foams. Several relative densities help tailor the trade-off between thermal resistance and stiffness. The stiffest solutions are made of a 0.039 relative density PVC foam (8.8 m²K/W and 0.57 µm) while the softest ones are made of a 0.0215 relative density PVC foam (21.32 m²K/W and 0.74 µm). This is the optimal material for stiffness as shown in Chapter 4 Section 2.1.
- The last optimal core material is glass foam which is the optimal choice for flexural stiffness with an optimal solution noted solution 3 with a 4.5 m²K/W thermal resistance and a 0.18 µm deflection. This material has also been identified as optimal material for stiffness as shown in Chapter 4 Section 2.1 but for very high stiffness requirements.

Thermal resistance and flexural stiffness are both proportional to core thickness. As a consequence the core thickness of solutions in the Pareto front is the maximum possible value regarding the density of the core material and the mass constraint of 50 kg/m².

Since almost all the thermal resistance is attributed to the core, optimal solutions are made of thin faces in order to maximize the ratio between core and face thickness. This is compatible with the stiffness requirements as most of the flexural stiffness comes from the gap between the faces.

Face material has a minor impact compared to the one of the core. However, stiff metallic faces will be the best choice for stiffness while low thermal conductivity ceramic faces will be on top for thermal insulation.

Effect of size constraint

Once again size constraint has a major influence on the achievable thermal resistance. The minimum deflection is raised from 0.18 to 0.67 µm. The trade-off surface obtained with the 50 mm thick constraint problem is more regular than the previous one but the same observations can be made.

Effect of mass as an objective

As shown in Figure A.3, mass constraint has a real effect on the performance space for very low value of accepted mass. For light sandwich panels, PVC foam core solutions are the optimal choice as Phenolic and glass foams vanish from the possible core material.

Optimal design of architected sandwich panels for multifunctional properties

Pierre Leite

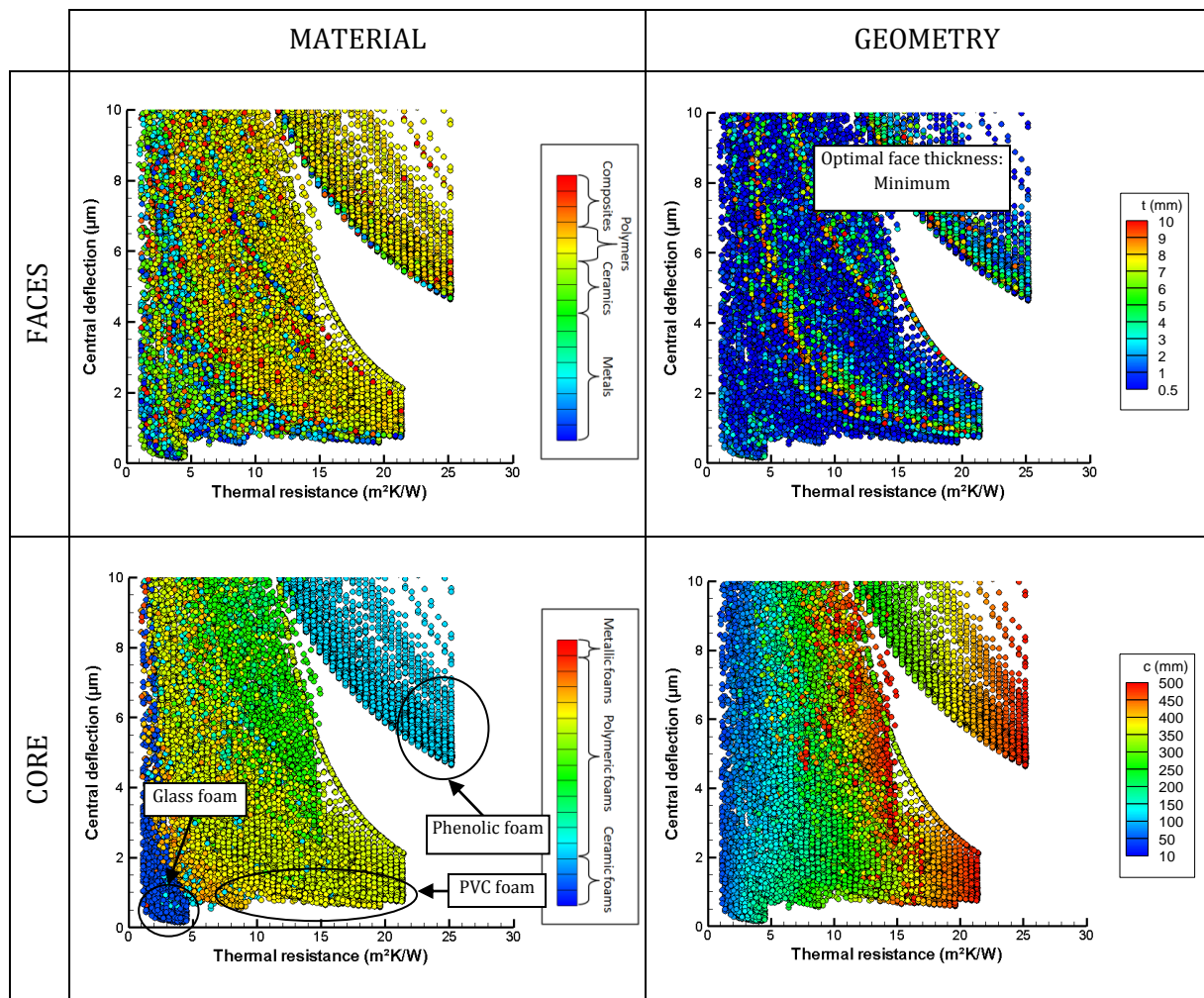


Figure A.2: Influence of design parameters on the optimal design of a sandwich panel for flexural stiffness and thermal resistance.

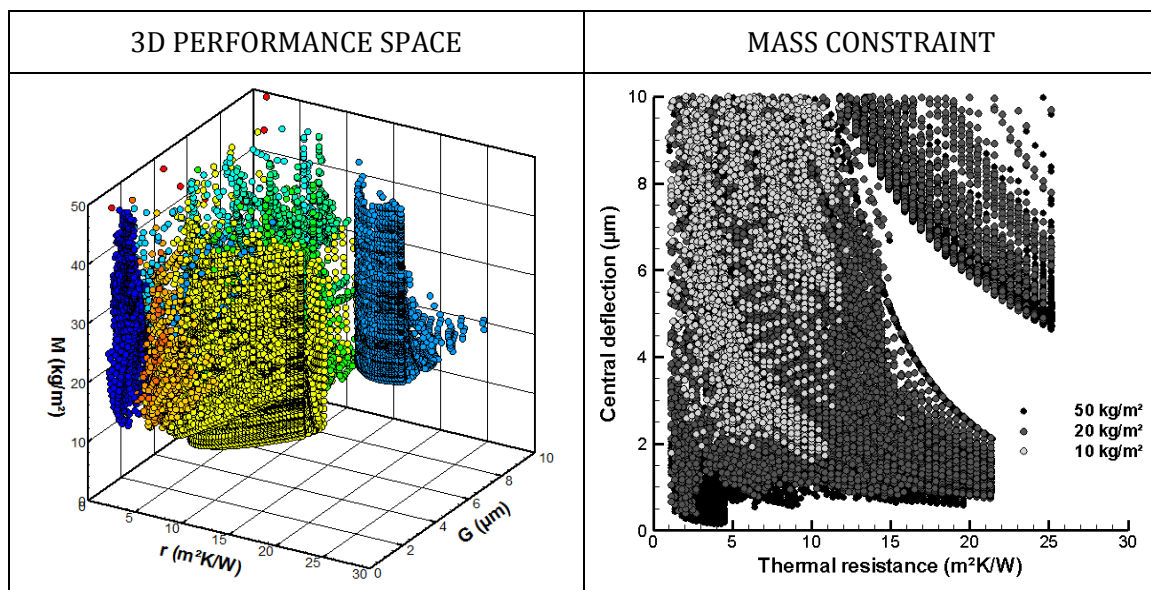


Figure A.3: On the left hand side: performance space for stiffness and thermal resistance at minimal weight. Colour legend represents core material. On the right hand side: evolution of the performance space for stiffness and thermal resistance as a function of mass constraint.

Effect of functional constraints

A value of $1 \text{ m}^2\text{K/W}$ for thermal insulation is not constraining regarding flexural stiffness as shown in Figure A.4. Increasing this constraint will mainly limit the flexural stiffness first by discarding glass foam from the optimal core material and finally by imposing Phenolic foam as the only optimal solution. The range of performances achieved by Phenolic foam core panels is tight, mainly due to the fact that for a $25 \text{ m}^2\text{K/W}$ thermal resistance, core thickness reaches the maximum possible value.

Regarding thermal insulation at a minimal weight, stiffness requirements limit the choice of core materials to Phenolic and PVC foam while melamine and PUR foams were optimal for thermal resistance. Then the trade-off surface is only composed of the sub-domain corresponding to Phenolic foam core sandwich panels or to PVC foam core ones when stiffness requirements is high.

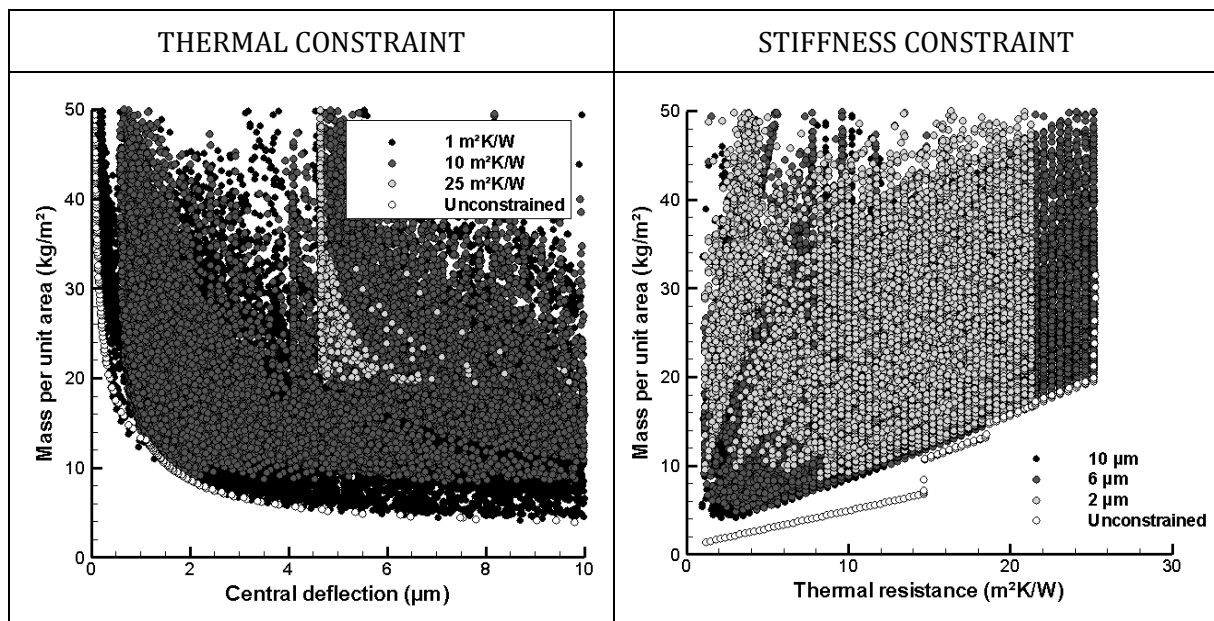


Figure A.4: On the left hand side: evolution of the performance space for stiffness at minimal weight as a function of thermal resistance constraint. On the right hand side: evolution of the performance space for thermal resistance at minimal weight as a function of stiffness constraint.

Advantage of sandwich solutions

Once again, these performances are compatible in terms of design guides and sandwich panels are better than solid plates for both flexural stiffness and thermal resistance.

b. A case of non-beneficial competition between specifications: flexural stiffness and strength

Design space:

- Face materials: Metals, Polymers, and Composites.
- Face thickness: from 0.5 to 10 mm.
- Core materials: Metal foams, Ceramic foams, Polymer foams.
- Core thickness: from 10 to 500 mm.
- Type of sandwich panel: symmetrical.

Objectives:

- Flexural stiffness: minimize the central deflection of a 1 m span sandwich beam submitted to a 1 N in a three-point bending test.
- Flexural strength: maximize the critical load corresponding to failure of a 1 m span sandwich beam submitted to a three-point bending test.
- Lightness: minimize the mass per unit area.

Constraints:

- Central deflection $< 10 \mu\text{m}$.
- Flexural strength $> 2 \text{ kN}$.
- Mass per unit area $< 50 \text{ kg/m}^2$.

Compatibilities

The compatibility between flexural stiffness and strength can be assessed using the performance space plotted in Figure A.5. It exhibits a pointed shape. For a large range of performances, increasing both strength and stiffness is possible. However, for very high stiffness requirements, corresponding to a deflection lower than $1 \mu\text{m}$, the Pareto front has a concave shape.

Two main solutions can be given as optimal solutions. The first one corresponds to the strongest sandwich panel, with a strength of 31.5 kN and a deflection of $1.19 \mu\text{m}$. The second one is the stiffest solution with a strength of 7.5 kN and a deflection of $0.18 \mu\text{m}$.

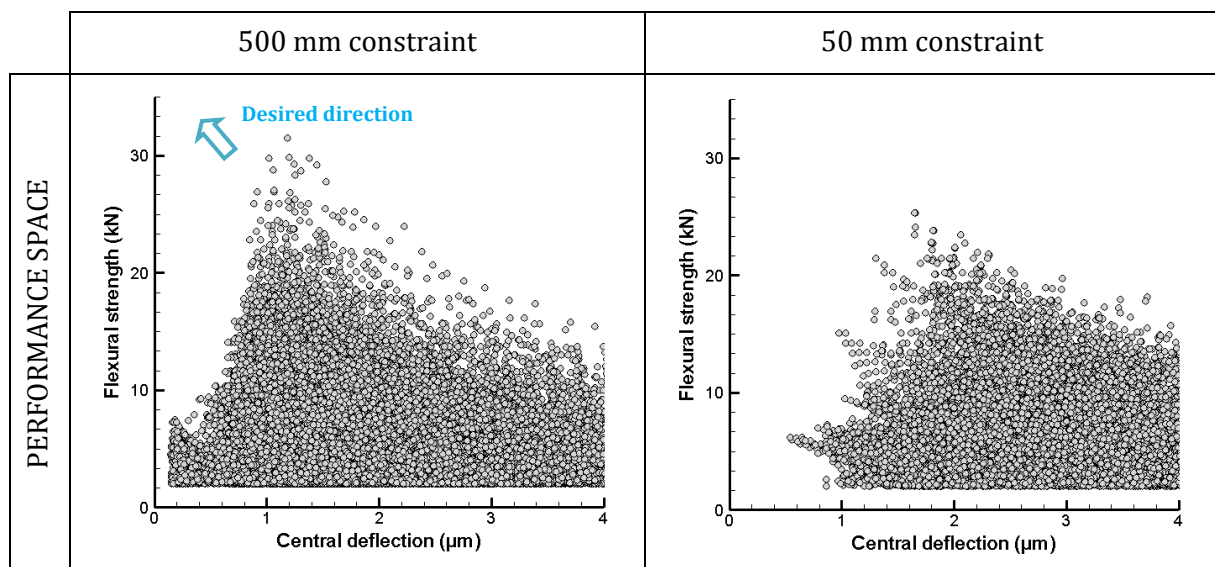


Figure A.5: Performance space for flexural stiffness and strength for two different size constraints.

Variability analysis

As shown in Figure A.6, the Pareto front is shared between three different core materials being PVC foams, alumina foam and glass foam, from the strongest to the stiffest respectively. Aluminium composite (Al-60%C) overcomes all other solutions as face material in almost all the Pareto front except for Alumina foam core solutions. The optimal choice as face material for Alumina foam core panels is a Duralcan MMC (Al-20%SiC) which is stiffer than Al-60%C. The optimal face thickness is 5 mm.

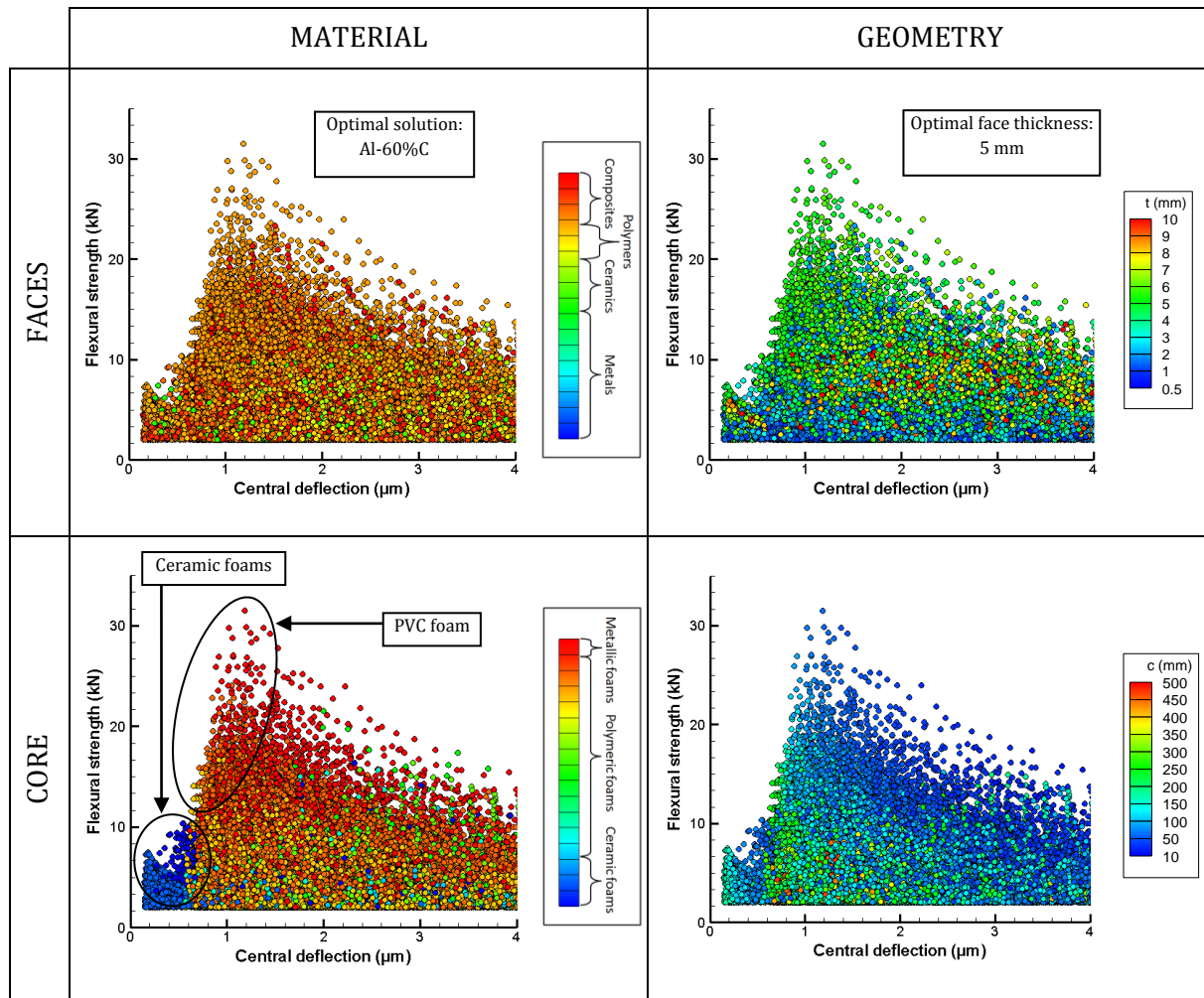


Figure A.6: Influence of design parameters on the optimal design of a sandwich panel for flexural stiffness and strength.

The aspect of the Pareto front is mainly due to the mass constraint. As shown in Figure A.6, core thickness has an influence on stiffness given that increasing the distance between the faces leads to an increase of the inertial moment, and thus to the increase of flexural stiffness. The optimal solution corresponding to the strongest design is made of a 60 mm PVC foam core (0.214 relative density) and 5 mm Aluminium composite face sheets panel. The weight of this solution is approximately 50 kg/m². To increase the flexural stiffness, core thickness has to be increased. To keep the weight under the constraint, foam relative density is reduced. This leads to a better stiffness but to a worse strength.

Optimal design of architected sandwich panels for multifunctional properties

Pierre Leite

There is a competition between geometrical requirements and material requirements in the design of the core. Strength is driven by the compressive strength and shear strength of the core while stiffness is driven by its thickness.

The optimal glass foam core solution is a 150 mm core with 5 mm Aluminum composite and it represents the stiffest solution within the chosen range of design variables.

To conclude on the compatibility between strength and stiffness, a trade-off is needed only when very high stiffness is required. Moreover, by being a ceramic based foam, glass foam is fragile. No consideration has been given on the toughness of solutions but for mechanical applications, this aspect could be an issue.

Effect of size constraint

Size constraint has a noticeable influence on the performance space, both on the range of achievable performances and on the trade-off surface. The performance space can be divided into several sub-domains considering the 50 mm thick sandwich panels with a sharp-pointed form pointing at the top left of the figure. This particular behaviour is translated into a slightly convex Pareto front composed of few points that are the solutions at the end of the peak.

This situation can be interesting in terms of trade-off given that a few solutions are considered as Pareto optimal and that they give different possibilities in terms of performances. However, the robustness of these solutions can be seen as an issue. A dense trade-off surface is preferable.

Effect of mass as an objective

When light panels are required, the shape of the trade-off surface between stiffness and strength passes from concave to linear as shown in Figure A.7. There are still different sub-domains corresponding to glass and PVC foam core solutions but Alumina foam core panels vanishes from the performance space quite quickly.

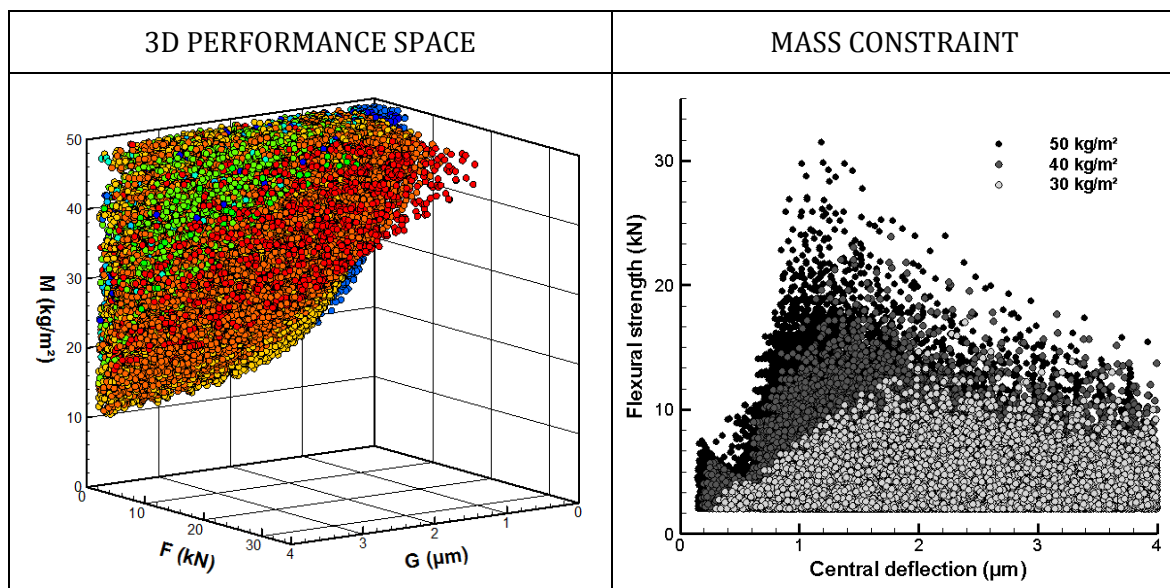


Figure A.7: On the left hand side: performance space for stiffness and strength at minimal weight. Colour legend represents core material. On the right hand side: evolution of the performance space for stiffness and strength as a function of mass constraint.

Effect of functional constraints

Strength requirements lead to designs with increased face thickness as shown previously. In terms of flexural stiffness at minimal weight, this leads to an increase of mass for a given stiffness as shown in Figure A.8. For high strength requirements, PVC foam is the optimal choice as core material and then the corresponding trade-off surface is only composed of PVC foam core panels.

On the other hand, flexural stiffness requires thick core material. This increase in thickness is balanced by a reduction of face thickness in order to satisfy mass constraints. In that case, strength is reduced as shown in Figure A.8.

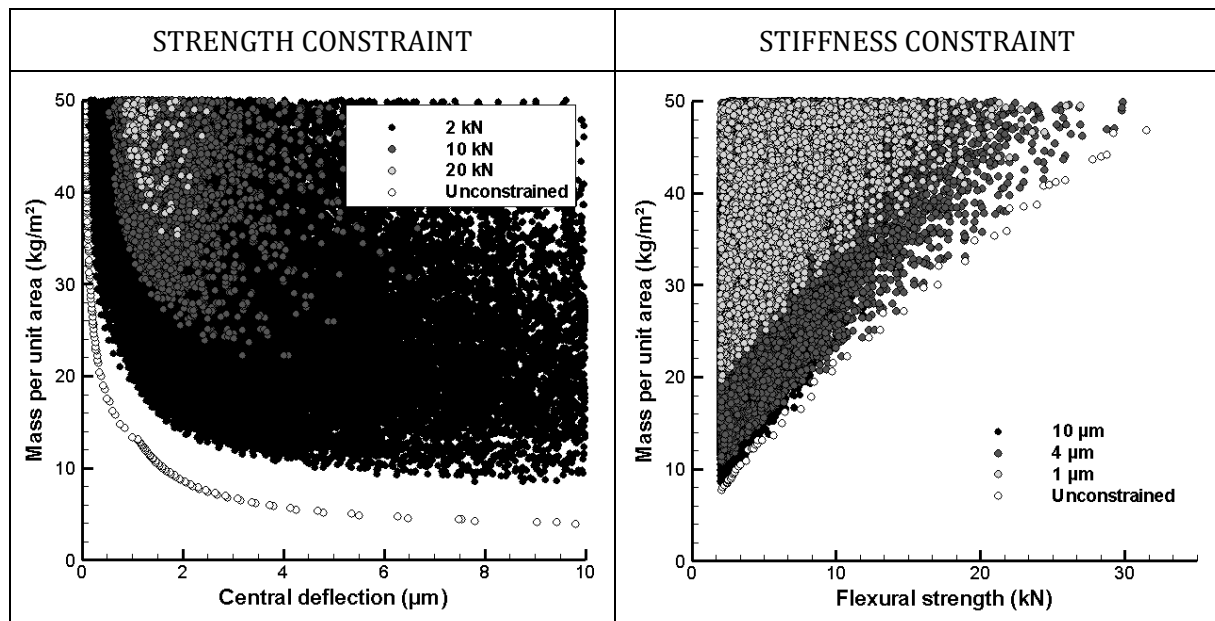


Figure A.8: On the left hand side: evolution of the performance space for stiffness at minimal weight as a function of strength constraint. On the right hand side: evolution of the performance space for flexural strength at minimal weight as a function of stiffness constraint.

Advantage of sandwich solutions

In Figure A.9 is represented the property chart corresponding to the performance indices of stiffness and strength at minimum weight of plates, $\rho/E^{1/3}$ and $\rho/\sigma^{1/2}$ respectively. The indices are written in such a way that optimizing performances requires a minimization of the performance indices. As shown, sandwich panels can exhibit far better performances than monolithic plates.

The results obtained are consistent with a performance index approach as shown in Figure A.9 in which PVC foam appears to be the optimal choice as core material.

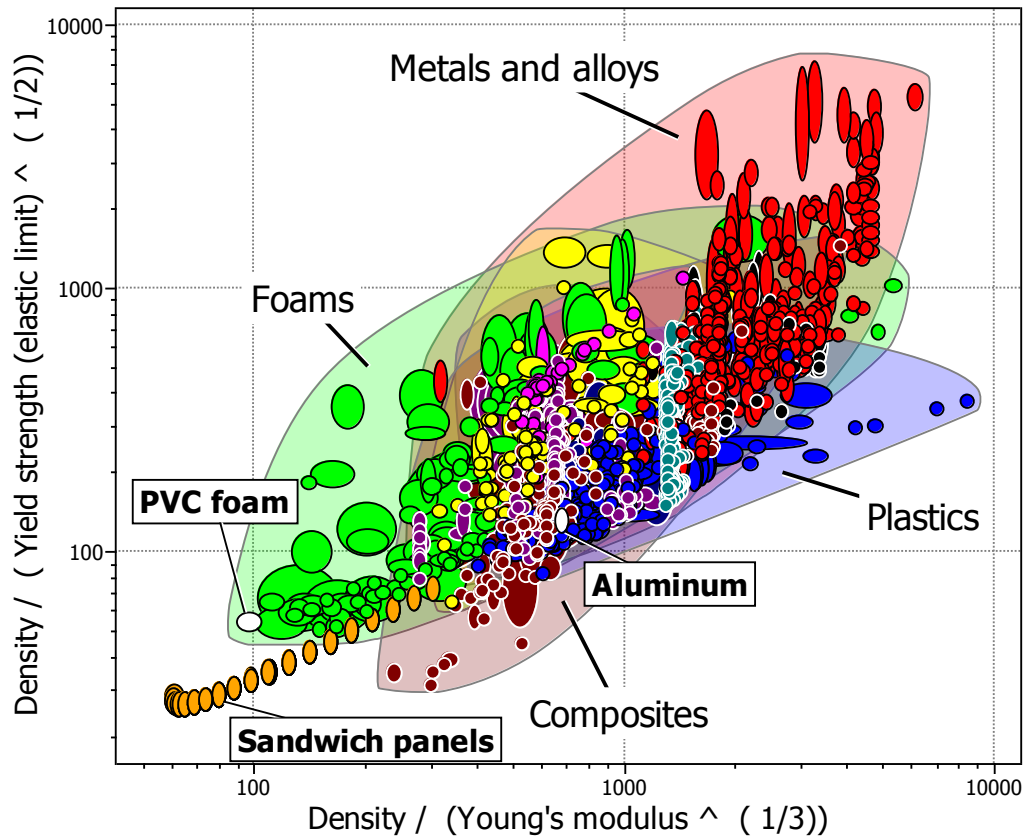


Figure A.9: Property chart plotting materials as a function of performance indices corresponding to strength at a minimal weight (vertical axis) and stiffness at a minimal weight (horizontal axis).

c. A case of incompatibility between specifications: flexural strength and acoustic damping

Design space:

- Face materials: Metals, Polymers, and Composites.
- Face thickness: from 0.5 to 10 mm.
- Core materials: Metal foams, Ceramic foams, Polymer foams.
- Core thickness: from 10 to 500 mm.
- Type of sandwich panel: symmetrical.

Objectives:

- Flexural strength: maximize the critical load corresponding to failure of a 1 m span sandwich beam submitted to a three-point bending test.
- Acoustic damping: maximize the mean value of the Acoustical Transmission Loss in the frequency range [1 000; 4 000] Hz.
- Lightness: minimize the mass per unit area.

Constraints:

- Flexural strength > 2 kN.
- Acoustical Transmission Loss > 20 dB.
- Mass per unit area < 50 kg/m².

Compatibilities

The obtained performance space for the bi-objective optimization problem involving acoustic damping and flexural strength is given in Figure A.10. As can be seen, the trade-off surface is very rough. Several solutions emerge, corresponding to different sub-domains pointing out on the Pareto front. However, only the solutions at the limits of the Pareto front are worthwhile in terms of trade-off even though some other solutions could emerge if additional constraints are set on the performances.

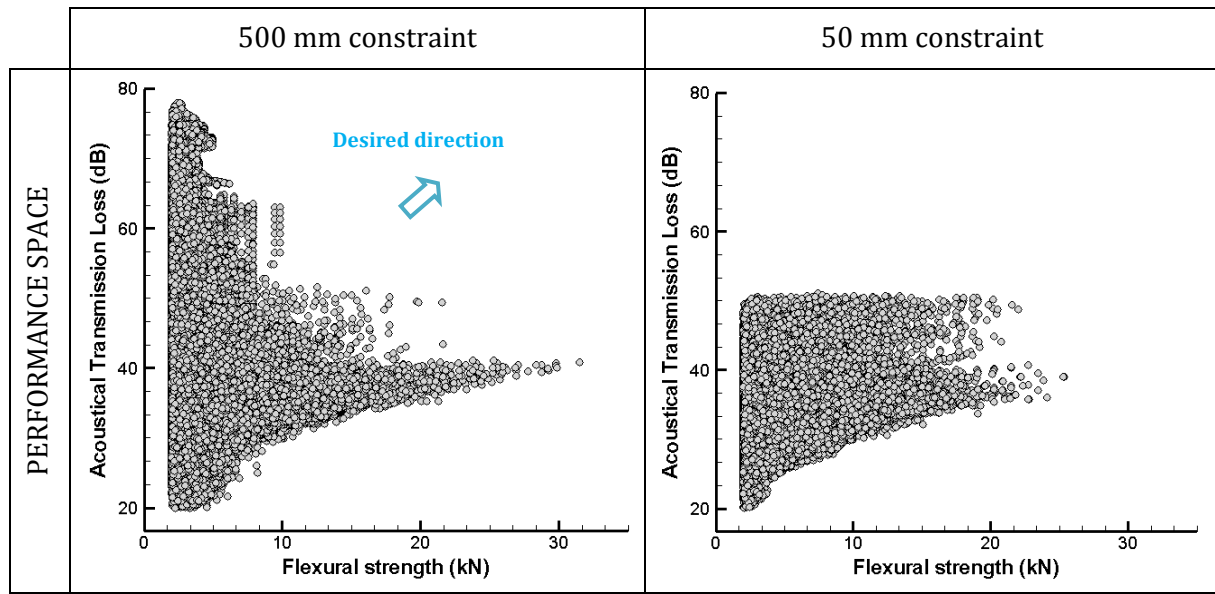


Figure A.10: Performance space for flexural strength and acoustic damping for two different size constraints.

Variability analysis

The performance space can be divided into two groups regarding the considered performances. A first group composed of solutions with good flexural strength and a second one composed of solutions with good Acoustical Transmission Loss.

Within the first group, two main core materials can be found on the Pareto front. The optimal core material for flexural strength is PVC foam of 0.214 relative density. The corresponding solutions are made of Aluminium alloy (7075) with a thickness between 5 and 5.5 mm. Core thickness reaches an optimal value of 60 mm for a 31.48 kN strength. Decreasing the flexural strength is achieved by decreasing foam relative density and core thickness as shown in Figure A.11.

The other solutions found in this group gather sandwich panels with a dense Polypropylene foam core. With a relative density of 0.62, a density of 620 kg.m⁻³ and a plateau stress of 13 MPa, this foam has a less interesting specific strength than the PVC foam (density of 257 kg.m⁻³ and plateau stress of 5.8 MPa). Moreover, the performance index for strong plates is the ratio between the square root of the yield strength and the density. The chosen PVC foam has a 9.4 performance index while the Polypropylene foam performance index is 5.8. Nevertheless, the latter is also softer which makes it a better candidate for sound insulation than the PVC foam. The strongest Polypropylene foam core solution is made of thin Chromium steel faces (1.5 mm thick) and has a 40 mm core thickness. This solution exhibits a 21.5 kN strength and a 49.43 dB transmission loss. Some Polypropylene foam core with Aluminium faces solutions are also observed on the Pareto front.

The second group, made of solutions with a high Acoustical Transmission Loss, is composed of very soft foam core sandwich panels. Solutions on the Pareto front are made of 3 mm Chromium Steel faces and of different Polystyrene foam core. The best solution for sound insulation is a 200 mm thick 0.019 relative density PS foam core. Increasing core thickness decreases transmission loss until reaching the 50 kg.m⁻² weight constraint. Increasing foam relative density increases the flexural strength but decreases the transmission loss.

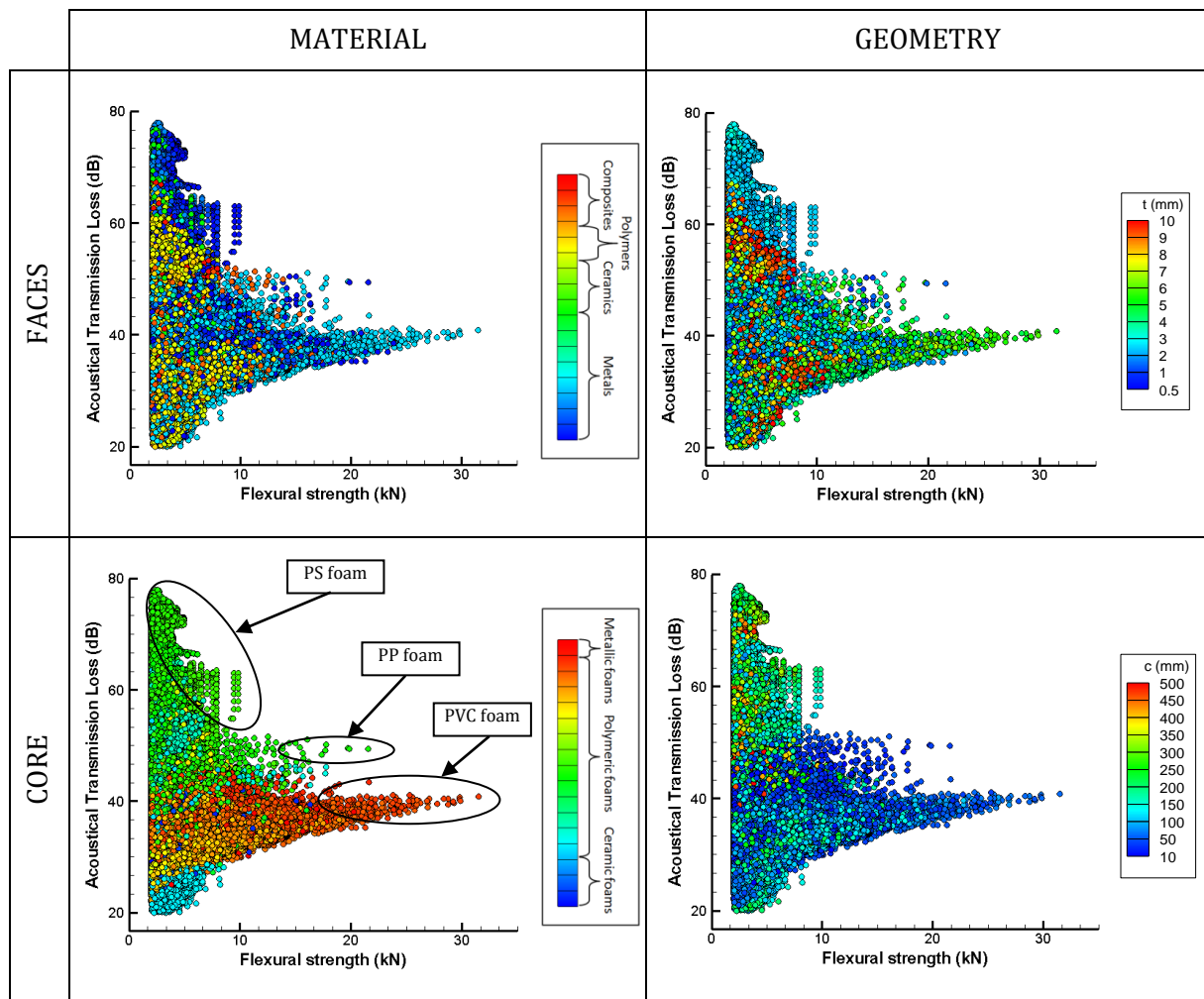


Figure A.11: Influence of design parameters on the optimal design of a sandwich panel for flexural strength and acoustic damping.

Effect of size constraint

The size constraint mainly limits the range of achievable Acoustical Transmission Loss while maximum flexural strength is only slightly reduced (from 31.48 to 25.35 kN). Acoustical Transmission Loss is limited at 51.02 dB while it can attain 77.9 dB for a 500 mm thick constrained panel. This limitation comes from the poor strength of the PS foams. Figure 4.54 shows the evolution of the flexural strength as a function of core thickness for a PS foam (0.019) core sandwich panel with 2.5 mm Steel faces. For a core thickness under 65 mm the strength is below the constraint of 2 kN. For thin sandwich panels, flexural strength and Acoustical Transmission Loss lead to comparable optimal designs.

Effect of mass as an objective

As shown in Figure A.12, mass constraint has a major impact on achievable performances, particularly on strength. Although, the overall shape of the trade-off surface remains likewise as there are still two different groups of solutions according to the two different required performances. In general, PVC foam is the optimal choice for flexural strength while PS foam is the one for Acoustical Transmission Loss.

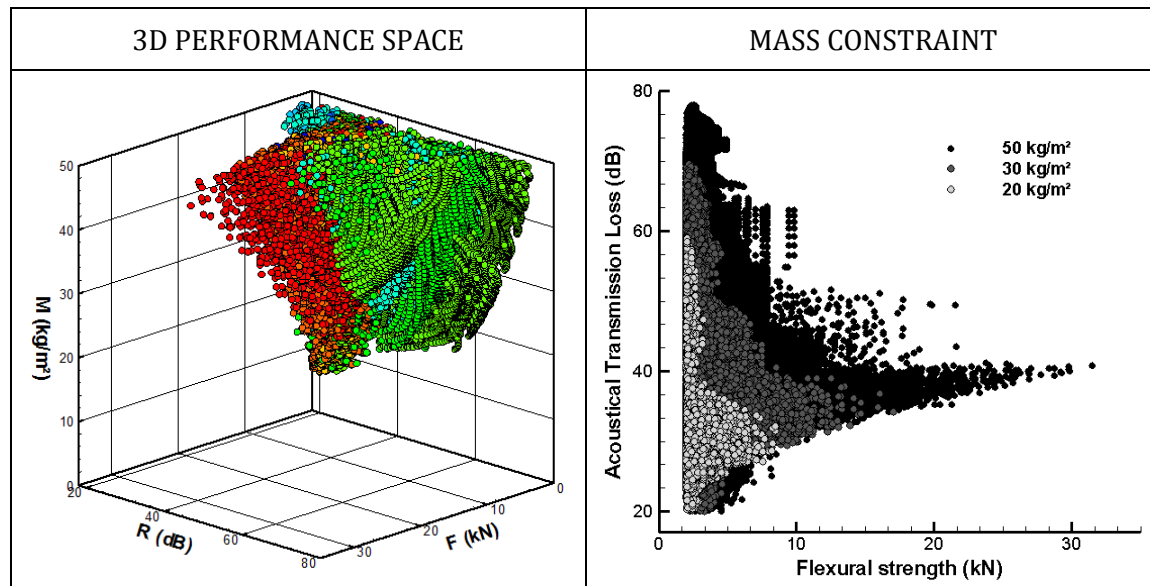


Figure A.12: On the left hand side: performance space for flexural strength and acoustic damping at minimal weight. Colour legend represents core material. On the right hand side: evolution of the performance space for strength and acoustic damping as a function of mass constraint.

Effect of functional constraints

Strength constraint mainly influences core material selection, discarding PUR foam of the performance space and thus imposing PS and PVC foams as optimal choices. The Acoustical Transmission Loss is dramatically limited by strength requirements.

Similarly, for an Acoustical Transmission Loss constraint higher than 40 dB, PVC foam is discarded as optimal core material leading to a deterioration of strength properties. Acoustical properties has no effect on strength for Acoustical Transmission Loss requirements under 40 dB as shown in Figure A.13.

Advantage of sandwich solutions

In this case, the two considered performances present compatible geometrical requirements. The core is to be relatively thin and the faces relatively thick, depending on the constitutive material. The major difference comes from the requirements in terms of core material. For acoustic damping, a soft core is required in order to allow the occurrence of symmetric vibration modes. In addition, the Acoustical Transmission Loss follows a “mass law”. On the contrary, flexural strength requires strong core material. Then, the only real trade-off is to choose between soft or strong foam, leading to a design driven by acoustical or strength requirements.

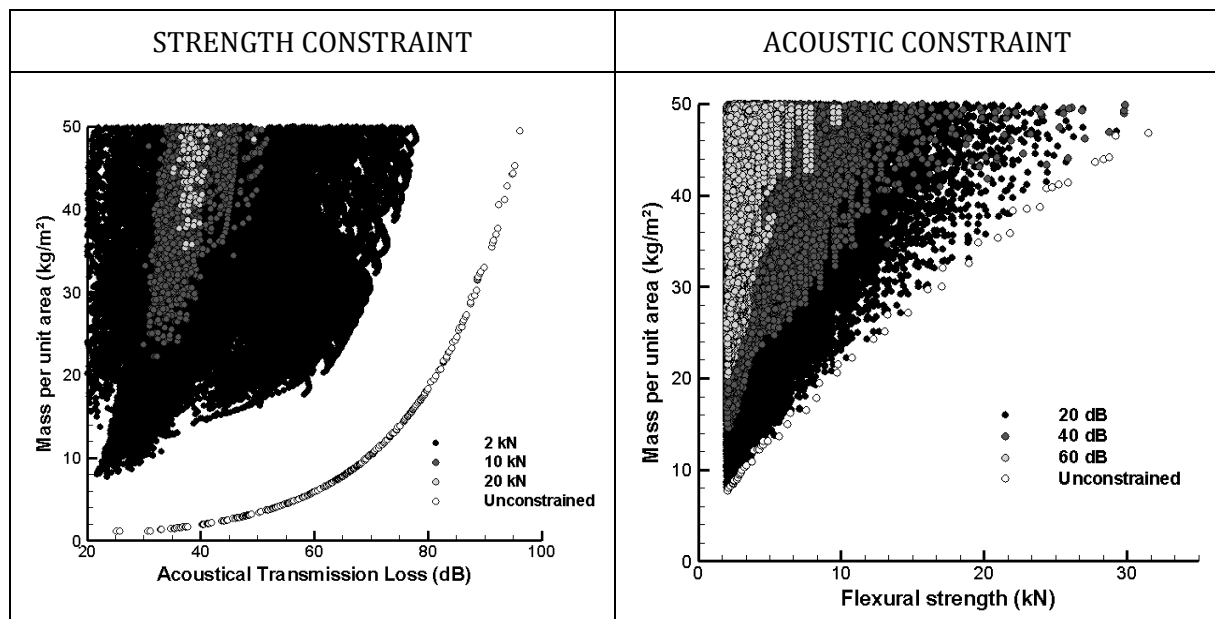


Figure A.13: On the left hand side: evolution of the performance space for acoustic damping at minimal weight as a function of strength constraint. On the right hand side: evolution of the performance space for flexural strength at minimal weight as a function of acoustic constraint.

d. A case of compatibility between specification: blast resistance and flexural stiffness

Design space:

- Face materials: Metals, Polymers, and Composites.
- Face thickness: from 0.5 to 10 mm.
- Core materials: Metal foams, Polymer foams.
- Core thickness: from 10 to 500 mm.
- Type of sandwich panel: symmetrical.

Objectives:

- Blast resistance: minimize the normalized back deflection which is the central deflection of the back face normalized by the span of the panel when the panel is submitted to a blast impulse of 10^4 Nsm^{-2} .
- Flexural stiffness: minimize the central deflection of a 1 m span sandwich beam submitted to a 1 N in a three-point bending test.
- Lightness: minimize the mass per unit area.

Constraints:

- Normalized back deflection $< 0.2 \text{ m/m}$.
- No face failure.
- Central deflection $< 10 \mu\text{m}$.
- Mass per unit area $< 50 \text{ kg/m}^2$.

Compatibilities

Instinctively, flexural stiffness and blast mitigation should be compatible in a way that increasing one should lead to increasing the other one. As shown in Figure A.14, this is quite true as the performance space is formed as a tip pointed at the bottom left of the plot, which

represents the direction of best performances. The obtained trade-off surface has a convex shape which is very close to a right angle. Two solutions arise. The stiffest one exhibits a $0.65 \mu\text{m}$ deflection for a three-point bending test and a normalized deflection of 0.028 m/m while the other one has a $1.17 \mu\text{m}$ deflection for a three-point bending test and a 0.026 m/m normalized deflection after blast loading. These two solutions are very close in terms of performances.

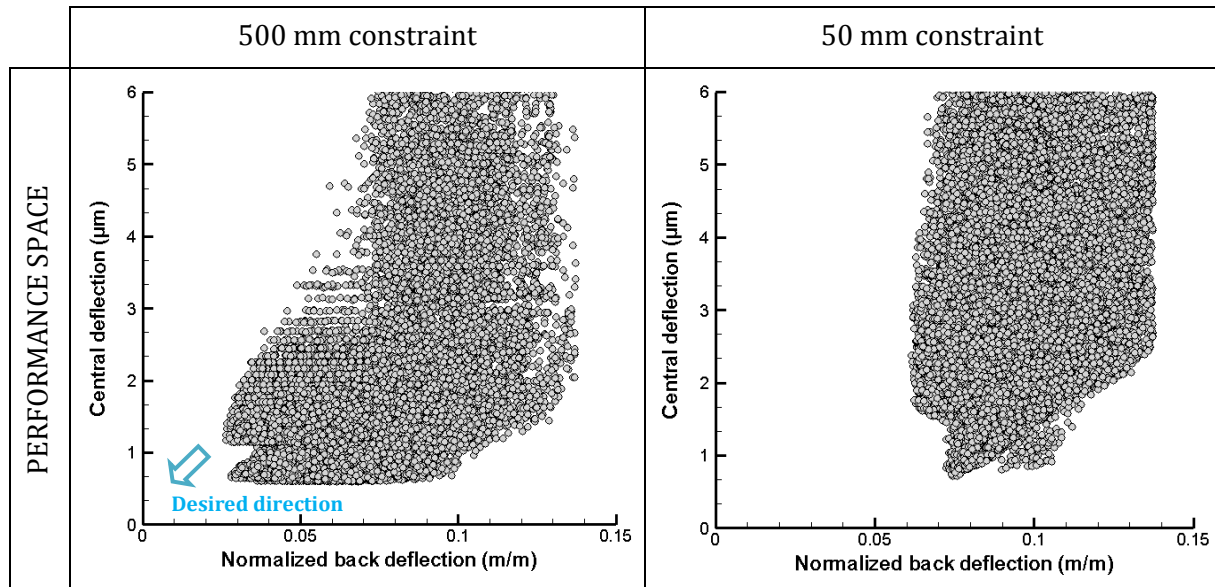


Figure A.14: Performance space for blast resistance and flexural stiffness for two different size constraints.

Variability analysis

The two solutions previously mentioned correspond to two different core materials. The stiffest one corresponds to a 410 mm thick PVC foam core solution with a 1.5 mm Aluminum composite (Al-60%C) faces. The second one is a 480 mm thick PS foam core sandwich panel with the same faces. As shown in Figure A.15, Carbon reinforced Aluminum is the optimal choice for face material. The optimal face thickness is around 1.5 mm.

The higher the core thickness is, the better the solution is for both stiffness and blast mitigation.

Effect of size constraint

Reducing the possible thickness of the panel from 500 to 50 mm has a major effect on the achievable blast mitigation of the solutions, increasing the minimum normalized deflection from 0.026 to 0.06 m/m . Flexural stiffness being less sensitive than blast mitigation, then the trade-off surface mainly retracts itself in the horizontal axis by reducing the possible thickness of the panel.

Effect of mass as an objective

The evolution of the trade-off surface between blast mitigation and flexural stiffness as a function of mass can be extracted from Figure A.16. The overall shape of the performance remains similar with the two sub-domains corresponding to PS and PVC foams as core material. For light panels, below about 32 kg/m^2 , there is no sandwich effect for blast mitigation. This transition in the behaviour has been discussed previously for the design of panels for blast mitigation at a minimal weight.

Optimal design of architected sandwich panels for multifunctional properties

Pierre Leite

The deterioration of the performances is due to a reduction of core thickness in order to decrease mass. However, stiffness of PVC foam core solutions is preserved by increasing foam density and thus foam stiffness.

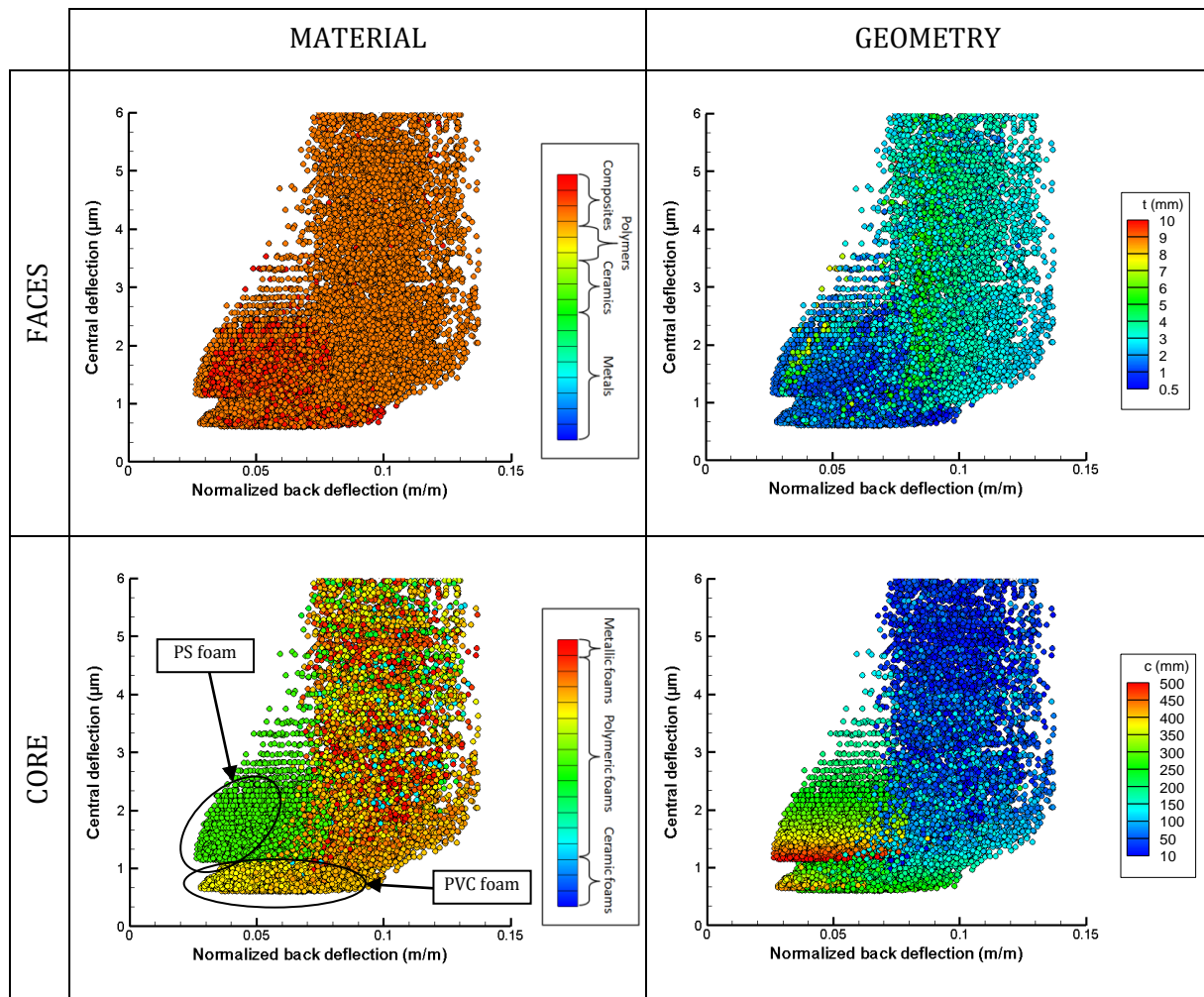


Figure A.15: Influence of design parameters on the optimal design of a sandwich panel for blast resistance and flexural stiffness.

Effect of functional constraints

Blast mitigation requires faces able to sustain high loads. In terms of design for flexural stiffness, this is translated by a limitation in the achievable lightness as shown in Figure A.17. The optimal choice as core material for flexural stiffness is PVC foam.

As shown in Figure A.17, stiffness requirements have a minor effect on blast mitigation at minimal weight. PS foam is slightly better than PVC foam for that performance. The limitation in terms of mass for high stiffness requirements comes from the fact that thick core is needed and implies a mass higher than 35 kg/m^2 for a $1 \mu\text{m}$ constraint.

Advantage of sandwich solutions

As related by Xue and Hutchinson [XUE03], a sandwich panel optimally designed would be more weight efficient for blast mitigation than solid plates. As flexural stiffness requirements are compatible with blast resistance ones, sandwich panels are better candidates than solid plates as soon as these performances are required.

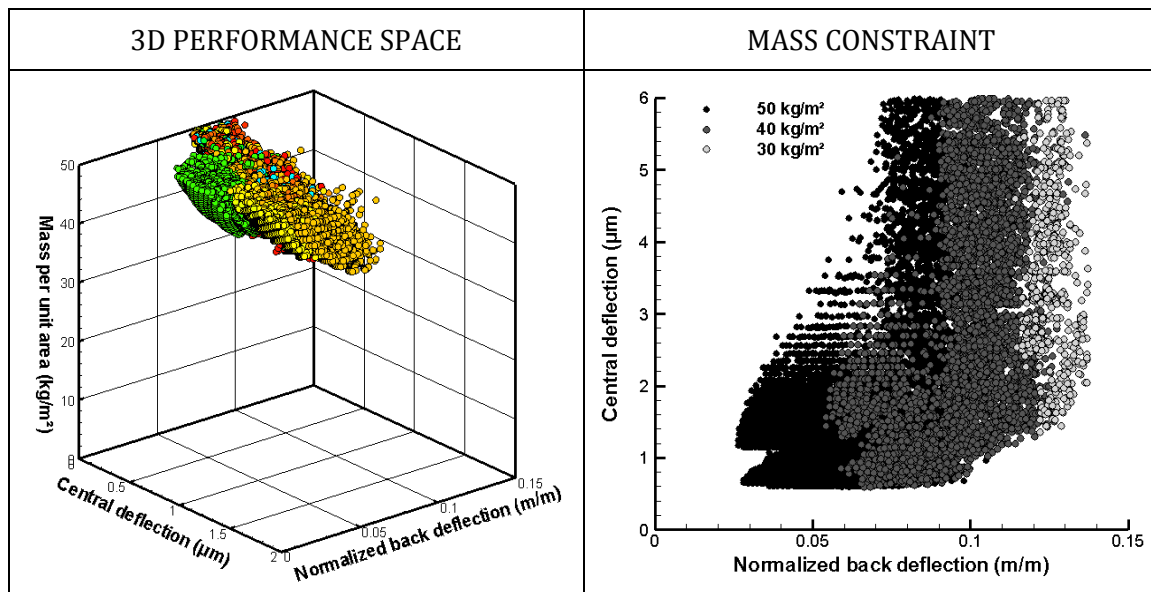


Figure A.16: On the left hand side: performance space for blast resistance and flexural stiffness at minimal weight. Colour legend represents core material. On the right hand side: evolution of the performance space for blast resistance and stiffness as a function of mass constraint.

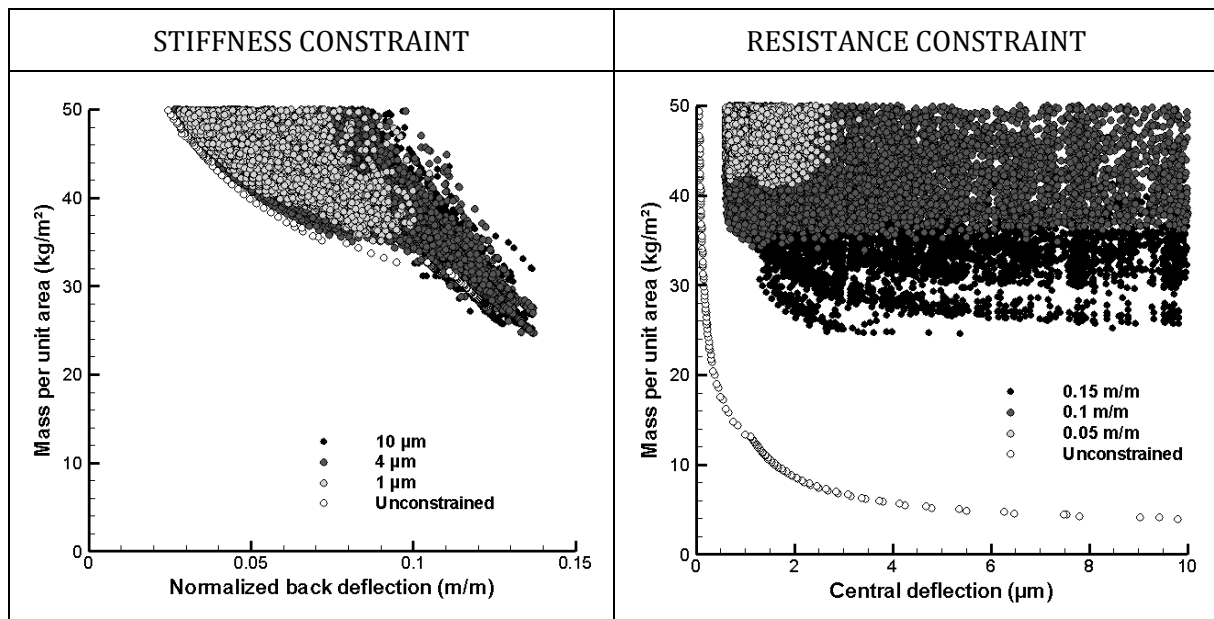


Figure A.17: On the left hand side: evolution of the performance space for blast resistance at minimal weight as a function of stiffness constraint. On the right hand side: evolution of the performance space for flexural stiffness at minimal weight as a function of blast resistance constraint.

e. A case of compatibility between specification: blast resistance and flexural strength

Design space:

- Face materials: Metals, Polymers, and Composites.
- Face thickness: from 0.5 to 10 mm.
- Core materials: Metal foams, Polymer foams.
- Core thickness: from 10 to 500 mm.
- Type of sandwich panel: symmetrical.

Objectives:

- Blast resistance: minimize the normalized back deflection which is the central deflection of the back face normalized by the span of the panel when the panel is submitted to a blast impulse of 10^4 Nsm^{-2} .
- Flexural strength: maximize the critical load corresponding to failure of a 1 m span sandwich beam submitted to a three-point bending test.
- Lightness: minimize the mass per unit area.

Constraints:

- Normalized back deflection $< 0.2 \text{ m/m}$.
- No face failure.
- Flexural strength $> 2 \text{ kN}$.
- Mass per unit area $< 50 \text{ kg/m}^2$.

Compatibilities

The optimization of a sandwich panel for blast mitigation and flexural strength gives the performance space which is illustrated in Figure A.18. The obtained Pareto front is slightly convex but is very close to a straight shape. Optimal solutions can be restricted to the two limit solutions with performances of 33.62 kN and 0.133 m for the first one and 7.9 kN and 0.049 m for the second one.

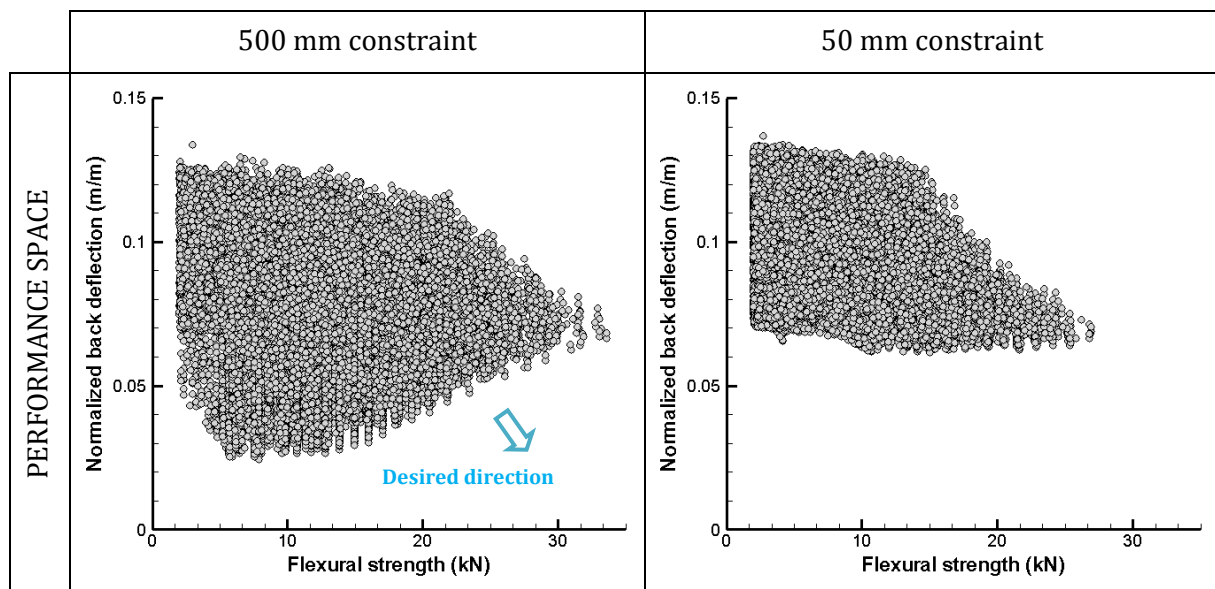


Figure A.18: Performance space for blast resistance and flexural strength for two different size constraints.

Variability analysis

As shown in Figure A.19, the optimal face sheet is a 1.5 mm Al-60%C. Regarding the core material, the trade-off surface is divided between PS and PVC foams. Increasing core thickness leads to an improvement of blast mitigation. PS foam is the best choice for blast mitigation. In terms of flexural strength, the dominant failure mode for thick panels is indentation. In this case, in order to increase flexural strength, an increase in core compressive strength is required, leading to an increase in foam relative density. To satisfy mass constraint, this increase in relative density comes along with a reduction of core thickness as shown in Figure A.19. This leads to the deterioration of blast mitigation.

PVC foams are preferred for high strength requirements as PS foam relative density is limited to 0.049. PVC foam relative density can go up to 0.214. The switch between PS and PVC foam is made between a 0.049 relative density PS foam and a 0.054 relative density PVC foam.

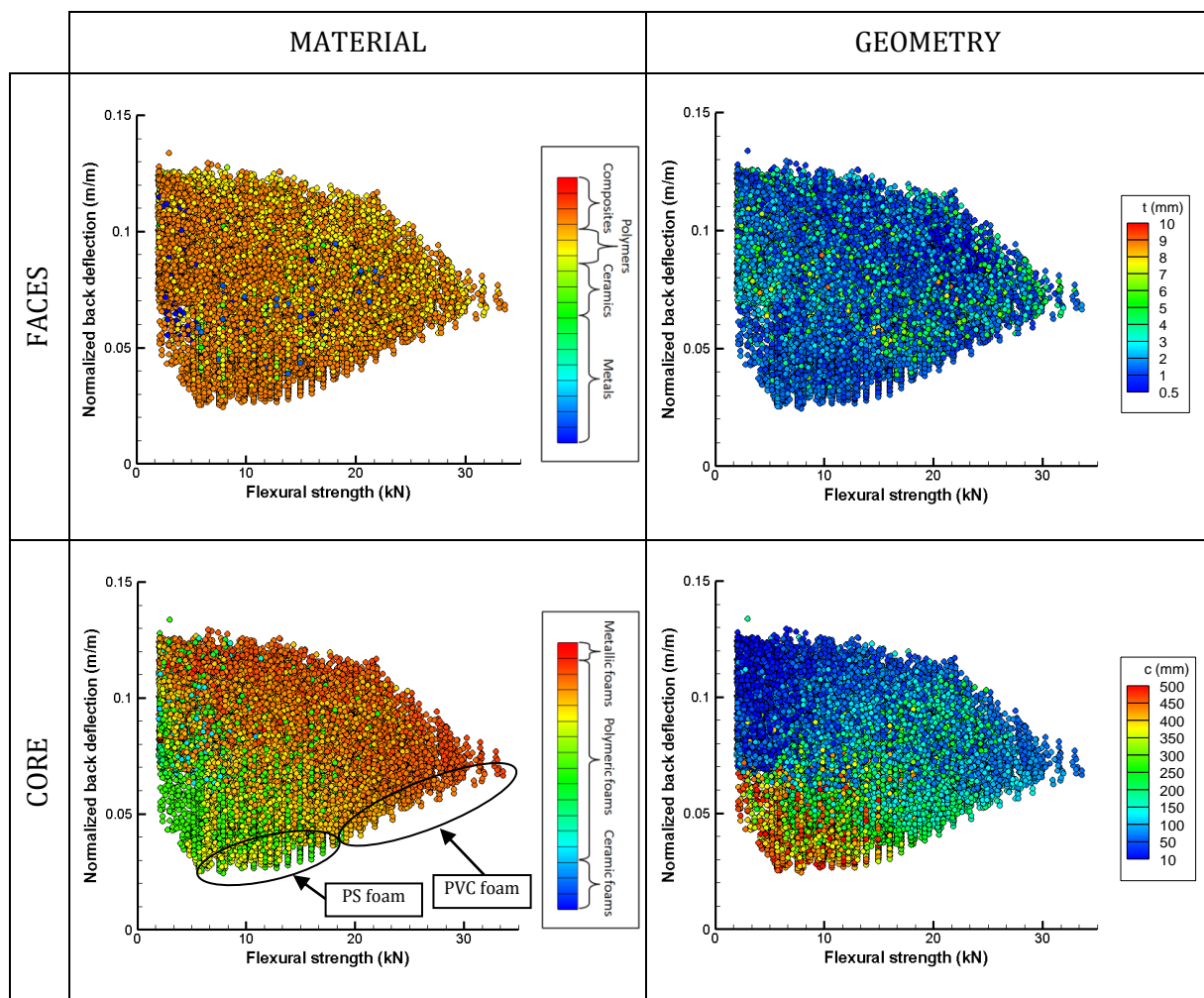


Figure A.19: Influence of design parameters on the optimal design of a sandwich panel for blast resistance and flexural strength.

Effect of size constraint

Size constraint has an influence on the achievable performances but is also translated in a change on the Pareto front shape. In terms of flexural strength, limitations in core thickness lead to a design for which the dominant failure is core shear instead of indentation as before. Increasing strength is mainly made by increasing core thickness and strength. Then,

Optimal design of architected sandwich panels for multifunctional properties

Pierre Leite

requirements in terms of materials selection and geometrical design are compatible between flexural strength and blast mitigation as shown in Figure A.20. This leads to a performance space with a pointed form.

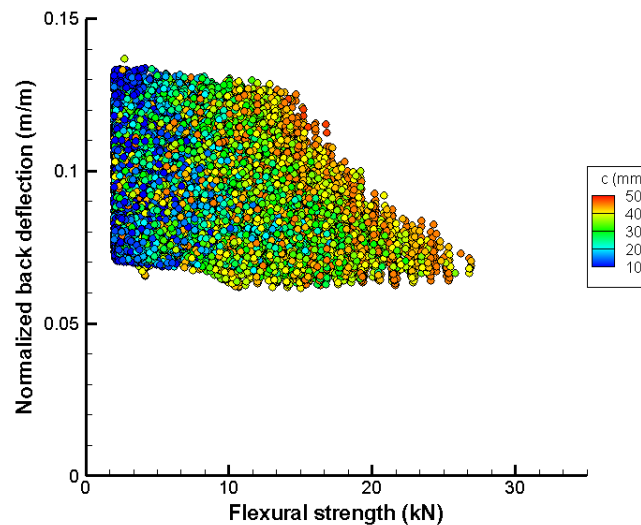


Figure A.20 Influence of core thickness on the performance space considering a 50 mm core thickness constraint.

Effect of mass as an objective

As shown in Figure A.21, mass constraint has an impact on the achievable performances but the shape of the trade-off surface remains the same, except for very light solutions. When mass constraint is very tough, the sandwich effect vanishes regarding blast mitigation. A decrease in mass is mainly achieved by a decrease in core thickness. Except for very light panels, the optimal choices as core material are PS and PVC foams.

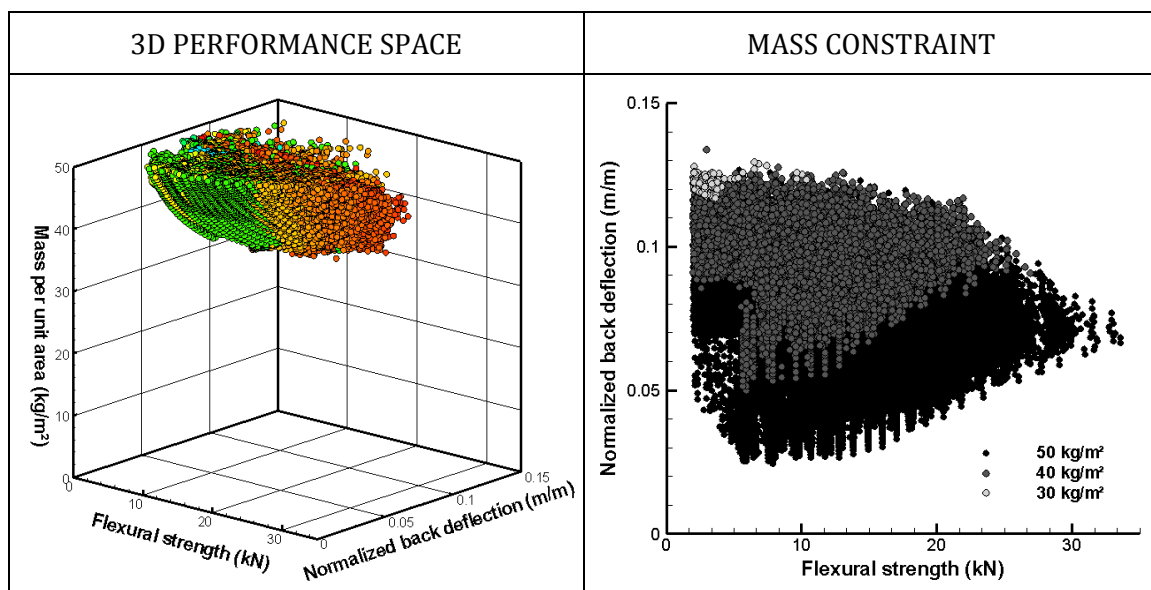


Figure A.21: On the left hand side: performance space for blast resistance and flexural strength at minimal weight. Colour legend represents core material. On the right hand side: evolution of the performance space for blast resistance and flexural strength as a function of mass constraint.

Effect of functional constraints

As shown previously, optimal design for blast mitigation and strength requirements are alike. Strong faces and core are required. Figure A.22 shows the influence of strength requirement on the trade-off surface between blast mitigation and mass. A noticeable impact is observed for high strength requirements of about 25 kN. At this strength level, mass requirements imply thin core, less than 100 mm. With such a thin core, the sandwich effect is lost in terms of blast mitigation.

On the other hand, for high blast mitigation, a thick core is required. Thus, the mass of the panel is not optimal in flexural strength design as shown in Figure A.22 for a 0.05 m/m constraint on the blast resistance. Blast mitigation requirements also imply a mass higher than about 28 kg/m² as lighter panels cannot sustain the considered blast load. This is translated into a truncation of the performance space as shown in Figure A.22.

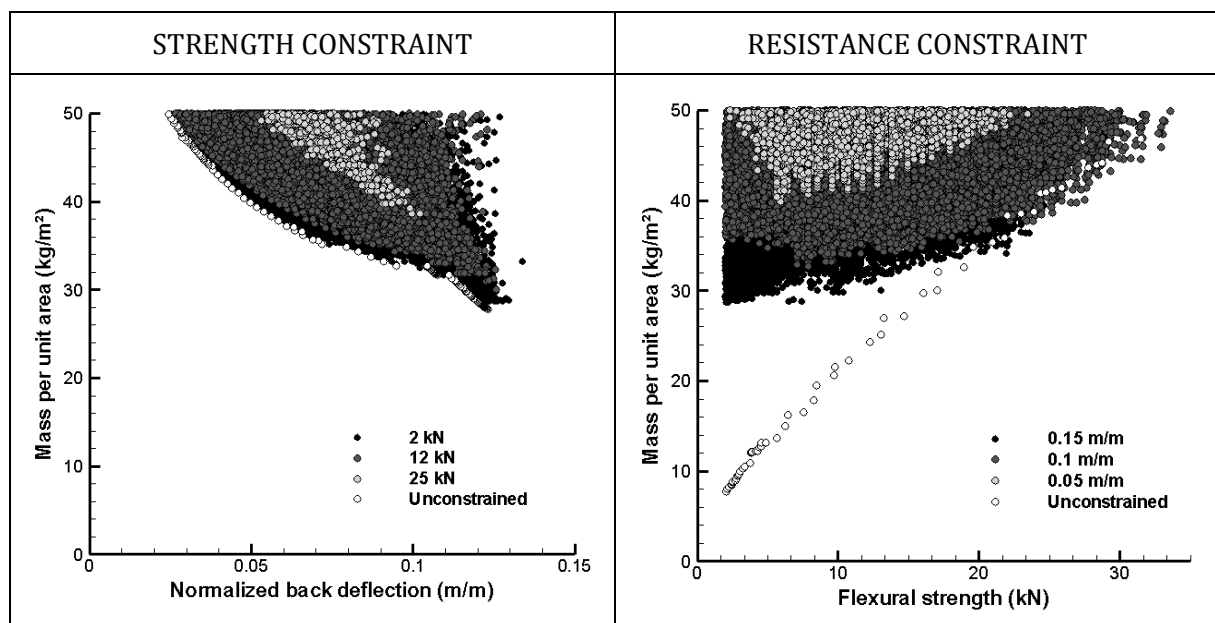


Figure A.22: On the left hand side: evolution of the performance space for blast resistance at minimal weight as a function of strength constraint. On the right hand side: evolution of the performance space for flexural strength at minimal weight as a function of blast resistance constraint.

Advantage of sandwich solutions

These two performances are compatible and sandwich panels overcome solid plates regarding both performances.

B. Performances of the genetic algorithm

The following tables display some data on the optimization calculations presented in the present work. For instance, the indicated data are:

- The function(s) that is (are) optimized along with mass.
- The number of objectives considered.
- The size of the search space, i.e. the number of solutions that could possibly be generated by the genetic algorithm.
- The n° of evaluations, i.e. the actual number of solutions that were generated by the genetic algorithm.

Optimal design of architected sandwich panels for multifunctional properties

Pierre Leite

- The n° of Pareto optimal solutions, which is the number of non-dominated solutions at the end of the optimization process.
- The shape of the trade-off surface or the compatibility between specifications when appropriate.

The first table, Table B.1, concerns the data from the “real path” approach” while the second one, Table B.2, gathers information on the optimizations by “virtual path”.

Table B.1: Data on the optimization process for the “real path” approach.

Function	N° objectives	Size of search space	N° evaluations	N° Pareto optimal solutions	Shape (Compatibility)
Flexural stiffness	2	1,37E+07	4,24E+04	127	Convex
Flexural strength	2	1,37E+07	3,63E+04	60	Concave
Acoustic damping	2	1,42E+07	8,59E+03	278	Convex
Thermal resistance	2	1,37E+07	3,52E+04	120	Linear
Thermal insulation	2	2,64E+10	9,73E+04	163	Convex
Blast resistance	2	2,09E+10	1,63E+05	365	Convex
<ul style="list-style-type: none"> • Stiffness • Acoustic damping 	3	1,24E+07	8,67E+05	21067	Convex
<ul style="list-style-type: none"> • Strength • Thermal resistance 	3	1,70E+07	4,42E+05	7637	Concave
<ul style="list-style-type: none"> • Blast resistance • Thermal insulation 	3	2,64E+10	2,57E+05	1155	Compatible
<ul style="list-style-type: none"> • Blast resistance • Acoustic damping 	3	2,09E+10	2,37E+05	1233	Incompatible

Table B.2: Data on the optimization process for the “virtual path” approach.

Function	Pattern	N° objectives	Size of search space	N° evaluations	N° Pareto optimal solutions	Shape (Compatibility)
Flexural stiffness	Foam	2	8,93E+07	4,36E+04	181	Convex
	Honeycomb	2	1,09E+08	3,80E+04	139	Convex
	Truss	2	4,02E+08	5,68E+04	226	Convex
Flexural strength	Foam	2	8,93E+07	3,56E+04	50	Concave
	Honeycomb	2	1,09E+08	3,65E+04	72	Concave
	Truss	2	4,02E+08	4,34E+04	106	Concave

Acoustic damping	Foam	2	8,93E+07	1,31E+04	154	Convex
	Honeycomb	2	1,09E+08	4,15E+04	522	Convex
	Truss	2	4,02E+08	3,35E+04	670	Convex
Thermal resistance	Foam	2	8,93E+07	3,27E+04	45	Linear
	Honeycomb	2	1,09E+08	3,10E+04	39	Linear
	Truss	2	4,02E+08	3,55E+04	42	Linear
Thermal insulation	Foam	2	1,91E+11	9,57E+04	72	Convex
	Honeycomb	2	1,91E+11	9,51E+04	83	Convex
	Truss	2	6,02E+11	1,32E+05	112	Convex
Blast resistance	Foam	2	1,91E+11	1,98E+05	669	Convex
	Honeycomb	2	1,91E+11	1,37E+05	463	Convex
	Truss	2	6,02E+11	3,28E+05	1025	Convex
<ul style="list-style-type: none"> Stiffness Acoustic damping 	Foam	3	8,43E+07	3,36E+05	1057	Convex
	Honeycomb	3	9,92E+07	2,69E+05	3125	Convex
	Truss	3	3,13E+08	4,20E+05	4246	Convex
<ul style="list-style-type: none"> Strength Thermal resistance 	Foam	3	9,43E+07	7,94E+04	1135	Concave
	Honeycomb	3	1,59E+08	2,10E+05	2193	Concave
	Truss	3	8,48E+08	2,98E+05	2934	Concave
<ul style="list-style-type: none"> Blast resistance Thermal insulation 	Foam	3	1,91E+11	5,25E+05	2618	Compatible
	Honeycomb	3	1,91E+11	5,22E+05	4575	Compatible
	Truss	3	6,02E+11	1,11E+06	20442	Compatible

Optimal design of architected sandwich panels for multifunctional properties

Pierre Leite

<ul style="list-style-type: none"> Blast resistance Acoustic damping 	Foam	3	1,91E+11	8,63E+05	604	Incompatible
	Honeycomb	3	1,91E+11	7,47E+05	579	Incompatible
	Truss	3	6,02E+11	5,78E+05	592	Incompatible

C. Design Of Experiments for acoustic damping

A Box-Behnken Design Of Experiments has been used to create a polynomial model of the Acoustical Transmission Loss R of a sandwich panel.

As far as a symmetrical sandwich panel is concerned, there are six factors which are:

- t_f , ρ_f and E_f , the thickness, density and Young's modulus of the face sheets respectively.
- t_c , ρ_c and E_c , the thickness, density and Young's modulus of the core respectively.

The initial data is provided by the PIAMCO software. Using these data, the plot of main effects of the factors is obtained and displayed in Figure C.1:

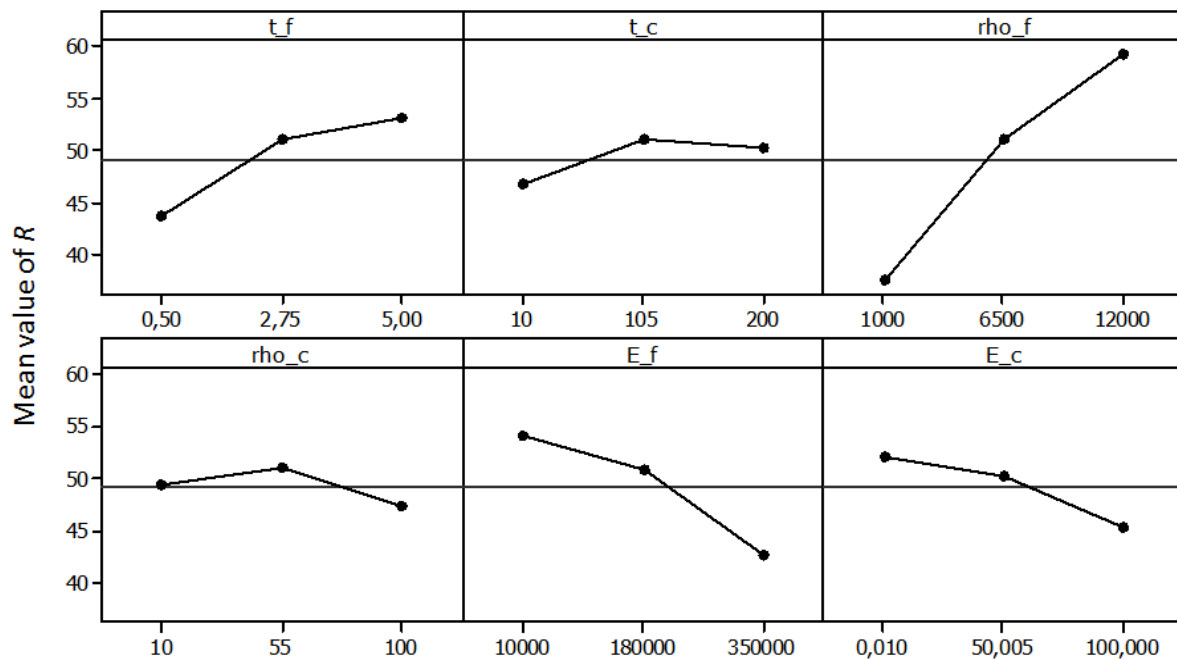


Figure C.1: Main effects of factors on the response R calculated based on the DOE.

The interactions between factors can also be taken into account. The interactions between two factors have been investigated through the plot presented in Figure C.2. These results are used to identify a polynomial model that fits the values of the experiments. This model can then compute an approximated value of the Acoustical Transmission Loss R in the whole range of variation of the factors. The contour plots calculated by this model are represented in Figure C.3.

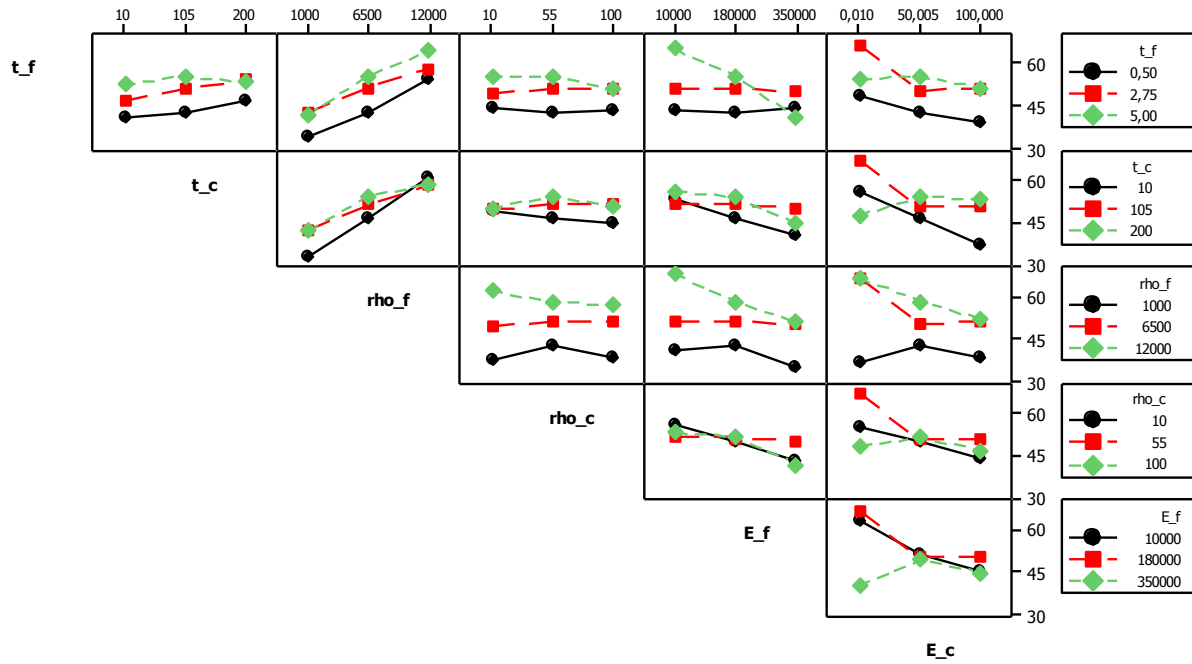


Figure C.2: Interaction plots for the creation of a surrogate model of the Acoustical Transmission Loss R .

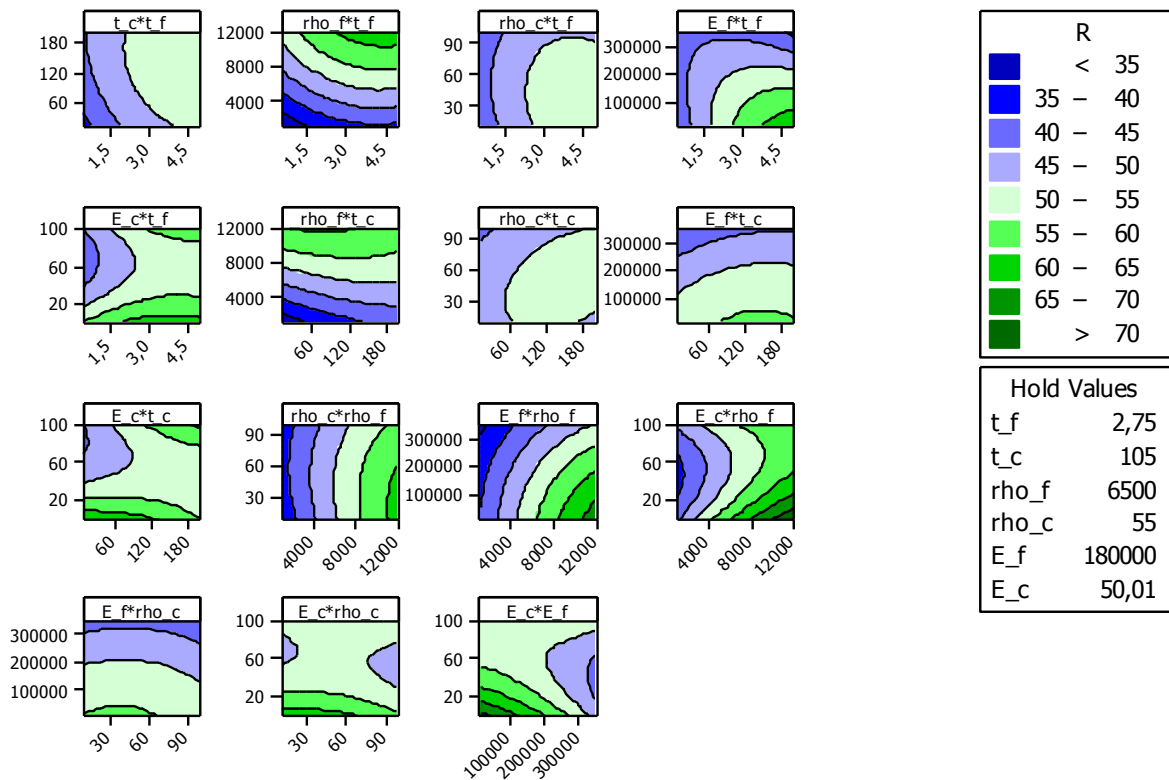


Figure C.3: Contour plots of the approximated model of the Acoustical Transmission Loss R calculated using the DOE.

References

- [ALD10] A. Alderson, K.L. Alderson, D. Attard, K.E. Evans, R. Gatt, J.N. Grima, W. Miller, N. Ravirala, C.W. Smith, K. Zied, *"Elastic constants of 3-, 4- and 6-connected chiral and anti-chiral honeycombs subject to uniaxial in-plane loading"*, Composites Science and Technology, 70, pp. 1042-1048, (2010).
- [ALL69] H.G. Allen, *"Analysis and design of structural sandwich panels"*, Oxford: Pergamon Press, (1969).
- [AMI12] M. Amiot, *"Mise en œuvre et étude de structures de nontissés et de composites poreux multifonctionnels en para-aramide : absorption acoustique et résistance à l'impact"*, [in french], Ph.D. thesis, Université des Sciences et Technologies, Lille, (2012).
- [ASH89] M.F. Ashby, *"On the engineering properties of materials"*, Acta Metallurgica, 37, pp.1273-1293, (1989).
- [ASH99] M.F. Ashby, *"Materials selection in mechanical design"*, 2nd edition, Oxford: Butterworth Heinemann, (1999).
- [ASH00a] M.F. Ashby, *"Multi-objective optimization in material design and selection"*, Acta Materialia, 48, pp. 359-369, (2000).
- [ASH00b] M.F. Ashby, A.G. Evans, N.A. Fleck, L.J. Gibson, J.W. Hutchinson, H.N.G. Wadley, *"Metal foams: a design guide"*, London: Butterworth Heinemann, (2000).
- [ASH03] M.F. Ashby, Y. Bréchet, *"Designing hybrid materials"*, Acta Materialia, 51, pp. 5801-5821, (2003).
- [ASH07] M.F. Ashby, H.R. Shercliff, D. Cebon, *"Materials – engineering, science, processing and design"*, 1st edition, Oxford: Butterworth Heinemann, (2007).
- [ASH11] M.F. Ashby, *"Hybrid materials to expand the boundaries of material-property space"*, Journal of the American Ceramic Society, 94, pp. 3-14, (2011).
- [ASH13] M.F. Ashby, *"Designing architected materials"*, Scripta Materialia, 68, pp. 4-7, (2013).
- [AUT07] A. Autruffe, F. Pelloux, C. Brugger, P. Duval, Y. Bréchet, M. Fivel, *"Indentation behaviour of interlocked structures made of ice: influence of the friction coefficient"*, Advanced Engineering Materials, 9, pp. 664-666, (2007).

Optimal design of architected sandwich panels for multifunctional properties

Pierre Leite

- [BAN08] J. Banhart, H.-W. Seeliger, *“Aluminium foam sandwich panels: manufacture, metallurgy and applications”*, Advanced Engineering Materials, 10, pp. 793-802, (2008).
- [BAR01] H. Bart-Smith, J.W. Hutchinson, A.G. Evans, *“Measurement and analysis of the structural performance of cellular metal sandwich construction”*, International Journal of Mechanical Sciences, 43, pp. 1945-1963, (2001).
- [BAS98] D. Bassetti, *“Aides informatisées à la sélection des matériaux”*, Thèse de Doctorat, Institut National Polytechnique de Grenoble, (1998).
- [BAU11] V. Baudoui, *“Optimisation robuste multiobjectifs par modèles de substitution”*, [in french], Ph.D. thesis, Institut Supérieur de l'Aéronautique et de l'Espace, Toulouse, (2011).
- [BER96] J.M. Berthelot, *“Matériaux composites – comportement mécanique et analyses des structures”*, 2^{ème} édition, Masson, (1996).
- [BHA02] A. Bhattacharya, V.V. Calmide, R.L. Mahajan, *“Thermophysical properties of high porosity metal foams”*, International Journal of Heat and Mass Transfer, 45, pp. 1017-1031, (2002).
- [BOL13] P. Bollen, N. Quiévy, I. Huynen, C. Bailly, C. Detrembleur, J.M. Thomassin, T. Pardoën, *“Multifunctional architected materials for electromagnetic absorption”*, Scripta Materialia, 68, pp. 50-54, (2013).
- [BOO01] K. Boomsma, D. Poulikakos, *“On the effective thermal conductivity of a three-dimensionally structured fluid-saturated metal foam”*, International Journal of Heat and Mass Transfer, 44, pp. 827-836, (2001).
- [BOU08] O. Bouaziz, Y. Bréchet, J.D. Embury, *“Heterogeneous and architecture materials: a possible strategy for design of structural materials”*, Advanced Engineering Materials, 10, pp. 24-36, (2008).
- [BOU12] O. Bouaziz, J.P. Masse, *“Extension of Ashby's performance indexes in mixed tension-bending solicitations”*, Advanced Engineering Materials, 14, pp. 497-498, (2012).
- [BOX60] G.E.P. Box, D.W. Behnken, *“Some new three level designs for the study of quantitative variables”*, Technometrics, Vol. 2, No. 4, pp. 455-475, (1960).
- [BRE13] Y. Bréchet, J.D. Embury, *“Architected materials: expanding materials space”*, Scripta Materialia, 68, pp. 1-3, (2013).
- [CAS09] G. Castillo, H. Wagnier, M. Danis, Y. Bréchet, *“Determination of materials selection performance indices through the combination of numerical modeling and optimization methods”*, Advanced Engineering Materials, 11, pp. 938-944, (2009).
- [CES] CES, Cambridge Engineering Selector, (Software), Granta Design Ltd, Cambridge, (2010).
- [CHE01] C. Chen, A-M. Harte, N.A. Fleck, *“The plastic collapse of sandwich beams with a metallic foam core”*, International Journal of Mechanical Sciences, 43, pp. 1483-1506, (2001).

-
- [CHU07] J.G. Chung, S.H. Chang, M.P.F. Sutcliffe, *"Deformation and energy absorption of composite egg-box panels"*, Composites Science and Technology, 67, pp. 2342-2349, (2007).
- [COL02] Y. Colette, P. Siarry, *"Optimisation multiobjectif"*, Editions Eyrolles, France, (2002).
- [COU12] L. Courtois, *"Monofilament entangled materials: relationship between microstructural properties and macroscopic behaviour"*, Ph.D. thesis, Institut National des Sciences Appliquées, Lyon, (2012).
- [DAK] M.S. Eldred, B.M. Adams, D.M. Gay, L.P. Swiler, K.R. Dalbey, K. Haskell, W.J. Bohnhoff, J.P. Eddy, P.D. Hough, *"Design Analysis Kit for Optimization and TeraScale Applications (DAKOTA)"*, Version 5.0 User's Manual, Sandia National Laboratories, (2009).
- [DAN09] *"Major accomplishments in composite materials and sandwich structures"*, edited by I.M. Daniel, E.E. Gdoutos, Y.D.S. Rajapakse, Springer, London, (2009).
- [DAV01] J.M. Davies, *"Lightweight sandwich construction"*, Blackwell Science, London, (2001).
- [DAV09] C. Davoine, A. Götzfried, S. Mercier, F. Popoff, A. Rafray, M. Thomas, V. Marcadon, *"Metallic hollow sphere structures manufacturing process"*, Proceedings of MRS Spring meeting, San Francisco, (2009).
- [DES01a] V.S. Deshpande, M.F. Ashby, N.A. Fleck, *"Foam topology: bending versus stretching dominated architectures"*, Acta Materialia, 49, pp. 1035-1040, (2001).
- [DES01b] V.S. Deshpande, N.A. Fleck, *"Collapse of truss core sandwich beams in 3-point bending"*, International Journal of Solids and Structures, 38, pp. 6275-6305, (2001).
- [DES05] V.S. Deshpande, N.A. Fleck, *"One-dimensional response of sandwich plates to underwater shock loading"*, Journal of the Mechanics and Physics of Solids, 53, pp. 2347-2383, (2005).
- [DIR12a] J. Dirrenberger, S. Forest, D. Jeulin, *"Elastoplasticity of auxetic materials"*, Computational Materials Science, 64, 57-61, (2012).
- [DIR12b] J. Dirrenberger, *"Effective properties of architected materials"*, Ph.D. thesis, Ecole Nationale Supérieure des Mines, Paris, (2012).
- [DUG13] M. Dugué, *"Expériences et simulations de matériaux autobloquants"*, [in french], Ph.D. thesis, Institut National Polytechnique, Grenoble, (2012).
- [DYM74] CL. Dym, M.A. Lang, *"Transmission of sound through sandwich panels"*, Journal of the Acoustical Society of America, 56, pp. 1523-1532, (1974).
- [DYS03a] A.V. Dyskin, Y. Estrin, A.J. Kanel-Belov, E. Pasternak, *"Topological interlocking of platonic solids: a way to new materials and structures"*, Philosophical Magazine, 83, pp. 197-203, (2003).
- [DYS03b] A.V. Dyskin, Y. Estrin, E. Pasternak, H.C. Kohr, A.J. Kanel-Belov, *"Fracture resistant structures based on topological interlocking with non-planar contacts"*, Advanced Engineering Materials, 5, pp. 116-119, (2003).

Optimal design of architected sandwich panels for multifunctional properties

Pierre Leite

- [EDD01] J.P. Eddy, K. Lewis, "*Effective generation of Pareto sets using genetic programming*", Proceedings of ASME Design Engineering Technical Conference, DETC2001/DAC-21094, (2001).
- [EHR05] M. Ehrgott, "*Multicriteria optimization*", Berlin: Springer, (2005).
- [EVA91] K.E. Evans, M.A. Nkansah, I.J. Hutchinson, S.C. Rogers, "*Molecular network design*", Nature, 353, pp. 124-, (1991).
- [FAH85] F. Fahy, "*Sound and structural vibration radiation, transmission and response*", academic Press, London, (1985).
- [FIS97] G.S. Fishman, "*Monte-Carlo: concepts, algorithms and applications*", New-York: Springer-Verlag, (1997).
- [FLE01] V.S. Deshpande, N.A. Fleck, M.F. Ashby, "*Effective properties of the octet-truss lattice material*", Journal of the Mechanics and Physics of Solids, 49, pp. 1747-1769, (2001).
- [FLE04] N.A. Fleck, V.S. Deshpande, "*The resistance of clamped sandwich beams to shock loading*", Journal of Applied Mechanics, 71, pp. 386-401, (2004).
- [FUL61] R.B. Fuller, "*Octet truss*", U.S. Patent 2,986,241, (1961).
- [FUZ] Fuzzymat, (Software), Bassetti, Grenoble, (1997).
- [GAS04] S. Gasser, Y. Bréchet, F. Paun, "*Materials design for acoustic liners: an example of tailored multifunctional materials*", Advanced Engineering Materials, 6, pp. 97-102, (2004).
- [GAS05] S. Gasser, F. Paun, Y. Bréchet, "*Absorptive properties of rigid porous media: application to face centered cubic sphere packing*", Journal of the Acoustical Society of America, 117, pp. 2090-2099, (2005).
- [GIA10] S. Giacobi, F.X. Kromm, H. Wargnier, M. Danis, "*Filtration in materials selection and multi-materials design*", Materials and Design, 31, pp. 1842-1847, (2010).
- [GIB97] L.J. Gibson, M.F. Ashby, "*Cellular Solids*", Cambridge University Press, (1997).
- [GLO97] F. Glover, M. Laguna, "*Tabu search*", Boston: Kluwer Academic Publishers, (1997).
- [GOL89] D.E. Goldberg, "*Genetic algorithms in search, optimization and machine learning*", New-York: Addison-Wesley, (1989).
- [GU01] S. Gu, T.J. Lu, A.G. Evans, "*On the design of two-dimensional cellular metals for combined heat dissipation and structural load capacity*", International Journal of Heat and Mass Transfer, 44, pp. 2163-2175, (2001).
- [GUP12] N. Gupta, D.D. Luong, K. Cho, "*Magnesium matrix composite foams – density, mechanical properties, and applications*", Metals, 2, pp. 238-252, (2012).
- [HEI12] J. Hein, M. Kuna, "*Optimizing thermal shock resistance of layered refractories*", Advanced Engineering Materials, 14, pp. 408-415, (2012).

-
- [HOL75] J. Holland, *"Adaptation in natural and artificial systems"*, Ann arbor: University of Michigan Press, (1975).
- [HUT05] J.W. Hutchinson, Z. Xue, *"Metal sandwich plates optimized for pressure impulses"*, International Journal of Mechanical Sciences, 47, pp. 545-569, (2005).
- [IRI11a] F.X. Irisarri, M.M. Abdalla, Z. Gurdal, *"Improved Shepard's method for the optimization of composite structures"*, American Institute of Aeronautics and Astronautics Journal, Vol 49, N° 12, pp. 2726-2736, (2011).
- [IRI11b] F.-X. Irisarri, F. Laurin, F.-H. Leroy, J.-F. Maire, *"Computational strategy for multiobjective optimization of composite stiffened panels"*, Composite Structures, 93, pp. 1158-1167, (2011).
- [KIR83] S. Kirkpatrick, C. Gelatt, M. Vecchi, *"Optimization by simulated annealing"*, Science, Tome 220, n°4598, pp. 671-680, (1983).
- [KOL12] A. Kolopp, *"Impact sur structures sandwiches pour applications de blindage aéronautique"*, [in french], Ph.D. thesis, Université Toulouse 3 Paul Sabatier, Toulouse, (2012).
- [KRO02] F.X. Kromm, J.M. Quenisset, R. Harry, T. Lorriot, *"An example of multimaterials design"*, Advanced Engineering Materials, 4, pp. 371-374, (2002).
- [LAN60] A. H. Land, A. G. Doig, *"An automatic method of solving discrete programming problems"*, Econometrica, 28, pp. 497-520, (1960).
- [LAN00] D. Landru, *"Aides informatisées à la sélection des matériaux et des procédés dans la conception des pièces de structure"*, [in french], Ph.D. thesis, Institut National Polytechnique de Grenoble, (2000).
- [LeR95] R. Le Riche, R.T. Haftka, *"Improved genetic algorithm for minimum thickness composite laminate design"*, Composites Engineering, Vol. 5, No. 2, pp. 143-161, (1995).
- [LU98] T.J. Lu, H.A. Stone, M.F. Ashby, *"Heat transfer in open cell metal foams"*, Acta Materialia, 46, pp. 3619-3635, (1998).
- [LU99] T.J. Lu, *"Heat transfer efficiency of metal honeycombs"*, International Journal of Heat and Mass Transfer, 42, pp. 2031-2040, (1999).
- [LU05] T.J. Lu, L. Valdevit, A.G. Evans, *"Active cooling by metallic sandwich structures with periodic cores"*, Progress in Materials Science, 50, pp. 789-815, (2005).
- [MAX64] J.C. Maxwell, *"On the calculation of the equilibrium and stiffness for frames"*, Philosophical Magazine, 27, pp. 294-299, (1864).
- [MER08] A. Merval, *"Application des modèles réduits à l'optimisation multiniveaux d'une structure aéronautique"*, [in french], Ph.D. thesis, Institut Supérieur de l'Aéronautique et de l'Espace, Toulouse, (2008).

Optimal design of architected sandwich panels for multifunctional properties

Pierre Leite

- [MEZ10] L. Mezeix, *“Développement de matériaux d’âme pour structures sandwich à base de fibres enchevêtrées”*, [in french], Ph.D. thesis, Université Toulouse 3 Paul Sabatier, Toulouse, (2010).
- [McC01] T.M. McCormack, R. Miller, O. Kesler, L.J. Gibson, *“Failure of sandwich beams with metallic foam cores”*, International Journal of Solids and Structures, 38, pp. 4901-4920, (2001).
- [McS06] G.J. McShane, D.D. Radford, V.S. Deshpande, N.A. Fleck, *“The response of clamped sandwich plates with lattice cores subjected to shock loading”*, European Journal of Mechanics A/Solids, 25, pp. 215-229, (2006).
- [MIN83] M. Minoux, *“Programmation mathématiques : Théories et algorithmes”*, Paris: Dunod, vol. 1, Paris (1983).
- [MUR98] Y. Murer, *“Etablissement de modèles prévisionnels du comportement thermo-acoustique de structures composites multicouches et sandwichs”*, thèse de doctorat, ENSAE, (1998).
- [NEL65] J.A. Nelder, R. Mead, *“A simplex method for function minimization”*, Computer Journal, 7, pp. 308-313, (1965).
- [PAR96] V. Pareto, *“Cours d’économie politique”*, Vol. 1 et 2, F. Rouge, Lausanne, (1896).
- [PET99] A. Petras, M.P.F. Sutcliffe, *“Failure mode maps for honeycomb sandwich panels”*, Composite Structures, 44, pp. 237-252, (1999).
- [QIU03] X. Qiu, V.S. Deshpande, N.A. Fleck, *“Finite element analysis of the dynamic response of clamped sandwich beams”*, European Journal of Mechanics - A/Solids, 22, pp. 801-814, (2003).
- [RAD06] D.D. Radford, N.A. Fleck, V.S. Deshpande, *“The response of clamped sandwich beam subjected to shock loading”*, International Journal of Impact Engineering, 32, pp. 968-987, (2006).
- [RAT06] H.J. Rathbun, D.D. Radford, Z. Xue, M.Y. He, J. Yang, V.S. Deshpande, N.A. Fleck, J.W. Hutchinson, F.W. Zok, A.G. Evans, *“Performance of metallic honeycomb-core sandwich beams under shock loading”*, International Journal of Solids and Structures, 43, pp. 1746-1763, (2006).
- [SIM95] F. Simon, S. Pauzin, *“Sound transmission loss model of orthotropic sandwich panels”*, Proceedings of Euronoise '95, 855-860, Lyon, (1995).
- [SIM04] F. Simon, S. Pauzin, D. Biron, *“Optimization of sandwich trim panels for reducing helicopter internal noise”*, Proceedings of ERF30, Marseille, (2004).
- [SIR04] P. Sirisalee, M.F. Ashby, G.T. Parks, P.J. Clarkson, *“Multi-criteria material selection in engineering design”*, Advanced Engineering Materials, 6, pp. 84-92, (2004).
- [SIR06] P. Sirisalee, M.F. Ashby, G.T. Parks, P.J. Clarkson, *“Multi-criteria material selection of monolithic and multi-materials in engineering design”*, Advanced Engineering Materials, 8, pp. 48-56, (2006).

-
- [STE04a] C.A. Steeves, N.A. Fleck, *"Collapse mechanisms of sandwich beams with composite faces and a foam core, loaded in three-point bending. Part I: analytical models and minimum weight design"*, International Journal of Mechanical Sciences, 46, pp. 561-583, (2004).
- [STE04b] C.A. Steeves, N.A. Fleck, *"Collapse mechanisms of sandwich beams with composite faces and a foam core, loaded in three-point bending. Part II: experimental investigation and numerical modelling"*, International Journal of Mechanical Sciences, 46, pp. 585-608, (2004).
- [STE04c] C.A. Steeves, N.A. Fleck, *"Material selection in sandwich beam construction"*, Scripta Materialia, 50, pp. 1335-1339, (2004).
- [TAG10] V.L. Tagarielli, V.S. Deshpande, N.A. Fleck, *"Prediction of the dynamic response of composite sandwich beams under shock loading"*, International Journal of Impact Engineering, 37, pp. 854-864, (2010).
- [TIA04] J. Tian, T. Kim, T.J. Lu, H.P. Hodson, D.T. Queheillalt, D.J. Sypeck, H.N.G. Wadley, *"The effects of topology upon fluid-flow and heat-transfer within cellular copper structures"*, International Journal of Heat and Mass Transfer, 47, pp. 3171-3186, (2004).
- [TIA07] J. Tian, T.J. Lu, H.P. Hodson, D.T. Queheillalt, H.N.G. Wadley, *"Cross flow heat exchange of textile cellular metal core sandwich panels"*, International Journal of Heat and Mass Transfer, 50, pp. 2521-2536, (2007).
- [TRI87] T.C. Triantafillou, L.J. Gibson, *"Failure mode maps for foam core sandwich beams"*, Materials Science and Engineering, 95, pp. 37-53, (1987).
- [VEN99] S. Venkataraman, T.R. Haftka, *"Optimization of composite panels – a review"*, Proceedings of the 14th annual Technical Conference of the American Society of Composites, Dayton, OH, pp. 27-29, (1999).
- [VEN04] S. Venkataraman, R.T. Haftka, *"Structural optimization complexity: what has Moore's law done for us?"*, Structural Multidisciplinary Optimization, 28, pp. 375-387, (2004).
- [WAN09] T. Wang, S. Li, S.R. Nutt, *"Optimal design of acoustical sandwich panels with a genetic algorithm"*, Applied Acoustics, 70, pp. 416-425, (2009).
- [WEN06] T. Wen, J. Tian, T.J. Lu, D.T. Queheillalt, H.N.G. Wadley, *"Forced convection in metallic honeycomb structures"*, International Journal of Heat and Mass Transfer, 49, pp. 3313-3324, (2006).
- [WIC01] N. Wicks, J.W. Hutchinson, *"Optimal truss plates"*, International Journal of Solids and Structures, 38, pp. 5165-5183, (2001).
- [XUE03] Z. Xue, J.W. Hutchinson, *"Preliminary assessment of sandwich plates subject to blast loads"*, International Journal of Mechanical Sciences, 45, pp. 687-705, (2003).
- [XUE04] Z. Xue, J.W. Hutchinson, *"A comparative study of impulse-resistant metal sandwich plates"*, International Journal of Impact Engineering, 30, pp. 1283-1305, (2004).
- [ZEN97] D. Zenkert, *"An introduction to sandwich construction"*, Sheffield: Engineering Materials Advisory Service, (1997).

Optimal design of architected sandwich panels for multifunctional properties

Pierre Leite

- [ZHA92] J. Zhang, M.F. Ashby, "*The out-of-plane properties of honeycombs*", International Journal of Mechanical Science, 34, pp. 475-489, (1992).
- [ZHU09] F. Zhu, Z. Wang, G. Lu, L. Zhao, "*Analytical investigation and optimal design of sandwich panels subjected to shock loading*", Materials and Design, 30, pp. 91-100, (2009).
- [ZUP03] M. Zupan, C. Chen, N.A. Fleck, "*The plastic collapse and energy absorption capacity of egg-box panels*", International Journal of Mechanical Sciences, 45, pp. 851-871, (2003).

Abstract:

The present thesis aims at developing a design method dedicated to the optimization of architected sandwich panels for multifunctional properties following a “materials-by-design” approach. This method is based on a genetic algorithm which enables to deal with materials selection (discrete variables) and geometrical dimensioning (continuous variables) simultaneously. Three core architectures have been investigated: foams, hexagonal honeycombs and tetrahedral truss structures. In this thesis, two main paths for material selection are defined. In the first one, architected materials are considered as existing materials with properties referenced in a closed materials database. This is called the “real path” optimization. In order to expand the range of possibilities in terms of materials selection, a semi-continuous description of the architected materials is considered in the second path, which is called “virtual path” optimization. The core material is described by a constitutive material (discrete variable) and a set of continuous geometrical variables representing the architecture. Using these two aforementioned approaches, several working properties of sandwich panels have been evaluated: flexural stiffness and strength, acoustic damping, thermal resistance and insulation, and finally blast mitigation. Bi-objective optimizations were performed in order to optimize each property in a minimal weight design. Some tri-objective cases are also presented, thus assessing the compatibility between different specifications. Indeed, this is achieved by relating trade-off surface shape to the compatibility between specifications. The optimization results also help identify the optimal design regarding the different criteria. Using the “virtual path” approach, a direct comparison between the different core architectures is achievable. Nevertheless, by being global and dealing with mixed variables, the obtained optimization process is complex. Two mixed methods where genetic algorithm is coupled with other approaches are proposed in order to increase the analysis complexity while providing a reasonable optimization complexity.

Keywords: Multi-objective optimization, sandwich panels, materials selection, architected materials.

Résumé :

Cette thèse suit une démarche « materials-by-design » avec pour objectif le développement d’une méthode de conception dédiée aux panneaux sandwichs architecturés pour l’obtention de propriétés multifonctionnelles. Cette méthode s’appuie sur l’utilisation d’un algorithme génétique permettant simultanément une sélection de matériaux (variables discrètes) et un pré-dimensionnement du panneau (variables continues). Trois architectures de cœur ont été étudiées : les mousses, les nids-d’abeilles hexagonaux et les treillis tétraédriques. Dans cette thèse, on définit deux approches différentes de sélection des matériaux. Dans un premier temps, les matériaux architecturés sont considérés comme des matériaux existants, dont les propriétés sont référencées dans une base de données fermée. Cette approche est appelée optimisation par « voie réelle ». Afin d’ouvrir les possibilités en termes de sélection de matériaux, la deuxième approche considère une description semi-continue des matériaux architecturés et est appelée optimisation par « voie virtuelle ». Le matériau cœur est décrit par un matériau constitutif (variable discrète) et par une ou plusieurs variables géométriques continues représentant l’architecture. Utilisant ces deux approches, différentes propriétés d’emploi des panneaux sandwichs sont évaluées : rigidité et résistance en flexion, atténuation acoustique, résistance et isolation thermique, et enfin résistance aux chocs impulsifs. Chaque fonction est optimisée à masse minimale par optimisation bi-objectifs. Différents cas d’optimisation tri-objectifs sont également présentés afin d’évaluer la compatibilité entre propriétés. En effet, la forme de la surface de compromis obtenue donne une indication sur la compatibilité entre les différents critères. Cette étape d’optimisation permet également l’identification des paramètres de conception optimaux. Dans le cas d’une optimisation par « voie virtuelle », une comparaison directe entre architectures est aussi possible. Cependant, la démarche d’optimisation mise en place est complexe car globale et travaillant avec des variables mixtes. Deux méthodes mixtes, couplant l’algorithme génétique avec d’autres approches, sont proposées pour permettre un accroissement de la complexité de l’analyse tout en garantissant une complexité raisonnable de l’optimisation.

Mots-clés : Optimisation multifonctionnelle, panneaux sandwichs, sélection de matériaux, matériaux architecturés.